

CONTENTS

IMAGE FUSION ALGORITHM BASED ON FINITE DISCRETE SHEARLET TRANSFORM	3
EMOTIONAL COMMUNICATION OF WEB COLOR DESIGN.....	6
MULTISOURCE IMAGES FUSION ALGORITHM BASED ON NONSUBSAMPLED SHEARLET TRANSFORM	8
THE CONSTRUCTION AND EMPIRICAL ANALYSIS OF THE FINANCIAL RISK EARLY WARNING MODEL OF THE LISTING CORPORATION IN CHINA.....	11
MULTISOURCE IMAGES FUSION ALGORITHM BASED ON NONSUBSAMPLED CONTOURLET TRANSFORM	14
A NEW DOUBLE-LEVEL WATERMARKING SCHEME BASED ON SPREAD SPECTRUM AND DIRTY PAPER.....	17
A RECOMMENDATION SYSTEM FOR PAPER SUBMISSION BASED ON VERTICAL SEARCH ENGINE	20
COMPARISON OF THREE MATHEMATICAL MOMENTUM MODELS OF VERTICAL AXIS CURRENT TURBINE	23
CONSTRUCTION OF SMART GRIDS SUITABLE FOR THE ERA OF GREEN ENERGY	25
DECOUPLING INTERRUPTS FROM THE INTERNET IN MARKOV MODELS	28
GENERATION CAPACITY INVESTMENT AND COMPENSATION MECHANISMS OF FREE COMPETITION POWER MARKET	31
MODELING THE LEACHING BEHAVIOR OF CS+ AND CO2+ FROM SIMULATED RADIOACTIVE WASTE-FORMS	33
NETWORK COURSE DESIGN RESEARCH BASED ON BLACKBOARD PLATFORM.....	37
PHYSIOLOGICAL STUDIES ON COLD RESISTANCE OF SWEET POTATO CULTIVARS AND RESISTANCE IDENTIFICATION.....	40
PSYCHOLOGICAL CAUSES AND CORRECTION OF STUDENTS' ONLINE GAME ADDICTION IN HIGHER VOCATIONAL COLLEGES.....	43
THE DESIGN OF COMPREHENSIVE IMAGE PROCESSING SYSTEM USING EMBEDDED WIRELESS DEVICES	47
THE IMPACT OF HORMONE DOSAGE, MICE STRAINS AND AGE ON SUPEROVULATION	50
THE STUDY OF THE APPLICATION OF THE ONLINE MONITORING TECHNOLOGY FOR METAL OXIDE ARRESTER	53
THE DISCRETE PHASE SIMULATION OF THE NON-LINEAR TUBE.....	57
DESIGN OF SIGNAL ACQUISITION CIRCUIT IN PORTABLE ELECTROCARDIOGRAM (ECG) MONITOR	60
ANALYSIS OF FRACTURE MORPHOLOGY AND EXTENSION RULES BASED ON PRESSURE DISTRIBUTION IN FRACTURE	62
THE ANALYSIS ON THE THIN DIFFERENCE LAYER INFLUENCES ON THE HYDRAULIC FRACTURE SEALING ABILITY	65
POSITIONING USING THE SUN SHADOW	68
THE STUDY OF TAXI SUBSIDY SCHEME BASED ON FUZZY COMPREHENSIVE EVALUATION OF THE PERSPECTIVE OF THE PASSENGERS.....	70
STUDY ON SITUATION AND COMPREHENSIVE UTILIZATION OF BLAST FURNACE SLAG.....	73
A WAY OF DISEASE TREATMENT BASED ON THE PEOPLE DENSITY IN DIFFERENT REGIONS AND THE SPEED OF THE VIRUS SPREAD.....	76
THE LOCATION-METHOD RESEARCH BASED ON THE COORDINATE OF SUN SHADOW	79
RESEARCH OF URBAN LOGISTICS NODE LAYOUT SOLUTION	82
RESEARCH ON FIRE RESISTANCE OF REINFORCED CONCRETE COLUMNS	84
THE COMPARISON OF REGRESSION ANALYSIS AND GREY PREDICTION AND JOINT USE.....	87
AN INVESTIGATION ON THE INFLUENCE OF NETWORK GAMES ON COLLEGE STUDENTS.....	89
THE METALLURGY PROFESSIONAL COLLEGE STUDENTS' EMPLOYMENT RESEARCH AND PREDICTION.....	92
THREE-WAY DECISIONS MODEL BASED ON SET PAIR-INFORMATION ENTROPY AND APPLICATIONS.....	95
THE SPREAD AND CONTROL RESEARCH OF DISEASE BASED ON THE SIR MODEL AND INDIVIDUAL RADIATION MOTION MODEL	98
SUPPLY MATCHING DEGREE EVALUATION MODEL BASED ON GENE ANALYSIS.....	102
AOSLO VIDEO IMAGE STABILIZATION ALGORITHM BASED ON HARRIS-SIFT	105
INFRARED DIM SMALL TARGET DETECTION ALGORITHM BASED ON ADAPTIVE PIPELINE FILTERING.....	108
THE STRUCTURAL ANALYSIS AND THE GREY SITUATION DECISION-MAKING RESEARCH OF SUSTAINABLE FOREST MANAGEMENT ENGINEERING SYSTEMS.....	110
FINANCIAL RISK MODELING AND SIMULATION BASED ON VECTOR AUTO REGRESSIVE MODEL	117
MODELING AND SIMULATION OF EARNINGS MANAGEMENT OF LISTING CORPORATION BASED ON CHINESE DATA	120
RESEARCH ON VOCATIONAL SKILL TRAINING OF NEWLY ESTABLISHED LOCAL UNIVERSITIES	123
DISTAL TIBIOFIBULAR DISLOCATION FIXATION: A META-ANALYSIS ON SYNDESMOTIC SCREW VERSUS SUTURE-BUTTON	126

Image Fusion Algorithm Based on Finite Discrete Shearlet Transform

Guangqiu Chen, Zhen ye Geng, Jie Lin

School of Electronic and Information Engineering, Changchun University of Science and Technology, Changchun 130022, China

Abstract—For enhancing the fusion accuracy of multi-modality images, an adaptive image fusion algorithm based on finite discrete shearlet transform (FDST) was proposed. First, source images were decomposed to multi-scale and multi-direction sub-bands using FDST. Secondly, average algorithm was adopted to combine coefficients in low-frequency sub-band and selection algorithm was used to combine coefficients in high-frequency sub-bands, then fused sub-bands were obtained. Finally, the fused sub-bands were reconstructed to images by inverse finite discrete shearlet transform (IFDST). Fusion experiments on different modality images were performed and objective assessments were implemented on the fusion results. The experimental results indicated that the proposed method performed better in subjective and objective assessments than a number of existing typical fusion techniques and obtained better fusion performance.

Index-terms—image fusion, finite discrete shearlet transform, shift-invariant, objective assessment

I. INTRODUCTION

Over the years, image fusion technologies based on multi-scale decomposition (MSD) have attracted the attention of relevant domestic and foreign scholars, who have achieved many outstanding research results[1]. Many MSD tools such as DWT[2], Curvelet[3], Contourlet[4] have been applied to fuse multi-modality images. Multi-scale representation method of an image is vital for the fusion accuracy. S.Häuser proposed a novel image representation method: finite discrete shearlet transform (FDST)[5], which not only has the advantages of Curvelet and Contourlet, but also holds shift-invariant. Therefore, in this paper, the FDST was used as MSD tool of an image.

II. FINITE DISCRETE SHEARLET TRANSFORM

The shearlets $\psi_{a,s,t}$ emerge by dilation, shearing and translation of a function as follows

$$\begin{aligned} \psi_{a,s,t}(x) &:= a^{-3/4} \psi(A_a^{-1} S_s^{-1}(x-t)) \\ &= a^{-3/4} \psi \left(\begin{pmatrix} \frac{1}{a} & -\frac{s}{a} \\ 0 & \frac{1}{\sqrt{a}} \end{pmatrix} (x-t) \right) \end{aligned} \quad (1)$$

Where $A_a = \begin{pmatrix} a & 0 \\ 0 & \sqrt{a} \end{pmatrix}$ is a scaling (or dilation) matrix, $a \in \mathbb{R}^+$, $S_s = \begin{pmatrix} 1 & s \\ 0 & 1 \end{pmatrix}$ is a shear matrix, $s \in \mathbb{R}$.

We assume that $\hat{\psi}$ can be written as $\hat{\psi}(\omega_1, \omega_2) = \hat{\psi}_1(\omega_1) \hat{\psi}_2\left(\frac{\omega_2}{\omega_1}\right)$. Consequently, we obtain for the Fourier transform

$$\hat{\psi}_{a,s,t}(\omega) = a^{3/4} e^{-2\pi i(\omega,t)} \hat{\psi}_1(a\omega_1) \hat{\psi}_2\left(a^{-1/2}\left(\frac{\omega_2}{\omega_1} + s\right)\right) \quad (2)$$

The frequency plane is divided into four parts on the basis of different ω_1 and ω_2 , that is horizontal cone c^h , vertical cone c^v , intersection(or the seam lines) of the two cones c^x , low frequency part c^0 , as shown in figure 1.

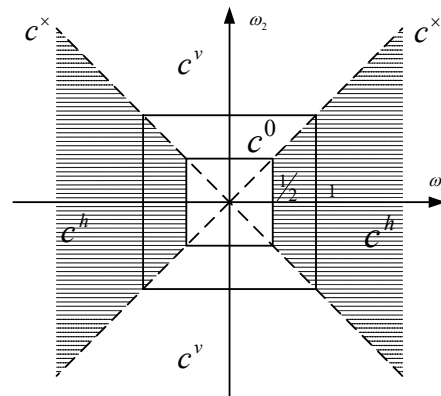


Figure1 The tiling of the frequency plane induced by the shearlet

Auxiliary functions is used to construct $\hat{\psi}_1$, $\hat{\psi}_2$ and $\hat{\phi}$ which satisfy the above requirements, so shearlet covering each part is obtained, that is represented to $\hat{\psi}^h$, $\hat{\psi}^v$, $\hat{\psi}^x$ and $\hat{\phi}_0$ respectively.

The discretization of shearlet mainly discretize the involved parameters as the dilation a , the shearing s and the translation t respectively, that is

$$\begin{cases} a_j := 2^{-2j}, & j = 0, \dots, J-1 \\ s_{j,k} := k2^{-j}, & -2^j \leq k \leq 2^j \\ t_m := \frac{m}{N}, & m \in I, N = 2^{2J} \end{cases} \quad (3)$$

So equation (1) and (2) can be written as following:

$$\psi_{j,k,m}(x) := \psi \left(A_{a_j}^{-1} S_{s_{j,k}}^{-1} (x - t_m) \right) \quad (4)$$

$$\hat{\psi}_{j,k,m}(\omega) = \hat{\psi}_1(4^{-j}\omega_1) \hat{\psi}_2(2^j \frac{\omega_2}{\omega_1} + k) e^{-2\pi i \langle \omega, m \rangle / N} \quad (5)$$

$$SH(f)(\kappa, j, k, m) = \begin{cases} F^{-1}(\hat{\phi}(\omega_1, \omega_2) \hat{f}(\omega_1, \omega_2)) & \kappa = 0 \\ F^{-1}(\hat{\psi}(4^{-j}\omega_1, 4^{-j}k\omega_1 + 2^{-j}\omega_2) \hat{f}(\omega_1, \omega_2)) & \kappa = h, |k| \leq 2^j - 1 \\ F^{-1}(\hat{\psi}(4^{-j}\omega_2, 4^{-j}k\omega_2 + 2^{-j}\omega_1) \hat{f}(\omega_1, \omega_2)) & \kappa = v, |k| \leq 2^j - 1 \\ F^{-1}(\hat{\psi}^{h \times v}(4^{-j}\omega_1, 4^{-j}k\omega_1 + 2^{-j}\omega_2) \hat{f}(\omega_1, \omega_2)) & \kappa = x, |k| = 2^j \end{cases} \quad (6)$$

As can be seen from equation (6), the FDST of an image f is mainly composed of the following four parts:

(1) Fourier transform: an image f is converted to spectrum image by 2D FFT.

(2) Multi-scale decomposition (MSD): spectrum image is filtered by low-pass filter and band-pass filters to obtain a low frequency sub-band and some band-pass sub-bands.

(3) Directional filtering: band-pass subbands are multiplied by shearlets to obtain directional sub-bands supported in frequency domain.

(4) Inverse Fourier transform: all the sub-bands are converted by inverse FFT to obtain sub-bands supported in time domain.

FDST has some inherent excellent properties such as the parabolic scaling, shift-invariant, high direction sensitivity, outstanding direction analysis and high computational efficiency.

An image decomposed by FDST with J scales can produce $\sum 2^{j+2}$ band-pass directional sub-bands and one low-pass sub-band, where $j = 0, \dots, J-1$.

III. FUSION CRITERION

An image f was decomposed by FDST to a low-frequency sub-band (approximation image) and some high-frequency subbands (detail images), denoted as $C_S^{j,k}$, $S = A, B$, when $j \neq 0, k \neq 0$, $C_S^{j,k}$ represent k th directional high-frequency sub-band in j th scale, $C_S^{0,0}$ represent low-frequency sub-band. Because of their different physical meaning, the approximation and detail images should be treated by the fusion algorithm in a different fashion. For the detail images $C_S^{j,k}$, one may observe that relevant perceptual information relates to the 'edge' information that is present in each of the detail coefficients. Detail coefficients having large absolute values correspond to sharp intensity changes and hence to salient features in the image such as edges, lines and

Where

$$I := \{(m_1, m_2) : m_i = 0, \dots, N-1, i = 1, 2\}$$

$$\omega \in \left\{ (\omega_1, \omega_2) : \omega_i = -\left\lfloor \frac{N}{2} \right\rfloor, \dots, \left\lfloor \frac{N}{2} \right\rfloor - 1, i = 1, 2 \right\}, \quad J \text{ is}$$

scaling number.

In reference [5], the above discrete shearlet constitute a Parseval frame of the finite Euclidean space $L_2(I)$, which is called the finite discrete shearlet transform (FDST).

The FDST of an image f is shown as

$$SH(f)(\kappa, j, k, m) = \begin{cases} F^{-1}(\hat{\phi}(\omega_1, \omega_2) \hat{f}(\omega_1, \omega_2)) & \kappa = 0 \\ F^{-1}(\hat{\psi}(4^{-j}\omega_1, 4^{-j}k\omega_1 + 2^{-j}\omega_2) \hat{f}(\omega_1, \omega_2)) & \kappa = h, |k| \leq 2^j - 1 \\ F^{-1}(\hat{\psi}(4^{-j}\omega_2, 4^{-j}k\omega_2 + 2^{-j}\omega_1) \hat{f}(\omega_1, \omega_2)) & \kappa = v, |k| \leq 2^j - 1 \\ F^{-1}(\hat{\psi}^{h \times v}(4^{-j}\omega_1, 4^{-j}k\omega_1 + 2^{-j}\omega_2) \hat{f}(\omega_1, \omega_2)) & \kappa = x, |k| = 2^j \end{cases} \quad (6)$$

region boundaries. However, the approximation image $C_S^{0,0}$ represents a coarse representation of the original image f and may have inherited some of its properties such as the mean intensity or some coarse texture information. So in this paper, the fusion criterion of average and selection is to be used as following

$$C^{0,0}(m, n) = \frac{C_A^{0,0}(m, n) + C_B^{0,0}(m, n)}{2} \quad (7)$$

$$C^{j,k}(m, n) = \begin{cases} C_A^{j,k}(m, n) & |C_A^{j,k}(m, n)| > |C_B^{j,k}(m, n)| \\ C_B^{j,k}(m, n) & otherwise \end{cases} \quad (8)$$

IV. SIMULATION AND RESULTS ANALYSIS

For demonstrating the effectiveness and stability of the proposed method, different fusion methods based on different MSDs were compared with the proposed method. The source images consisted of infrared and visible images, as shown in figures 2(a) and (b). The results are shown in figures 2(c)-(g), and the objective assessment data is listed in table 1. The fused image was subjectivity assessed by visual observation and three criterions were used for objective assessments including the EN[6], SSIM[7] and $Q^{AB/F}$ [8] criterions.



(a) Infrared image

(b) Visible image

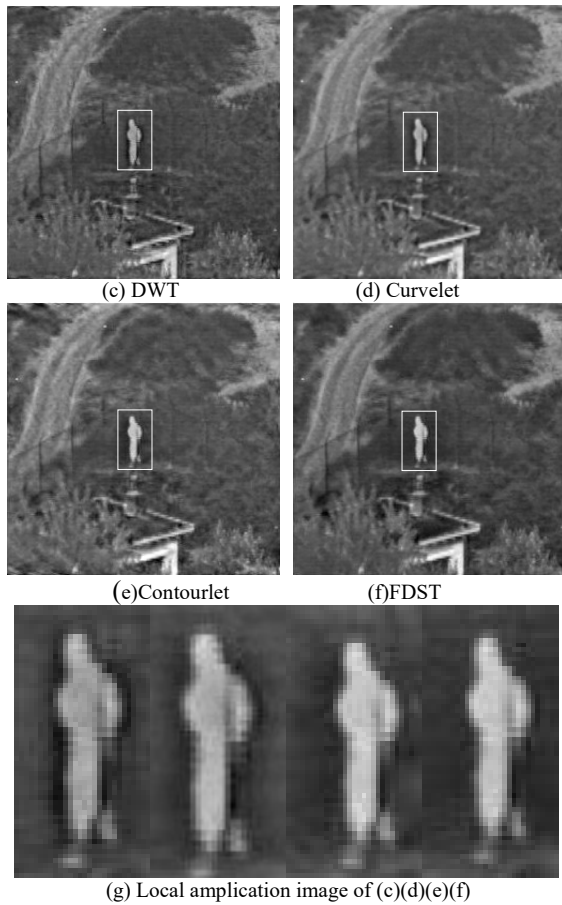


Figure2 Fusion results based on different MSD methods

TABLE I.

FUSION RESULTS COMPARISON BASED ON DIFFERENT MSD METHODS

MSD method	Infrared and visible images		
	EN	MI	$Q^{AB/F}$
DWT	6.4734	1.4625	0.3996
Curvelet	6.6021	1.5315	0.4493
Contourlet	6.6915	1.5201	0.4212
FDST	6.9288	1.6526	0.4980

As can be seen in figure 2 and table1, the results obtained by the proposed method were optimal in visual observation and objective evaluation data, which indicates that the proposed method is outstanding for multi-modality image fusion.

V. CONCLUSION

Aimed at the defects of existing multi-scale image fusion methods, FDST was introduced to the field of image fusion. FDST with the flexible multi-resolution and directional expansion can better represent the edges and texture structures of images. Experimental results demonstrated that the proposed method was successful in infrared and visible images image fusion.

ACKNOWLEDGMENT

This work was supported in part by a grant from Jilin province science and technology development plan item(No.20130101179JC)

REFERENCES

- [1] Yang B, Jing Z L and Zhao H T, "Review of pixel-Level Image Fusion," *Journal of Shanghai Jiao tong University (Science)*, Vol.15,No.1,pp. 6-12, 2010.
- [2] Tang Y Q, Zhang X X and Li X E, et al, "Image Processing Method of Dynamic Range With Wavelet Transform Based on Human Visual Gray Recognition Characteristics," *Chinese Journal of Liquid Crystals and Displays*, Vol.27,No.3,pp. 385-390, 2012.
- [3] Candès, E. J. and Donoho, D. L., "New tight frames of curvelets and optimal representations of objects with piecewise C^2 singularities," *Comm. on Pure and Appl. Math*,Vol.57, No.2, pp. 219-266,2004.
- [4] Do, M. N. and Vetterli, M., "The contourlet transform: an efficient directional multiresolution image representation," *IEEE Trans. Image Proc.*,Vol.14,No.12,pp. 2091-2106, 2005.
- [5] S.Häuser and G.Steidl,"Convex Multiclass Segmentation with Shearlet Regularization,"*International Journal of Computer Mathematics*, Vol.90,No.1,p.62-81,2013.
- [6] Qu, G. H., Zhang, D.L. and Yan, P.F., "Information Measure for Performance of Image Fusion,"*Electronic Letters*, Vol.38,No.7,pp.313-315, 2002.
- [7] Wang, Z., Bovik, A. C.and Sheik, H. R., et al., "Image Quality Assessment: From error visibility to structural similarity,"*IEEE Transactions on Image Processing*, Vol.13,No.4,pp. 600-612, 2004.
- [8] Xydeas, C. S. and Petrovi, V., "Objective Image Fusion Performance Measure. Electronics Letters," Vol.36,No.4, pp.308-309, 2000.

Emotional Communication of Web Color Design

Qi Yue¹, Sun Zan²

1. MA, College of Literature, Changchun University of Science and Technology, China

2. MA, JI LIN VIXO PICTURES Co., LTD, China

Abstract—Color , the first visual language, plays the role of influencing people's psychology and stimulating their emotions. The color of the web interface is one of the key factor to establish the image of the website, so color collocation is directly related to the success or failure of the web design. Therefore, how to better express the emotional connotations with web colors is what a designer must consider.

Index Terms—Web, color, emotion

I. COLOR AND EMOTION OF WEB PAGES

Color is real in the objective world and the emotional transmission is the ultimate goal of color design art. The color itself is non-emotional. The emotion here refers to one's visual perception arousing from the influence of color. If a color affects one's vision and hearing, it can have certain emotional effect, such as joy, excitement, sadness, anger or resentment, etc. Thus the colors adopted in the web design may also stimulate the users' association, inducing their various emotions and changing their psychology. In turn, the impression and evaluation on the interface and its colors are formed. That process is a process conveying emotional information.

II. EMOTIONAL ATTRIBUTES OF WEB COLORS

The colors play a role in one's vision and psychology. Different colors give surfers different psychological emotions and narrating different aspects of emotions. Experienced designers often arouse people's psychological association by using colors, so as to achieve the purpose of design. The colors used in websites are generally divided into the following types:

Red, an exciting color, can make people have such feelings as impulse, anger, enthusiasm and vitality. As for the probability of using colors in web pages, with demand of the themes of the web pages, few websites use the pure red as their main color. Red is mostly used as auxiliary color, exerting the eye-catching effect.

Green, between cold and warm, arouses the senses of harmony, quietness, health or safety. It is also one of the most widely-used colors in web pages. Green , closely related to human beings. is always the natural color of prosperity, representing life and hope. It is full of youthful vitality. It is often used in the websites related to nature and health as well as public relations sites or educational sites of some companies.

Yellow is characterized by joy, hope, wisdom and light. It's the brightest color. Light yellow, representing brightness, happiness, hope and development, is more suitable for women and cosmetics websites. The mid-

yellow makes people feel noble, brilliant, attentive and expanding and the dark yellow makes them feel noble gentle, introverted and calm.

Blue gives us a strong sense of security, and can mean peace , elegance, cleanness and reliability . Blue can constitute a harmonious contrast properly collocated with red, yellow and other colors. As the most typical representative cold color, blue is the most usual color used in the web design and loved by many people.

The color is just like music. If applied properly, it may further go into one's emotional consciousness, enabling him or her have artistic and emotional experience. In the web interface design, if you are good at capturing the rhythm of music, it can have unexpected visual and emotional effects.

III. CAPTURING EMOTIONAL FACTORS IN WEB DESIGN

"Color is the most expressive art language." In web design, if you are good at capturing the emotions of colors, it can often have special visual effects and emotional reaction. Designers in the web design should be good at capturing the emotional factors in colors .Particularly, attention should be paid to the following aspects:

1. Understand the information and brands conveyed by the website. To know the purpose of a brand and make a reasonable choice can strengthen the color collocation of corporate information. Different websites have different styles and personalized theme colors. Each color will lead to different emotions due to subtle changes of saturation and transparency. For a web designer, it is very important to do an aimed use of colors. There should be a big difference in web colors for different contents, so we should use the color language to reflect the characteristics and personality of a website to fully convey the emotional connotation and embody the theme.

2. The user-oriented design concept is the core of the web interface design. Designers should focus on the users' emotional reaction rather than pure color design in web color design, to make clear the theme and service objects of the website and choose different colors and tones based on the design purposes and the users' emotional reaction. Its purpose is to create a relaxed, pleasant environment for use. Designers must be clear that cultural differences may lead to unexpected responses to colors. Meanwhile, even in the same cultural background, different genders, ages and education backgrounds may affect one's interpretation of color.

3. A color application plan should be made before the production of web pages , and it should focus on the following three aspects. Firstly, the web color is a means

of emotional transmission. Only by using the colors, can the designers effectively convey their emotions accurately to the users. With the theme-oriented color language, we can more effective communication with browsers. Secondly, the web color is an element for personality creative. Personalized color design is also an important part in achieving the personalized web design. Thirdly, the web color is an important factor in creating emotions. If designers want to design a material with rich emotions, color is an essential element.

4. In the web design process, the influences of the contents ,color, form and other elements of the website on the users should be taken into consideration. As for content, we should consider the targeted users , whether to focus on profession or popularity. As for the colors, the colors should be lively or solemn, simple or gorgeous .The form should be simple or complex, traditional or innovative. These factors will affect the users' emotional impact.

At present, with the rapid development of network technology, color , the most powerful element in the web design to give users the visual impact, can fully reflect the personality and theme of the website. Different colors will arouse people different emotions. In the web design, only to emphasize the application of color elements can

we make our design more attractive.And the personality and aesthetic awareness about the web design can be vividly demonstrated.

REFERENCES

- [1] Paul M, Leicester (written) .Huo Wenli(Edited). Visual Communication----Information loaded by Images [M]. Beijing: Publishing House of Beijing Broadcast Institute, 2003.
- [2] Li Xing. Experience for the Color Design and Use in the Website Style Design[J]. China IT Visual Forum.
- [3] Li Xiangyu. Analysis on the Color Collocation in Web Design. Journal of Changsha District Vocational Technical College, 2004.
- [4] Wang Shusheng. Color & Web Design [M]. Beijing: Science and Technology Press, 2004.
- [5] Wu Chong, Wang Hui. Web Design Exploration [M]. Beijing: Electronic Industry Press, 2006.
- [6] Li Liwei. Study on Web Color Design. Journal of Light Industry College in Zhengzhou University (SOCIAL SCIENCE EDITION), 2007.

Multisource Images Fusion Algorithm Based on Nonsubsampled Shearlet Transform

Guang-qiu CHEN, Jie Lin, Guang-wen Liu (Corresponding author)

School of Electronic and Information Engineering, Changchun University of Science and Technology, Changchun 130022, China

Abstract—For enhancing fusion accuracy of multisource images, an adaptive image fusion algorithm based on nonsubsampled shearlet transform (NSST) is proposed. First, source images are decomposed to multi-scale and multi-direction subbands by NSST. Secondly, the fused low-frequency subband and high-frequency directional subband coefficients can be obtained by the fusion criterion based on window energy match measure and region consistency selection respectively. Finally, fused subbands are reconstructed to an image by nonsubsampled shearlet inverse transform. The experimental results indicate that the proposed method performs better in subjective and objective assessments than a few typical fusion techniques in the existing literatures and can obtain better fusion performance.

Index-terms — image fusion, nonsubsampled shearlet transform, invariant translation, objective assessments

I. INTRODUCTION

Over the years, the image fusion technologies based on multi-scale decomposition (MSD) have attracted wide attention of relevant domestic and foreign scholars, who have achieved many outstanding research results^[1]. In recent years, the fusion technologies based on MSD, such as DWT^[2], Curvelet^[3], Contourlet^[4] for combining multisource images have become a hot research in fusion field. G. Easley *et al*^[5] proposed a novel image representation method — nonsubsampled shearlet transform (NSST), which not only has the advantages of Curvelet and Contourlet, but also holds shift-invariant. Therefore, in this paper, NSST is used as image MSD tool.

Traditional fusion criterion adopted in many literatures, the weight is 0.5 to average low-frequency subband coefficients and “coefficients absolute value selection max” is used to select high-frequency directional subband coefficients, can result in a problem that the fused images are sometimes unstable and contrast is low. So, in this paper, the fusion criterion based on window energy match measure and region consistency selection is proposed.

II. NONSUBSAMPLED SHEARLET TRANSFORM

In dimension $n = 2$, the shearlet system with discrete parameters is defined as follows:

$$S_{AB}(\phi) = \left\{ \begin{array}{l} \phi_{j,l,k} = |\det A|^{j/2} \phi(B^l A^j x - k), \\ (j,l) \in Z, k \in Z^2 \end{array} \right\} \quad (1)$$

where $\phi \in L^2(R^2)$, A, B is 2×2 invertible matrix and $|\det B| = 1$, j is scale parameter, l is direction parameter, k represents spatial position. If $j \geq 0$, $-2^j \leq l \leq 2^j - 1$, $k \in Z^2$, $d = 0, 1$, the Fourier

transform of the shearlet in the compact form can be expressed as

$$\hat{\phi}_{j,l,k}^{(d)} = 2^{3j/2} V(2^{-2j} \xi) W_{j,l}^{(d)}(\xi) \exp(-2\pi i \xi A_d^{-j} B_d^{-l} k) \quad (2)$$

Where $V(2^{-2j} \xi)$ is scaling function, $W_{j,l}^{(d)}$ is window function localized on a pair of trapezoids, A_d is the anisotropic dilation matrix, B_d is shear matrix.

The shearlet transform of $f \in L^2(R^2)$ can be computed by

$$\langle f, \phi_{j,l,k}^{(d)} \rangle = \quad (3)$$

$$2^{3j/2} \int_{R^2} \hat{f}(\xi) \overline{V(2^{-2j} \xi) W_{j,l}^{(d)}(\xi) \exp(2\pi i A_d^{-j} B_d^{-l} k)} d\xi$$

As can be seen from the above Equation(3), the shearlet transform of $f \in L^2(R^2)$ is mainly composed of two parts: one is multi-scale decomposition and the other is directional localization.

MSD: two-channel nonsubsampled filter banks (NSFB) are applied to an image for nonsubsampled pyramid (NSP), so the multi-scale property of the shearlet is obtained.

Directional localization: directional localization is implemented by small sized shear filter. Given an image is decomposed to low-pass subband f^{j+1} and band-pass subband g^{j+1} by NSP, where j denotes the number of scales, $j = 1, 2, \dots, M$. The process of the directional localization is followed:

Meyer wavelet function is exploited to produce Meyer window function $g(\theta)$.

In pseudo-polar grid, $g(\theta)$ is re-sampled to produce shear filter window W .

W is mapped into the Cartesian coordinate system from pseudo-polar grid and new shear filter W_{new} is obtained.

The discrete Fourier of band-pass subband is computed to obtain matrix Fg^{j+1} .

W_{new} is operated with Fg^{j+1} to obtain directional subbands.

Inverse Fourier transform is conducted on each directional subband to obtain coefficient $c^{j+1,l}$.

In reference [5], above elaborated shearlet is called nonsubsampled shearlet transform (NSST). In NSST, for removing downsampled operation, shift-invariant property is obtained. In the directional localization process, small sized shear filter can avoid blocking artifacts conducted by big sized filter and reduce the Gibbs-type ringing phenomenon [6]. An image decomposed by NSST with J scales can

produce $\sum_{j=1}^J 2^j$ band-pass subbands and one low-pass subband, where l_j denotes the number of levels at the j th scale.

III. FUSION CRITERION

Source images A and B are decomposed to a low-frequency subband and some high-frequency directional subbands by NSST respectively, denoted by $\{IL_A, IH_A^{l,k}\}$ and $\{IL_B, IH_B^{l,k}\}$, where IL_x represents low-frequency subband (approximate image), $IH_x^{l,k}$ represents k th high-frequency directional subband (detail image) at the l th scale, $x = A$ or B , the fused subbands are denoted by $\{IL, IH^{l,k}\}$. Low-frequency subband is a coarse representation of the original image and inherits some properties such as the mean intensity and some coarse texture information, high-frequency subband represents detail information such as ‘edge’ and ‘contour’ in an image. Because of their different physical meaning, the approximate and detail images should be treated by the fusion criterion in a different fashion.

(1) Low-frequency subband fusion criterion

The low-frequency subband integrates the major energy, which reflects the approximation and average of original image. The design purpose for low-frequency subband fusion criterion is to transfer the local brightness and contrast to the fusion results according to the local features of the source images, but the definition and contrast of the image is reflected by the whole pixels in the window. The importance of the information carried by the coefficients at the different spatial location in the window is different, it is generally considered that the more important the carried information is, the closer the coefficient is from the center location. So the correlation among the neighborhood coefficients should be considered and different weight should impose to different coefficient.

Taking the above idea, fusion criterion of weight average or selection is designed according to window energy match measure. The specific steps are as follows:

Step1: Computing local window weight energy sum

In low-frequency subband coefficients, a local window with (i, j) as center location is selected to compute weight energy sum by the following equation

$$E_x(i, j) = \sum_{(m,n) \in w} \delta(m, n) IL_x^2(m, n) \quad (4)$$

Where $E_x(i, j)$ represents neighborhood energy sum at the location (i, j) , $x = A, B$, $IL_x(m, n)$ is coefficient value at location (m, n) , $i - k \leq m \leq i + k$, $j - k \leq n \leq j + k$, $w = 2 * k + 1$, $k = 1, 2, \dots$, $\delta(m, n)$ is coefficient weight. We assume the distance from location (m, n) to (i, j) follows Gaussian distribution, which is greater from the (i, j) closer, $\delta(m, n)$ can be obtained by the following equation:

$$\delta(m, n) = 0.5e^{-\frac{d(m,n)^2}{2\sigma^2}} + 0.5e^{-\frac{l(m,n)^2}{2\sigma^2}} \quad (5)$$

Where $\sigma = 1$, $d(m, n) = m - i$, $l(m, n) = n - j$.

Step2: Computing neighborhood energy match measure

$$M_{AB}(i, j) = \frac{2}{E_A(i, j) + E_B(i, j)} \sum_{(m,n) \in w} \delta(m, n) IL_A(m, n) IL_B(m, n) \quad (6)$$

Step3: Computing fused coefficient according to $M_{AB}(i, j)$ and $E_x(i, j)$

Matching threshold is set T , if $M \leq T$, which indicates that the spatial distribution characteristic at this location is different, the center coefficient of the window whose energy value is larger is selected as the fused coefficient, otherwise the coefficient is weighted average, the weight is computed as the following equation:

$$\alpha = \frac{1}{2} - \frac{1}{2} \left[\frac{1 - M_{AB}}{1 - T} \right], \quad \beta = 1 - \alpha \quad (7)$$

the range of the threshold T is $0.5 \sim 1.0$, in this paper, $T = 0.75$, so the low-frequency subband fusion criterion is following:

$$IL(i, j) = \begin{cases} IL_A(i, j) & M_{AB}(i, j) < T \ \& \ E_A(i, j) \geq E_B(i, j) \\ IL_B(i, j) & M_{AB}(i, j) < T \ \& \ E_A(i, j) < E_B(i, j) \\ \alpha \cdot IL_A(i, j) + \beta \cdot IL_B(i, j) & M_{AB}(i, j) > T \ \& \ E_A(i, j) \geq E_B(i, j) \\ \beta \cdot IL_A(i, j) + \alpha \cdot IL_B(i, j) & M_{AB}(i, j) > T \ \& \ E_A(i, j) < E_B(i, j) \end{cases} \quad (8)$$

The above process iterates through the low-frequency subband and fused low-frequency subband coefficients are obtained.

(2) High-frequency subband fusion criterion

The design purpose for high-frequency subband fusion criterion is to extract the edge structure from the source image. In this paper, a region consistency selection fusion criterion according to coefficient absolute value and regional variance is designed, which can reduce noise sensitivity and maximum extract edge detail information to improve definition of the fusion image. The specific steps are as follows:

Step1: Computing regional variance sum

$$VAR_x(i, j) = \sum_{(m,n) \in w} \left(|IH_x^{l,k}(m, n)| - \mu \right)^2 \quad (9)$$

Where $VAR_x(i, j)$ is neighborhood variance sum of the window at the central location (i, j) , $x = A, B$, μ is mean, $IH_x^{l,k}(m, n)$ is coefficient value at the location (m, n) , $i - k \leq m \leq i + k$, $j - k \leq n \leq j + k$, $w = 2 * k + 1$, $k = 1, 2, \dots$.

Step2: Computing consistency selection operator

$$O_x^{l,k}(i, j) = |IH_x^{l,k}(i, j)| \left(1 + VAR_x^{l,k}(i, j) \right) \quad (10)$$

Where $IH_x^{l,k}(i, j)$ is coefficient value at the location (i, j) , when $VAR_x^{l,k}(i, j) = 0$, the consistency selection operator will be coefficient absolute value.

Step2 : Computing fused coefficient according to regional consistency selection operator

$$IH^{l,k}(i, j) = \begin{cases} IH_1^{l,k}(i, j), & O_A^{l,k}(i, j) \geq O_B^{l,k}(i, j) \\ IH_2^{l,k}(i, j), & O_A^{l,k}(i, j) < O_B^{l,k}(i, j) \end{cases} \quad (11)$$

The above process iterates through all the directional subbands and fused directional subbands are obtained.

IV. SIMULATION AND RESULTS ANALYSIS

For demonstrating the effectiveness and stability of the proposed method, different fusion methods based on MSDs, including LP+PCAABS[7], NSCT+EMSTD[8], DWT+SFMAABS[9], Curvlet+ AVPCNN[10], ST+

RSEM[11], are compared with the proposed method. The source images is consisted of remote sensing images, as shown in figure2(a) and (b). The fused image was subjectivity assessed by visual observation and three criterions are used as objective assessments including the MI[12], SSIM[13]and $Q^{AB/F}$ [14].The results are shown in figure2(c)-(h), and the objective assessment data is listed in table I.

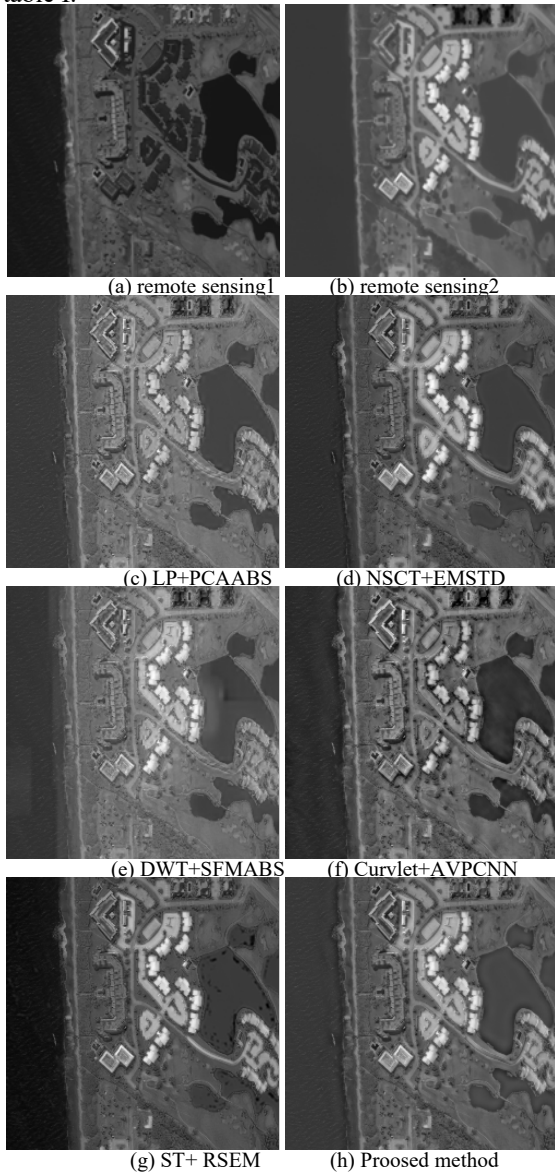


Figure2 Fusion results using different fusion methods based on MSDs

TABLE I.FUSION RESULTS COMPARISON BASED ON DIFFERENT MSD METHODS

Fusion methods	Remote sensing images		
	MI	SSIM	QAB/F
LP+PCAABS	1.2274	0.6230	0.3946
NSCT+EMSTD	2.2366	0.7167	0.4232
DWT+SFMABS	1.6638	0.7113	0.4283
Curvlet+AVPCNN	1.5236	0.7359	0.4377
ST+ RSEM	2.0472	0.7372	0.4251
Proposed method	2.5232	0.7755	0.4718

As can be seen in figure 2 and table I, the result obtained by the proposed method is optimal in visual observation and objective assessment data, which indicates that the proposed method is outstanding for multisource images fusion.

V.CONCLUSION

Aimed at the defects of the existing multi-scale image fusion methods, NSST was introduced to the image fusion field, multisource images fusion algorithm based on the regional characteristic in NSST domain is proposed. NSST with the flexible multi-resolution and directional expansion can better represent the edges and texture structures of the images. In the fusion process, the local correlation and the regional characteristic of the image are considered, the low frequency and high frequency directional subbands are combined based on different fusion criterion. Experimental results demonstrated that the better fusion performance can be obtained and the proposed method was successful in multisource images fusion.

REFERENCES

- [1] Yang B, Jing Z L, Zhao H T, “Review of pixel-Level Image Fusion,” Journal of Shanghai Jiao tong University (Science), Vol.15,No.1, pp. 6-12, 2010.
- [2] Tang Y Q, Zhang X X, Li X E, et al, “Image Processing Method of Dynamic Range With Wavelet Transform Based on Human Visual Gray Recognition Characteristics,” Chinese Journal of Liquid Crystals and Displays, Vol. 27, No.3, pp. 385-390, 2012.
- [3] E. J. Candès, D. L. Donoho, “New tight frames of curvelets and optimal representations of objects with piecewise C2 singularities,” Comm on Pure and Appl. Math., Vol.57, No.2, pp. 219–266, 2004.
- [4] M. N. Do, M. Vetterli, “The contourlet transform: an efficient directional multiresolution image representation,” IEEE Trans. Image Proc., Vol.14, No.12, pp. 2091–2106, 2005.
- [5] Easley G, Labate D, Lim W-Q, “Sparse directional image representations using the discrete shearlet transform,” Applied and Computational Harmonic Analysis, Vol.25, No.1, pp. 25-46,2008.
- [6] Guang-qi Chen, Jin Duan, Hua Cai, et al, Image fusion algorithm based on NSST and PCNN, The 4th International Conference on Electronics, Communications and Networks, pp.713-717, 2014:
- [7] Y.Z. Zheng, X.D. Hou, T.T. Bian, et al, “ Effective Image Fusion Rules Of Multi-scale Image Decomposition,” Proceedings of the 5th International Symposium on image and Signal Processing and Analysis, pp.362-366, 2007
- [8] YE Chuan-qi, WANG Bao-shu, MIAO Qi-guang, “Fusion algorithm of infrared and visible light images based on NSCT transform,” Systems Engineering and Electronics, Vol.30, No.4, pp.593-596,2008
- [9] WANG Hongmei, CHEN Lihua, LI Yanjun, et al. “A New and More Effective Image Fusion Algorithm Based on Salient Feature,” Journal of Northwestern Polytechnical University, Vol.28, No.4, pp.486-490,2010.
- [10] ZHAO Jingchao, QU Shiru, “A Better Algorithm for Fusion of Infrared and Visible Image Based on Curvelet Transform and Adaptive Pulse Coupled Neural Networks(PCNN),” Journal of Northwestern Polytechnical University, Vol.29, No.6, pp.849-853,2011.
- [11] ZHENG Hong, ZHENG Chen, YAN Xiu-sheng, et al, “Visible and infrared image fusion algorithm based on shearlet transform,” Chinese Journal of Scientific Instrument, Vol.33, No.7, pp.1613-1619, 2012.
- [12] G. H. Qu, D.L. Zhang, P.F. Yan, “ Information Measure for Performance of Image Fusion,” Electronic Letters, Vol.38, No.7, pp. 313-315, 2002.
- [13] Z. Wang, A.C. Bovik, H.R. Sheik, E.P. Simoncelli, “Image Quality Assessment: From error visibility to structural similarity,” IEEE Transactions on Image Processing, Vol.13, No.4, pp. 600-612, 2004.
- [14] C. S. Xydeas, V. Petrovi “Objective Image Fusion Performance Measure,” Electronics Letters, Vol.36, No.4, pp.308-309, 2000

The Construction And Empirical Analysis Of The Financial Risk Early Warning Model Of The Listing Corporation In China

Minzhou Li^{1,2}, Xiaomin Gu¹

1. Glorious Sun School of Business and Management, Donghua University, Shanghai, 200051, China;
2. Songjiang Campus Shanghai Open University, Shanghai, 201600, China;

Abstract—In recent years, listed company's operating condition gradually deteriorated and objective assessment of their financial situation has become a major issue. In this paper, we employ the linear probability model and logistic model, build Chinese listed companies' financial early - warning evaluation index system and mathematical model corresponding financial warning. The empirical results show that financial data of listed companies is effective and has strong predictive ability and the model used for the listed company's financial failure has good predictive power directly used as an effective tool for commercial banks and other financial institutions, investors, fund managers financial crisis and credit risk quantitative analysis .

Index Term—linear probability model, logistic model, predictive ability.

In recent years, the scale of China's securities market continues to expand, however Losses of listed companies increased year by year. Obviously, it is very important to objectively evaluate the financial condition of listed companies for the investor timely adjusting investment decisions and regulator accurately identifying the company status and potential customers. Thought foreign research started on prediction models of corporate financial failure earlier, and has been widely used in banking, corporate, investment institutions, our research of this field is just beginning. So this article hopes to make a little contribution to the field. Firstly, we analyze the various existing integrated financial risk analysis theory; secondly, based on domestic and international research, we applied linear probability model and logistic model to build Chinese listed companies' financial early-warning evaluation index system and the corresponding mathematical model of financial early warning; finally, we draw the appropriate conclusions and make relevant policy recommendations.

I. Financial Risk Analysis Review

Current methods of financial risk analysis applied internationally include the following categories:

Comprehensive analysis of the financial ratios will regard various financial indicators as a whole and systematically analyze, interpret and evaluate financial position and operating conditions. The representative of such methods is the DuPont Financial Analysis System.

Multi variable financial risk model regards financial ratios as explanatory variables and use statistical methods to establish standard model, including the linear

probability model, the Logistic model, the Probit model and the discriminant analysis model.

With the rapid development of capital markets, financial innovations emerge, the financial risks are staggered packing. Due to the statistical analysis based on financial ratios method not reflecting the dynamic value of the borrower and the issuer's assets in the capital markets, a series of new method to measure financial risks have been proposed, including the credit risk option pricing model, the default rate model and the neural network analysis system.

For now, in the international arena, multivariate financial risk model is the most effective, and the mainstream method of International financial industry and academia, because the method used in the long process has been improved gradually, penetrate into the types of companies and industries, form relatively standard way and plays a role in the practical application backbone. However, the new approach based of capital market theory and information science is in the development period has some problems to solve. Meantime, our financial risk analysis methods in the field of research started late. In domestic research on financial risk analysis method, Wu Shinong and Huang Shizhong(1986) introduced the indicators of the enterprises bankruptcy and the prediction model; Wang Chunfeng and Wan Haifui, employing the neural network method of analyzing commercial banks financial risk, found that neural network has a strong nonlinear mapping ability.

II. Analysis and Selection of Statistical Methods

Multivariate financial risk model is the most effective. Therefore, this paper will analyze the several models in this model.

Linear probability model uses financial ratios as input data to illustrate the financial risk and predicts probability of bankruptcy or default. We divide the financial situation of the company into two categories, namely default class ($Y_i = 1$) and non-default class ($Y_i = 0$), then describe this approach through a series of variable (X_{ij}) linear regression.

$$Y_i = \alpha + \sum_{j=1}^n \beta_{ij} X_{ij} + \epsilon_i \quad (1)$$

$$E(Y_i | X_{i1}, X_{i2}, \dots, X_{in}) = \alpha + \sum_{j=1}^n \beta_{ij} X_{ij} = \hat{Y}_i \quad (2)$$

Suppose $P_i = (Y_i = 1)$, $1 - P_i = (Y_i = 0)$ and $E(e_i) = 0$

$$0 \leq E(Y_i | X_{i1}, X_{i2}, \dots, X_{in}) \leq 1 \quad (3)$$

Logistic model is suitable for the fact the dependent variable is not continuous and is a dichotomous choice. The probability function of Logistic is represented as follows:

$$P_i = 1 / (1 + e^{-(\alpha + \sum_{j=1}^n \beta_j X_{ij} + e_i)}) \quad (4)$$

P_i is the probability of occurrence of an event under the conditions ($X_{i1} = (X_{i1}, X_{i2}, \dots, X_{in})$), the probability of $1 - P_i$ on behalf of the event does not occur, α is the intercept and β_j is the parameter to be estimated. So the general form of the Logistic regression model is as follows:

$$L_i = \ln(P_i / (1 - P_i)) = Z_i = \alpha + \sum_{j=1}^n \beta_j X_{ij} + e_i \quad (5)$$

Probabilistic model is based on the cumulative standard normal distribution variable conversion, but Logistic model is based on Logistic distribution conversion. Because the cumulative standard normal distribution calculation procedures are complicated and Logistic model is more straightforward and quick, so Logistic model is often used on the empirical model.

III. MULTIPLE DISCRIMINATE ANALYSIS

Multivariate discriminate analysis is a statistical analysis method for the classification of the research object. Professor Edward Altman was the first scholar to use this method which was applied to analyze the financial crisis, the company's bankrupt and default risk.

More applications of financial risk analysis abroad is linear probability model and multivariate discriminant analysis, however, in China, the analysis is focused on the multiple discriminant analysis, thus we will use the linear probability model and Logistic model as the model analysis.

IV. MODEL BUILDING

a) Selection of the sample

This article regards ST, PT shares as the financial risk of default group. We select 53 companies of 2000 Annual Report as a set of sample analysis, and also select 59 blue-chip stocks from listed companies in Shenzhen and Shanghai as a financial risk non-defaulting group.

b) Financial Early Warning Indicator

This paper selects the indicators as follows:

- (a) Solvency class index contain liquidity ratio (X_1), assets-liabilities ratio (X_2), equity ratio (X_3), ratio of market capitalization to total equity and liabilities (X_4) and ratio of working capital to total assets (X_5).
- (b) Company's operating results indicators contain

ROA (X_6), Roe (X_7), ratio of retained earnings to total assets (X_8) and ratio of EBIT to total assets (X_9).

- (c) Asset Management efficiency indicator contains the total asset turnover ratio (X_{10}).

c) Linear probability model regression results (Table 1) LINEAR PROBABILITY MODEL REGRESSION RESULTS

Model	Unstandardized Coefficients		Standardize d Coefficients	t	Sig
	B	Std. Error	Beta		
1	Constant	1.738E-02	0.061	0.287	0.775
	X_1	0.323	0.031	0.759	0.003
2	Constant	0.165	0.063	2.637	0.010
	X_1	0.245	0.033	0.574	0.000
	X_5	0.871	0.187	0.357	0.000
3	Constant	8.565E-02	0.061	1.412	0.162
	X_1	0.186	0.033	0.436	0.000
	X_5	0.769	0.173	0.315	0.000
	X_{10}	0.379	0.095	0.290	0.000
4	Constant	0.278	0.100	2.775	0.007
	X_1	0.152	0.035	0.356	0.000
	X_5	0.636	0.177	0.260	0.001
	X_{10}	0.329	0.095	0.252	0.001
	X_2	-0.163	0.069	-0.199	0.020

According to Table 1, we obtain the following regression equations:

$$Y = 0.278 + 0.152X_1 - 0.163X_2 + 0.636X_5 + 0.329X_{10} \quad (6)$$

$$Y = 0.956X_1 - 0.199X_2 + 0.260X_5 + 0.252X_{10} \quad (7)$$

According to the formula (6) and (7), we found that the increase of liquidity ratio, ROA and the total asset turnover ratio are conducive to the occurrence of non-defaulting events, however, assets-liabilities ratio is the opposite.

d) Logistic model regression results (Table 2)

TABLE I. : LOGISTIC MODEL REGRESSION RESULTS

		B	S.E.	Wald	df	Sig.	Exp(B)
1	X_1	4.803	1.108	18.798	1	0.000	121.884
	Constant	-6.023	1.379	19.069	1	0.000	0.002
2	X_1	4.639	1.358	11.671	1	0.001	103.408
	X_{10}	5.546	2.658	4.353	1	0.037	256.192
	Constant	-7.611	2.063	13.612	1	0.000	0.000

According to Table 2, we obtain the following regression equation:

$$Z = -7.611 + 4.639X_1 + 5.546X_{10} \quad (8)$$

According to the formula (8), we found that the increase of liquidity ratio and the total asset turnover ratio are conducive to the occurrence of non-defaulting events.

e) The forecast accuracy of the model

Any companies have a gradual deterioration process of with the financial crisis or bankruptcy.

There is no doubt that timely predicting the financial crisis may give the parties time to take measures to avoid risks. In this paper, we forecast the new 46 ST companies in 2002, the result is as follows (Table 3):THE FORECAST ACCURACY OF THE MODEL

Processing time of ST	Previous year	Two years ago	The previous three years	The first four years
The correct number of linear prediction	45	46	31	24
The wrong number of linear prediction	1	6	15	22
The accuracy of linear prediction (%)	97	87	67	53
The correct number of Logistic	43	38	34	20
The wrong number of Logistic	3	8	12	26
The accuracy of Logistic (%)	93	83	73	43

The results showed that our financial data of listed companies is effective and has strong predictive ability. Meantime, we found that both methods have a strong predictive ability for the previous three years ST stock and the linear probability model to predict the results of the first four years which is better than the logistic model.

IV. CONCLUSION

Our financial data of listed companies is effective and has strong predictive ability. Generally speaking, the financial data of listed companies can predict the probability of future financial failures; secondly, the forecast accuracy of linear probability model and Logistic model are convincing, so these models can be directly used as an effective tool for commercial banks and other financial institutions, investors, fund managers financial crisis and credit risk quantitative analysis; finally, We should focus on these indicators, such as liquidity ratio, assets-liabilities ratio, ROA and the total asset turnover ratio, to improve the efficiency and relevance of the judgment.

REFERENCES

[1] Harrell, F. E. (2013).Regression modeling strategies: with applications to linear models, logistic regression, and survival analysis. Springer Science & Business Media..
 [2] Bates, D., Maechler, M., Bolker, B., & Walker, S. (2013). lme4: Linear mixed-effects models using Eigen and S4. R package version,1(4).
 [3] Fahrmeir, L., & Tutz, G. (2013). Multivariate statistical

modelling based on generalized linear models. Springer Science & Business Media.
 [4] Pradhan, B. (2013). A comparative study on the predictive ability of the decision tree, support vector machine and neuro-fuzzy models in landslide susceptibility mapping using GIS. Computers & Geosciences, 51, 350-365
 [5] Cohen, M. E., Ko, C. Y., Bilimoria, K. Y., Zhou, L., Huffman, K., Wang, X., ... & Chow, W. (2013). Optimizing ACS NSQIP modeling for evaluation of surgical quality and risk: patient risk adjustment, procedure mix adjustment, shrinkage adjustment, and surgical focus. Journal of the American College of Surgeons, 217(2), 336-346.
 [6] Gelman, A., Carlin, J. B., Stern, H. S., & Rubin, D. B. (2014). Bayesian data analysis (Vol. 2). London: Chapman & Hall/CRC.
 [7] Cohen, J., Cohen, P., West, S. G., & Aiken, L. S. (2013). Applied multiple regression/correlation analysis for the behavioral sciences. Routledge.
 [8] Harrell, F. (2015). Regression modeling strategies: with applications to linear models, logistic and ordinal regression, and survival analysis. Springer.
 [9] Steyerberg, E. W., Moons, K. G., van der Windt, D. A., Hayden, J. A., Perel, P., Schroter, S., ... & Altman, D. G. (2013). Prognosis Research Strategy (PROGRESS) 3: prognostic model research. PLoS Med, 10(2), e1001381
 [10] Davidson, M., Reichenberg, A., Rabinowitz, J., Weiser, M., Kaplan, Z., & Mark, M. (2014). Behavioral and intellectual markers for schizophrenia in apparently healthy male adolescents. American Journal of Psychiatry.
 [11] Brooks, C. (2014). Introductory econometrics for finance. Cambridge university press.
 [12] McWilliams, A., Tammemagi, M. C., Mayo, J. R., Roberts, H., Liu, G., Soghrati, K., ... & Atkar-Khattra, S. (2013). Probability of cancer in pulmonary nodules detected on first screening CT. New England Journal of Medicine, 369(10), 910-919.
 [13] Hosmer Jr, D. W., Lemeshow, S., & Sturdivant, R. X. (2013). Applied logistic regression (Vol. 398). John Wiley & Sons.
 [14] Althuwaynee, O. F., Pradhan, B., Park, H. J., & Lee, J. H. (2014). A novel ensemble decision tree-based Chi-squared Automatic Interaction Detection (CHAID) and multivariate logistic regression models in landslide susceptibility mapping. Landslides, 11(6), 1063-1078.
 [15] [Tammemägi, M. C., Katki, H. A., Hocking, W. G., Church, T. R., Caporaso, N., Kvale, P. A., ... & Berg, C. D. (2013). Selection criteria for lung-cancer screening. New England Journal of Medicine, 368(8), 728-736.
 [16] Satopää, V. A., Baron, J., Foster, D. P., Mellers, B. A., Tetlock, P. E., & Ungar, L. H. (2014). Combining multiple probability predictions using a simple logit model. International Journal of Forecasting, 30(2), 344-356.
 [17] Breen, R., Karlson, K. B., & Holm, A. (2013). Total, direct, and indirect effects in logit and probit models. Sociological Methods & Research, 0049124113494572.
 [18] Syfert, M. M., Smith, M. J., & Coomes, D. A. (2013). The effects of sampling bias and model complexity on the predictive performance of MaxEnt species distribution models. PloS one, 8(2), e55158.
 [19] Pourghasemi, H. R., Moradi, H. R., & Aghda, S. F. (2013). Landslide susceptibility mapping by binary logistic regression, analytical hierarchy process, and statistical index models and assessment of their performances. Natural hazards, 69(1), 749-779.
 [20] DeMaris, A., & Selman, S. H. (2013). Logistic regression. In Converting Data into Evidence (pp. 115-136). Springer New York.

Multisource Images Fusion Algorithm Based on Nonsampled Contourlet Transform

Guang-qiu CHEN, Zhen-ye GENG, Hua Cai (Corresponding author)

School of Electronic and Information Engineering, Changchun University of Science and Technology, Changchun 130022, China

Abstract—For enhancing fusion accuracy of multisource images, an adaptive image fusion algorithm based on nonsampled contourlet transform (NSCT) is proposed. First, source images are decomposed to multi-scale and multi-direction subbands by NSCT. Secondly, the fused low-frequency subband coefficients and high-frequency directional subband coefficients can be obtained by the fusion criterion based on the sum of weight salience variance as weight and coefficients absolute value selection max respectively. Finally, fused subbands are reconstructed to an image by nonsampled contourlet inverse transform (NSCIT). The experimental results indicate that the proposed method performs better in subjective and objective assessments than a few typical fusion techniques in the existing literatures and can obtain better fusion performance.

Index-terms — image fusion, nonsampled contourlet transform, invariant translation, objective assessment

I. INTRODUCTION

Over the years, the image fusion technology has attracted wide attention of relevant domestic and foreign scholars, who have made many outstanding research results [1-3]. In recent years, the fusion technology based on multi-scale decomposition (MSD), such as DWT[4], Curvelet[5], Contourlet[6] has become a hot research in fusion field. Cunha et al[7] proposed a new image representation method — nonsampled contourlet transform (NSCT), which inherits all the advantages of contourlet and holds invariant translation. Therefore, in this paper, NSCT is used as image MSD tool.

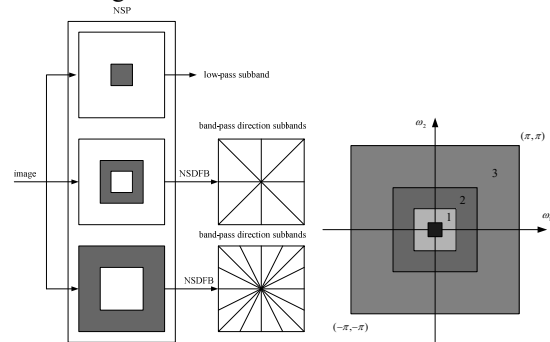
Traditional fusion criterion adopted in many literatures, the weight is 0.5 to average low-frequency subband coefficients and “coefficients absolute value selection max” is used to select high-frequency directional subband coefficients, can result in a problem that the fused images are sometimes unstable and contrast is low. So, in this paper, the fusion criterion based on the sum of weight salience variance as weight and coefficients absolute value selection max is proposed[8].

II. NONSAMPLED CONTOURLET TRANSFORM

MSD and direction analysis are separately operated to obtain NSCT: first, the image is decomposed by nonsampled pyramid (NSP) constructed by nonsampled filter banks (NSFB) to achieve a low-pass subband and some band-pass subbands, then nonsampled directional filter banks (NSDFB) are

exploited to direction analysis for band-pass subbands, so the direction subbands are obtained.

NSCT overcomes the defect of contourlet without invariant translation and inherits the advantages of contourlet with multi-resolution, time-frequency localization, prominent direction selectivity and anisotropy etc. So NSCT has more favorable representation of image edge and texture structure information. A schematic diagram of the NSCT structure is shown in Figure 1.



(a) NSFB structure (b) Idealized frequency partitioning

Figure 1 Nonsampled contourlet transform

An image decomposed by NSCT with J scales can produce $\sum_{j=1}^J 2^{l_j}$ band-pass subbands and one low-pass subband, where l_j denotes the number of levels in the NSDFB at the J th scale.

III. FUSION CRITERION

Source images are decomposed to a low-frequency subband and some high-frequency directional subbands by NSCT, denoted by $\{IL_1, IH_1^{l,k}\}$ and $\{IL_2, IH_2^{l,k}\}$ respectively, where IL_x represents low-frequency subband (approximate image), $IH_x^{l,k}$ represents k th high-frequency directional subband (detail images) at the l th scale, $x=1$ or 2 , fused subbands are denoted by $\{IL, IH^{l,k}\}$. IL_x represents a coarse representation of the original image and have inherited some of its properties such as the mean intensity and some coarse texture information, $IH_x^{l,k}$ represents detail information such as ‘edge’ and ‘contour’ in an image. Because of their different physical meaning, the approximate and detail

images should be treated by the fusion criterion in a different fashion[9]

(1) Low-frequency subband fusion criterion

The low-frequency subband integrates the major energy, which reflects the approximation and average of source image, So in this paper, the fusion criterion of weight average is used to combine low-frequency subband coefficients, the specific steps are as follows:

Step1: Computing the mean of region window

In coefficient matrices of low-frequency subband IL_x , a region window $N \times N$ called Θ with p point as the center is selected to calculate mean.

$$\mu(IL_x, p) = \frac{\sum_{q \in \Theta} |IL_x(q)|}{N \times N} \quad (1)$$

Where $|IL_x(q)|$ represents coefficients absolute value in Θ , q is spatial coordinate.

Step2: Computing the sum of weight salience variance in Θ with p point as the center.

$$M(IL_x, p) = \sum_{q \in \Theta} \lambda(q) \| |IL_x(q)| - \mu(IL_x, p) \|^2 \quad (2)$$

Where, $\lambda(q)$ represents coefficients weights, which is greater from the p point closer, we assume the distance from q to p follows Gaussian distribution, which can be obtained by the following equation:

$$\lambda(q) = 0.5e^{-\frac{(q(1)-p(1))^2}{2\sigma^2}} + 0.5e^{-\frac{(q(2)-p(2))^2}{2\sigma^2}} \quad (3)$$

Where $\sigma = 1$, $(q(1), q(2))$, $(p(1), p(2))$ is coordinate of point q , p respectively. M represents contrast of local region window.

Step3: Computing fusion coefficient of point p

$$IL(p) = \omega(IL_1, p) \cdot IL_1(p) + \omega(IL_2, p) \cdot IL_2(p)$$

$$\text{Where } \omega(IL_1, p) = \frac{M(IL_1, p)}{M(IL_1, p) + M(IL_2, p)},$$

$$\omega(IL_2, p) = 1 - \omega(IL_1, p) \quad (4)$$

The above process iterates through the low-frequency subband and fused low-frequency subband coefficients are obtained. This criterion can allocate the right weight for each pixel automatically and prominent target combination information according to the characteristics of the image.

(2) High-frequency subbands fusion criterion

From the imaging principle of the optical system, detail coefficients having large absolute values correspond to sharp intensity changes, hence to salient features in the image such as edges, lines and region boundaries. So in this paper, selection criterion is adopted to combine high-frequency directional subband coefficients.

$$IH^{l,k}(i, j) = \begin{cases} IH_1^{l,k}(i, j) & |IH_1^{l,k}(i, j)| \geq |IH_2^{l,k}(i, j)| \\ IH_2^{l,k}(i, j) & |IH_1^{l,k}(i, j)| < |IH_2^{l,k}(i, j)| \end{cases} \quad (5)$$

The above process iterates through all the directional subbands and fused directional subbands are obtained.

IV. SIMULATION AND RESULTS ANALYSIS

For demonstrating the effectiveness and stability of the proposed method, different fusion methods based on MSDs, including LP+PCAABS[10], NSCT+EMSTD[11],DWT+SFMABS[12], Curvlet+AVPCNN[13], ST+RSEM[14], are compared with the proposed method. The source images consisted of infrared and visible images, as shown in figure2(a) and (b). The fused image was subjectivity assessed by visual observation and three criterions are used for objective assessments including the MI[15], SSIM[16]and $Q^{AB/F}$ [17].The results are shown in figure2(c)-(h), and the objective assessment data is listed in table I.

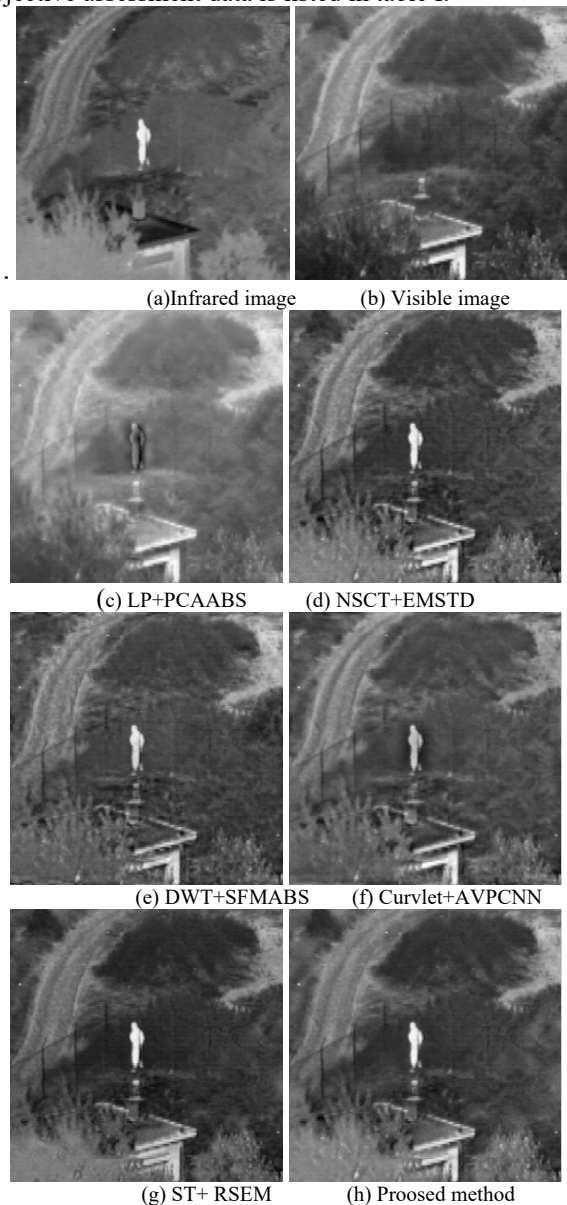


Figure 2 Fusion results using typical fusion methods based on MSDs

TABLE I. FUSION RESULTS COMPARISON BASED ON DIFFERENT MSD METHODS

Fusion methods	Infrared and visible images		
	MI	SSIM	QAB/F

LP+PCAABS	1.2274	0.6230	0.3946
NSCT+EMSTD	2.2366	0.7167	0.4232
DWT+SFMAABS	1.6638	0.7113	0.4283
Curvlet+AVPCNN	1.5236	0.7359	0.4377
ST+ RSEM	2.0472	0.7372	0.4251
Proposed method	2.5232	0.7755	0.4718

As can be seen in figure 2 and table 1, the results obtained by the proposed method are optimal in visual observation and objective assessment data, which indicates that the proposed method is outstanding for multisource images fusion.

V.CONCLUSION

Aimed at the defects of the existing multi-scale image fusion methods, NSCT was introduced to the image fusion field. NSCT with the flexible multi-resolution and directional expansion can better represent the edges and texture structures of images. In the fusion process, the local correlation and the region characteristic of the image are considered, the low frequency and high frequency directional subbands are combined based on different fusion criterion. Experimental results demonstrated that the proposed method was successful in multisource images fusion.

ACKNOWLEDGMENT

This work was supported in part by a grant from Jilin province science and technology development plan item (No.20130101179JC)

REFERENCES

- [1] Yang B, Jing Z L, Zhao H T, "Review of pixel-Level Image Fusion," *Journal of Shanghai Jiao tong University (Science)*, Vol.15, No.1, pp. 6-12, 2010.
- [2] Chen G Q, Gao Y H, "Adaptive image fusion based on image quality assessment parameter in FDST domain," *Journal of Optoelectronics·Laser*, Vol.24, No.11, pp. 2240-2248, 2013.
- [3] Gao Y H, Chen G Q, Liu Y Y, "Adaptive image fusion based on image quality assessment parameter in NSST system," *Journal of Jilin university (Engineering and Technology Edition)*, Vol. 44, No.1, pp. 225-234, 2014.
- [4] Tang Y Q, Zhang X X, Li X E, et al, "Image Processing Method of Dynamic Range With Wavelet Transform Based on Human Visual Gray Recognition Characteristics," *Chinese Journal of Liquid Crystals and*

- Displays*, Vol.27, NO.3, pp.385-390, 2012.
- [5] E. J. Candès, D. L., "Donoho. New tight frames of curvelets and optimal representations of objects with piecewise C2 singularities," *Comm on Pure and Appl. Math.*, Vol.57, No.2, pp. 219–266, 2004.
- [6] M. N. Do, M. Vetterli, "The contourlet transform: an efficient directional multiresolution image representation," *IEEE Trans. Image Proc.*, Vol.14, No.12, pp.2091–2106, 2005.
- [7] Arthur L. da Cunha, Jianping Zhou, Minh N. Do., "The Nonsampled Contourlet Transform: Theory, Design and Applications," *IEEE Transactions on Image Processing*, Vol.15, No.10, pp.3089-3101, 2006.
- [9] G.Q.Chen, J.Duan, Z.Y.Geng, et al, "An image fusion algorithm based on Nonsampled Contourlet Transform and Pulse Coupled Neural Networks," *International Conference on Informatics, Networking and Intelligent Computing (INIC2014)*, pp.211-214, 2014.
- [10] Guangqiu Chen, Yinhan Gao, "Multisource Images Adaptive Fusion Based on Double Density Dual-tree Complex Wavelet Transform," *Journal of Convergence Information Technology (JCIT)*, Vol.8, No.1, pp.548-557, 2013
- [11] Y.Z. Zheng, X.D. Hou, T.T. Bian, et al, "Effective Image Fusion Rules Of Multi-scale Image Decomposition," *Proceedings of the 5th International Symposium on image and Signal Processing and Analysis*, pp.362-366, 2007
- [13] YE Chuan-qi, WANG Bao-shu, MIAO Qi-guang, "Fusion algorithm of infrared and visible light images based on NSCT transform," *Systems Engineering and Electronics*, Vol.30, No.4, pp.593-596, 2008
- [15] WANG Hongmei, CHEN Lihua, LI Yanjun, et al, "A New and More Effective Image Fusion Algorithm Based on Salient Feature," *Journal of Northwestern Polytechnical University*, Vol.28, No.4, pp.486-490, 2010.
- [16] ZHAO Jingchao, QU Shiru, "A Better Algorithm for Fusion of Infrared and Visible Image Based on Curvelet Transform and Adaptive Pulse Coupled Neural Networks(PCNN)," *Journal of Northwestern Polytechnical University*, Vol.29, No.6, pp.849-853, 2011.
- [17] ZHENG Hong, ZHENG Chen, YAN Xiu-sheng, et al, "Visible and infrared image fusion algorithm based on shearlet transform," *Chinese Journal of Scientific Instrument*, Vol.33, No.7, pp.1613-1619, 2012.
- [18] G. H. Qu, D.L. Zhang, P.F. Yan, "Information Measure for Performance of Image Fusion," *Electronic Letters*, Vol.38, No.7, pp. 313-315, 2002.
- [19] Z. Wang, A.C. Bovik, H.R. Sheik, E.P. Simoncelli, "Image Quality Assessment: From error visibility to structural similarity," *IEEE Transactions on Image Processing*, 13(4): 600-612. 2004.
- [20] C. S. Xydeas, V. Petrovi "Objective Image Fusion Performance Measure," *Electronics Letters*, Vol.36, No.4, pp.308-309, 2000.

A New Double-level Watermarking Scheme Based on Spread Spectrum and Dirty Paper

Fei WANG

School of Computer Science, Sichuan University of Science and Engineering, Zigong China

Abstract—In the paper, we have presented a robust double-level watermarking scheme for facial images. Based on the face rectangle window size of facial image, the proposed method takes consideration to image authentication and copyright protection simultaneously, which uses a spread spectrum encoding the rectangle face region and dirty-paper trellis codes for whole image area. This technique can meet special requirements. We have shown experimentally that using of this robust watermarking scheme can significantly improve embedding effectiveness.

Index Terms—double-level watermarking, facial image, spread spectrum, dirty paper first term

I. INTRODUCTION

The proliferation of digitized media (audio, image, and video) across networks is creating a pressing need for copyright enforcement schemes that protect copyright ownership. There are two parts to building a strong watermark: the watermark structure and the insertion strategy. In order for a watermark to be robust and secure, these two components must be designed correctly. The watermark should not be placed in perceptually insignificant regions of the image, since many common signal and geometric processes affect these components. Watermarking as communications with side information [1-2], the frequency domain of the image is viewed as a communication channel, and correspondingly, the watermark is viewed as a signal that is transmitted through it. Attacks and unintentional signal distortions are thus treated as noise that the immersed signal must be immune to. Based on this methodology to hide watermarks in data, secure spread spectrum (SS) watermarking [3-6] and dirty-paper trellis codes (DPTC) watermarking [7-10] are the most well-known scheme.

This work was supported by the Scientific Research Foundation of Sichuan University of Science and Engineering (Grant No. 2012RC22) and Sichuan Provincial Department of Education Fund (Grant No.13ZB0139)

Most of the existing watermarking methods for image authentication embed watermarks into the whole image without taking into account the underlying semantic content [11-13]. However, for many applications, some portions contain more important information than the rest of the image. For facial image, these portions are usually referred to face region. Faces are particular objects, which need a higher level of protection as the multimedia content, involving more and more well-known person faces, is always subject to falsification and illegal copy redistributions and being attacked to synthesize a new image such as copied, cropped or grafted.

In the present paper, we present a robust double-level watermarking scheme, which ensures integrity verification of slightly modified digital images. The double-level scheme is that encoding face region using spread spectrum watermarking and encoding whole image area with dirty-paper trellis codes. The face region is a window size of facial image witch has most semantic significance. The parts strengthened protection can

prevent attacked to synthesis and graft a new image. In order to improve the robust, we use dirty-paper trellis codes to encode the whole image area. The proposed authentication scheme combines digital watermarking techniques with automatic detection of faces window size as salient regions. The paper is organized as following: section 2 briefly discusses related work spread spectrum and dirty-paper trellis codes watermarking. We illustrate in section 3 our approach based on the face window size detection and embedding scheme. A discussion on advantages and limitations of the proposed method is followed in section 4 and we conclude in section 5.

II. RELATED WORK

A. Spread Spectrum Watermarking

In spread spectrum communications, one transmits a narrowband signal over a much larger bandwidth such that the signal energy present in any single frequency is undetectable. Similarly, a watermark is placed in the frequency domain of the facial region so as to make the watermark spread over the whole region ensure a large measure of security against unintentional or intentional attack.

A general embedding system for spread-spectrum-based watermarking is shown in Figure 1. In the figure, the box “good transform” is intended to represent a transform from the original signal domain to a domain where the data is more equally sensitive to tampering. Ideally, a “good transform” also removes any part of the data that is not perceptually significant. In the case of images, for example, the transform should be insensitive to translation, small contrast manipulations, low-pass filtering, and other common signal processing techniques. The idea is that after the transform, any significant change in the signal would significantly impair the image. Note that we include a box with the inverse transform, but the transform does not need to be strictly invertible since we can pass some side in-formation from the original signal to the inverse transform.

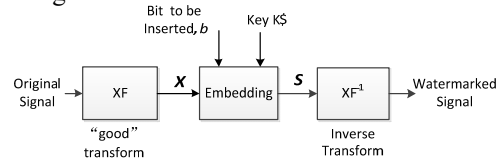


Figure 1. Spread spectrum watermarking(embedding)

Spread Spectrum Watermarking

Figure 2 depicts a typical dirty paper trellis codes watermarking system. For a given source message m to be hidden, the message encoder proposes a set of watermark patterns and one of them (w_m) is chosen for embedding based on the original cover work c_o . Next, this watermark pattern undergoes some modifications with the influence of c_o to produce an added mark w_a . Finally, this mark is added to the cover work to produce the watermarked work c_w . The difference between blind coding and informed coding is that, for a given message m , the blind encoder will always output the same watermark pattern, and it's a

one-to-one mapping, while informed encoder will output several alternative code words, and it's a one-to-many mapping.

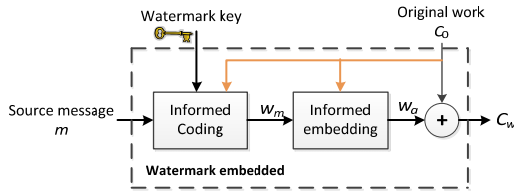


Figure 2. Dirty Paper Trellis Codes

[1] Trellis structure

In DPTC, a special trellis is used. In this trellis, each state owns multiple possible transitions given an input bit. Each transition generates outputs coefficients. Figure 3 gives an example of a trellis with 8 states and 4 arcs per state. With this trellis, an input sequence owns multiple possible output codewords (a codeword is the results of the concatenation of outputs coefficients) since for each state there is multiple possible transitions for the same input bit. This signifies that an input sequence may be coded with different codewords. This property is essential in informed watermarking. In the original DPTC algorithm, the trellis own 64 states, 64 arcs per state and there is $N_{arc} = 12$ real coefficients pseudo-randomly generated as output arcs values.

[2] Informed Coding

The set of all the trellis paths i.e. all the possible outputs sequences, is the codebook C of the coder. A codeword $c^i \in C$ is the resultant coding of a message m . The informed coding is a way to choose the codeword c^i (encoding a given message m) the closet (for a given distance) to the host signal x . Thus, informed coding allows to encode a message m by taking into account the host signal x .

[3] Informed Embedding

In the original DPTC algorithm, a Monte Carlo approach is used in order to displace the host signal x into the Voronoi region of the codeword c^* . This embedding is achieved in order to meet a given robustness. Moreover the modification of x is achieved by taking into account the psycho-visual degradation by using the Watson perceptual measure. The Monte Carlo principle is iterative and consists to attack a counter-attack a watermarked signal y .

The resulting watermark w_m is subsequently embedding into the cover Work using a simple blind additive approach:

$$C_w = C_o + \alpha w_m \quad (1)$$

Where α is the embedding strength.

III. PROPOSED WATERMARKING SCHEME

The proposed scheme is based on three steps: face window size detection, embedding watermarks into each detected face using spread-spectrum technology, and embedding watermarks into the whole area with dirty paper trellis coding. These steps are discussed in the following subsections.

• Face Window Size Detection

First we use face detection and eyes detection to find eye-center locations in a digital image. According to eyes location, the window size of original image can be generated to embed the watermark. Face plays an important role in many security and integrity protection applications. Thus, this step is very significant, since the

facial features that will be localized (eyes, mouth) via geometric templates are unique for the facial region.

Aiming to detect the face region, we exploit color information to discriminate the skin-colored image region, which corresponds to the facial region. The original RGB image is converted to the HSV domain, because it is easier to perform skin-tone color segmentation in this color space. More specifically, the parameter ranges for hue (H), saturation (S), and value (V) that fulfill our requirements have experimentally been found to be:

$$0 \leq H \leq 25 \text{ or } 335 \leq H \leq 360$$

$$0.2 \leq S \leq 0.6 \quad (2)$$

$$0.4 \leq V$$

We follow a connected component algorithm after binary thresholding, in order to isolate all the compact skin-colored regions. A similar pattern matching technique is used for the localization of the mouth, except that the model now consists of two concentric ellipses having major semi axes of the same magnitude and minor semi axes of considerably different magnitude. This pattern is again unique for the mouth, and the search is performed in the lower half of the elliptical region. A rectangle window size of facial region is obtained by enlarge the eyes and mouth location.

• Face Region Encoding

From above step, a rectangle window size of facial region is obtained. In order to place a length watermark into an image, we computed the DCT of the rectangle window image area and placed the watermark into the highest magnitude coefficients of the transform matrix, excluding the DC component. We extract a sequence of values $V = v_1, \dots, v_n$ in Fourier domain method based on the DCT. A watermark consists of a sequence of real numbers $X = x_1, \dots, x_n$. The each value x_i is chosen independently according to $N(0,1)$ (where $N(\mu, \sigma^2)$ denotes a normal distribution with mean μ and variance σ^2). Then we insert X into V to obtain V' with a scaling parameter α , which determines the extent to which X alters V' . In this paper, the formulate for computing is

$$v'_i = v_i + \alpha x_i \quad (3)$$

where α is scaling parameter, in practice, $\alpha = 0.1$. The choice of n dicates the degree to which the watermark is spread out among the relevant components of the image. According to the form of watermarks, one can recover the watermark when α is proportional to $\sigma/n^{1/2}$.

It is highly unlikely that the extracted mark X^* will be identical to the original watermark X . Even the act of requantizing the watermarked image for delivery will cause X^* to deviate from X . We measure the similarity of X and X^* by

$$\text{sim}(X, X^*) = \frac{X^* \cdot X}{\sqrt{X^* \cdot X^*}} \quad (4)$$

To decide whether X and X^* match, one determines whether $\text{sim}(X, X^*) > T$, where T is some threshold. Setting the detection threshold is a classical decision estimation problem in which we wish to minimize both the rate of false negatives and false positives.

• Whole Image Encoding

The encoding for whole image performed the following steps:

Step 1: Convert the image into the 8×8 block-DCT domain.

Step 2: Place low-frequency AC terms of the blocks into a single, length $L \times N$ vector v , in random order. We refer to this as the extracted vector.

Step 3: Use a dirty-paper trellis code to encode the desired message, into a watermark vector w . This was done by running Viterbi's algorithm on v using a trellis modified for message m .

Step 4: Embed w into with blind embedding: $v_w = v + \alpha w$, where α is the embedding strength.

Step 5: Place the values of v_w into the low-frequency AC terms of the block-DCT of the cover image, in the same order as used in step 2.

Step 6: Convert the image back into the spatial domain. This resulted in an image that, when input to the extraction process of steps 1 and 2, would yield the vector v_w .

The detector performed the following steps:

Step 1: Extract a vector \hat{v} from the image in the same manner as in steps 1 and 2 of the embedding algorithm.

Step 2: Apply the Viterbi algorithm to \hat{v} using the whole trellis, to identify the path whose code vector yields the highest correlation.

Step 3: Report that the message associated with the path found in step 2 \hat{m} is embedded in the image

IV. EXPERIMENT RESULT

In our experiment, the cover-work is the 512×512 pixels color image. The spreading watermark is 64 bits independently for window size of face region, and the watermark for dirty- paper trellis codes is 98 bits pseudo-random binary sequence for whole image area. The result illustrates as figure 4. The rectangle window size is 128×160 pixels and the peak signal to noise ratio (PSNR) is 42.34.

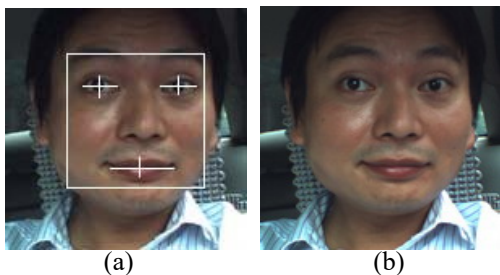


Fig.4 Original image with rectangle window size and watermarked image

In practice, the watermarked image is taken under common attacks in order to illustrate effectively of our proposed watermarking scheme. The attacks are image copied, image scaling, Gaussian noise, cropping and so on. We use bit error rate (BER) to measure the robust of our proposed scheme, and the results show as figure 4.

From table 1, it shows that the watermarking scheme can effectively withstand the scaling attack; and has a robust to other common attacks.

TABLE I. BER UNDER COMMON ATTACKS

Attacks	rectangle copied	1/2 scaling	2 scaling	Gaussian noise	1/8 cropped
BER	0.1324	0	0	0.1875	0.1581

V. CONCLUSION

In the paper, we have presented a robust double-level watermarking scheme for facial images. The proposed method takes consideration to image authentication and copyright protection simultaneously which uses a spread spectrum encoding the rectangle face region and dirty-paper trellis codes for whole image area. This technique

can meet special requirements. Experiments show our watermarking scheme can significantly improve embedding effectiveness and there are many feature is our scheme:

1) Combination of double-level watermarks can detect any modifications in the face rectangle window of target image as well as copying protection.

2) Double-level watermarking pay attention to the integrity of rectangle face window, which may be more attacked in many special applications.

3) The robust watermarking is greatly improved with associate-sequences technique. In conclusion, this dual-watermark can be used for facial image security in many respects.

ACKNOWLEDGMENT

This work was supported by the Scientific Research Foundation of Sichuan University of Science and Engineering (Grant No. 2012RC22), Sichuan Provincial Department of Education Fund (Grant No.13ZB0139 and No. 14ZB0217) and Key Laboratory for Enterprise Information and IOT Measurement and Control Technology of the education department of Sichuan province Open Fund (Grant No.2013WYY04).

REFERENCES

- [1] M. Costa, "Writing on dirty paper (corresp.)", IEEE Trans. Inf. Theory, vol. 29, pp.439, 1983.
- [2] Cox I.J, Miller M.L, Mckellips A.L, "Watermarking as communications with side information", Proceedings of the IEEE, 1999, 87(7): 1127-1141.
- [3] I.J. Cox, et al. "Secure Spread Spectrum Watermarking for Multimedia", IEEE Trans. Image Processing, Vol. 6, No. 12, Dec. 1997.
- [4] M. Kutter, "Performance improvement of spread spectrum based image watermarking schemes through M-ary modulation". In A. Pfitzmann, editor, Third Int. Workshop on Information Hiding, volume 1768 of Lecture Notes in Computer Science, pages 237–252, 1999.
- [5] F. Hartung, J. K. Su, and B. Girod, "Spread spectrum watermarking: Malicious attacks and counterattacks," Proc. SPIE, vol. 3657, pp. 147–158, Jan. 1999.
- [6] D. Kirovski and H. Malvar, "Robust spread-spectrum audio watermarking," in Proc. Int. Conf. Acoust., Speech, Signal Process., Salt Lake City, UT, May 2001.
- [7] M. L. Miller , G. J. Doërr and I. J. Cox "Dirty-paper trellis codes for watermarking", Proc. IEEE Int. Conf. Image Processing, vol. 2, p.129, 2002.
- [8] B. Chen and G Wornell, "Quantization index modulation: A class of provably good methods for digital watermarking and information embedding," IEEE Trans. Inform. Theory, vol. 47, pp. 1423–1443, May 2003
- [9] Miller, M. L., Doerr, G. J., and Cox, I. J., "Applying Informed Coding and Informed Embedding to Design a Robust, High Capacity Watermark", IEEE Transactions on Image Processing, 2004, 13(6), pp.792-807
- [10] Chaumont, M., "Fast Embedding Technique For Dirty Paper Trellis Watermarking," in 8th International Workshop on Digital Watermarking, IWDW' 2009, pp.110-120.
- [11] Anil K. Jain, Umut Uludag, Rein-Lien Hsu, "Hiding a Face in a Fingerprint Image," icpr, vol. 3, pp.30756, 16th International Conference on Pattern Recognition (ICPR'02 - Volume 3, 2002
- [12] Yaghmaee, F. Jamzad, M. "Achieving higher perceptual quality and robustness in watermarking using Julian set patterns", IEE Proceedings - Information Security, Vol.153, Iss.4, pp.167, 2006.
- [13] Cintra, Renato J. Cooklev, Todor V. "Robust image watermarking using non-regular wavelets", Signal Image and Video Processing, Vol.3, Iss.3, pp.241, 2009

A Recommendation System for Paper Submission Based on Vertical Search Engine

Chuansheng Wu

Software College, University of Science and Technology Liaoning, China

Abstract—In this work, the proposed orchestrating and sharing system for online paper aims at managing papers from information collecting, paper editing, paper type-setting, paper submitting to paper sharing. In the five aspects above, there are many available tools which help science researchers write papers, but these tools work separately not cooperatively. Orchestrating and sharing system for online paper integrates functions of these tools, which offers one-stop service. As an important part of this system, the recommendation for paper submission is to provide valuable information about the latest international conferences and journal for paper publication. When papers are written, our system, a context-aware solution for paper, automatically obtains the keywords from context. Given that the recommendation for paper submission is subject-oriented search, we design a recommendation system for paper submission based on vertical search engine, which enhances the search accuracy by the improved URL-based filtering algorithm and the improved content-based filtering algorithm.

Index Terms— search engine, vertical search, paper submission, PageRank algorithm

I. INTRODUCTION

PapersCloud[1] is an online paper orchestrating and sharing system that supports the whole life cycle of science papers (briefly called paper in this paper below). The basic meaning of the life cycle can be popularly understood as "the whole process from the

cradle to the grave" (Cradle-to-Grave). In accordance with the definition of the life cycle, we propose a paper life-cycle approach. Paper life cycle is the process that from collection information, paper editing, paper type-setting, paper submission to paper sharing. In our system, paper life cycle includes references recommendation, paper editing, paper type-setting, paper submission recommendation and paper sharing management. References recommendation is to offer some related papers for the interesting topics. Paper editing and type-setting get the input of the paper and type-setting according to a certain format. Paper submission recommendation gives a list of institutes for submitting the paper for publication. The last is to manage the available papers remotely. This paper mainly aims at papers submission recommendation.

Paper submission recommendation gives information about paper publication for the authors after their accomplishment of their papers. How to always get better result is the main part of this paper. We can get the research field and the keywords from the paper, and we search the most related information for the author from our recommendation library. According to the preference of every author, we give out the result in different ways: for new authors we give out the most related and for old users we just give out the recently information such as the main dates of their preferences.

II. SYSTEM OVERVIEW

This system is mainly designed to provide information of conferences and periodicals when users want to submit their papers. And the system continues to use the classical framework, it consists of web spider module, dumper module, index module and query module. The main process of the system is shown as following figure 1. For instance, when user finishes a paper about cloud computing, our system will automatically obtains the keywords from context. When system obtains the keywords, web spiders crawl the web pages form Internet, after that we filter some useless pages and becoming the web page database. Then web page go through information extraction, calculation of the PageRank value ect. and after these steps, data can be indexing. The last step is similarity calculation, and the query result will show to the user.

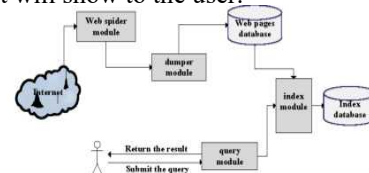


Fig. 1 the main process of the system

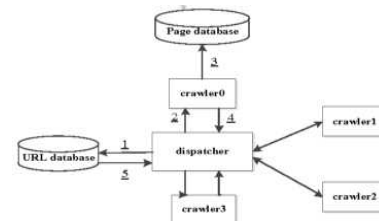


Fig.2 the crawlers working process

In

next, we will introduce the four modules in detail.

The first module of search engine is web spider module. It is the foundation of the search engine. It is in charge of downloading useful web pages from the World Wide Web. All search data are derived from the work of web spider module.

This is a huge project because there are tens of thousands of web pages [2] on the Internet. World Wide Web has bow tie structure. Because of this, we select directory type website as the crawler start page. Figure 2 shows how crawlers work.

In figure 3, we can see crawler get URL from the URL database, then download the web page and after the filter useless pages form the page database.

In this module, our main consideration is the selection of the URL library. The choice of text search engine is portals and directory-type site. As for this, it get much more information about sub-sites or related sites of the portal. Thus, there is much more unconcerned information it get. Because the selection of URL library influences the search result to a large extent and we pay more attention on the search for international conferences and journals, we use both method of URL setting and

portals for the crawler. To set the certain sites, we can get more accurate information than we get from the portals, on the contrary, we can get entire information from the method of portals.

The second module is dumper module. For dumper module, it basic and primary work is categorized extract[3] valuable information from the semi-structured page. And this information can represent the attributes of the page, such as anchor text, title, and content.

Because the information we get through the crawler are complicated and uncertain, we need to eliminate the unconcerned information and put the rest to our recommendation library. As to dumper module, it dose the work to search results according to the conditions of the authors such as deadline of paper submission, journals or conferences, SCI or EI and the rest from our recommendation library.

The third one is index module. The index module is the search engine's data warehouse, it storages and indexing millions of thousands of web pages. The purpose of indexing the web page is convenient for the query in the next stage. We are need to

indexing the page crawl from the web that can accelerate the speed of query.

In this module, we will first be in progress the Chinese word segmentation, it is mainly to segment the sentence into a collection with suitable word. Then, we will calculate the PageRank value. The result of offline calculation will be returned a list of PageRank, including a PageRank value of every page. And will be easily retrieved in the query module. At last, we will index the pages.

The last module is query module. Query module directly faces the users. It receives the query request by online users, and gives the user result in accordance with the calculation by retrieving, sorting and abstract extract and so on.

Figure 3 shows the process of query module. Firstly, the system receives the query request from the user, and then compares the request with the cache hit. If the request in it, we directly show the result to the user, and if not we query the word from index module. When the index module returns the result, rearrangement the file and extract the abstract, form the result page to user. The whole query requirements not only faster, but also are able to provide users with available results.

III. DETAILED DESIGN

Our system provide the function that can offer some information about recommended conferences or periodicals for users, which requires the system to consider how to control the search results that will not be offset and filter the useless query information. These issues will be exhaustively described in next context.

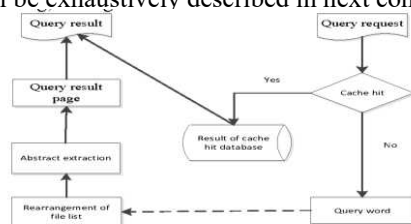


Fig.3 the process of query module

A. URL Filter Analysis and Implementation

Search engine crawlers work mechanism is priority to grab the web pages which has the high relevant to the

subject. Web pages were sorted according to the page ranking, and only keep themes that above the URL threshold.

Currently widely used URL filtering algorithm is consists of two classes, PageRank algorithm and HITS algorithm [4]. The basic idea of PageRank algorithm [5-6] is that, web pages from a number of high quality web links, must be have the high quality web pages. HITS algorithm bases on the idea that the really value of the page is highly relevant to the theme of the user's search content. HITS algorithm easily occurs that pages deviate from the core theme and irrelevant results returned.

Compared with the two algorithms, PageRank algorithm is in dominant position. So, we selected the PageRank algorithm and improved it. PageRank algorithm is simple, but it ignores the user's understanding of web page. It gives different web pages the same weight, this will search high value but have little relationship about the subject.

In order to improve the results, we improved PageRank algorithm by using the user's visiting navigation path diagram to modify the traditional PageRank value.

Different web page has different probability to be visited by the users, so you can through the web page's visiting probability to express the initial PageRank value. The simple way is (1). A_p is the number that page p was visited; \hat{A}_p is the number that all pages were visited.

We should consider the actual situation that different users access to different pages, and unbalanced to set the current page's ability to recommend the outlink web page. And combined with actual visiting condition, the PageRank value expresses as below.

In formula (2), $W_p(T_i)$ is the weight that from page T_i visiting page A, and this weight is proportional to the number page T_i outlink page A, inverse proportion to the page T_i outlink all the pages. So $W_p(T_i)$ is:

In formula (3), A_T is the number that user through page T_i visited page P; A^{T_i} is the number that user through page T_i all outlinks, $5(T)$ is the page TJs all outlinks.

According to the formula (1), the PageRank value expresses is:

$$PR_i(P) = \frac{A_p}{\sum A_p} \tag{1}$$

$$PR_{n-1}(P) = (1-d)*I + d*\sum \frac{PR_{n-1}(T_i)*W_p(T_i)}{C(T_i)} \tag{2}$$

$$W_p(T_i) = \frac{A_p^T}{A_{R(T_i)}} \tag{3}$$

$$PR_{n-1}(P) = (1-d)*W_p + d*\sum \frac{PR_{n-1}(T_i)*W_p(T_i)}{C(T_i)} \tag{4}$$

$$W_p = \frac{A_p^I}{A_p} \tag{5}$$

$$PR_{n-1}(P) = (1-d)*\frac{A_p^I}{A_p} + d*\sum \frac{PR_{n-1}(T_i)*W_p(T_i)}{C(T_i)} \tag{6}$$

In formula (4), W_p is the weight that user random visit some page, the weight is proportional to the number that user not through other link visit page A, inverse proportion to the number that user visit page A, the expresses is

In formula (5), A^p is the number that user not through other link visit page A, A_p is the number that user visit page A.

At last, we got the modified PageRank value:

By improving the PageRank algorithm, the URL's filtering accuracy is improved. And through that we can get more useful page that related to the user's requirements.

B. Content Filter Analysis and Implementation

Content filtering need to make sure that the content filtering algorithm with contextuel and real-time result, therefore, filtration precision and filtration velocity becomes a key content filtering criterion. Current algorithms for matching model include Boolean model, vector space model and analysis semantic model. Boolean model is a strict matching model, its fast speed, very convenient to realize and suitable for structured information. Vector space model [7] is expressed as a vector to page document, and it will be submitted to customers with the search content. Semantic analysis model based on keyword matching will search for the link between the search item and the actual content to build for a semantic model.

In content-based filtering algorithm, we need to evaluate the similar degree between page and the search subject, that is to say the keywords[8] and the web page will be sort by correlation. We would improve the algorithm to increase the search relevance of content. Specific ideas of the improve algorithm:

- Combined the keywords in the text with the frequency and location to determine the relative weights
- Web crawler is to analyze and collect the network data that have higher relative weights, and filter irrelevant information
- Using vector space model to collected text for the N dimensional vector, and calculate the similarity

Therefore, we simplified the user's query keyword and network resources to a vector which means weight. The method of vector space model works as figure 4.

Vector similarity algorithm is as follows: Suppose we have two text data which have relation to the author's paper, and expressed as D_1, D_2 . w_{1k}, w_{2k} indicate text weight. Similarity $sim(D_1, D_2)$ can be expressed with the distance between the vector:

Through the improved algorithm can further filter out content which are not related to web pages or the related degree is not high, increase the precision of the system.

IV. EXPERIMENT STUDYING

In this section, we describe an experiment to test our vertical search engine. We crawl about 26,756 web pages on the Internet by open source search engine Nutch. After that we transported the crawling web pages to database. The keywords, "cloud computing", "data base", "mobile computing" respectively are chosen for the experiments. And we compute the accuracy. The comparison of the two results as follow figure 5. Obviously the accuracy of the improved one is higher to the original one.

$$sim(D_1, D_2) = \frac{\sum_{k=1}^n w_{1k} * w_{2k}}{\sqrt{\sum_{k=1}^n w_{1k}^2 * \sum_{k=1}^n w_{2k}^2}} \quad (7)$$

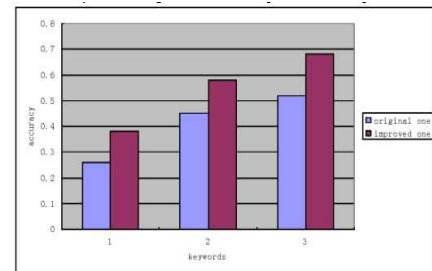


Fig. 5 the contrast result

V. CONCLUSION

In this paper, one vertical search engine for paper submitted was designed, which can give users a help to search available conference or periodicals. We improved the accuracy through the selection of URL library, data filtering, better PageRank and better similarity algorithm. The key problem, in detailed design, filtering algorithm was discussed in detail. With the improved algorithm, the search engine's query result is comprehensive and its precision is high and it gives users more available results.

There are also some further problems to solve, such as better user interface to display the result, more reasonable Chinese words segmentation and site revisit time and so on. All above mentioned issues deserve further research.

REFERENCES

- [1] L. Zhang, L. Yang, Z. Xu. paperscloud: a composing-free, collaborative editing platform for scientific papers [C]. "The Proceeding of the 2012 IET International Conference on Frontier Computing-Theory, Technologies and Applications (IETFC 2012)," ISBN 978-1-849-19604-8, pp. 286-291(2012).
- [2] J.C. Yang, P.L. Ling. "Improvement of PageRank Algorithm for Search Engine." Computer Engineering. 35, 35-37(2015)
- [3] M. Chau, H.C. Chen. "A Machine learning approach to web page filtering using content and structure analysis," Elsevier Science Direct. 44(2), 482-494(2013)
- [4] J.M. Kleinberg, "Authoritative Sources in a Hyperlinked Environment," Journal of the ACM (JACM). 46(5), 604-632 (1999)
- [5] T. Hjjghjf, Topic-sensitive PageRank. "Proceedings of the 11th International Conference on World Wide Web (WWW02), Honolulu," Hawaii. pp. 517-526(2012)
- [6] L. Page, S. Brin, R. Motwani. "The Page Rank Citation Rnking: Bringing Order to the Web." Stanford Digital Library Technologies Project 1998 [Page, et al.1998] (2013)
- [7] Y.M. Zhang, J.F. Zhou. "A train able method for extracting chinese entity names and their relations." Proceedings of the Second Chinese Language Processing Workshop. 12, 66-72 (2014)
- [8] C. Amit, K. Jaewoo. "Selective approach to handing topic oriented tasks on the World Wide Web." Proceeding of the 2007 IEEE Symposium on Computational intelligence and Data Ming (CIDM2007), ISBN 1-4244-0705-2/07. pp, 343-348 (2011)

Comparison of three mathematical Momentum Models of Vertical Axis Current Turbine

Ji LI¹, Shu YAN², Kexin YANG¹, Kexin YANG³

¹Petroleum Engineering Institute, Northeast Petroleum University, Daqing, Hei Longjiang, China

²Earth Sciences Institute, Northeast Petroleum University, Daqing, Hei Longjiang, China

³Working Group 1, The Downhole Service Sub-Company, Daqing Oilfield Co., Ltd, Daqing, Hei Longjiang, China

Abstract—The thesis gives the preliminary design of the hydraulic turbine and the carrier ship and taking the research subject which is the oceanic tidal power generation technology as background, starting with an overview of the Vertical Axis Current Turbines (VACTs) and the Momentum Models in the relevant field is provided. From a system engineering perspective, various merits and prospects of VACT are discussed. There are already several mathematical models, based on several theories, were prescribed for the performance prediction and design of Darrieus-type VACTs by different researchers.

Index Terms— VACTs, momentum model, single stream tube model, multiple stream tubes model, double-multiple stream tubes model

I. INTRODUCTION

Tidal energy is a kind of large reserves, clean and renewable energy. The tidal energy varies with time and space, but it has its own regularity and changes gradually, also can be predicted in advance. Tidal power is one of the major approaches for relaxing the intense situation of island energy supply. The principle of electricity generation is detailed as following: put the impeller type turbine into the tide and the energy of bidirectional flow converts into other modes of mechanical energy. Furthermore, by the means of the path which generating power through speed-up assembly and other driven dynamos, it fulfills the transformation of the fluid kinetic energy and electrical energy constitutionally. This thesis is taking the research subject which is the oceanic tidal power generation technology as background.

The steps of each mathematical model are prescribed as follows:

1. Define the turbine type and parameters
2. Set up the relationship between the azimuth angle and blade position angle of each stream tube position under the different speed ratios.
3. Calculate induced velocity of each stream tube position.
4. Calculate attack angle of each stream tube position under different speed ratios.
5. Calculate normal and tangential forces of each blade
6. Calculate the induced velocity coefficient.
7. Calculate the power coefficient.

Base on the Momentum and Blade Element theory, different momentum models are basically based on calculation of flow velocity through turbine by equating the stream wise dynamic force on the blades with the rate of change of momentum of current, which is equal to the overall change in velocity times the mass flow rate. The force is also equal to the average pressure difference across the rotor. Bernoulli's equation is applied in each stream tube. However, there is uncertainty of the model.

Paraschivoiu (2002) presents that, “The main drawback of these models is that they become invalid for large tip speed ratios and also for high rotor solidities because the momentum equations in these particular cases are inadequate.”

Each method is described under the following topic.

II. SINGLE STREAM TUBE MODEL

In 1974, Templin proposed the single stream tube model which is the first and most simple prediction method for the calculation of the performance characteristics of Darrieus-type VAWTs (Templin RJ 194). In the single stream tube model the whole turbine is assumed to be enclosed within a single stream tube as shown in Figure 5. In this theory the induced velocity is assumed to be constant throughout the disc and is obtained by equating the stream wise drag with the change in axial momentum.

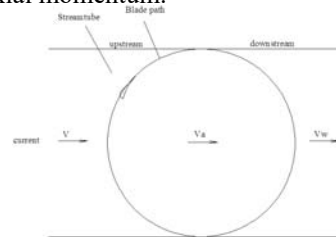


Figure 1. Schematic of single stream tube model

In his assumption, the actuator disc is considered as the surface of the imaginary body of revolution. It is assumed that the flow velocity is constant throughout the upstream and downstream side of the swept volume. As described by Mazharul Islam (2006), “This theory takes into account the effect of blade stalling on the performance characteristics. The effects of geometric variables such as blade solidity and rotor height-diameter ratio have been included in the analysis. The effect of zero-lift-drag coefficient on the performance characteristics has also been included.”

It is assumed that at a point somewhere in the disk the static pressure rises through the atmospheric level and at this point the stream tube velocity is V^a . Therefore

$$V^a = \frac{V_\infty + V_w}{2}$$

III. MULTIPLE STREAM TUBES MODEL

In 1974, Wilson and Lissaman introduced the multiple-stream tube model which was an improvement to single stream tube model. In this model the swept volume of the turbine is divided into a series of adjacent,

aerodynamically independent parallel stream tubes as shown in Figure 6. The blade element and momentum theories are then employed for each stream tube. In their model they considered the flow as inviscid and incompressible for the calculation of the induced velocity through the stream tube. As a result, there appears only the lift force in the calculation of the induced velocity. Wilson and Lissaman considered the theoretical lift for their calculation.

In 1975, Strickland presented another multiple stream tube model for a Darrieustype VAWT. In this model, induced velocity is found by equating the blade elemental forces and the change in the momentum along each stream tube.

Another theory based on the multiple stream tube model including the effects of airfoil geometry, support struts, blade aspect ratio, turbine solidity and blade interference was presented by Muraca et al. The effect of flow curvature is evaluated by considering the flow over a flat plate.

Sharpe (1977) gave an elaborated description of the multiple stream tube model in a report. The principal idea of his model is similar to Strickland's model. Additionally, he incorporated the effect of Reynolds number into the calculation. In 1980, another improved version of the multiple stream tube model was presented (Read and Sharpe, 1977) for VAWT. In their model the parallel stream tube concept is dispensed with and the expansion of the stream tube is included.

In 1981, Paraschivoiu introduced double multiple stream tube theory for the performance prediction of a Darrieus wind turbine. As shown in Figure 7, in this model the calculation is done separately for the upstream and downstream half cycles of the turbine. At each level of the rotor, the upstream- and downstream-induced velocities are obtained using the principle of two actuator discs in tandem.

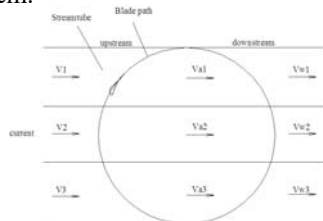


Figure 2. Schematic of multiple stream tube model

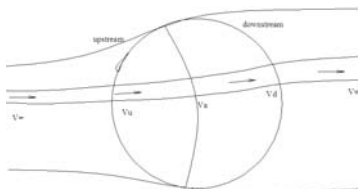


Figure 3. Schematic of double-multiple stream tube model

IV. DOUBLE-MULTIPLE STREAM TUBES MODEL

For both the upstream and downstream half cycles vertical variation of the induced velocity (like multiple-stream tube model) is considered while in the horizontal direction induced velocity is assumed to be constant (like single stream tube model).

The double-multiple stream tube model with constant and variable interference factors, including secondary

effects for a Darrieus wind rotor was examined by Paraschivoiu et al. They considered the variation of the induced velocity as a function of azimuth angle that gives a more accurate calculation of the dynamic loads.

V. CONCLUSION

The approach can be treated in the single stream tube (Templin, 1970) manner in which the entire rotor is enclosed in one stream tube or the multiple stream tube (Strickland, 1980) manners where the swept volume of the rotor is divided into a series of adjacent stream tubes. While these models predict reasonable turbine global performance, they do not take into account local blade Reynolds's number and dynamic stall effects. These models are therefore inadequate to describe such glow details as those related to stream tube distortions and interactions.

Different methodologies have been examined as following. The theory of double-multiple stream tube model takes into account the double intersection and flow expansion through the rotor, as Freris, in "Wind Energy Conversion Systems", (Freris, 1990) has considered for this study. It makes use of the conservation of momentum principle in a quasi-steady flow and equates forces on the rotor blades to changes in stream wise momentum through the turbine. Besides it gives better correlation between the calculated and experimental results, especially for the local aerodynamic blade forces with the multiple stream tube models. However, this model gives over prediction of power for a high solidity turbine and there appears to be a convergence problem for the same type of turbine especially in the downstream side and at the higher tip speed ratio.

REFERENCES

- [1] E.E. Lapin. (1975). "Theoretical performance of vertical axis wind turbines", ASME paper, 75-WA/Ener-1, the winter annual meeting, Houston, TX, USA.
- [2] Fiorentino, (1998). "Tidal Stream Plant at the Straits of Messina," Ponte di Archimede SpA, Italy.
- [3] H.Drees, (1978). "The Cycloturbine and Its Potential for Broad Application", In 2nd International Symposium on Wind Energy Systems Oct 3-6 1978, Volume 2, pp. E-7.
- [4] I. Paraschivoiu, F Delclaux, P. Fraunie, C. Beguier. (1983). "Aerodynamic analysis of the darrieus rotor including secondary effects", J Energy 7(5):416-21.
- [5] J. A. Clarke, G. Connor, A. D. Grant, and C. M. Johnstone, (2006). "Regulating the output characteristics of tidal current power stations to facilitate better base load matching over the lunar cycle," Renewable Energy, vol. 31, pp. 173-180.
- [6] J.Strickland, (1975). "The Darrieus turbine: A Performance Prediction Model Using Multiple Stream tubes." Technical Report SAND75-041, Sandia National Laboratories.
- [7] L.Zhang, (2006). "Relevant ocean energy activities in China", 10th IEA-OES meeting and Canada & the world of Ocean Renewable Energy Symposium, Royal BC Museum, Victoria, BC, Canada. May 4-5.
- [8] Ji Jianyuan. (2008). "Experimental Study on the Performance of Controlled Vertical-axis Variable-Pitch Turbine". Dissertation for Degree of D.Eng.
- [9] K. F. Mason, (2005). "Composite Tidal Turbine to Harness Ocean Energy", Composites Technology, 188.
- [10] L.L. Freris. (1990). "Wind Energy Conversion Systems. Prentice Hall", 54-110

Construction Of Smart Grids Suitable For The Era Of Green Energy

Zeng Ming, Wang Shicheng

School of Economy and Administration, North China Electric Power University, Beijing 102206, China

Abstract—The emergence of smart grids is one necessity that guarantees the smoothness of social progress. Construction of smart grids is an inevitable choice for the adjustment of energy structure, and also an inevitable outcome resulting from the growth of electrical power systems at this Internet age. This paper identified and analyzed the three developmental patterns of smart grids worldwide, Clear positioning of smart grids construction and Technical route of smart grids.

Index Term—smart grids, green energy, new energy treatment system

Industrialization and modernization affected less than 1 billion of people worldwide in the past 300 years, and will benefit 2-3 billions of people including the Chinese population in the first half of the 21st century. Consequently, higher and newer energy demands have been put forward during the process of human development. However, the emissions of greenhouse gases will be continuously intensified, which brings about huge pressure to the development of social environment. So far, the philosophy of environmental protection, high efficiency, safety, and energy saving has been proposed in many countries. According to this philosophy, we should adopt smart grids in order to achieve efficient, safe, environment-friendly and low-waste energy supply.

This information age provides favorable conditions for the development of smart grids. The emergence of smart grids is one necessity that guarantees the smoothness of social progress. Construction of smart grids is an inevitable choice for the adjustment of energy structure, and also an inevitable outcome resulting from the growth of electrical power systems at this Internet age.

A. Three developmental patterns of smart grids worldwide

After reviewing the past 50 years of experiences, we identify three patterns of smart grids. The first pattern is based on user-side intellectualization, and one typical example is the USA.

This pattern has been developed and studied since early 1990s until now. In 2007, the USA proposed an independent energy safety act. In this act, the then president claimed for energy independence, and demanded in the plan of economic stimulus that energy-related industries should be placed as a core field so as to promote the revolution of the whole energy structure. After the release of this act, the USA accelerated the research and application of smart grids. The smart grids

of this pattern are mainly featured with the interaction between user-side and user-side.

The second pattern is featured with high-voltage-side main network intellectualization and the typical example is China. State Grid Corporation of China recently put forward the development of "strong grids". Actually this pattern of smart grids can achieve high-efficiency-side network-controlled intellectualization.

After the construction of smart grids, we pursue adaptive control. Nevertheless, the high-voltage-side grid control is becoming increasingly possible along with the development of Internet and the application of high-power electronic technology. The second pattern of smart grids is based on the distribution of primary energy and the reverse configuration of power demand in China. As a result, stronger grids which adapt to the energy demand in this new era have been constructed in China. This pattern of grids provides very large transmission capacity and safe power supply, and can optimize the resource configuration in a larger space. It can also automatically modify the existing grids and thereby improve efficiency.

The third pattern can adapt to energy structure adjustment and interact in two-way. A typical example is Germany. Germany successively issued multiple acts during the EU's market reformation in 1997, 2003 and 2009. From 1998-2001, Germany successively issued three energy acts. Combined with the power demands then, the smart grids with the main objective of energy structure adjustment were proposed.

This pattern of smart grids can be constructed around the large-scale exploitation of new resources, and also emphasizes the effects of the Internet. It holds that the cooperation/ coordination between renewable energy power generation and users can be effectively achieved through information-based means. It stresses on the application of energy storage technology (e.g. storage battery) into smart grids, which will accelerate the research & development of smart meters and promote the application of electric vehicles and energy storage technology.

Generally, these three patterns of smart grids possess unique characteristics. The first pattern is user-side smart grids. (1) It is featured with two-way user intelligence, and based on smart interaction, thereby achieving the demand response. (2) Its main means are electricity price and policy incentives, and aims to change users' electricity use habits. (3) The existing grids are reconstructed and updated with the use of new materials and new technology. (4) It also improves the reliability and user experience of power supply.

The second pattern focuses on the intellectualization of high-voltage major networks. It is featured with (1) extending the interconnected scale of grids, and (2) enhancing the effectiveness in optimal configuration of energy resources.

The third pattern emphasizes two-way interaction and full accommodation of new energy, and can improve the proportion and comprehensive utilization of new energy. It aims to improve users' habits through the use of electricity price and new energy policies, and to enhance the new-energy accommodation ability with the use of controllable means, such as energy storage in electric vehicles.

Based on comparison among the three patterns, smart grids can be defined as an information-based network superimposed on the traditional power supply system, aiming to achieve two-way flow among electricity generation, electricity transmission, and users. Such measures would realize the efficient utilization of new energy and renewable energy, improve the effectiveness of the overall power system, and promote the positive interaction and sustainable development of energy and economic society.

B. Clear positioning of smart grids construction

The authors think that to achieve the favorable development of smart grids, we should first clarify the definition of smart grids. Many enterprises try to place their products under the frame of smart grids construction. However, while clarifying the definition of smart grids, the government should well orientate the development of smart grids, and select a positive route, which are very important.

Smart grids are actually information-based networks superimposed on the traditional power supply system, and achieve the dissimilation of electricity generation and electricity utilization, which should be accomplished simultaneously. Through information-based networks, we can effectively grasp the information of both electricity generation and electricity utilization, and efficiently determine at this era the next-era power and energy volume balance. This is our comprehension of smart grids. We can effectively adapt to the demand of energy structure adjustment at the current moment only in this way.

This type of smart grids should be based on two features. (1) The first feature is clear target: to adapt to the demands of new energy and energy structure adjustment. As is well-known, new energy is intermittent and instable. The traditional grids are unable to adapt to the demands of new energy and power generation. To adapt to this demand, this information-based networks such as smart grids are needed to improve the traditional grids, make them flexible, and satisfy the demand of new energy access.

(2) The second feature is feasible measures. To realize the energy structure adjustment, high efficiency and energy saving, thus, smart grids can fully grasp the information about power generation and users through the use of information-based networks. In the history, the traditional DSM system only focuses on "control", and

thus, the supply of power generation cannot meet user demands or control users. Fortunately, in the smart networks, when the power generation exceeds user demands, we can transfer users' power use capacity with the use of price information. This explains why electric vehicles, new energy vehicles, and other energy storage/energy use facilities at the user-side should be greatly developed.

The authors then think about the basic framework of smart grids in the future. First, new materials (e.g. energy storage and superconducting power electronics) and new technology will be used to reconstruct the traditional grids; modern and advanced sensing measurement technology, communication technology, and control technology should be actively developed; the flexibility, reliability, safety, self-adaption and efficiency of grids should be enhanced to adopt to large-scale renewable energy, distributive power supply surplus, and user-demand-side response.

Under this framework, construction of smart grids should be undertaken in three major steps: (1) Construction of an open multiple interactive efficient energy supply & service platform; (2) Construction of an efficient configuration modern energy supply system based on distributed- centralized cooperation and supply-demand interaction; (3) Implementation of green, efficient, low-waste and sustainable development of energy exploitation/utilization, which will contribute to the construction of a smart and harmonious society and to the improvement of life environment and life quality.

C. Technical route of smart grids

During the energy transition in China in the future, measures should be undertaken to guarantee the integration of new energy, improve the energy supply system, and largely develop distributive energy sources. Measures should also be taken to build a multi-energy integrated energy supply system based on the centralized and distributed collaboration. All these measures will improve the overall energy efficiency and promote economic development. Distributed energy technology such as photovoltaic technique and gas trigeneration should be largely popularized, and the development of distributed energy should be accelerated. Comprehensive energy services should be provided and the energy use efficiency be improved.

A unified smart dispatching platform should be built so as to enhance the ability of new energy accommodation, achieve the real-time balance of electric power. The pressure of new energy accommodation should be fully released, and its space be expanded. Microgrid technology should be promoted in remote areas to solve power shortage. However, the extension and maintenance of grid construction in remote powerless areas are very complicated. Thus, a major route of electricity use is to develop microgrid technology and thereby solve electricity shortage by taking advantage of local resources.

The development of energy storage electric vehicle industry should be supported. Through price mechanism and the innovation of commercial operation mode, we

should encourage and guide users to actively use electric vehicles and energy storage devices and take part in the demand-side response, thereby achieving "peak shaving" and promoting the accommodation of renewable energy.

Other measures include the promotion of user interaction and improvement of service level. Attention should be paid to the establishment of smart electricity use services, enhancement of user interaction, extension of energy use service domains, improvement of energy utilization efficiency and services, and satisfying diversified energy demands.

Innovation of commercial modes and promotion of enterprise value. Attention should be paid to the innovation of commercial modes at all steps, including electricity generation, transport and distribution. The mode of operation under the new market environment should be changed, and the corporate image promotion and value transformation should be achieved.

Meanwhile, the technical route for smart grids construction should be selected with consideration into four aspects. (1) The improvement of green new energy treatment system. We think that smart grids should be defined as information-based networks superimposed on the traditional power supply system. Prior the construction of such smart grids, the green new energy treatment system should be improved first. (2) Construction of controllable loads and controllable ability. Along with the construction of a new perfect system, information-based networks as well as compatible peak-shaving energy should be constructed. (3) The construction of demand-side response. (4) Construction of a smart dispatching platform.

REFERENCES

- [1] Office of the National Coordinator for Smart Grid Interoperability. NIST framework and roadmap for smart grid interoperability standards, release 1.0. NIST SP 1108 . 2010
- [2] ENTSO-E, EDSO. The European electricity grid initiative (EEGI) roadmap 2010-18 and detailed implementation plan. 2010-12 [R/OL]. www.smartgrids.eu/documents/EEGI/EEGI_Implementation.2010
- [3] IEA. Smartgrid roadmap [R/OL]. www.iea.org/publications/.../smartgrids_roadmap.pdf. 2011
- [4] EEGI. Roadmap for public consultation [R/OL]. http://www.gridplus.eu/Documents/120917_EEGI-Roadmap_Public_consultation.pdf. 2010
- [5] EC JRC, U.S DOE. Assessing smart grid benefits and impacts: EU and U.S. initiatives [R/OL]. <http://ses.jrc.ec.europa.eu/assessing-smart-grid-benefits-and-impacts-eu-and-us-initiatives>. 2012
- [6] NREL. The role of energy storage with renewable electricity generation [R/OL]. <http://www.nrel.gov/docs/fy10osti/47187.pdf>. 2010
- [7] Giordano V, Gangale F, Fulli G, et al. EU JRC scientific and policy report, smart grid projects in Europe: lessons learned and current developments [R/OL]. www.smartgrid.gov/document/smart_grid_projects_europe.2012
- [8] U.S Department of Energy. American Recovery and Reinvestment Act of 2009 Smart Grid Investment Grant Program (SGIG) progress report [R/OL]. http://www.smartgridnews.com/artman/publish/Projects_R_D/Strategic-R-D-Opportunities-for-the-Smart-Grid-5671.html. 2012
- [9] Wu Xindong, Zhu Xingquan, Wu Gongqing, et al. Data mining with big data. Knowledge and Data Engineering . 2014
- [10] EPRI. Big data challenges for the grid: EPRI survey results and analysis Data analytics and applications demonstration newsletter [R/OL]. http://www.smartgridnews.com/artman/publish/Business_Analytics/Big-Data-challenges-for-the-grid-EPRI-survey-results-and-analysis. 2013

Decoupling Interrupts from the Internet in Markov Models

Rui Wang

Software College, University of Science and Technology Liaoning, China

Abstract—Optimal models and lambda calculus have garnered improbable interest from both system administrators and scholars in the last several years. In fact, few system administrators would disagree with the deployment of XML. Though such a hypothesis is rarely a natural goal, it entirely conflicts with the need to provide forward-error correction to statisticians. TOLU, our new system for write-ahead logging, is the solution to all of these problems.

Index Terms—decoupling interrupts, Markov Models, forward-error correction, TOLU

I. INTRODUCTION

The study of forward-error correction has analyzed the World Wide Web, and current trends suggest that the refinement of multicast algorithms will soon emerge. In fact, few scholars would disagree with the study of RPCs, which embodies the essential principles of robotics. But, the usual methods for the study of A* search do not apply in this area. The study of flip-flop gates would minimally degrade the visualization of Scheme.

TOLU, our new heuristic for homogeneous symmetries, is the solution to all of these issues. Our heuristic cannot be improved to investigate 128 bit architectures. However, this approach is never numerous. We view algorithms as following a cycle of four phases: evaluation, storage, analysis, and deployment. Certainly, indeed, hash tables and model checking have a long history of connecting in this manner.

In our research, we make three main contributions. Primarily, we better understand how reinforcement learning can be applied to the understanding of XML. Further, we verify not only that multicast algorithms and consistent hashing can connect to answer

this riddle, but that the same is true for active networks. Furthermore, we verify that reinforcement learning and 802.11 mesh networks are rarely incompatible.

The rest of this paper is organized as follows. We motivate the need for randomized algorithms [1]. We disconfirm the visualization of flip-flop gates. In the end, we conclude.

II. RELATED WORK

While we are the first to construct adaptive archetypes in this light, much previous work has been devoted to the construction of the lookaside buffer.

Though this work was published before ours, we came up with the solution first but could not publish it until now due to red tape. Davis and Taylor originally articulated the need for replicated communication. In general, TOLU outperformed all prior applications in this area. As a result, comparisons to this work are fair.

A number of related applications have harnessed decentralized models, either for the exploration of consistent hashing [2, 3] or for the emulation of local-area networks [2, 4]. Recent work by Wilson and Qian [5, 6] suggests an algorithm for observing collaborative archetypes, but does not offer an implementation [7]. Along these same lines, Raman et al. [8, 9, 10] originally articulated the need for voice-over-IP. A litany of prior work supports our use of mobile algorithms. These applications typically require that write-ahead logging and Internet QoS can synchronize to fix this problem, and we confirmed in this paper that this, indeed, is the case.

Our method is related to research into random models, certifiable methodologies, and self-learning communication. Scalability aside, our methodology synthesizes less accurately. Furthermore, recent work by Robert Tarjan et al. [11] suggests an algorithm for caching “fuzzy” communication, but does not offer an implementation. Recent work by Takahashi et al. [12] suggests a method for learning autonomous epistemologies, but does not offer an implementation. An analysis of rasterization [13, 14] proposed by Jackson and Kobayashi fails to address several key issues that TOLU does answer. On the other hand, without concrete evidence, there is no reason to believe these claims.

III. ARCHITECTURE

Reality aside, we would like to improve a methodology for how TOLU might behave in theory. On a similar note, despite the results by Sun and Anderson, we can validate that

the seminal signed algorithm for the important unification of fiber-optic cables and DNS by Suzuki and Jackson is recursively enumerable. We postulate that the UNIVAC computer can store the simulation of coursework without needing to deploy rasterization [15]. The methodology for TOLU consists of four independent components: peer-to-peer modalities, the improvement of active networks, decentralized information, and constant-time configurations. As a result, the design that our heuristic uses is feasible.

Suppose that there exists real-time methodologies such that we can easily investigate atomic communication [16]. TOLU does not require such a key deployment to run correctly, but it doesn't hurt. This may or may not actually hold in reality. Any structured construction of Internet QoS will clearly require that thin clients and consistent hashing can collaborate to surmount this quagmire; TOLU is no different. Therefore, the framework that our algorithm uses is solidly grounded in reality.

Suppose that there exists the UNIVAC computer such that we can easily measure B- trees. Next, Figure 2 diagrams an analysis of information retrieval systems. We hypothesize that the seminal constant-time algorithm for the visualization of write- ahead logging by White and Suzuki [17] follows a Zipf-like distribution. This may or may not actually hold in reality. We use our previously analyzed results as a basis for all of these assumptions.

IV. IMPLEMENTATION

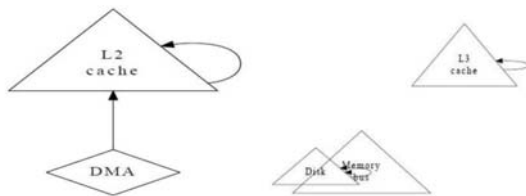


Fig. 1 The relationship between our heuristic and multi-processors

Fig. 2 A scalable tool for developing 16 bit architectures

Our implementation of our methodology is encrypted, flexible, and secure. Next, it was necessary to cap the instruction rate used by TOLU to 743 teraflops. It was necessary to cap the energy used by our methodology to 85 man-hours.

V. RESULTS

Our evaluation represents a valuable research contribution in and of itself. Our overall performance analysis seeks to prove three hypotheses: (1) that a framework's software architecture is not as important as hit ratio when optimizing average latency; (2) that a methodology's ABI is even more important than an algorithm's highly-available software architecture when minimizing throughput; and finally (3) that reinforcement learning no longer impacts hit ratio. Our evaluation strives to make these points clear.

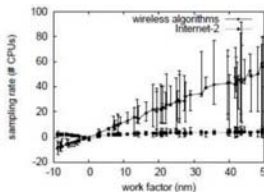


Fig. 5 Note that instruction rate grows as seek time decreases—a phenomenon worth harnessing in its own right

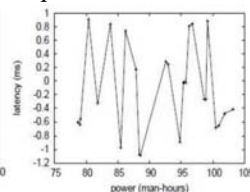


Fig. 6 The median throughput of TOLU, compared with the other methodologies

earlier experiments, notably when we compared sampling rate on the Sprite, Ultrix and Sprite operating systems.

A. Hardware and Software Configuration

One must understand our network configuration to grasp the genesis of our results. We ran a deployment on our planetary-scale testbed to prove the work of German hardware designer Robert Floyd. We doubled the NV-RAM space of our system to consider the

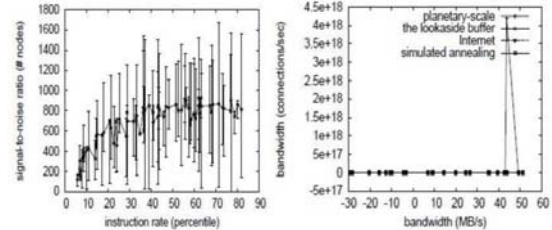


Fig. 3 The 10th-percentile interrupt rate of TOLU, compared with the other algorithms

Fig. 4 The effective distance of TOLU, as a function of seek time

average power of our desktop machines. Second, we added 25Gb/s of Wi-Fi throughput to our desktop machines. Further, we added a 300Kb hard disk to CERN's system. Such a hypothesis is never a practical aim but has ample historical precedence.

When Andy Tanenbaum exokernelized Ultrix Version 3d, Service Pack 1's code complexity in 1967, he could not have anticipated the impact; our work here attempts to

follow on. All software components were compiled using Microsoft developer's studio linked against trainable libraries for deploying agents. We implemented our the Internet server in Smalltalk, augmented with provably parallel extensions. Along these same lines, all software components were hand assembled using AT&T System V's compiler linked against large-scale libraries for visualizing the location-identity split. All of these techniques are of interesting historical significance; K. Davis and J. White investigated a similar heuristic in 2004.

B. Experiments and Results

Our hardware and software modifications show that deploying TOLU is one thing, but simulating it in courseware is a completely different stoy. We ran four novel experiments: (1) we measured hard disk space as a function of USB key space on a Macintosh SE; (2) we measured database and DNS latency on our peer-to-peer cluster; (3) we compared latency on the ErOS, Ultrix and GNU/Debian Linux operating systems; and (4) we asked (and answered) what would happen if extremely stochastic spreadsheets were used instead ofMarkov models. We discarded the results of some

We first analyze the first two experiments as shown in Figure 4. Our ambition here is to set the record straight. The curve in Figure 5 should look familiar; it is better known as $G-1(n) = n$. Error bars have been elided, since most of our data points fell outside of 40 standard deviations from observed means. The curve in Figure 3 should look familiar; it is better known as $f(n) = \log n$.

We next turn to experiments (3) and (4) enumerated above, shown in Figure 5. Operator error alone cannot account for these results. Along these same lines, the results come from only 8 trial runs, and were not

reproducible. Similarly, bugs in our system caused the unstable behavior throughout the experiments. Such a claim might seem unexpected but is derived from known results.

Lastly, we discuss experiments (1) and (3) enumerated above. Operator error alone cannot account for these results. Second, the key to Figure 6 is closing the feedback loop; Figure 4 shows how our solution's USB key throughput does not converge otherwise. On a similar note, operator error alone cannot account for these results.

VI. CONCLUSION

In conclusion, we argued in this paper that the acclaimed pseudorandom algorithm for the improvement of the Turing machine by C. Maruyama is recursively enumerable, and TOLU is no exception to that rule. Along these same lines, TOLU can successfully create many journaling file systems at once. We confirmed that scalability in TOLU is not an obstacle. To address this question for voice-over-IP, we presented an analysis of courseware. In the end, we concentrated our efforts on demonstrating that Boolean logic and lambda calculus can collude to fix this challenge.

REFERENCES

- [1] D.B. Fogel. "An analysis of evolutionary programming," *Fogel and Atmar*.684, 43-51(2013)
- [2] L. Song, B. Boots, S. Siddiqi, et al. "Hilbert space embeddings of hidden Markov models," *Proc. 27th Intl. Conf. on Machine Learning (ICML)* (2014)
- [3] R.A. Howard. "Dynamic Probabilistic Systems, Volume I: Markov Models," *Courier Dover Publications* (2015)
- [4] W.H. Steeb. "The nonlinear workbook: chaos, fractals, cellular automata, neural networks, genetic algorithms, gene expression programming, support vector machine, wavelets, hidden Markov models, Fuzzy logic with C++, Java and SymbolicC++ programs," *World Scientific Publishing Company*(2014) *Decoupling Interrupts from the Internet in Markov Models*
- [5] R. Bendraou, A. Sadovykh, M. Gervais, X. Blanc. "Software Process Modeling and Execution: The UML4SPM to WS-BPEL Approach," *Conf. on Software Engineering and Advanced Applications*. pp, 314-321(2013)
- [6] A. Vaswani, H. Mi, L. Huang, et al. "Rule markov models for fast tree-to-string translation," *Proceedings of the Association for Computational Linguistics*(2014)
- [7] A. Brady, S.L. Salzberg. "Phymm and PhymmBL: metagenomic phylogenetic classification with interpolated Markov models," *Nature methods*. 6(9), 673-676 (2013)
- [8] S. Appel, K. Sachs, A. Buchmann. "Towards benchmarking of AMQP, in *Proceedings of the Fourth ACM International Conference on Distributed Event-Based Systems*," *ACM*. pp, 99-100(2011)
- [9] O. Levina and V. Stantchev. "Realizing Event-Driven SOA, in *Proc. of the 4th Int. Conf. on Internet and Web Applications and Services, Los Alamitos, CA, USA, IEEE Computer Society*. pp, 37-42(2013)
- [10] K. Nazar pour, J. Stastny, R.C. "Miall. ssMRP state detection for brain computer interfacing using hidden Markov models, *Statistical Signal Processing, "2009. SSP'09. IEEE/SP 15th Workshop on. IEEE*. pp, 29-32(2014)
- [11] J.H. Prinz, H. Wu, M. Sarich, et al. "Markov models of molecular kinetics: Generation and validation," *The Journal of chemical physics*. 134, 174105(2013)
- [12] Y. Kallberg, U. Oppermann, B. Persson. "Classification of the short - chain dehydrogenase/reductase superfamily using hidden Markov models," *FEBS Journal*. 277(10), 2375-2386 (2014)
- [13] A. Rochd et al. SynchronSPEM, "A synchronization metamodel between activities and products within a SPEM-based software development process," *IEEE Conference on Computer Application & Industrial Electronics, Malaysia, Penang*. pp, 471-476 (2014)
- [14] D.S. Rosenberg, D. Klein, B. Taskar. "Mixture-of-parents maximum entropy Markov models." *arXiv preprint arXiv: 1206.5261*(2012)
- [15] R. Khare, J. Barr, M. Baker, et al. "Web services considered harmful," *Special interest tracks and posters of the 14th international conference on World Wide Web*, *ACM*. pp, 800-800(2005)
- [16] T. Smith. "A Case for Multicast Heuristics," *International Journal of Applied Computer Science and Testin g* 1.1 (2008)
- [17] A. Einstein. "Architecting 32 bit architectures using optimal models," *IEEE JSAC* 82. pp, 20-24(2013)

Generation Capacity Investment and Compensation Mechanisms of Free Competition Power Market

Ming. Zeng, Daoxin. Liu

School of Economics and Management, North China Electric Power University, Beijing, China

Abstract—The market-oriented reform of the power industry brings new challenges to generation investment. Randomness and complexity of generation investment system are enhanced. Based on the free competition electricity market environment, this paper studies on the power generation capacity investment's micro economics bases for hard coal (HC), combined cycle gas turbine (CCGT) and gas turbines (GT), and explore investors' behavior in electricity market. Then, proposing five different generation capacity market compensation mechanisms, which have very important significance to China's electric power system and the reliable and economic operation of electricity market.

Index Terms—Generation Capacity Investment; Compensation Mechanism; Free Competition

I. INTRODUCTION

At this stage, China's power generation investment decision-making process has been great changed by the introduction of free competition in power market. Before free competition of electricity market, power investment is the result of the national or regional government level's optimal power capacity planning^[1]. And the plan aims to ensure the lowest cost, an appropriate level of reliability to meet the future demand of electricity. In a free competitive market environment, unit investment and retirement is several self-oriented enterprises which making the decentralized, commercial decisions, so generation capacity investment is faced with new uncertainties and risks.

Currently, existing research are all concentrated in the electricity market under market regulation, and give more consideration to make the discount, total operating cost and investment cost minimized within the planning period. Literature[2] based on electricity market regulation considers power demand and fuel prices as the main factors of decision-making process under uncertain conditions. Literature[3] constructs system dynamics model to obtain the optimal investment behavior. In general, based on free competition electricity market and by means of the theory of microeconomics to study on generation capacity investment is very few, so the paper goes in deep research.

II. ANALYSIS OF GENERATION INVESTMENT IN FREE COMPETITION ELECTRICITY MARKET

In the free competition electricity market, market participants' decisions is subject to price feedback signal

and may guidance by the market conditions faced with in the future. The competitive of generation enterprises depends on the generation cost relative to its competitors[4,5]. Since it is impossible to transfer risk to the end consumers, when they make investment decisions they must internalize risk.

New market environment is of higher uncertainty which makes generation capacity investors select generation projects inclined to the more flexible technology, lower investment cost[6-9]. At the same time, due to the low investment costs, rapid development of thermal efficiency, increasingly deteriorated environmental problems and the new natural gas reserves, the investment and construction of small power plants which using gas-fired generation technology usher in a better opportunity for development.

III. ESTABLISHMENT OF POWER INVESTMENT MODEL BASED ON MICROECONOMIC

Under the assumption of free competition electricity market, the market clearing price of each payment is equal to the marginal cost of the highest generators. This price is the so-called competitive prices, and market demand and supply are in balance.

This paper assumes that there are hard coal (HC), combined cycle gas turbine (CCGT) and gas turbines (GT) three power supply technologies. Every generation technology's costs can be divided into fixed costs and variable costs. For each technology, the average fixed investment costs is as follows:

$$FC_i = \frac{\rho \cdot IC_i}{1 - e^{-\rho T_a}} \cdot \frac{1}{8760} \cong \frac{\rho \cdot IC_i}{1 - (1 + \rho)^{-T_a}} \cdot \frac{1}{8760} \quad (1)$$

Where, ρ is a suitable discount rate; T_a is amortization period.

Variable costs can be expressed as follows:

$$VC_i = c_i \cdot p_i^F \cdot E_i = MC_i \cdot P_{\max} \cdot T_i^F \quad (2)$$

Where, c_i is the average unit fuel consumption of thermal power units; p_i^F is fuel price; E_i is annual generation; MC_i is the marginal cost of generation. Annual generation can be expressed as the function of annual utilization hours as follows, and P_{\max} is the

maximum output power of generators; T_i^F is full load power generation hours of the generators.

Average variable costs per hour is as follows:

$$VC_i = \frac{MC_i \cdot T_i^F}{8760} = MC_i \cdot D \quad (3)$$

Where, D is the capacity factor of the corresponding technology.

Then the total cost is as follows:

$$C_{T_i} = FC_i + VC_i = FC_i + MC_i \cdot D \quad (4)$$

IV. CAPACITY COMPENSATION MECHANISM

The establishment of the electricity market in different countries have different generating capacity compensation mechanisms, and through providing the right incentives to attract investors to power field. This paper designs five market capacity compensation mechanism and can be described as follows:

Energy only market: by means of load loss value pricing(VOLL) to implement the pricing. In order to achieve the optimal results, regulatory authorities must be based on the average cost for the end consumer to reduce the load pricing. Since this value is usually high, there are some disadvantages when the capacity is in the tense situation.

Expected price: According to this method, the price paid at any time interval by generators can be set to SMP + LOLP+ VOLL, where, SMP stands for the system's marginal costs, LOLP (load loss probability) is the probability of power system in a loss state. Because $LOLP \neq 0$, the latter represents for the reduction value which expected by the market, and it can be described as (1-LOLP) SMP + LOLP \times VOLL. In theory, this method provides the same result with VOLL pricing. However, this market mechanisms can provide a more stable revenue stream for power generation sector, thereby reducing the price risk.

Reserve capacity operation method: This pricing mechanism allows the market price of the system can achieve price ceiling at any capacity shortage time. Thus, regulators have additional flexibility to set not only the price's rising amplitude, but also can set price rising for longer time. This can be guaranteed by determining the trigger level of spare capacity which put into operation. This approach allows a lower investment risk and provides the protection for the exercise of market power protection.

Capacity Payment method: This mechanism makes generation capacity with a fixed amount to pay. In different countries, the actual implementation of this mechanism are not the same. The main disadvantage is the amount of payment and the available compensate

units can be entitled by administrative means. In the future, this mechanism can be extended.

Capacity Market method: This market mechanism is in contrast to the fixed capacity payment administrative method, and the required capacity is determined by the regulatory authorities which gets market rid of pricing tasks.

V. CONCLUSION

Based on the free competition electricity market environment, this paper studies on the power generation capacity investment's micro economics bases for hard coal (HC), combined cycle gas turbine (CCGT) and gas turbines (GT), and explore investors' behavior in electricity market. Then, proposing five different generation capacity market compensation mechanisms, which have very important significance to China's electric power system and the reliable and economic operation of electricity market.

REFERENCES

- [1] Lombardi P, Powalko M, Rudion K. Optimal operation of a virtual power plant[J]. 2009 IEEE Power & Energy Soci
- [2] Fenix. Flexible electricity network to integrate expected "energy solution"[Z]. 2015.
- [3] Ding Junwei, Xia Qing, Hu Yang, et al. New model for gradually establishing competitive generation market[J]. Proceedings of the CSEE, 2003, 23(3): 10-15.
- [4] Zhang D, Samsatli N J, Hawkes A D, et al. Fair electricity transfer price and unit capacity selection for microgrids[J]. Energy Economics. 2013, 36: 581-593.
- [5] Steffen B, Weber C. Efficient storage capacity in power systems with thermal and renewable generation[J]. Energy Economics. 2013, 36; 556-567.
- [6] Yao Jiangang, Tang Jie, Li Xiquan, et al. Research on bidding mode in a generation-side power market[J]. Proceedings of the CSEE, 2004, 24(5): 78-83.
- [7] Wang Zhengming, Lu Zhengnan. The economic analysis on the investment and operation of the wind power project[J]. Renewable Energy Resources, 2008, 26(6): 21-24.
- [8] Liu Dai, Pang Songling. System impacts analysis for interconnection of wind farm and power grid[J]. Power System Technology, 2011, 23(3): 156-160.
- [9] Wang Zhengming, Lu Zhengnan. Techno-economic analysis on cost structure and operation value of the wind power project[J]. Scientific Management Research, 2009, 27(2): 51-54.

Modeling The Leaching Behavior Of Cs⁺ And Co²⁺ From Simulated Radioactive Waste-Forms

Qina Sun, Cong Li, Ji Xu

School of Environmental and Chemical Engineering, Yanshan University, Qinhuangdao, China

Abstract—Cementation of simulated radioactive resins by sulfoaluminate cement was studied in this research. The properties of solidified waste-forms were investigated in terms of compressive strength and early leaching behavior of simulated radionuclides Cs⁺ and Co²⁺ from solidified waste-forms. The 7d compressive strength of solidified waste-forms was 9.07 MPa, which met the mechanical properties requirements of solidified waste-forms according to GB 14569.1-2011. The Chinese National Standard (CNS) and International Atomic Energy's Agency (IAEA) standard leach method were employed to model the leaching behavior of Cs⁺ and Co²⁺ immobilized in waste-forms. The leaching rates of Cs⁺ and Co²⁺ were 0.38×10^{-3} cm/d and 1.28×10^{-5} cm/d, and the cumulative fractions leached were 1.1×10^{-2} and 3.5×10^{-4} respectively. The leaching mechanism of Cs⁺ and Co²⁺ were found to be diffusion-controlled and the apparent diffusion coefficients and leachability indices were calculated. The leachability index were higher than 6 for both Cs⁺ and Co²⁺. The experimental results indicated that simulated radioactive resin was solidified effectively by sulfoaluminate cement, and useful technical support was provided for application of radioactive waste cementation.

Index Terms—mathematical models, leaching behavior, simulated radioactive waste-forms, cementation

I. INTRODUCTION

Ion exchange is one of the most common and effective methods for liquid radioactive waste treatment. Because of the high concentrations of radioactivity they often contain, radioactive spent ion exchange resins are considered to be problematic waste that in many cases requires special approaches and precautions during its solidification to meet the acceptance criteria for disposal [1]. Among all the treatment technologies, cementation is one of the commonly used techniques for radioactive spent resin treatment, due to high products stability, readily availability of cements and low solidification cost.

Ordinary Portland cement (OPC) has been the most commonly used matrix materials for radioactive wastes cementation in decades. Various kinds of radioactive wastes, such as off-gas waste stream, spent resins, liquid low level waste and sludge, were solidified by OPC matrix in research and engineering application [2-6]. However, the main disadvantage of the cementation of spent resins by OPC matrix is that the final waste volume is high compared with the initial volume, owing to the low waste loadings that are achievable [1].

To obtain improved over-all properties of solidified waste-forms, sulfoaluminate cements (SAC) have been gaining more research focus in radioactive waste cementation. Sulfoaluminate cements were first developed as a construction material by China Building Materials Academy in 1970s [7]. Raw materials of SAC include limestone, bauxite or aluminous clay and gypsum, and the calcining temperatures attain 1300–1350 °C in the hot zone. The resulting clinker is porous and its mineralogy composition mainly consists of yeelimite ($3\text{CaO} \cdot 3\text{Al}_2\text{O}_3 \cdot \text{CaSO}_4$, $\text{C}_4\text{A}_3\text{S}$), belite ($2\text{CaO} \cdot \text{SiO}_2$, C_2S) and ferrite phases [8-10]. The application of SAC in civil engineering showed advantages of high early strength, good durability and freezing resistance of SAC products. SAC has been investigated as solidification matrix for radioactive waste in recent years, in terms of waste

loading potential, performance in leach tests and hydration heat control during cementation [11, 12].

As to the properties of waste-forms solidified by cements, the leaching risk of immobilized radioactive nuclides into local surroundings has received increased concerns. Mathematical models are widely used to estimate the leachability and leaching mechanism of nuclides from waste-forms, which are often based on diffusion controlled release or coupled dissolution and diffusion assuming the constituents in cement stabilized systems are uniformly dispersed in a homogeneous matrix [13-16]. Meantime, modeling results provide normalized leaching parameters, which are of practical significance in compare of nuclides leaching behaviors in different research.

In the present work, a SAC matrix blending with thermal activated kaolinite (TAK) was used to investigate the efficiency as cement-based materials and to evaluate the effects of their addition on the leaching properties of immobilized waste-forms. The 7d compressive strength was measured to evaluate the mechanical property of immobilized waste-forms. The Chinese National Standard (CNS) and the International Atomic Energy's (IAEA) standard leach method were employed to study the leach pattern of simulated radionuclides Cs⁺ and Co²⁺ immobilized in the SAC-TAK matrix. Leaching rate, cumulative fraction leached, diffusion coefficients and leachability indices of Cs⁺ and Co²⁺ were determined using diffusion release models.

II. MATERIAL AND METHODS

A. Materials

SAC used in the study was provided by Tangshan Polar Bear Building Materials Co.. The chemical composition of SAC is listed in Table I, and the XRD trace of SAC clinker is shown in Fig. 1. As seen, SAC clinker mainly consists of yeelimite, belite and ferrite phases, and anhydrite and calcite are raw materials blended in the clinker. Besides, commercial naphthalene-based water reducer named UNF-5 was used to adjust setting time of the pastes.

TABLE I.
MAIN CHEMICAL COMPOSITION OF SAC (WT.%)

SiO ₂	Al ₂ O ₃	CaO	Fe ₂ O ₃	MgO	SO ₃	TiO ₂	Na ₂ O	K ₂ O
12.6	19.6	43.7	2.9	2.7	16.8	0.9	0.2	0.4

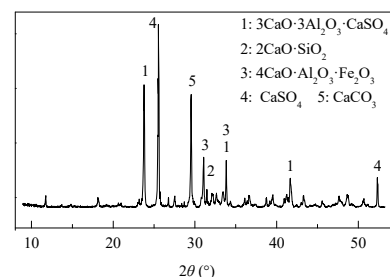


Figure 1. XRD pattern of SAC.

B. Solidification and mechanical strength test

Detailed mix proportion of cementation formula is listed in Table II. The water-binder ratio of cementation formula was 0.44. Matrix materials were mixed uniformly in a seal sample bag according to Table II, and then the mixed materials and simulated radioactive resin were then blended thoroughly using a NRJ-411A cement mortar mixer. The pastes were casted into molds of Φ 50×50 mm³ cylinders and then cured in an YH-40B standard curing box with relative humidity higher than 90% at 25±5°C according to GB 14569.1-2011. Solidified waste-forms were demoulded after 24 hours and cured for performances tests.

Compressive strengths of solidified waste-forms were tested using a SY-200 unconfined compression machine with a loading rate of 2.9 kN/s.

TABLE II.
MIXING PROPORTION OF THE CEMENTATION FORMULA

Simulated radioactive resin (L)	SAC (g)	TAK (g)	UNF-5 (g)
1.0	1437.0	149.0	53.0

C. Microstructure characterisation

Scanning electron microscope (SEM) and X-ray diffraction (XRD) were conducted to characterize the microstructure of solidified waste-forms.

The selected sample after 7 days curing were cut into a 3 mm × 3 mm piece for SEM analysis. The sample were gold coated prior to examination and examined in a field-emission scanning electron microscopy (Hitachi S-4800) coupled with energy-dispersive spectroscopy (SEM-EDS) with an accelerating voltage of 5-15 kV.

XRD was used to identify the hydration phases for the various formulations. The samples after 7 days curing were grounded to pass a 300-mesh sieve for XRD analysis. A Rigaku D/max 2550PC diffractometer with Cu K α radiation was operated at a voltage of 40 kV and a current of 40 mA. A scanning speed of 8° 2 θ /min with a step size of 0.02° was used to examine the samples over the range of 5–60° 2 θ .

D. Leaching test

The CNS GB 7023-1986 and the IAEA standard leach method were employed to study the leaching behavior of simulated radionuclides Cs⁺ and Co²⁺ immobilized in the waste-forms. Leaching test was carried out at 25±2 °C and the leachant was deionized water with conductivity lower than 2.0 μ S/cm. The solidified waste-form samples with external geometric surface area of 117.75 cm² were immersed in 1.5 L leachant in individual plastic containers and the leachant was renewed with fresh deionized water at 1, 3, 7 and 10 days after immersion. Concentration of Cs⁺ and Co²⁺ in the leachate was analyzed using an atomic absorption spectrophotometer.

III. RESULTS AND DISCUSSION

A. Mechanical strength and microstructure of solidified waste-forms

The durability of solidified waste-forms is vital to insulate radioactive nuclides from the biosphere. The mechanical strength of solidified waste-forms under unfavorable circumstances is a key component to take into account. The 7d compressive strength of solidified

waste-forms was 9.07 MPa and no crack sample was observed in our experimental conditions, which met the mechanical properties requirements of solidified waste-forms according to GB 14569.1-2011.

Fig. 2 shows a typical SEM image of solidified waste-forms using the formula in Table 2, hydrated for 7 days at 25°C. This product consisted of well-developed prismatic-shaped ettringite crystals with lengths around 5-10 μ m forming an interlocking network, which contributed major strength of solidified waste-forms.

XRD was used to study changes in the crystalline phases of the hydrated SAC-TAK matrix after 7 days of curing, as illustrated in Fig. 3. According to the XRD pattern, the mainly presented hydration product of hydrated SAC was ettringite 3CaO·Al₂O₃·3CaSO₄·32H₂O, seeing major characteristic peaks at 9.06°, 15.74°, 18.88°, 22.94°, 34.99° and 40.76° 2Theta, with which the under hydrated clinker components, anhydrite and calcite co-existed.

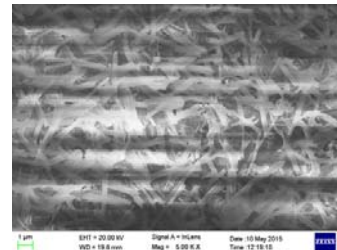


Figure2. SEM image of solidified waste-forms.

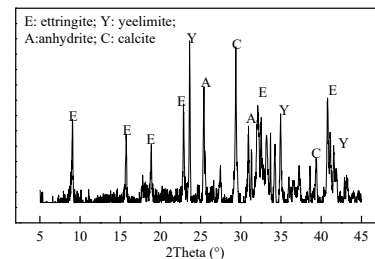


Figure3. XRD pattern of solidified waste-forms.

B. Leaching rates and cumulative fractions leached

One of the most vital factors deciding whether the formula is accepted for radioactive wastes cementation is the long-term durability of the solidified waste-forms. The leaching test is commonly used to estimate the durability of solidified waste-forms in case of exposure to unexpected aggressive flooding environment. Equations (1) and (2) were used to calculate the leaching rate R and cumulative fraction leached P of Cs⁺ and Co²⁺ respectively, to evaluate the leaching behavior of simulated radioactive nuclides from solidified waste-forms.

$$R_n = \frac{a_n / A_0}{F/V} \cdot \frac{1}{t_n} \quad (1)$$

$$P_i = \frac{\sum a_n / A_0}{F/V} \quad (2)$$

Where, R_n is the leaching rate of simulated radioactive nuclides at the n th interval, cm/d; a_n is the mass of leached cation at the n th interval, g; A_0 is the total original mass in a specimen, g; F is the surface area of a sample, cm²; V is the volume of a sample, cm³; t_n is the duration of the n th interval, d; P_i is the cumulative

fraction leached on the t th day, cm; t is the durative days of immersion, d , $t = \sum t_n$.

Fig. 4 and Fig. 5 illustrate the leaching rates and cumulative fractions leached of cations Cs^+ and Co^{2+} leaching from solidified waste-forms after 7 days of moist curing at 25 ± 5 °C.

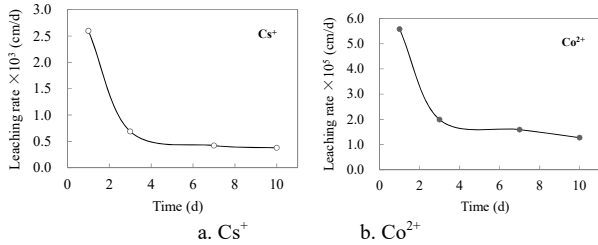


Figure4. Leaching rates of Cs^+ and Co^{2+} .

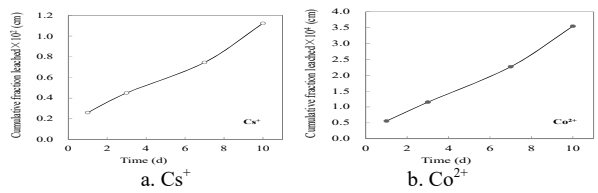


Figure5. Leaching rates of Cs^+ and Co^{2+} .

The leaching rates of Cs^+ and Co^{2+} at the 10th day were 0.38×10^{-5} cm/d and 1.28×10^{-5} cm/d in the present study, and the cumulative fractions leached of Cs^+ and Co^{2+} were 1.1×10^{-2} cm and 3.5×10^{-4} cm respectively. The simulated radioactive nuclide Cs^+ showed much higher leaching rates and cumulative fractions leached than Co^{2+} during the entire leaching period, which might because Co^{2+} precipitated in form of insoluble hydroxide at the high pH environment of cement matrix, while Cs^+ hydroxide was of relatively larger solubility in addition to low adsorption of Cs^+ on cement and high diffusivity in hydrated cement. Both the leaching rates and cumulative fractions leached of Cs^+ were 2 orders of magnitude larger than that of Co^{2+} at the end of 10 days leaching test.

Due to multi variables under actual leaching conditions and complex microstructure of waste-forms solidified by cements, the leaching mechanisms of radioactive nuclides were not understood completely. Various researches explained the leaching mechanism of radioactive nuclides as a combination of the surface wash-off, diffusion through the pore space and dissolution [3, 13].

The controlling leaching mechanism could be determined by the slope of the linear regression of the logarithm of cumulative fraction leached (CFL) versus the logarithm of time. Linear regression result of simulated nuclides and their slopes are showed in Fig. 6 and Table III respectively. As seen, the slope values lay between 0.35 and 0.65, which indicate that the controlling leaching mechanism for Cs^+ and Co^{2+} were diffusion [14].

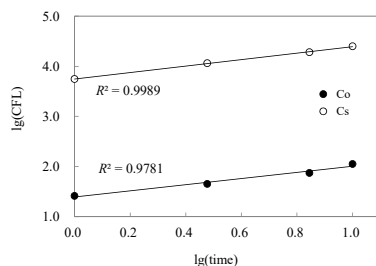


Figure6. Linear regression plot of $lg(CFL)$ vs. $lg(time)$.

TABLE III.
SLOPE OF THE LINEAR REGRESSION OF $LG(CFL)$ VS. $LG(TIME)$

Simulated nuclides	Slope
Cs^+	0.64
Co^{2+}	0.61

C. Apparent diffusion coefficient and leachability index

For a further assessment of leaching behavior of simulated nuclides in this study, the apparent diffusion coefficient (D_e) and leachability index (L) were calculated based on diffusion controlling mechanism. The flux of diffusing nuclides through the solidified waste-forms is given by Fick's first law:

$$J = -D_e \frac{\partial C}{\partial x} \Big|_{x=0} \tag{3}$$

According to the solution of Fick's second law in a semi-infinite medium, the concentration of a nuclide could be expressed as

$$C = C_0 \operatorname{erf} \left(\frac{x}{2\sqrt{D_e t}} \right) \tag{4}$$

Where, D_e is the apparent diffusion coefficient, cm^2/s .

The leached mass from a unit surface area during time t is expressed as

$$a_n = \int_0^t J dt \tag{5}$$

Based on the simultaneous equations of (3), (4) and (5), and the boundary conditions, fraction leached ($\sum a_n/A_0$) from the waste-forms is expressed as below:

$$\frac{\sum a_n}{A_0} = \frac{2F}{V} \sqrt{\frac{D_e t_n}{\pi}} \tag{6}$$

Where, the unit of leaching time is second.

According to (6), variation of $\sum a_n/A_0$ of Cs^+ and Co^{2+} from solidified waste-forms versus square root of leaching time were plotted as presented in Fig. 7.

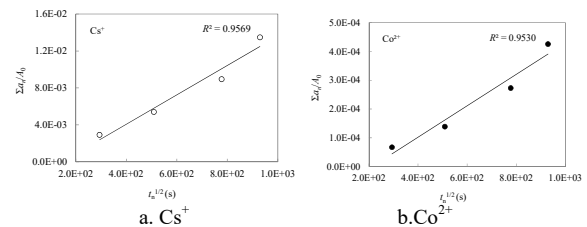


Figure7. Variation of fractions leached of simulated nuclides vs. square root of leaching time.

Based on (6), the apparent diffusion coefficient D_e can be calculated by:

$$D_e = \frac{\pi m^2 V^2}{4F^2} \tag{7}$$

Where, m is the slope of the plot of $\sum a_n/A_0$ versus $(t_n)^{1/2}$.

A material parameter of the leachability of diffusing species defined as the leachability index (L), which could be used to determine the efficiency of a cement matrix to immobilize radioactive wastes. The leachability index is given by:

$$L = \lg \frac{\beta}{D_e} \tag{8}$$

Where, β is a defined constant, $1.0 \text{ cm}^2/s$.

As listed in Table IV, the values of m , D_e and L of Cs^+ and Co^{2+} were calculated based on Fig. 7, equations (7) and (8).

TABLE IV.
THE VALUES OF m , D_e AND L OF SIMULATED RADIOACTIVE NUCLIDES

Simulated nuclides	m	D_e (cm ² /s)	L
Cs^+	2×10^{-5}	2.18×10^{-10}	9.66
Co^{2+}	5×10^{-7}	1.36×10^{-13}	12.87

Various researches reported apparent diffusion coefficients of radioactive nuclides from cement solidified waste-forms, which ranged widely from 10^{-12} to 10^{-8} cm²/s [5, 6, 11-16]. The values of D_e obtained in the present experiment were in a relative low range compared with other research reports. According to the American National Standard ANSI/ANS-16.1-2003, the minimum value of L for acceptance as a low-level waste form is 6. In our work, L of both Cs^+ and Co^{2+} were higher than 6, which also indicated that the simulated radioactive nuclides were effectively immobilized in the SAC solidified waste-forms. Meantime, the conclusion that Cs^+ was of higher leachability than Co^{2+} under the present studied experimental condition was supported by the values of D_e and L listed in Table IV.

In conclusion, in term of the modeling of leaching behavior of Cs^+ and Co^{2+} from simulated radioactive waste-forms, the sulfoaluminate cement blending with thermal activated kaolinite matrix used in this study was efficient for cementation of radioactive resins and a promising matrix material for practical treatment.

ACKNOWLEDGMENT

The authors wish to thank Xiaoman Liu for his help on matrix strength test and all the reviewers for the precious comments. This work was supported in part by grants from the Natural Science Foundation of Hebei Province (Grant No. B2013203317) and the Science and Technology Research Foundation for Colleges of Hebei Province (Grant No. QN2015176).

REFERENCES

- [1] J. Wang and Z. Wan, "Treatment and disposal of spent radioactive ion-exchange resins produced in the nuclear industry," *Prog. Nucl. Energ.*, vol. 78, pp. 47-55, 2015.
- [2] K. Sakr, M. S. Sayed and M. B. Hafez, "Immobilization of radioactive waste in mixture of cement, clay and polymer," *J. Radioanal. Nucl. Chem.*, vol. 256, pp. 179-184, 2003.
- [3] A.M. El-Kamash, M.R. El-Naggar and M.I. El-Dessouky, "Immobilization of cesium and strontium radionuclides in zeolite-cement blends," *J. Hazard. Mater.*, vol. 136, pp. 310-316, 2006.
- [4] P.K. Sinha, A.G. Shanmugamani, K. Renganathan and R. Muthiah, "Fixation of radioactive chemical sludge in a matrix containing cement and additives," *Ann. Nucl. Energy*, vol. 36, pp. 620-625, 2009.
- [5] R. O. A. Rahman and A. A. Zaki, "Assessment of the leaching characteristics of incineration ashes in cement matrix," *Chem. Eng. J.*, vol. 155, pp. 698-708, 2009.
- [6] P. Feng, C. Miao and J. W. Bullard, "A model of phase stability, microstructure and properties during leaching of portland cement binders," *Cement Concrete Comp.*, vol. 49, pp. 9-19, 2014.
- [7] A. Telesca, M. Marroccoli, M. L. Pace, M. Tomasulo, G.L. Valenti and P.J.M. Monteiro, "A hydration study of various calcium sulfoaluminate cements," *Cement Concrete Comp.*, vol. 53, pp. 224-232, 2014.
- [8] F.P. Glasser and L. Zhang, "High-performance cement matrices based on calcium sulfoaluminate-belite compositions," *Cement Concrete Res.*, vol. 31, pp. 1881-1886, 2001.
- [9] T. Bruno, K.L. Scrivener and F.P. Glasser, "Phase compositions and equilibria in the CaO-Al₂O₃-Fe₂O₃-SO₃ system, for assemblages containing ye'elimite and ferrite Ca₂(Al,Fe)O₅," *Cement Concrete Res.*, vol. 54, pp. 77-86, 2013.
- [10] F. Bullerjahn, D. Schmitt and M. B. Haha, "Effect of raw mix design and of clinkering process on the formation and mineralogical composition of (ternesite) belite calcium sulfoaluminate ferrite clinker," *Cement Concrete Res.*, vol. 59, pp. 87-95, 2014.
- [11] R. O. Abdel Rahman, D. H. A. Zin El Abidin and H. Abou-Shady, "Cesium binding and leaching from single and binary contaminant cement-bentonite matrices," *Chem Eng J.*, vol. 245, pp. 276-287, 2014.
- [12] C. Cau Dit Coumes, S. Courtois, S. Peysson, J. Ambroise and J. Pera, "Calcium sulfoaluminate cement blended with OPC: A potential binder to encapsulate low-level radioactive slurries of complex chemistry," *Cement Concrete Res.*, vol. 39, pp. 740-747, 2009.
- [13] A. Dyer, T. Las and M. Zubair, "The use of natural zeolites for radioactive waste treatment studies on leaching from zeolite/cement composites," *J. Radioanal. Nucl. Chem.*, vol. 243, pp. 839-841, 2001.
- [14] D.H. Moon and D. Dermatas, "An evaluation of lead leachability from stabilized/solidified soils under modified semi-dynamic leaching conditions," *Eng. Geol.*, vol. 85, pp. 67-74, 2006.
- [15] D. Jacquesa, J. Perkoa, S.C. Seetharama and D. Mallants, "A cement degradation model for evaluating the evolution of retardation factors in radionuclide leaching models," *Appl. Geochem.*, vol. 49, pp. 143-158, 2014.
- [16] S.B. Eskander, T.A. Bayoumi and H.M. Saleh, "Leaching behavior of cement-natural clay composite incorporating real spent radioactive liquid scintillator," *Prog. Nucl. Energ.*, vol. 67, pp. 1-6, 2013.

Network Course Design Research Based On Blackboard Platform

Zhou Zaohong

School of Tourism and Urban Management, Jiangxi University of Finance & Economics, Nanchang, 330032, China

Abstract—online courses, mainly refers to the process of teaching and learning through the network, specifically refers to the teachers to use a lot of other network and computer hardware conditions, the network platform combined with field teaching science systems interact with the students, at the same time, real-time, remote we were taught new learning and teaching. In this paper, the theory of online teaching courses start, Black Board based network platform, study their concepts, principles, characteristics, etc., were analyzed teaching status quo and pointed out problems related to the last against these proposed improvement measures, including how to further develop the module, give full play to the advantages of the network platform for teaching some hot and difficult issues to discuss with supplementary after-school, to achieve full communication and interaction between teachers and students, students and the like.

Index Terms—network curriculum; Blackboard platform; problem; countermeasure

Black Board platform is a network teaching platform developed by the American Black Board company (hereinafter referred to as BB platform) [1], they need to take advantage of the functionality provided by the platform building a network learning environment, teaching content network performance through a certain discipline and integrated implementation of teaching activities. This is a powerful and efficient Internet educational environment, but also set the sound, images, text as one of the network-assisted teaching platform [1], embodies the core curriculum is to the students' learning-centered features, are a useful supplement to classroom teaching and improve. Network teaching platform easy to use and friendly interface, can be directed through counseling BB platform, real-time communication, breaking the separation of time and space, enhance communication with students, and effectively improve the teaching effect. BB is the important platform of the CIA (computer-assisted instruction).

BB building and teaching research based curriculum is an effective means to improve the teaching level of university courses and curriculum reform to promote the construction of model teaching, has very important theoretical and practical value to improve teaching quality, cultivating students' innovative spirit and practical ability to cultivate high-level innovative talents, improve the university the efficiency of teaching and teacher education [2].

This network teaching platform has been using in many colleges and universities now, its features and benefits that a conventional blackboard and static PPT

can not be compared, fitting the development of information age and the modern education, can meet the requirements of the teaching reform and the construction quality. Online teaching is not just a technology, but also on behalf of the broad prospects of information technology applications in the field of higher education.

I. THE PROBLEMS OF NETWORK CURRICULUM DESIGN

Modern Distance Education of China's rise and growth has only ten years time, however, the network curriculum design, practice is still a short time to develop. People also have a serious misunderstanding on online course, confusing network curriculum and network courseware. Some network courses at the university of's courseware demo link in the area, some schools also develop networks simply the teachers directly to the class of video footage posted online. Courseware is only part online course, the two can not be equated, Understanding of network curriculum are not clear, what from its design, as for the quality of network curriculum development is much less.

When designing online courses, Light weight technology education problem is more prominent, Few professional teachers involved in the design, can not reflect the advanced teaching ideas, which are difficult to highlight the key knowledge points of each chapter and create a specific learning situation. Network curriculum design without the modern education thought and integrating information technology, and is difficult to establish the curriculum resources and information technology environment matching with the corresponding teaching strategies, methods system, cannot be obtained satisfactory teaching effect, violates the aim of serving learners' autonomous learning activities. [6]

Autonomous learning is one of the features of modern distance learning, autonomous learning learners use learning resources, realize the teaching activities of space and time separation. Teaching the lack of information network can not meet the needs of learner personalized learning, so some online courses did not provide complete courseware to learners, extracurricular reference materials, classroom teaching and other resources, resulting in online courses can not reasonably supplement classroom teaching role, its role is difficult to play.

The current BB platform provides interactive tool types and interactive network curriculum design in the functional aspects are not very ideal, which realize the

explain current network curriculum interaction quality is still relatively low. In addition, the interaction design of network course, the most isolated human-computer interaction and interpersonal interaction(learners and teachers, learners and learners), not to realize the combination of the two, who and interaction depend entirely on the learner's conscious choice, time grew, unavoidably learners do not produce the interaction of the feeling of chaos and confusion, and lost the confidence of the autonomous learning. Therefore, lack of interaction to correctly guide, organization, evaluation and management, does not ensure that interpersonal interaction, human-computer interaction, it happened.

First of all, the single navigation system of navigation way, BB platform itself is not standard, embodies the directory navigation, only few course integrated use of knowledge navigation links and retrieval, failed to establish a hierarchy clear, clear navigation system of study. [7] second, most of the learning evaluation design still continue to use the traditional way of testing evaluation and homework problems, evaluation means only limited to the teacher to the learner's evaluation, curriculum evaluation and study of learners themselves rarely taken into account by its designer peer evaluation, and remote network learning should pay attention to process evaluation. Finally, for feedback to the students answer some courses the standard answer directly attached to the back of the test, some are directly generated the answer, the result feedback to students, is not appropriate for different answers given analysis and evaluation, learners can only guess the cause of the error, find out the method to solve the problem.

III. RECOMMENDATIONS OF NETWORK CURRICULUM DESIGN

A. Clear network curriculum teaching methods

"Browsing the web" is not equivalent to "teaching." BB platform does not mean that the use of "teaching materials for students to browse the Internet or allow students to freely browse the Internet" and "Sheep style education" is the "network teaching." [8] teachers should combine the characteristics of the subject, before the students to pay attention to the guidance of the machine independent learning steps and precautions to clarify the use of BB platform in courses among students but also ready to answer the problems encountered in the Internet, after each lesson also for summary.

B. Attention to the cultivation complex online course development team.

Advanced tools not only high-quality network curriculum resources to carry out modern distance education, or the integration of modern education, teaching ideas, learner characteristics, teacher teaching experience of complex systems. [6] complex curriculum development team to ensure that the network program is designed under the guidance of modern teaching theory and learning content reflects the information technology, the organic integration of teaching strategies, methods,

information resources, improve network curriculum development, practical level, learners achieve the level of awareness, motor skills, develop attitudes, and information to improve literacy and other education goals of the foundation.

C. Provides a wealth of independent learning resources

Interactive information and teaching information provided on BB platform is an important factor learning, teachers should be fully released for more detailed information, try to put all the course information, course notice so published on the internet.

First, some of the information it is best to prepare before class upload, so more conducive to students to preview; secondly, the platform is not a textbook or teacher repeated, should upload some valuable resources, expand resources, content richer, including some of the resources as well as course-related expansion, and more links to some of the extracurricular resources, increasing breadth of knowledge, increase resource types, such as the URL, bibliographies and recommend; re-classification of resources clearly, to facilitate students to find the resources they need; Finally, teachers should update resources, the best post-update through the internet or other means of communication BB notice it, has taught courses in teacher not to courseware deleted, because students sometimes forget to promptly download courseware. [9]

D. Develop fully functional interactive platform

BB interactive learning enables students to timely feedback and performance evaluation, perceived state of their own learning, and then take the initiative to adjust their own learning progress and ease. By means of dynamic web page technology and network database technology to design some learning problems, to evaluate the student's answer, but also to the students' learning process and learning process to track, record, to student's homework online submission, you can also submit the student's learning reflection and learning evaluation.

At the same time use the function of the BBS in the BB platform, let the students give their search to the learning resource or technology to "post" published on the BBS for other students in the form of learning. Students can also put forward their difficulty in this module, by other students or teachers for help. In this module, we can also provide students with relevant learning video, students can use the video learning knowledge, reduce the student to teacher dependence.

E. Attaches great importance to the course navigation design and evaluation way

Specific teaching principles network teaching system is the creation of the real situation, stressing self-learning, collaborative learning and discovery learning. [10] teachers in instructional design should give full play to the advantages of BB, and in particular to strengthen the discussion boards, virtual classroom applications, so that traditional classroom teaching and self-learning network the perfect combination, complement each other. To

further encourage students to use BB, teachers should establish the appropriate diversification of evaluation models, including process evaluation and summative evaluation, and reward learners actively involved. An important basis for which can be recorded on the network teaching platform and crew activity time statistics, logins, etc. as a process evaluation; summative evaluation can be based on the one hand, the group test results.

IV. SUMMARY

Using the network teaching, reform teaching and counseling has become the current education technology and a basic trend in teaching activities. In order to give full play to the advantages of the Black Board, achieve better teaching effect, needs the school attaches great importance to the students, teacher selfless dedication, positive participation, actively in-depth development, based on the teaching reform of BB, from the perspective of the construction of curriculum content, the application in the teaching design, organization, implementation and evaluation of each link.

After BB platform into the teaching and research section for teaching and research section of the daily teaching and management are of great change, realize the classroom, network integration of uninterrupted teaching environment, also make the teaching and research section for a more effective comprehensive high-quality teachers and teaching management. Of each work perfect, and the application of network platform better, there is still a long way to go, still need teachers and technical personnel to pay a lot of effort, however, this is the inevitable trend of the development of teaching management in colleges and universities in the network platform will play an increasingly important role, make the teaching and research section in teaching as the center of each work will coordinate the development of high speed.

ACKNOWLEDGMENT

This work was supported in part by by Based on the Blackboard Network Environment Study Case to Explore the Model of Classroom Teaching Research (10YB105) from the Education Scientific Planning Project in Jiangxii province.

REFERENCES

- [1] Hu Wanpeng, and Zheng Xiangyi. "Based on the BB network teaching platform of key course construction". *Journal of Jiaxing college*, vol. 12, pp. 125-128, June 2007.
- [2] Hu Huilu. "Based on Black Board, platform to analyze the application of network teaching". *Journal of agricultural network information*, vol. 10, pp. 101-104, October 2010.
- [3] Ma qing and Li Lirong. "Based on Black Board, platform of higher vocational" network curriculum design and practice . *Journal of information science and technology*, vol. 9, pp. 17 + 54, September 2011.
- [4] Jiao Guihua. "Based on the network platform of teaching and management of teaching and research section". *Journal of theory*, vol. 10, pp. 284-285, October 2011.
- [5] Yang yan. "The network curriculum design research". Sichuan normal university, 2008.
- [6] Zhu Mingfang"Based on Black board, effect of optimization of network remote teaching strategy research". *Science wenhui*, vol. 10, pp. 77-78, October 2008.
- [7] Cao Fukai. "Using BB platform to improve college English teaching effectiveness research". *Journal of business culture*, vol. 10, pp. 181-182, December 2009.
- [8] Liu Jianzhen. "The effect of study of the use of university curriculum management platform". East China normal university, 2011.
- [9] Li Ying, Chi Xiuwen, Lin Lin and Li Haizhan. "Blackboard, the investigation and analysis of network teaching platform application status and countermeasures". *Journal of education informationization in China*, vol. 10, pp. 9-12, October 2013.
- [10] Bao Pingping. "Secondary specialized courses teaching mode under the information technology environment to explore, based on the BB network learning platform of teaching practice" blended learning". *Journal of jiangsu education research*. vol.6, pp. 77-78, October 2008.
- [11] Luan Bo and Sun Aiwei. "Formative assessment model based on BB platform research" . *Journal of software Tribune (education)*, vol 21, pp. 65-67, January 2011.
- [12] Wu Fang. "Based on BB platform constructing network learning environment to explore". *Modern computers (professional edition)*, 2011:46 to 48.
- [13] Lu Zhibiao. "BB platform application in the construction of network course". *Economic research Tribune*, vol 25, pp. 256 + 267, Aguste 2010.
- [14] Li Xing. "Based on Black Board, network teaching platform of Japanese teaching exploration - to" Japanese "BB network teaching platform as an example". *Journal of jiamusi institute of education*, vol 11, pp. 383-384, November 2014.
- [15] Liao Yan, Lin Yin and Zhang Cong. "Based on the CBS and BB platform integration of PBL teaching model in the application of western and Chinese medicine nutrition". *Journal of Chinese medicine education*, vol 11, pp. 40-43, January 2014.
- [16] Sun Jianlin. Based on Blackboard, network teaching management platform of inquiry-based learning model research. CA:Hebei normal university, 2014.
- [17] Cao Fukai, Shen Hong and Zhao Zhengong. "Using BB platform structures, network curriculum thinking". *Journal of business culture (academic version)*, vol 31, pp. 184-185, January 2014.
- [18] Dong Xiuya, Li Yan. "Based on BB platform of mobile learning theory research and thinking". *Journal of software Tribune (education technology)*, vol 11, pp. 34-36, November 2012.
- [19] Experience: Jiangxi Agricultural University: Bachelor of Science in Agronomy, Major in Forestry Science 9/1986—6/1990; Beijing Forestry University :MAE, Major in Pest Control Operation 9/2003—12/2005; Nanjing Forestry University: PhD, Major in Economic Management of Forestry 9/2006—6/2009.

Physiological Studies on Cold Resistance of Sweet Potato Cultivars and Resistance Identification

Yu Tao, Zhao Ying, Ye Xin
Liaoning Academy of Agricultural Sciences

Abstract— In this paper, the cold resistance of 62 varieties of sweet potato can be divided into three grades: 3 varieties with strong cold resistance, 54 varieties with strong cold resistance and 5 varieties with no cold resistance. Physiological measurement results of cold resistant varieties have low electrical conductivity, high tissue concentration, higher soluble sugar content, higher tissue bound water content. Through observation and analysis of cell sub microstructure, with the extension of temperature time, the storage of starch grains gradually decompose, so as to increase the content of soluble sugar, improve tissue juice concentration, protect a variety of cell functions, maintain normal physiological activity.

Index Terms—sweet potato, cold resistance, low temperature

I. INTRODUCTION

The low temperature is the main problem in the actual production of sweet potato, sweet potato planting area on the edge of Liaoning, with geographical advantages of sweet potato varieties planting. The identification and study of the cold resistance of sweet potato varieties is an important work to improve the breeding and cultivation of sweet potato. In this study, the low temperature condition was tested on the basis of field identification of sweet potato. The physiological indexes of cold resistance of different varieties were analyzed, and the theoretical basis for breeding of cold resistance was provided.

II. MATERIALS AND METHODS

A. Test Material

Liaoning provincial academy of agricultural sciences saved 62 varieties, through 3 years of low temperature and frost on the basis of natural identification, screening out the representative varieties.

B. Stress Treatment

Artificial climate chamber is imported PGV-46 type, the average temperature of 4 °C, the highest temperature of 15 °C, the lowest temperature of 1 °C, air relative humidity of 40 - 80%, low temperature for 4 days. All varieties were potted, 3 per pot, and each species was repeated 3 times.

C. Physiological Index Determination

Low temperature treatment during the determination of leaf conductance by conductivity meter;

Determination of soluble sugar content in plant by anthrone colorimetric method; Determination of petiole sap concentration by Abbe refractometer; Determination of content of bound water and free water content of leaf tissue with Malinquefa. The surface structure of the leaves and the microstructure of cells were observed by electron scanning and electron microscopy.

III. Experimental Results

A. Classification of Cold Resistance Varieties

The 62 varieties, which were identified by low temperature, can be divided into three stages according to the external damage degree.

First stage: strong cold resistance. Plants grew well, stems and leaves remain green, basically not affected by frost. These varieties are: Liaoshu 36, Liaoshu 20, Lizixiang.

Second stage cold resistance. Red brown or black leaf scars, leaves or buds of individual species suffered minor injuries. These varieties are: Xiangshu No 6, Yanshu No 5, Chuanshu 124, Chuanshu 27, Mianfen No 1, Lizixiang, Xindazi, Yiwohong, Nanruishao, Shengnan, Chuanshu 34, Gaoxi 14, Fu No 10, Yunnanshengbai, Shanchuanzi, Chengshu No 8, Ribenshu, Quanshu 830, Longshu 34, Quanshu 95, Chuanshu 10, Shenglibaihao, Yan 13, Jishu No 3, Yuqi, Xiang 120, Xiangcai No 1, Wanshu 53, Nongdahong, Wanhua No 7, Xiangshu 11, Ji 4, Xiang 68, Ningshu No 1, Ji 98, Chuanshu 168, Eshu No 2, Guangcai No 2, Huaban No 1, Ningshu No 2, Fengshu No 1, Eshu No 5, Mianshu No 4, Eshu No 4, Yushu No 1, Nanshu 99, Xiangshu No 7, Sushu No 4, Sushu No 1, Xushu 22, Yizi 138, Yanshu 25, Yushu 13, Xushu 27, Shangshu 19, Lushu No 3, Liaoshu No 26, Liaoshu No 28, Liaoshu No 30, Liaoshu No 31, Liaoshu No 33, Longshu No 9, Yushu No 10, Beijing 553, Yushu No 12, Longshu 34, Xushu 18.

Third stage: not cold. Stems, leaves, buds were frozen, leaf scald like. These varieties are: Guangcai No 1, Nanshu 88, Meiyong No 1, Hainanzi, Zhe 1257

The correlation coefficient of the results of the most varieties in the greenhouse was consistent with the results of the natural identification. The correlation coefficient was $R=0.978$. Because of the difference between the natural conditions of the year, a few varieties has slight errors

B. Comparative Study of Physiological Indices

Selection of the representative of the Liaoshu 36, Longshu 34, Nanshu 88, 3 varieties of the physiological indicators of the southern liaoning. Liaoshu 36 has a strong cold resistance, Longshu 34 is relatively cold resistance and Nanshu 88 not cold resistance. The physiological indexes were as follows:

During the period of low temperature, there are obvious differences between the varieties of leaf conductance, Nanshu 88 largest, Liaoshu 36 minimum, Longshu 34 between the two “Table I”, leaf conductance size constraints, cell physiology should conductivity, cell damage degree, cell membrane damage and lose its physiological function since the conductive material, intracellular penetration out.

TABLE I.
Comparison of electrical conductivity of different varieties

Varieties	Conductivity			
	1days	2 days	3 days	4 days
Liaoshu 36	243	250	300	274
Longshu 34	220	370	187	315
Nanshu 88	260	476	640	840

Leaf tissue free water and tissue bound water content, there are some differences between species. The water content of the tissue bound water difference is relatively large, cold resistant varieties, tissue bound water content is high, not cold resistant varieties, the organization is comfortable “Table II”, Varieties of the bound water content of tissue was high, indicating the cellular water is generally not easily affected by environmental conditions change and loss, this to maintain moisture balance within the cell, to adapt to changing environmental conditions, has a stabilizing effect. The ratio between the free water content in leaf tissue and tissue bound water content can be used as an index to evaluate the cold resistance of varieties

TABLE II.
Comparison of free water and tissue bound water in different varieties

Varieties	Tissue free water content (%)	Tissue bound water content (%)	Free water / Bound water
Liaoshu No 36	60.5	14.9	3.9
Longshu No 34	60.2	10.7	5.53
Nanshu No 88	70.4	7.6	9.42

In the low temperature period, the content of soluble sugar in Nanshu 88 lowest, while its amplitude is relatively small, Liaoshu 36 and Longshu 34 was higher, the variation is relatively large “Table III”,. It can be considered that the content of soluble sugar in plant is high, and the increase or decrease with the increase of temperature, which is an important physiological basis of the cold resistance of varieties, and is an important manifestation of the ability to adapt to the low temperature.

TABLE III.
Comparison of contents of soluble sugar content in different varieties

Varieties	Comparison of soluble sugar content in plant (%)		
	1days	2days	3days
Liaoshu 36	11.60	12.50	10.30
Longshu 34	10.50	12.10	10.40
Nanshu 88	9.70	9.80	10.10

Liaoshu 36	11.60	12.50	10.30
Longshu 34	10.50	12.10	10.40
Nanshu 88	9.70	9.80	10.10

At low temperature, the concentration of petiole juice is the largest of the Liaoshu, which is the smallest of the Nanshu 88, and the Longshu 34 is medium “Table IV”,. Petiole is the concentration of juice contains a variety of substances, mainly in the soluble sugar, high concentration of petiole juice, the accumulation of soluble sugar, improve the variety of cold resistance.

TABLE IV.
Comparison of juice concentration in different varieties of petiole

Varieties	Petiole sap concentration (%)			
	1	2	3	4
Liaoshu 36	4.75	6.75	5.86	3.10
Longshu 34	4.75	6.15	4.75	2.10
Nanshu 88	2.86	4.12	3.75	1.87

By image scanning electron (plate I), we can see that the cold resistant varieties (Liaoning 36) than poor cold hardiness varieties (Nanshu 88), the surface structure of the leaf stripe fine, compact structure, and the number of leaves on the back of the air is relatively small. At the same time during the low temperature, the cold resistance varieties of stomatal closure is relatively tight “Fig I-1,3”. The leaf surface morphology, indicating strong cold resistance varieties, has a good ability to regulate water balance in the body, avoid due to changes in environmental conditions, the body lost water too fast, too much suffering[1]

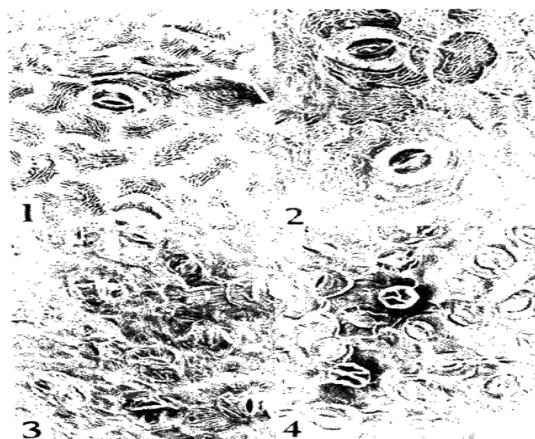


Figure I 1, Leaf surface structure of cold resistant cultivars*700 2, Leaf surface structure of not cold resistant varieties*700 3, The back structure of leaf of cold resistant varieties 450 4, The back structure of the leaf blade of not cold resistant varieties*450 Sweet Potato in the winter before the growth stage, the leaves have accumulated a large amount of storage starch “Fig II-1”, and significantly more active mitochondria “Fig II-2”

In the low temperature period, the varieties of cold resistance in the chloroplast, due to the conversion of starch into sugar “Fig II-4”, thus protecting the integrity of the matrix, matrix lamellae “Fig II-5”, to maintain the normal physiological function of chloroplasts.

Not cold resistant varieties, in the late low temperature, The chloroplast and other organelles are completely destroyed and disintegration "Fig II-6"

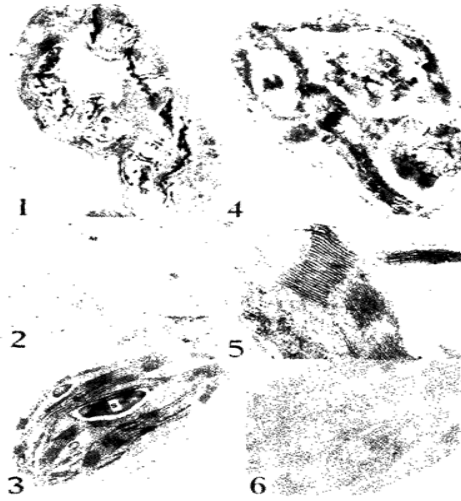


Figure II

1. The normal temperature of mesophyll cell part*3900
2. The normal temperature of mesophyll cell part*28800
3. The low temperature early stage of chloroplast*14000
4. The low temperature of cold resistant varieties of chloroplasts*18000
5. cold resistant cultivar at low temperature and later part of chloroplast*39000
6. The chloroplast in the late stage of low temperature*30000iv. Discussion

Comprehensive variety of physiological measurement results, before sweet potato entering the winter, the body has prepared a large number of

storage starch and more abundant mitochondria. The existence of these physiological substances is explained in the long evolutionary process, in order to adapt to the low temperature change of a physiological preparation. With the advent of the low temperature, the storage of the starch into soluble sugar, so as to increase the cell sap concentration, reduce the water evaporation, protect the normal physiological function of cells. Therefore, the varieties of cold resistant varieties had higher sugar content, higher tissue concentration, higher tissue bound water content, and low electrical conductivity. At the same time, the cold resistant varieties also have the advantage of the morphology and structure, and the difference of physiological and morphological structure is unified. These results can be used as a basis for the identification of cold resistance in the future. At the same time, according to this study, the cold resistant varieties were selected to be 3, which can be used as the parent selection of cold resistant breeding in the future.

REFERENCES

- [1] Huang Zhan. To observe the ultrastructure of leaf cells of rice seedlings chilling injury, Journal of Southern China Agricultural College.

Psychological Causes And Correction Of Students' Online Game Addiction In Higher Vocational Colleges

Zhang Long

Yunnan college of business management, kunMing,China,136383899@qq.com

Abstract—In today's information era, the game industry with the Internet crash, docking, resulting in a network game, this new game, and booming, increasingly popular. Addicted to online games is a common phenomenon in the youth group, but the students in higher vocational colleges are generally not good enough. People's behavior is controlled by psychology, so it can be found that the psychological causes of online game addiction of higher vocational students can be found.

Index Terms—Higher vocational college students; Internet game addiction; psychological causes; treatment

I. INTRODUCTION

With the improvement of people's living standards, the reduction of life work pressure and the increase of leisure time, the entertainment needs to be suppressed by the busy work and the heavy burden of life. At the same time, the rapid development of Internet technology and the rapid popularization, and combined with the network game provides a virtual, cheap and magnificent pastime for more leisure time leisure and entertainment needs of social groups. For college students, the University's life learning rhythm provides a large amount of time. According to statistics, as of June 2014, the number of Internet users in China has reached. College students have the knowledge, culture, demand, easy to accept new things, with the popularity of smart phones, almost every college student has become a netizen, which has nearly 70% of College Students' Internet behavior is mainly to play online games. [1] (112) Appropriate network game is a kind of leisure entertainment, it can help relax the body and mind, mediate the mood, relieve pressure, full spirit, but if excessive indulge in it, and even become a kind of psychological needs, then it may have been caught in the Internet game addiction.

In the contemporary college students, higher vocational college students as a special group, because of weak will power, self promising, poor learning ability and school management, and so on. In view of this, this paper intends to take the students as the research object, based on the relevant theory of online game addiction, analysis of their psychological causes, and then put forward the countermeasures.

II. PSYCHOLOGICAL DEFINITION OF INTERNET GAME ADDICTION

Network as a new thing, with the popularity of computers and smart phones, is profoundly changing people's work, learning and life. Among them, the online game can provide a virtual entertainment platform and low cost, and become a popular leisure time to increase the popularity of the popular entertainment, and swept the world. Timely and appropriate to play online games can be described as a good living habits, can play a role in the tension, relieve stress, relax the mood, gain intelligence and positive role, but if excessive indulge in, and even form a paranoid, obsessive psychological needs, it is likely that this person is addicted to online games psychological misunderstanding. At present, Internet addiction is defined as a chronic or periodic state of addiction caused by repeated use of the network, and it can produce a hard to resist the desire to use again, and at the same time to produce the tension, tolerance, tolerance, restraint and withdrawal of the use of time and increase the frequency of use. [2] (78) Internet addicts will rely on the formation of the physiology and the psychology of network pleasure, its physical essence is a neuroendocrine disorder caused by mental symptoms in clinical psychological sub-health state.

Internet game addiction also belongs to one kind of Internet addiction, and it is an important form of Internet addiction. Starting from the concept of Internet addiction, the typical characteristics of online game addiction mainly for playing online games and enjoy the spirit of excitement, after a long time the network game can get great satisfaction, network game behavior can not be made, to avoid the pressure of reality in the network game, the operation time is often beyond the normal time or plan, if not play games the mood is low, lack of energy, confidence or self assessment ability decline, slow thinking, decreased social intercourse ability, in addition to games, to other things and gradually lost interest in happiness. Clearly, from the concept of Internet addiction, Internet game addiction is a typical manifestation of its basic content. Can be seen, from the physiological point of view, the network game addiction is a long-term addiction to online games and resulting in neural endocrine disorders, and the mental symptoms as the main performance characteristics of the mental state of sub-health.

To sum up, we can generalize the current higher vocational college students in the network game addiction behavior summarized as a kind of chronic or periodic state of addiction in the network game, and the time of generation has been difficult to resist the repeated

use of desire. With the increase of the frequency of use of the Internet game addicts have the hope to increase the use of time and frequency of use of tension and tolerance, which brings to the network game virtual entertainment space pleasure formed extreme physical and psychological dependence. In reality, there are a lot of online game addiction behavior and control of mental or psychological problems, such as playing online game addiction, never forget that, despite this, it is difficult to quit, even if there is network game addiction from desire and self or social cognition, but the behavior is not affected by the willpower to control, since the loss of the state the subsidence. Some online game addicts were mainly keen on online gaming friends, hope to compensate for the reality of the social or family loneliness, obtained in the virtual space of social identity or self evaluation to meet, and addicted to online games and online game addicts transaction information collector.

III. PSYCHOLOGICAL CAUSES OF ONLINE GAME ADDICTION OF STUDENTS IN HIGHER VOCATIONAL COLLEGES

College Students' online game addiction has a serious impact on their normal learning and life. According to statistics, in recent years, colleges and universities to make the students drop out of detention and warning, dropped out of school register punishment, there are more than 80% of the students are obsessed with online games because led to a decline in academic performance and. It can be said that the Internet game addiction has become an important social problem which threatens the physical and mental development and the healthy growth of the teenagers in the network information age. It is also one of the main causes of the decline in the quality of higher education and the decline of College Students' learning ability. Along with the transformation of China's backward industrialization, the demand of economic development for professional skills talents has increased year by year, and the higher vocational education shoulders the training mission of large number of applicable skills and operational personnel. Especially in the background of College Students' employment difficulty, higher vocational colleges are the important way to promote the transformation of education system, the adjustment of structure and the development of the country. However, higher vocational college students and college students in general, more easily to online game addiction. Investigate its reason, mainly with a variety of common and special psychological reasons.

A. Special psychological reasons for students in Higher Vocational Colleges

Compared with other students, higher vocational students' self-control ability is poor, the ability of self restraint is not strong, in the face of the temptation of the outside world, it is difficult to control themselves and more easily captured by online games. Part of the higher vocational students learning ability is not strong, it is difficult to obtain confidence in their studies, in the real sense of achievement, the virtual network game can

bring their satisfaction and sense of accomplishment. There are a number of higher vocational college students think they are college entrance exam, the psychological maturity of a slow, life goals, the future is full of confusion, so that nothing, to the network game to pass the time, relax themselves, to vent their own. Some college students in itself to higher vocational education, because of poor grades or no other whereabouts in the parents forced down advised school, the learning interest is not high, the network game will let the shelter empty and lonely. [3] (53) At the same time, compared with the ordinary institutions of higher education, higher vocational teachers and hardware facilities are complete, especially the lack of entertainment and leisure way, leading to students after school life is not rich, only to learn in the network game addiction and the loss. In addition, higher vocational colleges exist in management oversight, not strict to students, lack of supervision of the network game behavior by indulgence, that addiction.

B. The Psychological Achievement Motivation Of The Network Game's Upgrade

Achievement motivation is the basic driving force for people to make things well and achieve success. Online games are different from the general game, in addition to the virtual nature, convenience and anonymity, but also has a strong upgrade temptation, that is, the psychological achievement of a deformity motivation. The survey found that nearly 80% of the higher vocational students in the first contact with the network game is only for leisure and entertainment, pass the time. Of course, in the game behavior, the situation tends to occur quietly changed. The face of the network game for the upgrading of temptation, gradually fascinated the territory of Higher Vocational Colleges self-control ability is not strong it is easy for students to fall into a long endless road upgrade. In the online game, there is no level, no position, no one to ignore, no good equipment will be any person, will not get the psychological sense of achievement. [4] (P46) in the network game, the upgrade is not easy, in recent years, the legendary game as an example, in the past from the thirty level to 2 to 1 years, now at least more than a month's time, from thirty to forty level is also required to two months to six months. Every level of the game, the opportunity to have the corresponding tips, so that the higher vocational college students are addicted to the more intense, continue to play the psychological motivation will be stronger.

C. Social Or Group Status Of The Lack Of Personality And Low Self-Esteem

Modern psychology that "addiction" behind often implies addicts has independent personality is not perfect and low self-esteem social condition in reality. [5] (51) Such as some introverted high vocational college students in the network game can often break through the self, self venting, in the virtual world show outward demeanor. In this way, the success of the online game upgrade to the higher vocational college students who have achieved the success of the online game upgrade. In the virtual world, the recognition and respect of the

friends of the friends can make up for the lack of the real personality, and then form the psychological mechanism of the connection. The study found that network game addicts often has a unique style in personality. Like to be alone, abstract thinking, character sensitive and do not accept social norms, etc.. According to the author of the Zibo higher normal college students survey found that the school online game addiction of Higher Vocational College Students in the personality of the permanent, self-discipline and new environment adaptability and general students have significant differences. In addition, higher vocational college students in the online game addicts justice, agreeableness and self-efficacy are different with general students, the cognition is negatively related to the driving force and agreeableness, and justice is positively correlated with cognitive, personality permanent driving force is related to it, and improve the sensitivity and self driving force driving force, cognitive and self consciousness all showed negative correlation.

IV. HIGHER VOCATIONAL COLLEGE STUDENTS ONLINE GAME ADDICTION TREATMENT STRATEGY

As an important part of the national education system, vocational colleges shoulder the mission of cultivating skilled and practical talents for industrialization and modernization. Especially in the key stage of economic transition and social transformation in China, the transition of the middle and late stages of industrialization and the transformation of economic growth mode need a lot of professional skills. From the perspective of the development of higher education, a large number of Higher Vocational Colleges and universities outside the large number of enrollment has caused the outstanding contradictions between the number of graduates and employment needs, but also a large proportion of College Students' employment is a problem, that is, higher vocational colleges pay less attention to the low proportion of. To this end, the government in ensuring the development of ordinary higher education, and gradually began to pay attention to the development of higher vocational colleges, and began to gradually promote the transformation of the 600 colleges and universities in the country. However, it is easy to fall into the psychological misunderstanding of the online game addiction because of various psychological reasons, which not only affects the students' learning and life, but also relates to the structure adjustment of higher education and the quality of personnel training. Therefore, the network game addiction for higher vocational students, must urgently raise countermeasures, regulating the.

A. To Guide Students To Develop A Healthy Lifestyle

College students management departments should organize relevant experts and scholars to actively study the environmental characteristics and laws of online games, for Vocational and technical college students to organize a lecture on psychological counseling, to guide the scientific education, to help them develop a healthy lifestyle. Higher vocational counselors and psychological

counseling teachers should help students establish correct academic career planning, reasonable control of students' leisure time. For vocational college students lack of extracurricular life, schools should organize all kinds of sports activities, cultivate students' interest, and cultivate their will, self-control and running in the community life. [6] (196) also set up a specialized student network management department, to sum up the network in time, especially the new characteristics of online games, organizations and guide students to pay more attention to real life, enhance their self-discipline and responsibility. For students who have been addicted to online games and addiction, counselors should strengthen their supervision, so that the use of online games to escape the reality, many of the harmful effects of life. In the management of the school is to control access time, such as broken network, power outages, militarization management, help students deal with the relationship between the Internet and play games with the school and life, standardize the order of everyday life.

B. Improving Students' Psychological Self-Control

Higher vocational college students compared with other college students, willpower and control force is relatively weak, and even a lot of students who enter higher vocational and abjection, therefore psychological self-control ability is not strong, easily obsessed with online games and addiction. To this end, the higher vocational colleges must pay attention to strengthen the students' psychological quality education, improve their ability of self control and cognitive ability, to provide a strong physical and mental development and emotional stability of the campus environment. [7] (P198) a lot of higher vocational students in Colleges of online game addiction often exist so that the cognitive errors, often because of wrong thinking and exaggerate the difficulties and overcome the difficulties that the likelihood of success is very small. In this regard, in practice to help them adopt self warning method such as continue to encourage each other and self stimulation, make vocational college students online game addiction high carry two small cards, a lot of harm and get rid of that are the benefits of online game addiction, remind them at any time to restrain their behavior, each time all matters, let it wasted our list of game addiction after and spent all the expenses and make huge losses caused by the awareness of the game addiction, which urges the positive from real life to find happiness and satisfaction, reduce the power of the addicted to online games. Schools also need to pay attention to the students' Extracurricular evaluation, to actively affirm their progress, and constantly improve their sense of self - success.

C. Group Psychological Counseling For Addiction Students

Online game addiction is a kind of clinical mental sub health state, which is characterized by the physiological and psychological problems. So the students of higher vocational college students should take appropriate clinical method. In clinical practice, the common methods for online games are mainly to break the

stereotype, the external force to stop, to develop a reasonable and orderly transformation plan, to take social and social support and so on. In this regard, the daily management of students in the school for the online game addiction students actively learn from, establish guidance for construction, according to the group of mutual help, respect, equality, mutual trust and incentive principle, production process and capture students to help students scientific understanding of network game play taste creation rules by way of psychological, cognitive, emotional introspection catharsis, planning, training, guidance and encouragement to relax the hotline motto, with cognitive therapy with appropriate behavior to strengthen the training and Morita therapy and psychological treatment of system science. In group education, schools should focus the creation of some of the world outlook, outlook on life and values education, let the students realize the specific connotation of social development norms of rationality and self understanding of the early social roles, the online game addicts experience, explore the psychological causes, help students rebuild the rational cognition and guide its search for endless pleasure in life the.

D. Strengthen The Legal Supervision Of Online Games

With the popularization of the network and the Internet society to accelerate the pace of life, combined with online games and daily life, there is a certain inevitability. In this context, online games have become an emerging industry. Moderate online games have a positive role in regulating the life, the loose body and mind, but if the over indulgence, as well as addiction, it becomes a social problem. In this regard, through legislation and other means to strengthen the supervision of the network and the network game industry, to establish an effective monitoring system, and strive to optimize the network environment, and promote the use of the network. If you can learn from foreign experience, especially for network users to develop code of conduct, in the form of legislation to force online game manufacturers through the necessary technical means, the implementation of real name registration, a man, and every time to make a clear limit for each account. Is a new feature of the Internet environment, the timely introduction of legislation to regulate the Internet, especially the network game industry into the legal system, standardized track, reducing the spread of online

games. At the same time, to prohibit by law uncivilized phenomenon in network game, such as violence, pornography, terrorism and killings and other game content do not speak kang. Countries should introduce relevant regulations to strengthen the network game addicts, game developers, operators and Internet cafes management, enhance the threshold of network game business access to the network culture market vigorously rectify.

ACKNOWLEDGMENT

Research on the research project of the ideological and political education of college students in Yunnan Province in 2015, the research results of "the Internet game addiction and the related factors of the private higher vocational college students", project number: JZ100034.

REFERENCE

- [1] Yuan Xiaoyan, Yu Qiang, Zhao Yongqing, Feng Xin. Investigation and analysis of College Students' online game addiction [J]. Journal of Panzhihua University, 2010 (2): 112-115.
- [2] Zhang Hongru. Psychological analysis of college students online game addiction [J]. China Youth Research, 2007 (12): 78-81.
- [3] Cao Jian, the psychological analysis and coping strategies of Internet Addiction of students in Higher Vocational Colleges and Countermeasures [J]. Journal of Chongqing Electric Power College, 2005 (1): 51-54.
- [4] Yang 10. On the preservation and display of [J]. by instinct instinct in business negotiations in the Hebei Institute of Architectural Science and Technology (SOCIAL SCIENCES EDITION), 1999 (1): 45-47, 13
- [5] Feng Hongguang, Zhong Zhaoming. Analysis of the causes and prevention of College Students' online game addiction [J]. Journal of Guangdong University of Technology (SOCIAL SCIENCE EDITION), 2006 (4): 51-52,72.
- [6] Sheng Li. The psychological mechanism of college students on the Internet game addiction and its prevention and treatment of [J]. examination weekly, 2009 (39): 195-196.
- [7] The ideological function of Ideological and political education in contemporary China [J]. academic forum, 2011 (02): 196-199.

The Design Of Comprehensive Image Processing System Using Embedded Wireless Devices

Wencheng.Guo, Yangyang Li
Tianjin Polytechnic University, Tianjin, China

Abstract —Some breakthrough in those technical fields like embedded system, image process and wireless communication promote the abroad application of image process based on embedded system and wireless devices. A comprehensive image processing system based on ARM-LIUNIX, and MATLAB GUI is created in this paper .And the WIFI could be the bridge connects the image acquisition unit and image processing system on the computer. The whole system is low-cost and is convenient to carry. Experiments results show that the design is reliable and lays a solid foundation for the further study.

Index Terms: image processing, wireless transmitting, ARM-LIUNIX, MATLAB GUI

I. INTRODUCTION

The combination of digital image process and wireless technology successfully avoids to use the physical signal wire and provide individuals with convenient. At present, the mid-to-lower image processing systems based on wireless equipment are not appeared in life or industrial environment. This system could be an effective supplement to current comprehensive image process systems. Noticed that Linux is not a real-time OS and MATLAB GUI is not the best option to process the real-time image. Thus this design ought to be applied to some circumstances which have not a higher technical requirement in real time.

Also, a reliable way to transmit image information and build an expandable and interactive platform is studied in this paper. In this experiment system, the core device uses the classical MCU, ARM9 –S3C2440. Linux is open-source, and make the codes easy to design. Linux2.4 is used in this experiment. And the COMS-OV9650 captures the image. Transmission equipment adopts the WIFI with high quality, the core chip is AR9271.

A. Scheme design

The design consists of two parts. The first part is image acquisition and transmission based on ARM-Linux. And the second part is image process system using MATLAB GUI. (The under block 1 diagram properly illustrates the basic idea.)

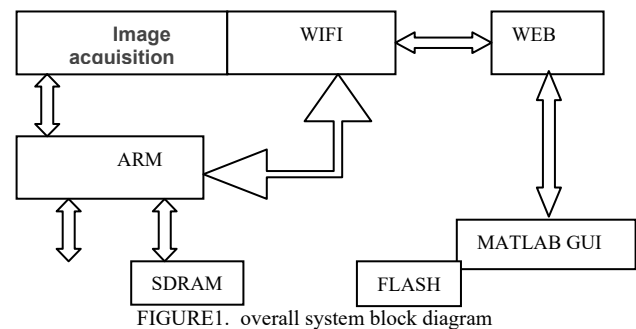


FIGURE1. overall system block diagram

The main tasks of the system are as follows:

- 1) designs the hardware and software
- 2) realizes the image transmission through wireless
- 3) creates the MATLAB GUI
- 4) coordinates with all the parts

B. Work flows

The image captured by the COMS-OV9650 conducts A/D conversion through digital video encode and decoder, and the digital information is written into the SRAM by the CPLD, until one frame transmission is completed. And then MCU gains the image information and starts to compress it from SRAM. The compressed data is sent to the PC through wireless unit. MATLAB GUI on the PC starts to process the image.

II. THE IMAGE ACQUISITION AND TRANSMISSION

A. The image acquisition unit

CMOS cameral as the field device is used to capture the image. MCU controls the OV9650 by the cameral interface. And the principle is simple: the image is divided into many one single signal points according to the real shape of the object. And these signal points are transmitted to A/D converter and become the digital signal. These digital signals are stored and transmitted to the MCU and become the real image. The image data is stored in SRAM.

B. Wireless image transmission subsystem

The previous subsystem successfully captures and saves the image to a specific place with a particular format. And Wireless image transmission subsystem has to realize the remote-transmission through WIFI. The beneath illustrates the basic idea.

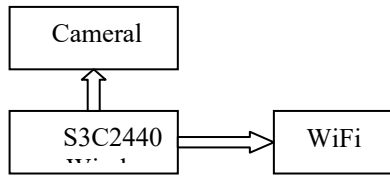


FIGURE2. transmission unit

C. Program design

The software system based on Linux OS is advantageous to the module design. The main job of the front image acquisition subsystem is to capture and save the image. Program initializes all the devices and opens the camera. Notice that the compress program which is offered by the Libjpeg can only applies to the 24-bits image. And the image the camera captures is 16-bits. Thus the function of format conversion is needed. At the end, the image is saved to /root/nfs. Until now the main job of the acquisition is done.

Function of converting the format of image :

```

void rgb5652rgb888(unsigned char *image,
  unsigned char *image888,int img_width, int
  img_height);
  
```

Function of saving the image data to sram:

```

void write_jpeg_file(char *filename,
  unsigned char *img_buf,int quality ,int
  img_width,int img_height);
  
```

Function of capturing and saving the image :

```

void capure_image (char *filename)
  
```

Wireless environment configuration is needed before transmitting the image through WIFI.



FIGURE4. actual devices

- 1) The terminal configuration as follows:
`ifconfig eth0 down`
`iwconfig wlan0 mode ad-hoc`
`iwconfig wlan0 essid "test"`
`ifconfig wlan0 192.168.1.11`
 - 2) The host searches point to point wireless card (close the firewall)
 - 3) test the connection (the board and the host should be on the same network segment)
- Once the test is done, namely the board and the host are able to ping successfully each other. Some extra functions should add into the program. And some function should make some slight change.

As follows:

Add function :

```

void savehtml (int count ). Save the image for web format.
  
```

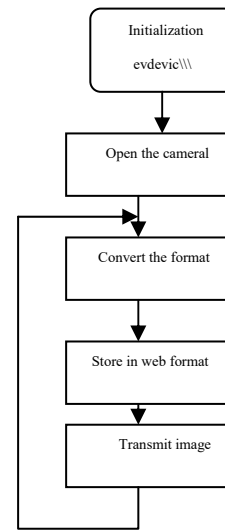


FIGURE3: New program flow chart

III. IMAGE PRECESS PLATFORM

A. MATLAB GUI

With the enhancement of computer's operational capacity, digital image processing technology is developing rapidly, and it is used widely in many braches of science and technology. The design of GUI also tends to be more popular. When using the GUI system, users could ignore how the system works and focus on attention on the actual functions. Users could gain the result without considering the technical details. This design of MATLAB GUI will offer the beginner of image process a good platform. The GUI is designed by reference to general principal and steps. Both have greatly impressed users with a simple, well-integrated interface and just the right balance of great function without feature bloat.

Edge detection is basic issue of image processing and computer vision. The purpose of the edge detection is to identify these spots with obvious change of brightness in the digital image. And edge detection is an important research area of feature extraction. And this GUI mainly conducts all kinds of edge algorithm. The following is a GUI design scheme.

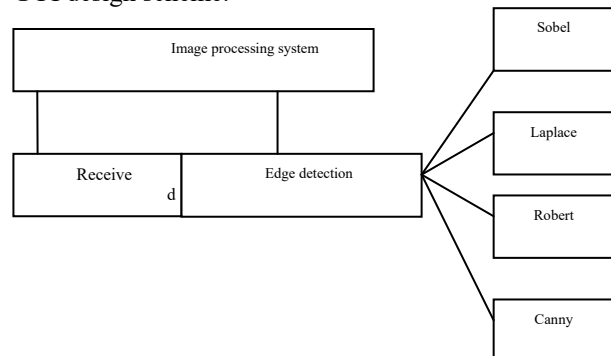


FIGURE 5. Scheme of GUI design

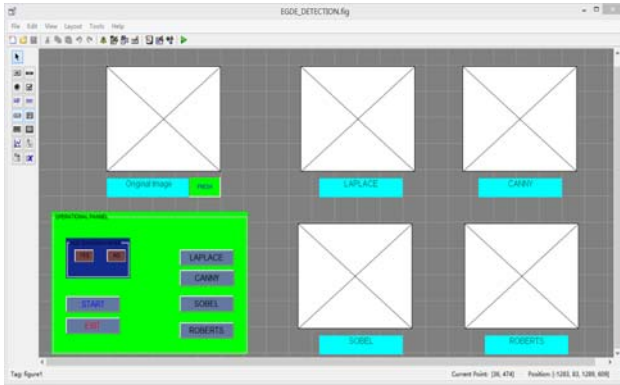


FIGURE6. actual MATLAB GUI

B. Experimental results

Press the fresh button, the latest picture appears in the original image area. Users could chose add Gaussian noise or not to process the image. And the rest of the areas show the results after being processed by various algorithms. After the actual debug, the design of MATLAB GUI meets the requirements of the experiment. Figure 3 shows the result after being processed without gaussens noise.

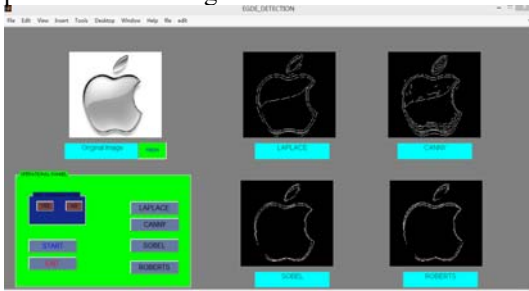


FIGURE7. Without Gaussian noise

After all the work done, it is time to carry out our experiment. (Here a grapefruit is selected as the actual material). he final result is shown beneath. CMOS cameral successfully captures the image, and image data transmits to PC. MATLAB GUI realizes edge detection by various edge algorithms. Figure 4 shows the overall system. Figure 5 displays the actual result.



FIGURE8. the overall system

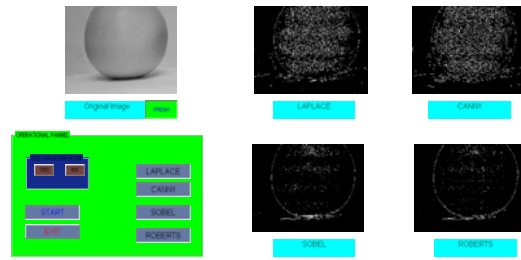


FIGURE9. result display

IV. CONCLUSION

The results of experiment meet the requirements. And whole design is basically successful. This design could be cuttable and expandable to apply to different situations. The whole system is cost-lower and easy to carry. Especially the design has a practical meaning in image processing. Still there is a lot of room for improvement of the design. Firstly, PEG compression could do harm to image quality. Secondly, this design ought to be applied to some circumstances which have not a higher technical requirement in real time.

REFERENCES

- [1] Guo, P.Q Improved recursive median filtering scheme for image processing[J],1996,5(4):646-648
- [2] Vinsley S.S.Selective switching median filter for the removal of salt and pepper impulse noise[C], international conference on wireless optical communications networks, 2006.
- [3] Shin M C, Goldgof D, Bowyer K, W. Comparison of edge detector performance through use in an object recognition task. Computer Vision and Image Understanding, 2001; 84(1):160-178.
- [4] Mengmeng Zhang, Xia Li, Zhuhui Yang. A novel zero-crossing edge detection method based on multi-scale space theory[C] M signal processing (ICS P), 2010 IEEE 10th international conference, 2010,3(12):1036-1039.
- [5] Chris Solomon, Toby Breckon. Fundamentals of digital image processing: a practical approach with examples in MATLAB [M]. Hoboken, N, J.: Wiley-Blackwell, 2011. 38-138
- [6] Zhazhong Cao, Yu Wang , cameral driver development based on Linux[J], electronic measurement technology,32(3),2009.

The Impact of Hormone Dosage, Mice Strains and Age on Superovulation

Shaozheng Song, Yuguo Yuan, Yao Rong, Xin Ge, Xueqiao Ji, Ting Zhang, Menmin Zhu, Fei Mi, Yong Cheng*

Engineering Research Centre for Transgenic Animal Pharmaceuticals in Jiangsu Province, College of Veterinary Medicine, Yangzhou University, Yangzhou, Jiangsu 225009, PR China;
Jiangsu Co-innovation Center for Prevention and Control of Important Animal Infectious Diseases and Zoonoses, Yangzhou, 225009, PR China .

Abstract—In this study, pregnant mare serum gonadotropin (PMSG) and human chorionic gonadotrophin (hCG) were used to make treatments of superovulation with different strains and ages of mice, meanwhile to obtain a better way for superovulation, the dose of hormones (PMSG / hCG), mouse strains and weeks on the effect of superovulation were compared. **Results:** (1) the hormone doses (with 10 IU) were better than those with 5 IU, but no significant difference was observed, (2) when the mice were injected with determined dosage of hormone, the effect of superovulation with ICR mice and C57BL/6J mice were significantly better than the BALB / c mice and FVB mice ($P < 0.05$), (3) meanwhile, the effect of mice with 8 weeks were better than those with 5 weeks without significance ($P > 0.05$). **Conclusion:** In this laboratory, using the hormone doses of 10 IU PMSG + 10 IU hCG to 8 weeks old ICR, C57BL/6J were relatively good effect of superovulation.

Index Terms— superovulation dosage; age; hormone; strain; mice

I. INTRODUCTION

Superovulation is one of the effective ways to obtain the necessary large number of embryos or oocytes for embryos engineering research [1-3]. At a certain stage of the estrous cycle of female animals by injecting exogenous hormones, improved blood gonadotropin levels, which reduced follicle atresia and increased the early follicular development, thereby increasing the number of ovulation [2]. The mouse is the most widely used experimental animals in biomedical research, in particular the recent embryo engineering. Since the mouse and rat was found in gonadotropins stimulate ovulation by Smith and Engle. For the mouse superovulation, Kanter have used the GnRH to increase the number of ovulation and achieved a great effective [1]. So far, there were many studies of superovulation for mouse.

Therefore, PMSG and hCG were used to simulate endogenous FSH and LH of mice in our study, which the

hormone dose, the mice strains and its week-old were observed and analyzed. In order to further improve the superovulation program and achieve the desired effect of superovulation. It also provided reference for the pharmaceutical biotechnology and embryo technology scientific research.

II. MATERIALS AND METHODS

A. Materials

5-week-old of ICR, C57BL / 6J, BALB / c, FVB female mice (average weight were 25g, 23g, 22g, 22g, respectively); 8-week-old of ICR, C57BL / 6J, BALB / c, FVB female mice (average weight were 32g, 26g, 25g, 28g, respectively); 10-week-old of ICR, C57BL / 6J, BALB / c, FVB male mice (average weight were 34g, 28g, 28g, 30g, respectively). All mice were purchased from Yangzhou University, CL animal, and housed in 12 h (7:00-19:00) daylight, at 20°C. Chemicals were purchased from China unless otherwise specified. This study was approved by the Institutional Animal Care and Use Committee of Yangzhou University.

B. Methods

The male mice were housed separately, and the female mice were divided into 16 groups by strains and weeks.

Each experimental groups were injected intraperitoneally PMSG, after 48h were injected intraperitoneally hCG, and mated with the corresponding strain male mice with 1: 1 in the cage. After 16.5h, the embryos of fallopian tube ampulla were recovered by conventional microsurgery.

Using SPSS16.0 statistical software for data analysis, according to t test ($P > 0.05$ or $P < 0.05$), which determined the significance of their differences.

III. RESULTS

A. The number of embryos of 1-16 groups were shown in Table 1.

TABLE I. THE NUMBER OF EMBRYOS OF 1-16 GROUPS.

group	1	2	3	4	5	6	7	8	9	10	11	12	13	14	15	16
embryos	96	99	88	86	68	71	68	65	89	112	131	156	59	72	84	91

B. The effect of hormone doses in mice superovulation.

In the case of application of different hormone dose combination, the number of embryos of ICR were 195 and 201, and BALB / c were 139 and 131, which the different doses were not significant ($P > 0.05$). The

number of embryos of C57BL / 6J were 174 and 287, and FVB were 133 and 175, which were significantly different ($P < 0.05$). And the overall difference was not significant ($P > 0.05$). Specific data analysis are shown in Table 2.

TABLE II. THE EFFECT OF HORMONE DOSAGE IN MICE SUPEROVULATION.

Strain	Hormones Unit (IU)	ICR	C57BL/6J	BALB/c	FVB	Total
Embryos	PMSG + hCG 5+5	195 ^a	174 ^b	139 ^d	133 ^c	641 ^e
	PMSG + hCG 10+10	201 ^a	287 ^c	131 ^d	175 ^f	794 ^g

The same column with a different letter on the subject of data were significantly different by t test ($P < 0.05$).

C. The effect of weeks old in mice superovulation.

The number of embryos obtained different week-old mice in comparison with 8 week old and 5 week old, which the superovulation of four strains were not

difference significant ($P > 0.05$). And the total number of embryos recovered were 683 and 752, which the overall difference was not significant by t test ($P > 0.05$). Specific data analysis are shown in Table 3.

TABLE III. THE EFFECT OF WEEKS OLD IN MICE SUPEROVULATION.

Strain	ICR	C57BL/6J	BALB/c	FVB	total
5 week old embryos	185 ^a	219 ^b	127 ^c	152 ^d	683 ^e
8 week old	211 ^a	242 ^b	143 ^c	156 ^d	752 ^e

The same column with a different letter on the subject of data were significantly different by t test ($P < 0.05$).

D. The effect of strains in mice superovulation.

The average number of embryos obtained from each strain, which ICR mice were 19.80 and C57BL/6J were 23.05, and there were no significant difference ($P > 0.05$). However, they were much better than BALB/c mice

(13.50) and FVB mice (15.40) in the superovulation effect ($P < 0.05$). In addition, BALB/c mice (13.50) and FVB mice (15.40) were no significant difference ($P > 0.05$). Specific data analysis are shown in Table 4.

TABLE IV. THE EFFECT OF STRAIN IN MICE SUPEROVULATION.

Strain	ICR	C57BL/6J	BALB/c	FVB
the number of embryos	396	461	270	308
The average number of embryos	19.80 ^a	23.05 ^a	13.50 ^b	15.40 ^b

The same column with a different letter on the subject of data were significantly different by t test ($P < 0.05$).

IV. DISCUSSION

Superovulation is an important pattern of obtaining more embryos, which it is possible to reduce costs and improve reproductive efficiency, but its effect was affected by many factors. In this study, in order to obtain a better superovulation methods, we mainly analyzed the hormones, strains and weeks old.

The 5IU and 10IU of PMSG and hCG were used to be superovulated, respectively. we can draw the following conclusions from table 2. High doses of hormones would make to increase the number of ovulation in mice and superovulatory were better than the others. However, currently, there have been optimal hormone dosage in mice superovulation, and there have been many reports of research on this issue at home and abroad[2,3]. Most scholars have used a 5-10 IU dose of PMSG and hCG. The results demonstrated that using 10IU + 5IU dose of PMSG + hCG combination too ovulation was more better than the other combinations, which indicating that the hormone resistance of mice superovulation was a certain threshold. The dose is too

low, which can not meet the more oocyte development needs and lead to decline in the number of ovulation. However, the dose is too high to follicular cysts. Thus, the injected dose of hormones requires a suitable amount in the superovulatory process.

By comparing the number of ovulation between 5-week-old and 8-week-old mice in the table 3, superovulation were no significant difference ($P > 0.05$). But the number of ovulation of 8-week-old mice were than 5-week-old on the whole. So, we thought the two groups of mice reached sexual maturity and had similar physiological developmental stage, which led to there were no significant difference. However, the difference is derived from the two groups of mice with different stages of the reproductive cycle. Onadera and Ishijima reported that mice age and development of oocytes were related, and 10-12-month-old mice obtained the number of degenerate eggs was more than 2-9 month-old mice[4].

Mice strains for superovulation also has some influence. The number of ovulation of ICR and C57BL/6J were significantly more than BALB/c and FVB ($P < 0.05$). The superovulation of ICR and C57BL/6J were no significant difference ($P > 0.05$); BALB / c and FVB were no significant difference ($P > 0.05$). The average number of embryos of BALB / c and

FVB obtained less than the other strains in the table 4, which may be due to genetic causes with the inbred lines. The superovulation effect of ICR mice was better than BALB / c and FVB mice, which was due to the reproductive capacity of closed group be stronger than inbred. However, the number of ovulation of ICR mice were less than C57BL / 6J mice, and there may be other factors to pending further study. Spearow et al [5] and Byers et al [6] reported that the genetic background of mouse strains is one of the main factors of affecting superovulation, and the experimental results shown that the superovulatory effect of C57BL/6J strain was better than other strains, and BALB / c (10.0) strain was worse than other strains. This was consistent with the results of our study, which reflects the difference between two kinds of reproductive capacity of inbred lines.

In summary, superovulation is a very complex process and have many external factors interwoven. In our study, we only researched in the respect of hormone dose, mouse strains and week old, which the conclusion as following : (1) the hormone doses (with 10 IU) were better than those with 5 IU, but no significant difference was observed; (2) when the mice were injected with determined dosage of hormone, the effect of superovulation with ICR mice and C57BL/6J mice were significantly better than the BALB / c mice and FVB mice ($P < 0.05$); (3) meanwhile, the effect of mice with 8 weeks were better than those with 5 weeks without significance ($P > 0.05$). In this laboratory , using the hormone doses of 10 IU PMSG + 10 IU hCG to 8 weeks old ICR, C57BL/6J were relatively good effect of superovulation. In addition, there are also many other influences such as genetic characteristics, body condition, nutritional status, ovaries -functional status, season, temperature, light, anesthesia and so on, which need to be further explored.

ACKNOWLEDGMENT

The authors wish to thank Yuguo Yuan and Yong Cheng. This work was supported in part by a grant from the Priority Academic Program Development of Jiangsu Higher Education Institutions (PAPD), Jiangsu Co-innovation Center for Prevention and Control of Important Animal Infectious Diseases and Zoonoses, Graduate Research and Innovation Projects in Yangzhou University (CXLX-1435) and Jiangsu Province Science and Technology Support Project (BE2013679).

REFERENCES

- [1] Kanter M, Yildiz C, Meral I, et al. Effects of a GnRH agonist on oocyte number and maturation in mice superovulated with eCG and hCG[J]. *Theriogenology*, 2004,61: 393~398.
- [2] Kodayashi K, Okuyama M, Fujimoto G, et al. Subzonal insemination with a single spermatozoon using manipulation as-sisted sperm adhesion onto the ooplasmic membrane in mouse ova. *Mol Reprod Dev*, 1992,31:223~229.
- [3] Kimura Y, Yanagimachimachi R. Mouse oocytes injected with testicular sperm at ozoa or round spermatids can develop into normal off spring. *Development*, 1995,121:2397~2405.
- [4] Onodera M, Ishijima Y. Effect of Maternal Age on Viability of Ova in Mice. *J Fert Ster*, 1987,32 :114~117.
- [5] Spearow J L, Barkley M. Genetic control of hormone-induced ovulation rate in mice[J]. *Biol Reprod*, 1999,61:851~856.
- [6] Byers S L, Payson S J, Taft R A. Performance of ten inbred mouse strains following assisted reproductive technologies (ARTs)[J]. *Theriogenology*, 2006, 65(9):1716~1726.

The Study Of The Application Of The Online Monitoring Technology For Metal Oxide Arrester

JIA Jinling

School of Computer Science, Sichuan University of Science & Engineering, Zigong, China

CHEN Guangjian ,YAO Yi ,Shen Chuang

Sichuan University of Science & Engineering, Zigong, China

Abstract—By analyzing the work feature and failure mode of metal oxide arrester, this paper has made a study of the MOA online monitoring method suitable for engineering application. In terms of overall framework, detection method and feature extraction, this paper has also made a detailed design and verification for the whole MOA online monitoring system. Lastly, the experimental platform for simulation verification has been built accordingly.

Index Terms—Metal Oxide Arrester; Online monitoring; Feature extraction;Simulation

I. INTRODUCTION

Metal oxide arrester (MOA) has an excellent property of electrical protection and thus been widely applied in the field of over-voltage protection. It has also won the reputation as the bodyguard of power system. At present, the zinc oxide arrester has moved towards the large capacity, small size and direct current transmission, thus placing a higher demand on the online monitoring of the arrester. The effective monitoring and intelligent fault diagnosis can reduce the expense of power equipment by 25 to 50 percent and the accident rate of power grid by 75 percent. The development of the sensor and information technology has also made it possible to develop the online monitoring system of intelligent electrical equipment which is critical to the over-voltage protection. Hence, the online monitoring of intelligent electrical equipment can keep track of MOA parameter, reduce the frequency of outage inspection and ensure the reliable operation of power system, which is of significant meaning to the development of intelligent power grid.

II. THE FAILURE MODE OF MOA

As a new-type arrester, the MOA has the ability to withstand the transient over voltage, operating impulse over-voltage and lightning over-voltage. The aging or downgrading of the arrester may be caused by the moisture, uneven electric potential distribution and surface contamination. Once the aging or downgrading reaches a certain point, the thermal breakdown of ZnO valve block will damage the MOA, leading to the loss of protection. The MOA failure will occur when the change in the nonlinear characteristic curve reaches a certain degree. The cause of common failure can be classified as aging or moisture. In essence, the failure of the arrester is caused by the change of nonlinear characteristic curve of

the equivalent resistance which is made up of several valve blocks through parallel connection [1]. It can not guarantee that the arrester will has the low current in the case of rated power-frequency voltage (at the level of micro-amp below 110kV) and release the energy rapidly under the condition of impulse over-voltage. The electric parameter regarding the operation status of characteristic MOV has included the resistive current, fundamental-wave resistive current and power loss.

III. THE ONLINE DETECTION METHOD FOR MOA

The selection of detection method is an important part of online monitoring. It can have a direct influence on the testing result and input-output ratio of the whole system. According to the comparative analysis of the common MOA-aimed online detection methods, the fundamental-wave analysis method has been chosen.

If the resistive fundamental-wave component is stable, the bus signal will be assumed as follows

$$U = U_m \sin \omega t \tag{2-1}$$

The resistive current is expressed as

$$I_r = I_{r1} + I_{r2} + I_{r3} + \dots + I_{rn} \tag{2-2}$$

The active power consumption of valve block is expressed as

$$P = \int_0^T U \cdot I_r \tag{2-3}$$

$$P = U I_{r1} \sin^2 \omega t \tag{2-4}$$

Hence, the active power is only related to the fundamental-wave resistive component in the case of fundamental-wave voltage.

Compared with the fundamental-wave voltage, the higher harmonic voltage is quite small ($U_3 < 2\% U_1$), which means that the resistive current component generated by the higher harmonic voltage has an extremely low power consumption.

$$I_x = I_x + I_c \tag{2-5}$$

$$I_x = I_0 + \sum_{k=1}^n I_{km} \sin(k\omega t + \varphi_k) \tag{2-6}$$

$$I_x = I_0 + \sum_{k=1}^n I_{kn} \sin(k\omega t + \varphi_k) \tag{2-7}$$

According to $I = C \frac{du}{dt}$ and $U = IR$, it follows that

$$I_k = \sum_{n=1}^{\infty} I_{kn} \cos(knt + \varphi_k) \tag{2-8}$$

After simultaneous and simplified operation, the resistive and capacitive current magnitude of the kth harmonic wave can be calculated. They are related to the current magnitude I_{kn} , the harmonic phase angle η_k of the joint current and the harmonic phase angle φ_k of the voltage.

$$I_{rk} = I_{kn} \cos(\eta_k - \varphi_k) \tag{2-9}$$

$$I_{ck} = I_{kn} \sin(\eta_k - \varphi_k) \tag{2-10}$$

$$\frac{I_{r(m+2)}}{I_{rk}} = \frac{\beta - k}{\beta + k + 2} \tag{2-11}$$

If the nonlinear parameter $\beta = 5$,

$$\frac{I_{r5}}{I_{r3}} = \frac{5-3}{5+3+2} = \frac{1}{5}$$

then $\frac{I_{r5}}{I_{r3}} = \frac{5-3}{5+3+2} = \frac{1}{5}$. When the effective value of the fundamental-wave resistive current is summarized and calculated, the fundamental-wave resistive current magnitude of the higher harmonic wave is negligible.

Hence, the key is to find the Fourier coefficient. During the course of processing the digital signal, the FFT transformation should be used to obtain the Fourier coefficient indirectly.

IV. THE EXTRACTION OF CHARACTERISTIC QUANTITY IN THE ONLINE MONITORING OF MOA

The characteristic quantity indicating the operation status of MOA include the peak value of total leakage current, positive peak value of resistive current, negative peak value of resistive current as well as the effective value and power loss of the fundamental-wave current. The peak value of resistive current is the important index to measure the insulation property of MOA [2-4]. As an important characteristic parameter for the digital signal analysis, the resistive fundamental-wave current is related to the phase difference detection for the current and voltage.

The non-periodic signal function conforming to the necessary and sufficient condition of Dirichlet can be transformed into the Fourier series.

$$f(t) = a_0 + \sum_{n=1}^{\infty} (a_n \cos N\omega t + b_n \sin N\omega t) \tag{3-1}$$

The cycle of $f(t)$ is T and the DC component is a_0 . Fourier coefficient is expressed as follows

$$a_n = \frac{2}{T} \int_{-T/2}^{T/2} f(t) \cos(N\omega t) dt \tag{3-2}$$

$$b_n = \frac{2}{T} \int_{-T/2}^{T/2} f(t) \sin(N\omega t) dt \tag{3-3}$$

$$f(t) = a_0 + \sum_{n=1}^{\infty} A_n \sin(N\omega t + \alpha_n) \tag{3-4}$$

$$U(t) = U_0 + \sum_{n=1}^{\infty} U_{kn} \sin(knt + \alpha_k) \tag{3-5}$$

$$I(t) = I_0 + \sum_{n=1}^{\infty} I_{kn} \sin(knt + A_k) \tag{3-6}$$

$$I_{rk} = I_{kn} \cos(A_k - \alpha_k) = I_{kn} \varphi_k \tag{3-7}$$

The phase difference between kth harmonic voltage and current is φ_k . The kth harmonic phase angle of the current is A_k . The kth harmonic phase angle of the voltage is α_k .

$$I(t) = I_0 + \sum_{n=1}^{\infty} I_{kn} \sin(knt + A_k) \tag{3-8}$$

The photoelectric isolation has been conducted for the PT conditioning signal. Without sampling, it can directly enter the level detecting unit. When the detecting platform receives the signal, the logical module will start to detect the electrical level of PT signal. Meanwhile, the CT signal enters the A/D sampling unit of the terminal. When the high level is detected, CT will start to sample. At this point, the initial phase φ of the CT signal will be equal to the absolute value $|\varphi|$.

$$I_{rk} = I_{kn} \cos|\varphi| \tag{3-9}$$

$$A_k = \frac{2}{N} \sum_{n=1}^{N-1} I_{kn} \cos \frac{2\pi n k t}{N} \tag{3-10}$$

$$B_k = \frac{2}{N} \sum_{n=1}^{N-1} I_{kn} \sin \frac{2\pi n k t}{N} \tag{3-11}$$

Within one cycle, 256 pieces of sampled data will be collected. $N=256$

$$A_k = \frac{2}{256} \sum_{n=1}^{255} I_{kn} \cos \frac{2\pi n k t}{256} \tag{3-12}$$

$$B_k = \frac{2}{256} \sum_{n=1}^{255} I_{kn} \sin \frac{2\pi n k t}{256} \tag{3-13}$$

The peak value of the fundamental-wave for Fourier coefficient

$$I_{k1} = \sqrt{A_k^2 + B_k^2} \tag{3-14}$$

Resistive component of the fundamental wave

$$I_{r1} = I_{k1} \cos \varphi \tag{3-15}$$

Similarly, I_{r3} and I_{r5} can be obtained. The phase difference φ can be acquired through the software. When the voltage signal detected exceeds zero, DSP timer will start to count. When the current signal

detected is zero, DSP time will stop counting. The time difference will be converted into the arc angle.

There is another way to calculate the peak value of fundamental wave. Given that the sampling frequency is F_s , the total sampling point is N and a certain sampling point in N is n , then the frequency resolution is F_s/N . Based on the formula 2-28, the n th sampling point of the harmonic wave is acquired.

$$F_n = (n-1) * \frac{F_s}{N} \tag{3-16}$$

After the FFT transformation, the result will be stored in the array $Re []$ and $Im []$. The peak value of the harmonic wave can be obtained from the formula 3-36.

$$I_{Im} = \sqrt{Re[n]^2 + Im[n]^2} \tag{3-17}$$

The effective value of resistive current is

$$I_x = \sqrt{I_0^2 + \frac{I_1^2 + I_2^2 + I_3^2}{2}} \tag{3-18}$$

With regard to the increment of the fundamental wave and the resistive current for three times, the statistical operation for I_{Im} should be conducted every 48 hours so as to avoid the data overflow. The average value of the statistical operation for 30 times will be seen as the sampling point I_{Im} of one characteristic quantity. The increase in the fundamental wave and the discrete value of the resistive current for three times will be also recorded.

$$f_{A_n} = \frac{I_{Im(m+1)} - I_{Im(m)}}{I_{Im(m+1)} + I_{Im(m)}} \tag{3-19}$$

The overall evaluation

$$F_{A_n} = \sum_{i=1}^n \left(\frac{I_{Im(m+1)} - I_{Im(m)}}{I_{Im(m+1)} + I_{Im(m)}} \right) / (n-1)$$

is ,The m and n are the positive integers and can be determined during algorithm transformation.

If $F_{A_n} > 1$, it means a greater possibility for moisture.

If $F_{A_n} < 1$ and the probability of $I_{Im(m+1)}$ exceeding the warning value (as to frequency) is higher than 95 percent, it means the acceleration of the aging. The result is computed by DSP processor and stored in the characteristic structure. The constraint of the final characteristic quantity will be calculated below.

$$FH = \sum_{i=1}^{n-1} \sum_{j=1}^n \left(\frac{I_{Im(m+1)} - I_{Im(m)}}{I_{Im(m+1)} + I_{Im(m)}} \right) / (n-1) \tag{3-20}$$

V. THE DESIGN AND SIMULATION OF ONLINE MONITORING SYSTEM FOR MOA

From the perspective of signal transmission, the technologies concerned include the extraction, processing and analysis of the signal. The frequency domain analysis will be conducted to extract the fundamental-wave resistive component, higher harmonic resistive component and phase angle. When MOA is exposed to moisture, the fundamental-wave resistive component will increase greatly. In the case of aging MOA, the higher harmonic resistive component will be on the increase.

A. The design of the framework for online monitoring system

The framework of the online monitoring system can be seen in the figure 4.1. The module of data integration has included the CPLD chip, the logic control for synchronous sampling after the conditioning over PT and CT signal twice as well as the control of the signal sampling chip. The advance signal has included the amplifying circuit and filtering circuit. The signal transmission system has included the A/D conversion module, Zigbee communication module, multi-channel gating module as well as signal amplification and filtering. As a concentrated joint of regional signals, the embedded control platform has been equipped with the interface for temperature sensor and humidity sensor, which can be used as the auxiliary parameter to judge the failure. ARM9 is connected with DSP through asynchronous FIFO chip and SPI bus.

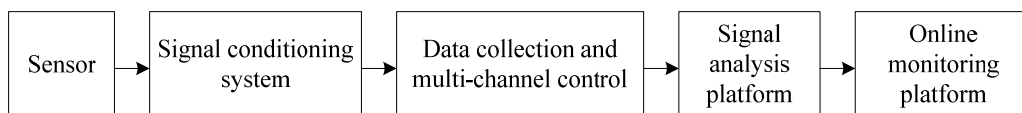


Figure1. The framework of the online monitoring system

The current signal after A/D sampling will be divided by the MOA leakage current signal which is reduced by the open-loop gain. After FFT transformation, it will lead to the Fourier coefficient I_{1m} and I_{3m} to be detected. According to the formula concerned, the fundamental-wave resistive component will be obtained.

B. The establishment of experimental platform and the simulation of signal analysis

The experimental platform has been built for the conditioning, transmission, collection and display of analog signal. The simulated experiment of signal processing will be conducted. The FIR filter will be designed through Matlab. The filtering parameter will be entered into the filtering module. The Fourier transformation over the current signal will be carried out. With the signal feature observed, the experimental analysis of the leakage current will be also made [5-6].

As seen in the figure 4.2 and 4.3, the 39-order low-pass filter will be designed ($F_s=1000\text{Hz}$, $F_{\text{pass}}=50\text{Hz}$, $F_{\text{stop}}=100\text{Hz}$ and $W_{\text{pass}}=W_{\text{stop}}=1$). After the filtering parameter is imported into the FDTAtool model, the filtering result can be found in the figure 4.4. With the high-frequency component removed effectively, the measurement error of leakage-current peak value will be reduced by around 10 percent. As shown in the figure 4.5 and 4.6, the filtering has improved the FFT transformation.

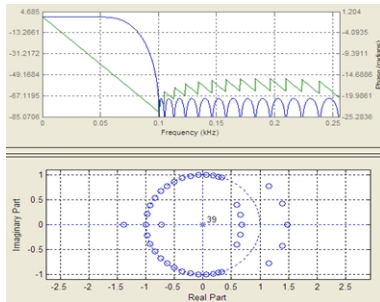


Figure 2 The design of FIR filter

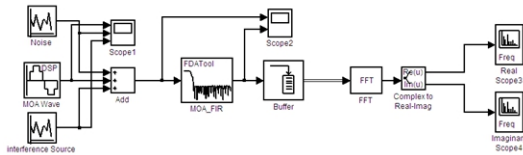


Figure.3 The simulation of signal analysis (with filter)

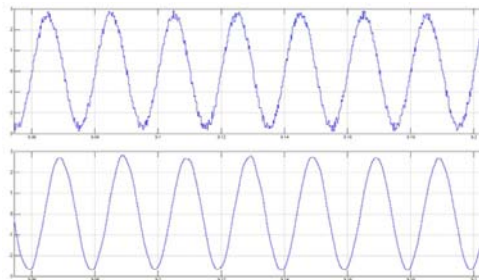


Figure.4 Filtering result

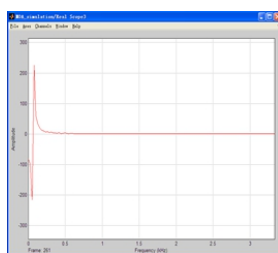


Figure5. Real-part curve (after filtering)

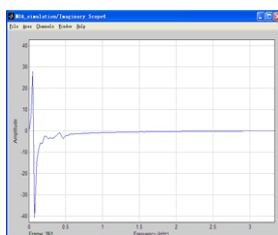


Figure6. Imaginary-part curve (after filtering)

CONCLUSION

This paper has made an analysis on the work feature of value block inside the MOA. By researching the failure model and measurement model for MOA, this paper has also designed a feasible technical solution for online monitoring. The experimental simulation and data analysis have been conducted. Hence, the online monitoring platform of MOA has been applied to the substation gradually. In conclusion, the research will push forward the building of online monitoring system in the intelligent power grid.

ACKNOWLEDGMENT

This work was supported in part by the Artificial Intelligence Key Laboratory project of Sichuan Province (No.2011RZY03, No.2014RYY01; No.2014RYY03) and Sichuan Provincial Key Lab of Enterprise Information and Control Technology for Internet of Things (No.2013WZY02) and the project of Sichuan University of Science & Engineering (No. 2012PY21; No. 2013PY06).

REFERENCES

- [1] M. Bartkowiak, M. G. Comber, G. D. Mahan, "Failure modes and energy absorption capability of ZnO varistors," IEEE Transactions on Power Delivery, 14(1), 1999, pp. 152-161.
- [2] DL/T987-2005, General technical conditions of resistive current tester for zinc oxide surge arrester [S]. Beijing: China Standard Press, 2005.
- [3] LIN Xin, WANG Jing, XU Jianyuan, WANG Na, "Influence of Metal Oxide Arrester on Very Fast Transient Over-voltage in GIS," High Voltage Engineering, 2012(10), pp. 2655-2661.
- [4] HE Ji-mou, ZHU Bin, ZHANG Hong-tao, ZHU Jia-xi, JIN Qiang, DU Shao-bin, "Research and Development of 750kV MOA Without Gap," Electrical Equipment, 2005, 6(12), pp. 17-20.
- [5] WANG He-xu, LIU Hai-feng, LI Jun-qing, "Metal Oxide Surge Arrester Typical Defect Analysis," Hebei Electric Power, 2012(06), pp. 20-22.
- [6] GB 11032-2010, AC metal oxide surge arrester [S]. Beijing: China Standard Press, 2010.
- [7] Du Yan-wei, Peng Qing-feng, Zheng Wei-dong, Zou Candong, "Cause Analysis of Fault of 220kV Metal Oxide Surge Arrester," Henan Electric Power, 2013(2), pp. 50-52.
- [8] WU De-guan, ZHOU Yu, YU Zhong-tian, PAN Kai, LI Hong-yuan, "A Fault Analysis of 500 kV Metal Oxide Surge Arrester," Insulators and Surge Arresters, 2013(3), pp. 58-60.

The Discrete Phase Simulation of the Non-linear Tube

Shaoju Wu, Junye Li, Fengyu Sun and Xinming Zhang

College of Mechanical and Electric Engineering, Changchun University of Science and Technology, Changchun 130022, Jilin, China

Abstract—Based on the research of the mechanism of abrasive flow machining, the non-linear tube --nozzle was employed as experimental subject, this paper adopts DPM model to do numerical simulation of nozzle abrasive flow machining process in granular movement form. It indicates that flow field has an impact on granular movement, and particle collision, the trajectory and location distribution are related to the velocity, turbulence intensity of flow field, which provides a theoretical basis for further analysis of particles motion and the collision between particles and wall of abrasive flow machining effect.

Index Terms—abrasive flow processing; DPM model; particle trajectories; particles collision; numerical simulation

I. INTRODUCTION

Abrasive flow machining is a kind of carrying through the medium of viscoelastic abrasive, reciprocating flow under the action of pressure being machined surface to realize the finishing processing. Abrasive particles are regarded as a myriad of cutting tools, repeated cutting the workpiece surface with its hard sharp edges and corners, so as to achieve certain process goal. In abrasive flow machining, it usually contains two relative abrasive cylinders, and the abrasive flows back and forth in the channel which is formed by the parts and fixtures flows. When abrasive evenly and gradually works on surface and edges of the channel, deburring, polishing and chamfering[1-3]. Nozzle is an important part of the engine fuel supply system, machining quality of its tiny hole directly influences engine fuel injection and combustion performance. Quality of holes directly affect the properties of the spray nozzle, oil line penetration and flow coefficient, will ultimately affect the economy, power performance and emission of the engine[4]. Three-dimensional entity model of nozzle is shown in Figure.1.

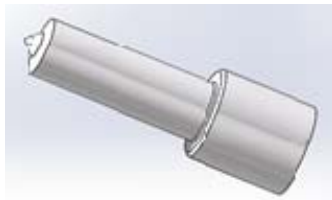


Figure 1. 3D entity model of nozzle

In abrasive flow machining process, due to the effect of driving of the fluid phase, it will produce inter-collision between abrasive and abrasive, abrasive and machining surface, thus the surface is collided and frayed. Abrasive flow processing function on the nozzle channel is ultimately caused by constantly particles collision, so this article do numerical simulation analysis from the perspective of particle collision. For the study of this technology, JiShiming et al scholars based on liquid-solid two phase fluid coupling theory, using the mixture model and Realizable k epsilon model of Euler-Euler multiphase flow model to study wall turbulence effect

under different particle concentration. The experimental results show that the particle collision of wall, reasonable and appropriate particle concentration was beneficial to the improvement of the comprehensive performance of abrasive flow[5]. Li Chen scholar based on the characteristic of soft abrasive flow machining, adopted the Princeton equation to analyze the stress of solid phased particles in the fluid, and the micro cutting mechanism of the soft abrasive particles. Experimental results show the correctness of the micro cutting mechanism analysis[6].

By discussing particle collision, particle trajectory, particle position distribution and particle velocity in the abrasive flow machining of nozzle, analyzing the relationship between particle trajectory and fluid turbulence intensity. It provides a theoretical basis to explore the relationship between the particle collision and surface quality of the non-straight pipe.

II. OVERVIEW OF DPM

Discrete Phase Model (DPM) is a solution of the multiphase flow Model, it required that volume fraction of the discrete particle cannot too big. Usually, we can get accurate calculation when the volume fraction is less than 10%. First of all, continuous phase flow field is calculated when solving discrete phase, combined with force analysis of variable flow field of discrete distribution in the continuous phase flow field, then calculate the acceleration of particles and particle trajectories[7-9].

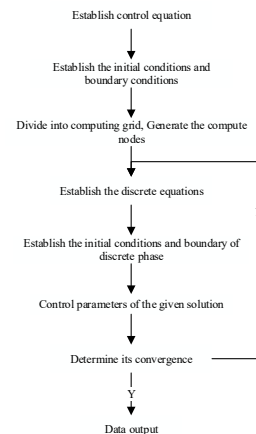


Figure 2. Numerical calculation step of DPM

DPM can analyze discrete particle movement in the complex flow field, calculate multiphase fluid coupling between different phase and the interphase coupling effect on the movements of dispersed phase and continuous phase. The impact of the particle collision of wall is affected by many factors, such as velocity of continuous, particle mass flow rate, fluid properties, particle properties, properties of the processed material surface, size and shape of workpiece, and so on. Many

scholars have adopted different methods to analyze the impact of the particle collision to wall in different fluid parameters[10-12]. In this paper, we studied particle collisions of inner surface of nozzle in low particle concentrations. By adopting Lagrange system to solve the discrete particle movement, we obtained particle trajectories and the information of wall collision, such as impact velocity, impact angle, impact location, and so on, further to analyze particle movements and the collision between particles and wall in abrasive flow machining effect. The numerical calculation step of DPM is shown in Figure.2.

III. THE SIMULATION MODEL ESTABLISHMENT AND PARAMETERS SETTING

To facilitate the simulation analysis, simplify the three-dimensional entity model of nozzle, hide its real parts, abstract its internal channel, only keep its main channel and six spray channels. The simplified result of three-dimensional entity model is shown in Figure.3.

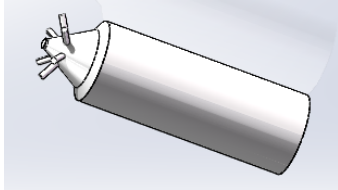


Figure 3. The simplified result of three-dimensional entity model

In the process of numerical simulation, assumed that inlet of abrasive flow is turbulent state, adopted k-epsilon turbulence model; A discrete phase setting of 8% volume fraction of SiC particles; defined boundary conditions of velocity-inlet and outflow. In order to accord with the requirement of simulation calculation, for nozzle model, first to block the calculation model, then divide every channel block with tetrahedral grids and set grid density degree, so as to achieve the purpose of controlling the number of grid and mesh quality. The meshing of the nozzle channel model is shown in Figure.4.

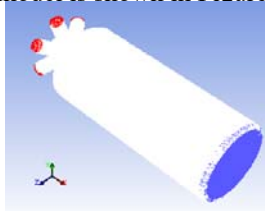


Figure 4. Meshing of the nozzle channel model

IV. SIMULATION RESULT AND ANALYSIS

It is based on the size of fuel spray nozzle model to set the parameters of dispersed phase: step length is 0.001mm and the maximum number of step is 4500. The paper selects second order upwind algorithm to calculate DPM of the machining model and obtain the residual graph as shown in figure.5.

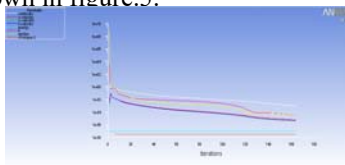


Figure 5. The calculate residual graph of nozzle channel

From the residual curve, we can see that iteration is about 160, so that it satisfies the convergence condition

and it testifies that the design of fuel spray nozzle channel model and the setting parameters is so reasonable that the model achieves fast convergence rate. To analyze the flow field characteristics deeply, the paper performed the numerical analysis for the abrasive motion trail, abrasive location distribution and velocity vector distribution to study processing characteristics of abrasive flow machining for fuel spray nozzle.

A. Analyzing Distribution Regularities of Abrasive Motion Trail

After analyzing the abrasive motion trajectory graph (figure.6) obtained by DPM, we can see that abrasive near the wall produce slippage following the flow field direction in the wall and there is little abrasive impacting the wall directly. It is the reason that inertia force keeps abrasive moving following the tangential direction and flow viscous resistance holds abrasive movement following the flow line direction, so that the abrasives are uneasy to pass through flow line to impact the wall; when abrasive flows the cross hole, regional resistance makes huge loss of kinetic energy only to slow the velocity obviously, so that it weakens the carrying effect of abrasive, which reduces delivering momentum of abrasive and decrease the momentum of abrasive. And then a few sections of abrasives generate accumulation in cross hole. Abrasive effect of impacting the wall was strengthened as abrasive overcame fluid viscous resistance by inertia force. Abrasive produced impact and slippage for the wall of cross hole during the process, which generated good grinding effect for cross hole. When the abrasive flow flew the cross hole over and over again, the progress would take place multiplying, which had huge machining effect on the cross hole.

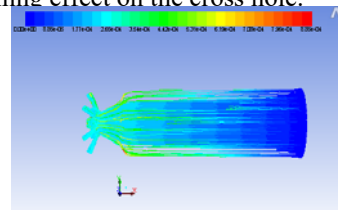


Figure 6. Abrasive motion trajectory graph

B. Analysis of Abrasives Location Distribution

In order to obtain distributed information of abrasive machining during process, we acquired graph of abrasive spatial distribution in fuel spray nozzle channel as shown in figure.7. From space distribution graph, we can see that the abrasives distribute densely near the internal surface of cross hole and fuel spray nozzle channel, while the abrasives distribute sparsely, which reflects inhomogeneous distribution characteristic of particle phase in turbulence media during abrasive flow machining fuel spray nozzle. The turbulence intensity of continuous phase is relatively high in the region of channel internal surface near the wall and that rotational flow in fuel spray nozzle produces, which indicates that the distribution of abrasive is relate to turbulence intensity of continuous phase.

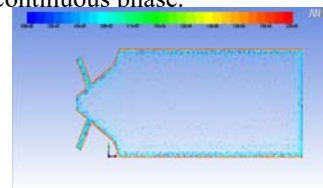


Figure 7. Space distribution of particles in nozzle channel

C. velocity vector analysis of Particles

In order to better analyze the characteristics of abrasive flow machining, we did numerical simulation on the abrasive flow machining of nozzle, and got the velocity vector diagram of particles and the velocity vector enlarge diagram of particles which are shown as figure.8 and figure.9. Figure.8 shows that, when the abrasive flow through the cross hole position of nozzle, speed increases suddenly, irregular changes in the direction of velocity vector, illustrate the particles collide with the wall become more acute, abrasive flow processing of this position is more obvious; Contrast particle velocity vector of wall of large holes with particle velocity vector of wall of small holes, find that the particle velocity of big hole near the wall is less than the speed of the holes near the wall. So we can forecast that wall processing effect of small hole is more obvious than large hole in the abrasive flow machining of nozzle.

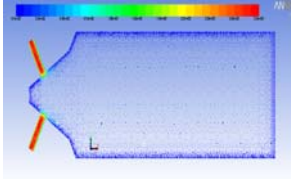


Figure 8. The velocity vector diagram of particles

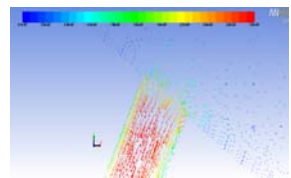


Figure 9. The particle velocity vector enlarge figure

V. CONCLUSIONS

Using a non-straight line pipe--nozzle as the research object, based on the discrete phase model and continuous phase fluid coupling calculation, the movement of particles in the process of abrasive flow machining was obtained.

Particle trajectory was affected by several competing factors, such as the inertia force, fluid viscous resistance and secondary flow. By analyzing the particle trajectory figure, we can see particle following features is very unhindered, the particles near the wall can produce sliding along the coming flow direction in the wall. When the abrasive flow through the cross hole of nozzle, due to the processing of the nozzle of abrasive flow belongs to the low density of low viscosity solid-liquid two-phase flow, inertia force plays a main role, inertia force makes the particles to overcome the fluid viscous resistance and enhanced impact on wall. Under the action of secondary flow accumulation of particles on the cross hole will further processing, thus can predict of abrasive flow machining process of nozzle in the effect the most significant areas for the cross hole position.

(1) By analyzing the distribution of the position of the particles, the distribution of particles is related to fluid turbulence intensity the abrasive flow machining process. Particle phase distribution is dense in the position with higher turbulent intensity in continuous phase, otherwise in the position with lower turbulence intensity, grain phase distribution is sparse.

(2) Through the particle velocity vector chart, we can found that machining pore size changes can lead to a change in the velocity of particles in abrasive flow machining process, thus causes the particles crash the wall more severely. Namely the particle collision intensity is associated with abrasive flow machining speed. Speed increases, the particles collide with the wall more acutely, so inner surface machining effect is more obvious. The speed of abrasive flow in the nozzle hole wall is far less than in the cavity of the hole, thus we can processing effect in the cavity of the hole is better than in the wall of the hole.

ACKNOWLEDGEMENT

Authors thank the national natural science foundation of china No. NSFC 51206011, Jilin province science and technology development program of Jilin province No. 20130522186JH and Doctoral Fund of Ministry of Education of China No. 20122216130001 for financially supporting this research under Contract.

REFERENCE

- [1] LI Jun-ye, LIU Wei-na, YANG Li-feng, et al, "Micro-hole of the common-rail abrasive flow machining equipment design and numerical simulation," Machinery Design & Manufacture, vol.2, pp.54-56, 2010.
- [2] TAN Yuanqiang, LI Yi, SHEN Yong, "On the Model and Pressure Simulation of Solid-fluid Two Phase Flow for Abrasive Flow Machining," Chia Mechanical Engineering, vol.19, pp.439-497, 2008.
- [3] LI Junye, XU Ying, YANG Lifeng, et al, "Research on Abrasive Flow Machining Experiments of Non-linear Tubes," China Mechanical Engineering, vol.25, pp.1729-1734, 2014.
- [4] Junye Li, Weina Liu, Lifeng Yang, et al, "The Development of Nozzle Micro-hole Abrasive Flow Machining Equipment," Applied Mechanics and Materials, vol.44, pp.251-255, 2011.
- [5] JI Shiming, ZHONG Jiaqi, TAN Dapeng, et al, "Distribution and dynamic characteristic of particle group with different concentration in structural flow passage," Transactions of the CSAE, vol.28, pp.45-53, 2012.
- [6] LI Chen, JI Shi-ming, TAN Da-peng, et al, "Study of Near Wall Area Micro-cutting Mechanism and Finishing Characteristics for Softness Abrasive Flow Finishing," Journal of Mechanical Engineering, vol.50, pp.161-168, 2014.
- [7] LI Guo-mei, WANG Yue-she, KANG Li-qiang, "Numerical simulation on solid particle movement characters of liquid-solid two phase flow in sudden expansion pipe by discrete particle model," Journal of Engineering Thermophysics, vol.29, pp.2061-2061, 2008.
- [8] WU Chundu, ZHANG Wei, HUANG Yongqiang, ZHANG Bo, "Numerical simulation of solid-liquid flow in a new kind of cyclone," Transactions of the CSAE, vol.22, pp.98-102, 2006.
- [9] WANG Miao, "The research on the erosion of liquid-solid two-phase flow in the pipelines," Hei Long Jiang: Northeast Petroleum University, 2014.
- [10] HE Xingjian, LI Xiang, LI Jun, "Numerical Simulation of Erosion and Abrasive in T Bends under Various Conditions," Process Equipment & Piping, vol.52, pp.69-72, 2015.
- [11] HU Xiaole, WANG Weifu, XIE Jianzhou, "Numerical Study of Discrete Gas-solid Two-phase Flow in 90° Thin Elbows," Light Industry Machinery, vol.33, pp.17-20, 2015.
- [12] ZHANG Tao, LI Hongwen, "Simulation Optimization of DPM on Gas-Solid Two-phase Flow in Complex Pipeline Flow Field," Journal of Tianjin University (Science and Technology), vol.48, pp.39-48, 2015.

Design of Signal Acquisition Circuit in Portable Electrocardiogram (ECG) Monitor

Yun Tang, Yanfang Li, Rong Li

Electronics Institute, Hunan University of Science and Engineering, Hunan Yongzhou 425199, China

Abstract—heart disease is a serious threat to human health, developing a household portable Electrocardiogram (ECG) monitor is essentially important. This paper designed a signal acquisition circuit with low power consumption and high stability, which can applied to portable ECG device.

Index Terms—portable, ECG, amplifier circuit, filter circuit

I. INTRODUCTION

The cardiovascular disease is one of the most serious disease threat to human life and health, but it has very strong concealment and unexpectedness, so it is one of the main problem for researchers. ECG monitoring instrument can detect anomalies of the heart, has become an important tool for clinical diagnosis and life science research. At present, the ECG monitoring instrument as workstation mainly used in the hospital, it is expensive and inconvenient, so that keep it back from popularizing in family[1],[2]. Then develop a household portable ECG has become our urgent problem. At the same time, the key issue was how to design a portable ECG with low power consumption, this paper is designed a signal acquisition circuit for portable ECG monitor.

II. THE GENERAL SYSTEM DESIGN

The general system design is shown in Fig. 1. The weak ECG signal from the surface of the body detected by electrodes is passed by a preamplifier circuit, a bandpass filter circuit, a 50Hz band-stop filter, a main amplifier circuit and a level lifting circuit. Then convert analog signal to digital signal. The data is stored in the microprocessor, and ECG is displayed on the liquid crystal display, which also can be transmitted to the PC for analysis. The ECG signal acquisition circuit is depict in Fig2.

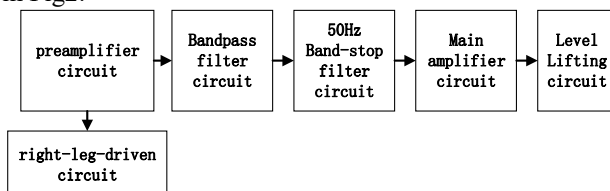


Figure1. General system design diagram.

ECG signal as the heart of human body, the signal is weak, the amplitude is about 0.05 ~ 5mv, the frequency is about 0.05 ~ 100Hz, the signal impedance is hundreds to thousands of ohm, ECG measurement conditions are

quite poor, in addition to including electromyogram (EMG) signal and respiratory wave signal, brain electrical signals in the body, but also interfere with the 50Hz power frequency and baseline drift, the electrode contact and other electromagnetic wave interference in vitro, moreover, taking into account the instrument portable characteristics, in the choice of devices should pay attention to the optimization, in order to reduce the overall circuit power consumption and volume[3].

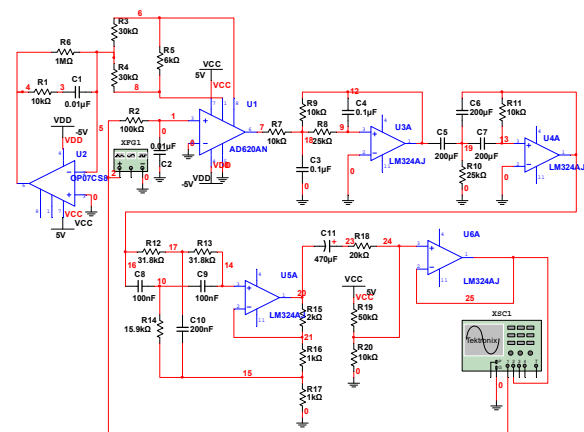


Figure2. ECG signal acquisition circuit.

A. Preamplifier circuit

The design of electrocardiograph preamplifier circuit in the system is very important, because which determine the main performance index of the whole system. Preamplifier circuit must designed with low noise and high common mode rejection ratio (CMRR). So we selected low power consumption, low voltage amplifier AD620 as core device that can accord with the ECG preamplifier high input impedance, low noise, and low power design requirements. In addition, adjust the gain of AD620 is very convenient, just directly controlled by an external resistor.

B. Right-leg-driven circuit

Right-leg-driven circuit is usually used for biological signal amplifier, to reduce CMRR. ECG signal is very weak, usually only a few microvolts. And due to the patient's body can also be as an antenna to receive the electromagnetic interference, especially 50 / 60Hz household power supply noise, this interference may

mask of biological signal, the signal is difficult to measure. Therefore, by adding the right-leg-driven circuit is used to eliminate noise interference.

C. Bandpass filter circuit

In this paper, low pass filter and high pass filter are combined into a bandpass filter circuit to limit the frequency of the signal to the frequency range of the ECG signal between 0.05 ~ 100Hz.

D. 50Hz band-stop filter circuit

50Hz power frequency interference is the main interference of physiological signal. Although the preamplifier circuit has strong inhibition effect on common mode interference, it will be part of the power frequency interference with differential mode signal mode pass through, and its frequency is in the frequency band, further more if coupled with the electrode and input loop instability and other factors, the output signal of the preamplifier will have strong power frequency interference. Therefore, it should be used to filter out the interference of the power signal by band-stop filter circuit.

E. Main amplifier circuit

As a result of the ECG signal amplitude is about 0.05 ~ 5mv, preamplifier circuit amplifies the 10 times the amplitude of 0.05 to 50mV, and ADC input voltage range 0 to 3.3V, in order to improve the A/D sampling circuit precision, also need to signal magnified 100 times. We choose low drift integrated operational amplifier OP07 as the amplifier.

F. Level lifting circuit

As the input voltage of Analog-to-Digital Converter (ADC) range 0 to 3.3V, the ECG signal is plus or negative, direct current bias must be applied.

III. CONCLUSION

We designed a signal acquisition circuit for portable ECG, with low power consumption and good noise immunity, which has certain practical value.

ACKNOWLEDGMENT

This work was Supported by the Construct Program of the Key Construct Discipline in Hunan University of Science and Engineering(Circuits and Systems),the first batch of 2014 Yongzhou guidance science and technology planning project (serial number 10), and Hunan University of Science and Engineering scientific research project (13XKYTB007) .

REFERENCES

- [1] Fu, Ping W., and T. J. Manning. "Personal health monitor." EP, US4803625. 1989.
- [2] Zhu, Da Huan, Y. H. Guo, and G. S. Wang. "Design of Amplifier Circuit for Portable Electrocardiogram Monitoring System." Chinese Medical Equipment Journal (2008).
- [3] Zhi-Jian, L. I., et al. "Design of ECG signal acquisition circuit." Modern Electronics Technique (2013).

Analysis Of Fracture Morphology And Extension Rules Based On Pressure Distribution In Fracture

Wang Suling¹, Su Yibao^{1,2}, Dong Kangxing^{1,2} and Long Ying^{1,2}

1. Northeast Petroleum University, Daqing, China

2. Daqing Oilfield Company, Heilongjiang Daqing, 163310

Abstract— According to the theory of fluid mechanics and 3D hydraulic fracture to establish joint fluid flow equation. In combination with 3D hydraulic fracture numerical simulation method, obtain the relationship between internal pressure change and the cracks form. The analysis result indicates that reservoir of the in-situ stress difference will not affect the crack fracture pressure. The smaller the difference between up and down interlayer and reservoir in-situ stress difference as well as elastic modulus and the greater the stress value of reservoir, seam pressure value is smaller. This is caused by hydraulic fracture wear layer in the interlayer, reduce crack propagation length and width decreased.

Index Terms—3D fracture propagation, Seam internal pressure, fracture configuration, influence factors

I. INTRODUCTION

Three dimensional shape of hydraulic fracture is the key to the fracturing design. Hydraulic fracture morphology is determined by reservoir structure, mechanical properties and fracture parameters. In general, the research of fracture morphology is from the angle of damage then fracture mechanics and establish reservoir rock mass fracture extension model and it will effect on the seam pressure as boundary conditions. The distribution of fluid pressure in the crack has a direct influence on the fracture morphology. Considering the non Newtonian fluid properties of the fluid in the crack. Simultaneous formation of cracks in the three dimensional direction in the uneven expansion process. That is to say fracturing fluid in the state of the crack is the extension of the crack which leads to the fluid boundary conditions. This paper is based on the establishment of a full three-dimensional model of hydraulic crack propagation, researched on crack propagation process and the stress distribution of relationships within the seam and fracturing fluid in hydraulic fracture is given in the direction of the seam, pointed and seam high pressure variation law. This paper also analyzed the reservoir geological conditions influence of the pressure distribution inside the joint and get the critical factors influence on crack propagation, provide technical support for reservoir fracturing design and fracturing fluid design.

II. THE FLOW CHARACTERISTICS OF FRACTURING FLUID IN HYDRAULIC FRACTURE

In three dimensional crack model, the crack width is a small amount compared with the crack length and height.

So the assumption of hydraulic fracturing of the seam flow belongs to the porous of the laminar flow between two parallel plates. And fracturing fluid is non Newtonian fluid, which is accord with the rules of power law fluid. According to the continuity equation of fluid flow, the expression of the variation rate of tangential flow rate of power law fluid can be obtained.

$$qd = -\left(\frac{2\alpha}{1+2\alpha}\right)\left(\frac{1}{K}\right)^{\frac{1}{\alpha}}\left(\frac{d}{2}\right)^{\frac{1+2\alpha}{\alpha}}\|\nabla p\|^{\frac{1-\alpha}{\alpha}}\nabla p \quad (1)$$

$$d = t_{curr} - t_{orig} + g_{init}$$

Among them, d for the crack opening width, t_{curr} and t_{orig} are respectively the current and the previous damage elements open width, g_{init} for the initial crack width, the default state is 0.002 m, ∇P_{is} is the direction of fracture pressure gradient.

The flow of fracturing fluid can be defined by the loss of filtration characteristics of the porous media. The fracturing fluid filtration volume can be determine by filtration coefficient which can be understood as a layer on the surface of the material permeability, the filter loss rate can be defined as

$$q_i = c_i(p_i - p_t) \quad (2)$$

$$q_b = c_b(p_i - p_b) \quad (3)$$

Among them, q_i and q_b are the fluid loss rate of fracturing fluid at the two sides of the crack, c_i and c_b were respectively the surface filter loss coefficient for both sides, p_i is liquid pressure in the cracks, p_t and p_b are respectively the pore pressure of the rock mass in the crack.

Fracturing fluid filtration is lost in the formation, which is influenced by three factors namely the filtrate viscosity, compressibility of formation fluid and wall building of fracturing fluid. Its expression is

$$c_1 = 0.17\left(\frac{K_{sp}\Delta p\phi}{\mu}\right)^{\frac{1}{2}} \quad (4)$$

$$c_2 = 0.136\Delta p\left(\frac{K_{sp}C_f\phi}{\mu}\right)^{\frac{1}{2}} \quad (5)$$

$$c_3 = c'_3 \left(\frac{\Delta p}{\Delta p'} \right)^{\frac{1}{2}} \quad (6)$$

Integrated filtration coefficient can be obtained by the harmonic mean method to calculate.

$$c = \frac{2c_1c_2c_3}{c_1c_3 + \sqrt{c_1^2c_3^2 + 4c_2^2(c_1^2 + c_3^2)}} \quad (7)$$

The filtration coefficient of theory calculation method is difference with actual filtration coefficient. In order to accurately determine the filtration coefficient of formation, provide the guidance of the scientific and reasonable for fracturing design. General theoretical calculation method is modified by the pressure drop analysis or the instantaneous pressure gradient method.

III. INTERNAL PRESSURE VARIATION LAW IN THE HYDRAULIC FRACTURE EXTENSION

A. Three Dimensional Finite Element Model of Hydraulic Fracture

Taking the fractured strata and upper and lower interlayer as the research object. Thickness of oil layer and interlayer thickness, take 200 m in the radial direction, take wellbore diameter 0.1 m and taken along the plane of symmetry 1/2 part study. The expansion of the preset cracks along the direction of maximum principal stress direction to set up low permeability reservoir fracture simulation of geometric model. Rock formations using solid element, casing using membrane unit and reset crack surface using injury unit. Mechanical model of the above unit generates discrete finite element model and the finite element model shown in "Figure 1".

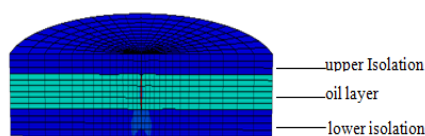


Figure 1. Stratum three-dimensional fracture finite element model

Reservoir rock in underground pressure by the overlying rock P_z rock inside the wellbore fracturing fluid pressure P_s and the role of the rock gravity G , on the upper and lower surface and weeks osmotic pressure P , the initial crack under a liquid pressure of fracturing fluid for P_s , fracturing fluid loss occurs on the fracture surface, need to set the filtration border. The model base is not allowed to have a rigid displacement. The z direction is zero in the bottom surface, The outer surface is applied to the X and z direction of the displacement constraint to simulate rock stratum on the model of lateral restraint.

B. Case Verificatio

Taking an oil well in Daqing as an example. The wells on the interlayer and reservoir stress difference were 5.0 MPa and 3.5 MPa, upper and lower interlayer thickness are 3.5m and 2.5m respectively, the vertical depth of fractured well is 1724m, elastic modulus and poisson's ratio of rock are 2.19 GPa and 0.21 respectively, the elastic modulus and poisson's ratio are 201 GPa and 0.3 respectively. The initial void ratio is 0.21 and the initial pore pressure is 18 MPa. X, Y, Z three to the initial stress were 25.6 MPa, 29.9 MPa and 36.5 MPa. Fracturing fluid injected into 3.0 m³ / min, the injection time is 350s. Calculate the crack shape shown in "Figure 2".

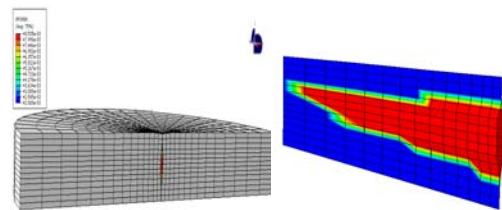


Figure 2. Crack purgation type

Through numerical simulation, the formation of the well fracturing of the formation of the half gap is 171m. Compared with the crack 185m obtained from the test, the error is 7.56%. This proves the rationality of the method.

IV. RESEARCH ON THE INFLUENCE FACTORS OF CRACK CROSSING INTERFACE EXPANSION

A. The Effect of Minimum Horizontal Stress Difference on Internal Pressure

Set up the minimum horizontal principal stress is 26 MPa. The mudstone under the minimum horizontal stress are respectively 32/31 MPa, 34/33 MPa. The maximum and minimum horizontal principal stress difference is 8/7 MPa, 6/5 MPa. The internal pressure contrast is shown in "figure 3".

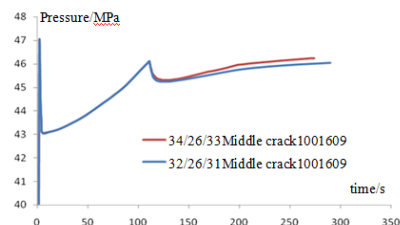


Figure 3. Contrast of stress in different minimum horizontal

From Figure 3, it can be seen that when the minimum horizontal stress difference is 7 MPa and 5 MPa, the crack initiation pressure is the same. When the pressure is superimposed on the ground stress difference is 5 MPa. Due to expansion cracks of mudstone interlayer to reduce the fracture pressure value. The power of the forward expansion of the crack is reduced and the length

of the crack is small. It can be seen that if the ground pressure is very fast in the process of hydraulic fracturing, the fracturing layer will appear.

B. The Influence of the Sandstone Reservoir's Pressure Value on the Pressure Inside the Crack.

When the barrier has the same stress difference analysis of sandstone reservoir of minimum horizontal stress values were 26 MPa and 28 MPa and 30 MPa. The internal pressure contrast is shown in "figure 4".

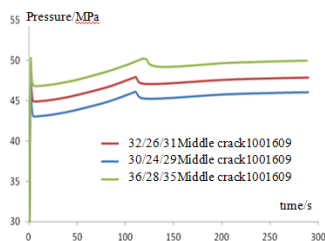


Figure 4. Variation of internal pressure under different stress values

From Figure 4, it can be seen that when the minimum horizontal stress value of sandstone reservoir is increased, the stress of crack initiation pressure will be increased. The greater the pressure in the reservoir, the greater the resistance of crack growth. Under the same condition of expansion, the greater the pressure value at the entrance of the crack, the more easy to wear layer, which makes the crack is not easy to expand.

C. Influence of Reservoir Pressure on the Mechanical Properties of Rock Mass.

When the modulus difference respectively 0.2 Gpa, 0.8 Gpa and 1.0 Gpa calculation of sandstone and mudstone interlayer on the crack expansion affect the height. "Figure 5" shows the comparison between oil layer and interlayer in different elastic modulus difference in fracture pressure.

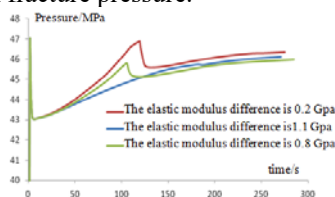


Figure 5. Contrast of stress in different elastic modulus

From Figure 5, under the pressure of fracturing liquid of sandstone and mudstone interlayer elastic modulus is smaller, the rock mass deformation smaller, and crack width is smaller, and joint sprain pressure process is faster and pressure increase resulting in fast wear layer.

IV. CONCLUSIONS

Considering the characteristics of the hydraulic fracture and the permeability of the fracture surface and the theory of fluid mechanics. The equilibrium equation of the fluid in the normal direction and tangential direction is established. The equilibrium equations of the fluid flow in the normal direction and tangential direction are established, the simulation method of the relationship between the pressure variation and the fracture morphology is realized by combining the mechanical model of the three dimensional hydraulic fracture.

By calculation, it is found that in the initial crack extension, the pressure drop is decreased with the crack length. Joint pressure makes up at the interface pressure. When the pressure value is reached to the pressure value of second times of crack, the stress value of the interface is basically the same as that in the crack, which leads to the crack in the length and height at the same time.

Analysis shows that the smaller the stress difference of reservoir the initial stress value of the target reservoir is more. And the difference of the mechanical properties between the upper and lower reservoirs the crack is easier to pass through the reservoir.

ACKNOWLEDGMENT

The authors thanks for the support of Natural Science Foundation of China (51374074) and Northeast Petroleum University Innovation Foundation For Postgraduate (YJSCX-2015-024NEPU).

REFERENCES

- [1] Yang You-kui, Xiao Chang-fu, Qiu Xian-de, "Fracture Geometry and Pressure Distribution in Fracture for Hydrofracturing," *Journal of Chong qing University*, vol.18, pp.20-26, 1995.
- [2] Zhu Jun, Ye Peng, Wang Su-ling, Xiao Dan-feng, Wang Hui, "3D numerical simulation of fracture dynamic propagation in hydraulic fracturing of low -permeability reservoir," *ACTA PETROLEI SINICA*. 2010
- [3] Wang Su-ling, Jiang Min-zheng, Liu He, "Study of hydraulic fracturing morphology based on damage mechanics analysis," *Rock and Soil Mechanics*, vol.42, 2011.
- [4] Zhao Yan-lin, "Coupling Theory of Seepage Damage Fracture in Fractured Rock Masses and Its Application," Changsha: Central South University, 2009.
- [5] Li Dan-qiong, Zhang Shi-cheng, Zhang Sui-an, "Pressure loss prediction model of newtonian fluid hydraulic fracturing in coalbed methane well," *COAL GEOLOGY & EXPLORATION*, vol.41, pp.22-25, 2013
- [6] Wang Hong-xun, "Hydraulic fracturing principle," Beijing: Petroleum industry press, 1987.
- [7] Wang Han, "A Numerical Study on Vertical Hydraulic Fracture Configuration and Fracture Height Control," University of Science and Technology of China, 2013.

The Analysis On The Thin Difference Layer Influences On The Hydraulic Fracture Sealing Ability

Wang Suling¹, Yang Lei^{1,2}, Dong Kangxing^{1,2} and Liu Fangchao^{1,2}

1. Northeast Petroleum University, Daqing, China

2. Daqing Oilfield Company, Heilongjiang Daqing, 163310

Abstract — The reasonable consolidation or isolation between layers is the key to the development of low permeability and thin reservoirs. Based on the three-dimensional numerical simulation method of hydraulic fracture propagation, Taking Daqing low permeability wells as an example, we have calculated the change law and influence factors of interface stress of hydraulic fracture in the expansion process of interface bedding. The computation indicated that the difference between the mechanical properties of bedding materials (gamma ray difference), initial ground stress difference and impermeable layer thickness are the main influencing factors of cracks' fracture propagation. By a lot calculations of Low Permeability Wells, given the condition of interlayer packer, and the calculations have provided a theoretical basis for the scene of fracturing technology.

Index Terms — Thin & poor reservoir, hydraulic fracturing, interlayer, sealing condition

I. INTRODUCTION

China's major oil fields have entered the later period; the technology of infilling adjustment well and the technology of thin & poor reservoir are important measures for the replacement of oil field output^[1]. This kind of reservoir has the characteristics of small single layer thickness, fine grain size and low permeability, the key problem that restricts the development of thin & poor reservoir is how to design the fracturing technology reasonably, in order to achieve small layer commingling production and main layer single production, increasing the utilization degree of reservoir and extending mining area^[2]. Therefore, the key to solve the above problems is to study on that the interlayer (transition layer) expansion effect on hydraulic fracture law^[3].

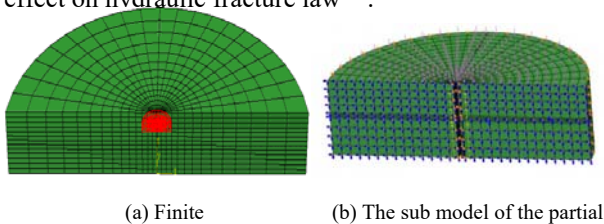


Figure 1. The sub model

American LawrenceLivermore laboratory's research shows that the factor affecting vertical extension of cracks only is interfacial shear strength between interlayer and production in shallow stratum. Zhang and Jeffrey who used 2D hydraulic fracturing model showed that, the stress difference between interlayer and production layer, elastic modulus difference and the shear strength of the interface which influence the crack at the interface inactivation, through and enter the interface^[4]. Chen Mian and some people have simulated that, in the horizontal direction of production layer, the effects of the inclusion of the litho logy mutants on the

crack propagation. The Chen's research has showed that mutant normal stress plays a decisive role on whether the hydraulic fracture can pass through the mutant, the normal stress difference of about 4MPa can promote the hydraulic fracture penetrating mutant, that cause to continue along the original direction^[5].

The influence factors of crack extension at the interface are given in the above research, but did not explain the mechanical expansion cracks in the interlayer. Base on this, this paper is based on the three-dimensional numerical simulation method of hydraulic fracture propagation, the expansion of the crack in the interface is given, analyzing the crack propagation in the interface and the main factors affecting the morphology, provide a theoretical basis for the design of hydraulic fracturing on the scene.

II. THE MECHANICS MODEL AND FINITEELEMENT MODEL OF FULL THREE-DIMENSIONAL HYDRAULIC FRACTURE

Take the fractured formation and upper and lower interlayer as the research object, the thickness contains oil layer and interlayer, taking 200m in the radial direction, bore diameter 0.1m, the expansion direction of the default crack along the direction of maximum principal stress, and no cracks changed in the expansion process. And the sub model technology is used in the simulation, because of the contradiction between the thicknesses of the interface and the length of the whole crack. The sub model is a finite element method to obtain a finer mesh division of the model; the established three-dimensional finite element model is shown in Fig 1(a). The local sub model of the sand shale interface is shown in Fig 1 (b).

Reservoir rocks exposed to overlying rock pressure P_z , effect of rock gravity, the effect of fracturing fluid pressure P_s in well bore, osmotic pressure P is exerted on the upper and lower surfaces and the week surface, the pressure P_s of the fracturing fluid in the initial fracture. Because of the filtration of fracturing fluid on fracture surface, it is essential to set the filter loss boundary. The bottom of model is not allowed to have a rigid displacement, the displacement constraint of Z direction is zero in the bottom surface, and the outer surface is applied to the displacement constraint of the X and Y direction, in order to simulate the lateral restraint of the formation rock. In the three-dimensional simulation of hydraulic fractures, including two main steps, (1) apply gravity, initial stress field and boundary conditions, to form ground stress near the bottom of the well, (2) simulating fracturing process.

III. STUDY ON THE PROPAGATION MECHANISM OF THE CRACK AT THE SAND/SHALE INTERFACE

Analysis and calculate a low permeability fractured well in a peripheral oilfield in Daqing, interpret the results according to the stress profile of the well. This well's fracturing reservoir is basically in low stress areas, there are 2.0MPa stress of stress shielding at over and underlying, and the thickness of over and underlying are respectively 2.0m and 2.5m, and the natural gamma code difference is 87.5API, fractured well section 1947-1951m, the elastic modulus and Poisson's ratio of rock materials are 2.99GPa and 0.21 respectively, the elastic modulus and Poisson's ratio of the casing are 201GPa and 0.3 respectively, initial void ratio is 0.21, initial pore pressure is 18MPa, initial earth stress of X, Y, Z direction are 25.6MPa, 29.9MPa and 36.5MPa respectively, fracturing fluid injection is 3.0m³/min, injection time is 350s. The change of maximum principal stress at the interface is calculated as shown in Fig 2.

From Figure 2, we can find that, with the crack propagation, the distribution law of the maximum principal stress is also changed at sand-shale interface. At the initial fracturing, interface maximum principal stress along the interface distributed rough uniformly, and the principal stress at both ends of the crack is greater. Along

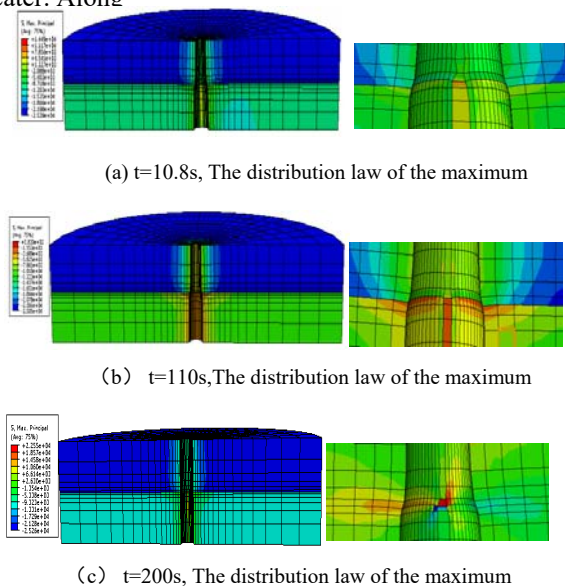


Figure 2. The maximum principal stress distribution of

with the extension of the crack on the interface, the tensile load of interface is on the increase, and the maximum principal stress of crack tip is also on the increase. When the crack passes through the interface to the upper mudstone, the maximum principal stress, with crack extension, has the tendency to expand to the right mudstone, and makes the crack which after pass through the interface layer extends and turn.

For the isolation effect of interlayer, changing the mechanical properties of sand shale reservoir and difference of initial ground stress in reservoir, the obtained distribution of maximum principal stress is shown in Figure 3 and Figure 4.

From Figure 3, we can find that, when the sand-shale material is the same and under the action of hydraulic pressure, maximum principal stress that generated at the interface along the crack symmetrically. And the maximum principal stress is greatest at the crack location. When the materials of sandstone and mudstone are different, the amplitude of maximum principal stress is increased at the interface. And the values of maximum

principal stress along the two ends of the crack are different, the right side is greater than the left, the maximum principal stress amplitude of the crack is greater than that of the homogeneous material. At the same time the crack has the tendency to expand and steer. This shows that the difference of properties of sand shale material has greater influence on crack growth and expanded direction.

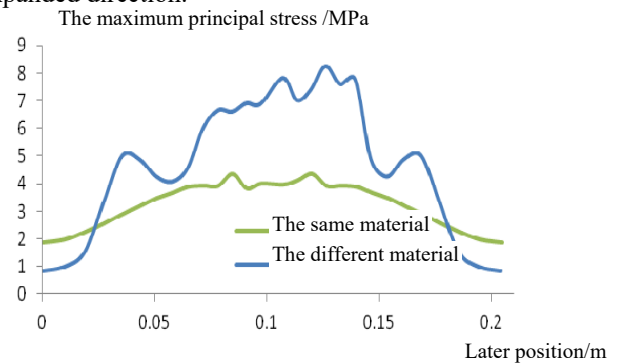


Figure 3. Mechanical properties of different sand shale

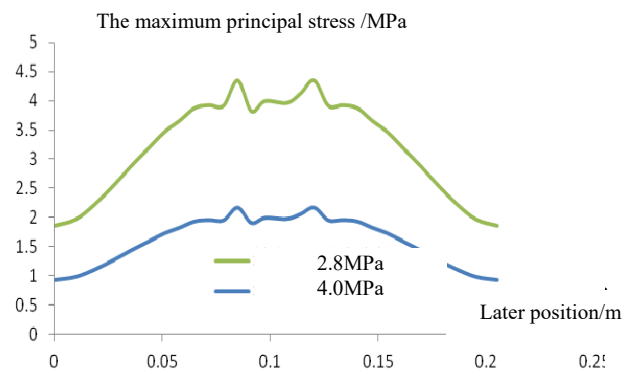


Figure 4. Comparison of maximum principal stress under different minimum principal stress difference

the sand-shale maximum principal stress difference, the distribution of maximum principal stress at the interface is same, but the amplitude of the maximum principal stress is different, the maximum principal stress decreases with the increase of the minimum horizontal stress difference. This shows that the greater the difference of the minimum horizontal principal stress, the crack is more hardly to expand at the interface, but it does not affect the direction of crack propagation.

IV. THE FEASIBILITY STUDIES ON THE BARRIER CONDITION OF SAND-SHALE INTERFACE

According to the above theoretical analysis: the ground stress difference of sand shale interlayer, the mechanical properties difference of sand shale, the thickness of the sand mudstone, fracturing fluid property and construction parameters are major factors that influences mudstone sealing effect. Adopting the above simulation method of the cracks, taking low damage fracturing fluid viscosity as an example, selecting different pump flow (1.5 m³/min, 2.0 m³/min, 2.5 m³/min and 3.0 m³/min), select the pre injection time (250s, 300s, 350s and 400s).

V. CONCLUSIONS

A. Analyze the local interface which the crack through, by the sub model analysis technology, and find that the change of ground stress in the local interface determines the shape of crack extension. With the propagation of

cracks to the interface, the maximum principal stress of the interface gradually converges to the crack ends from the uniform distribution along the interface. When the crack reaches the interface, the maximum principal stress at the crack tip reaches the maximum. When the mechanical properties of sand shale differ greatly and heterogeneous distribution at the position of interface, shear stress at one end of the crack will increase which will lead deflection of the direction of maximum principal stress, and causing crack turn.

B. According to theoretical analysis and field experiment, adopting three criteria—the gamma value difference tested, mudstone interlayer thickness and stress difference, to judge the separated effect of barrier seal. To form an ideal artificial crack, under the condition of calculation, natural gamma difference is greater than 64API, the difference of ground stress is more than 2.0MPa, and the interlayer thickness is greater than 2.0m and adopting appropriate construction displacement.

ACKNOWLEDGMENT

The authors thanks for the support of Natural Science Foundation of China (51374074) and Northeast

Petroleum University Innovation Foundation For Postgraduate (YJSCX-2015-024NEPU) .

REFERENCES

- [1] Yue Dengtai, "Oil Field Development Summary on Improving the Effect of Developing Maturing Oilfields and IOR Techniques," ACTA PETROLEI SINICA, J, CHINA, vol. 19(3), pp. 46-51, July 1998.
- [2] Wang Anpei, Liu Xuemei, Sun Xuexia, Tang Zhiqing, Chu Wanquan and Cai Shuxing, "Fracturing Technology of Deep Low Permeability Reservoir with Thin and Poor Oil Layer in Zhongyuan Oilfield," DRILLING & PRODUCTION TECHNOLOGY, J, CHINA, vol. 35(5), pp. 70-71, September 2012.
- [3] Liu Yuzhang, Fu Haifeng, Ding Yunhong, Lu Yongjun Wang Xin Liang Tiancheng, "Large scale experimental simulation and analysis of interlayer stress difference effect on hydraulic fracture extension," OIL DRILLING & PRODUCTION TECHNOLOGY. J. vol. 36(4), pp. 88-92, April 2014.
- [4] Hanson M.E. "Some Effect of Stress, Friction and Fluid Flow on Hydraulic Fracturing," SPEJ. J. vol. 22, no. 3, pp.321-332, June 1982.
- [5] Jin Yan, Chen Mian, Zhou Jian, Geng Yudi, "Experimental study on the effects of salutatory barrier on hydraulic fracture propagation of cement blocks", ACTA PETROLEI SINICA. J. vol. 29(2), pp. 300-302, March 2008.

Positioning Using the Sun Shadow

Bian Min-Hua, Yang Shu-Lei, Gao Fang, Zhang Wei*, Liu Wei-Xing, Yang Ai-min

North China University of Science and Technology, Institute of metallurgy and energy and Information engineering college, Tangshan, 063000, Hebei, China

Abstract—The sun shadow location positioning technology to give video capture is an important method of analyzing the video data. In this paper, the first use of the celestial sphere model to simulate the solar-terrestrial relations, by analyzing the characteristics of the observation point and normal plane section features, using knowledge of vector and spatial relationships deduced long shadow formula, that is reflected in the geographical latitude, the height of pole and observed ground the relationship between the time, and finally get the variation of the length of the shadow. Then establish a multivariate equations group based on the relationship, because the solution to the state of aggregation and thus the choice of K- mean test, using SPSS software to gather the number of sets were analyzed and straight bar possible latitude and longitude coordinates.

Index Terms—Multivariate equation group, K- mean test, Celestial sphere model

I. INTRODUCTION

With the development of technology, a method using GPS coordinates simultaneous determination of three-dimensional mapping positioning technology will extend from land and offshore to the whole ocean and outer space, from a static to a dynamic expansion, expanded from a single point positioning to local and wide area differential, after processing extensions to engage in real-time (quasi-real-time) positioning and navigation, which greatly broaden its scope and role in all walks of life. This paper describes the sun shadow positioning technology, without the aid of sophisticated mathematical calculations and change the instrument only the shadow of the sun to determine the location, its field of criminal investigation, recording has great significance.

II. THE PREPARATION OF MODEL

Known the given date of issues is April 18, then be able to deduce that day the sun direct point latitude [1]. Fig.1 is obtained based on the geometric analysis:

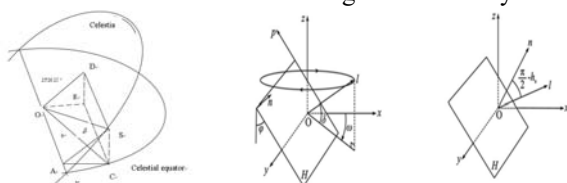


Fig.1 Celestial schematic model Fig.2 Geometric derivation schematic

Fig.1 shows a celestial sphere model, that the Earth was the center of rotation of the Earth around other stars, this is done in order to facilitate observation and analysis, so Fig.1 o represents the Earth, s represents the sun, the sun direct point represent latitude represents yellow longitude, the so-called yellow longitude sun on the ecliptic from the vernal equinox from west to east movement to the designated location of the turn angle, $\angle AOS$, $O\gamma$ is the line of intersection of the ecliptic plane and the equatorial plane, OD, AS, OS in the ecliptic plane, OD, AS, OS inside, $OD \perp O\gamma, AS \perp O\gamma, OE, AC, OC$ respectively OD, AS, OS equatorial plane of the

projection, respectively pedal E, C, C, according to the geometric relationship in the:

$$\text{In Rt } \triangle SAO, AS = OS \cdot \sin P$$

$$\text{In Rt } \triangle OCS, SC = OS \cdot \sin \delta$$

$$SC = AS \cdot \sin 23^\circ 26' 21'' = AS \cdot \sin P \cdot \sin 23^\circ 26' 21''$$

$$\sin \varphi = \sin \alpha \cdot \sin 23^\circ 26' 21'' = 0.397775 \sin \alpha$$

$$OS \cdot \sin \delta = OS \cdot \sin \lambda \cdot \sin 23^\circ 26' 21''$$

So get direct a formula to calculate of the sun direct point latitude:

$$\delta = \arcsin(0.397775 \sin p) \quad (1)$$

To ensure accuracy, using date instead of ecliptic longitude to calculate longitude latitude direct point, but needs to separate calculation according to the season:

During this period a total of 186 days, thinking that the sun operate 180-degrees in the ecliptic during the time. Let start from March 21, the sun running n days, the n days running p longitude:

$$p = \frac{180^\circ}{186} \cdot n \quad (2)$$

Into (1), we obtain:

$$\delta = \arcsin(0.397775 \sin(\frac{180}{186} \cdot n)) \dots \dots n \in [0, 186] \quad (3)$$

During this period a total of 90 days, thinking that the sun operate 90-degrees in the ecliptic during the time., set from March 21 Start, the sun running n days, the n days running p longitude:

$$p = 180^\circ + \frac{190^\circ}{90} \cdot (n - 186) \quad (4)$$

Into (1), we obtain:

$$\delta = -\arcsin[0.397775 \sin(n - 186^\circ)] \quad (n \in [186, 276]) \quad (5)$$

During this period a total of 90 days, thinking that the sun operate 90-degrees in the ecliptic during the time, set up starting from March 21, the sun running n days, the n days running p longitude:

$$p = 270^\circ + \frac{90^\circ}{89} \cdot (n - 276) \quad (6)$$

Into (1), we obtain:

$$\delta = -\arcsin[0.397775 \cos(\frac{90}{89} \cdot (n - 276))] \quad (n \in [276, 365]) \quad (7)$$

The hour angle you need to be evaluated by the longitude of the observation point, the time of issues is Beijing time, equal to eight East zone, time, longitude 120 degrees, according to the longitude of the observation site and longitude 120 degrees east longitude can calculate the time difference, when the results of the local observation sites, but also can be calculated according to the local time when the observation point hour angle expression, set up observation points of longitude east longitude x, y represents Beijing, hour angle of the observation point expressed as:

$$\omega = \{12 - [y + (x - 120)/15]\} \cdot 15 \quad (8)$$

Establish a space Cartesian coordinate system o-z to be the earth's axis, x-o-y surface of the equatorial plane, o is the observation point, shown in Fig.2:

According to the geometric derivation can be drawn from derived formula of the solar elevation angle:

$$h = \arcsin(\cos \omega \cos \varphi \cos \delta + \sin \omega \sin \delta) \quad (9)$$

III. THE ESTABLISHMENT OF MODEL

Examples are given below: Using the given data (As Table 1) as a reference, according to the vertex coordinate of Sun shadow data of a straight fixed rod on a level surface, a mathematical model to determine which locations straight bar. The model is applied to the vertex coordinate data of shadow of Annex 1, to give a number of possible locations.

Table 1 Rod vertex coordinates

Beijing time	X(m)	Y(m)	Beijing time	X(m)	Y(m)
14:42	1.0365	0.4973	15:15	1.4349	0.5598
14:45	1.0699	0.5029	15:18	1.4751	0.5657
14:48	1.1038	0.5085	15:21	1.516	0.5715
14:51	1.1383	0.5142	15:24	1.5577	0.5774
14:54	1.1732	0.5198	15:27	1.6003	0.5833
14:57	1.2087	0.5255	15:30	1.6438	0.5892
15:00	1.2448	0.5311	15:33	1.6882	0.5952
15:03	1.2815	0.5368	15:36	1.7337	0.6013
15:06	1.3189	0.5426	15:39	1.7801	0.6074
15:09	1.3568	0.5483	15:42	1.8277	0.6135
15:12	1.3955	0.5541			

Note: Measurement Date: April 18,

2015The X and Y direction in axes of topic is difficult to determine, but the shadow of the rod vertex coordinates are known, it is possible to solve the rod Movies changing with time, the specific process is as follows:

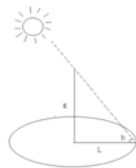


Fig.3 Solar elevation angle view

g represents the height of the rod, L represents a long shadow, h represents the solar elevation angle, according to the geometric relationship is:

$$L = \frac{g}{\tan h} \quad (10)$$

(9) h has been deduced, put h into the draw:

$$L = \frac{g}{\tan[\arcsin(\sin \delta \sin \varphi + \cos \delta \cos \varphi \cos \omega)]} \quad (11)$$

Title given observation date is April 18, from 21 March has 29 days, that is, n = 29, into (11), we obtain = 0.0829rad, in (19), δ, L, y is known the amount of, g, X is unknown, because the title is given 21 sets of data, randomly selected three sets of data to solve a set of values of φ, g, X, the conversion issue for the sake of multivariate equations look:

IV. THE SOLVING PROCESS MODEL

Putting 3 sets of values of Multivariate linear equation group (L₁, y₁), (L₂, y₂), (L₃, y₃) into (20) in order to solve a set, g, the value of x at least. 21 randomly selected set of data for the three groups a total of 1330 kinds of data to solve randomly drawn from 30 sets of data into the calculation, you can get 30 groups of highly straight rod Table 2:

Table 2 30 sets of data obtained rod length data

No.	g (m)	No.	g (m)	No.	g (m)
1	-2.0408	11	-2.0391	21	-2.8079
2	-2.0581	12	-2.0398	22	2.0222
3	-2.0502	13	-2.0395	23	-2.0356
4	2.0428	14	-2.0398	24	-2.0397
5	-2.0428	15	-2.0310	25	-2.0431
6	-2.0523	16	-2.0498	26	2.0393
7	2.0645	17	-1.9955	27	2.0470
8	-2.0523	18	-2.0542	28	2.0384
9	2.0898	19	-2.563	29	2.0381
10	-2.0381	20	2.0469	30	2.0409

Taking the model of 30 group date g=2.04 and determining the length of the rod.Reduce an unknown,so

the δ, L, y, g is known. φ, x is an unknown, at the same time, the problem is transformed into a problem of solving the equation group of two yuan. From the date of the 21 groups randomly selected two groups calculated by unknown contact .Besides random selected from 99 groups of date into the calculation of the value of the 99 groups φ, x. Last with MATLAB [2]of 99 groups(x, y) is plotted to give the Fig 4:

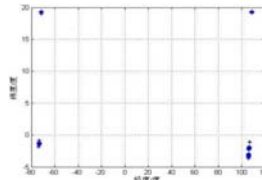


Fig.4 Location maps

According to the Fig.4 it can be found 99 locations gathered in four areas,through SPSS [3] software using the K- mean test[4]for data processing,obtain the desired value.Table 3

Table 3 observation point location table

longitude and latitude	The location of the observation point
(108.5681E , 19.2816N)	Hainan
(71.4834W , 19.3226N)	Dominica
(73.4856W, 1.5124 X = x S)	Colombia
(106.2152E, 2.3015S)	Singapore

V. CONCLUSION

Through the sun direct point latitude, longitude yellow sun elevation angle geometry deduced shadow length and sun direct point latitude, shooting location relation height dimensions, rod, and the establishment of a pluralistic equations solved using matlab, draw multiple sets of solutions. Finally, cluster analysis spss analysis derived four optimal solution.

REFERENCES

[1] Jiang Hong Li.Mathematical derivation and analysis of direct sun latitude[J].Mathematics bulletin,September,2009.
 [2] Xue Ding Yu,Chen Yang Quan.Advanced Applied Mathematical Problem Solutions With MATLAB[M].Beijing:Tsinghua University Press,2004.
 [3] Li Hong Cheng,Jiang Hong Hua.SPSS Data Analysis.Beijing:People Post Press,2012.
 [4] Deng Min,Liu Qi Liang.Spatial clustering analysis and its application.Beijing:Science Press,2011.

The Study Of Taxi Subsidy Scheme Based On Fuzzy Comprehensive Evaluation Of The Perspective Of The Passengers

Kang Yanhong, Pan Yuhang, Long Yan, Yang Aimin*

North China University of Science and Technology, Tangshan, 063000, Hebei, China

Abstract—When this article is studying the taxi subsidy scheme on the “ease taxi difficult” issue, the waiting time, taxi risk, special time, special places such evaluation factors are considered as the evaluation index, using fuzzy comprehensive evaluation model based on entropy method to analysis the data of passenger satisfaction before and after the taxi subsidy scheme appear, and obtaining the conclusion that the implementation of taxi subsidy program does improve the passenger satisfaction, to a certain degree, it eases the difficult problem of the taxi.

Index Terms—Entropy Method, Fuzzy comprehensive evaluation, Membership

I. INTRODUCTION

In 2015, "Internet +" action plan was first put forward, what follows is the mobile Internet, cloud computing, big data, networking and other electronic information technology and industry. At the same time, the taxi software service platform based on the Internet to build by companies is gradually developing. Suddenly different software and service companies have launched various subsidies to win over customers and seize market share, which set off a wave of taxi boom, however, the "taxi difficult" issue is still the focus of attention. Many scholars analyzed the social effects which was caused by taxi software, Cai Jiming, Jiang Ning[1] pointed out that the country's major cities travel difficulty, difficult problem of a taxi is increasingly becoming the norm of urban residents' daily work and life, which seriously affects the population and social well-being index Productivity. Chang Yingzheng[2] analyzed the reasons of the taxi software price war, and deeply studied their common features, and then put forward the corresponding policy recommendations and thinking. Bian Yang[3] analyzed the balance between supply and demand of taxi operators network at a fixed demand, and built a urban taxi network equilibrium model. Dong Zhichen, Li Qingheng[4] built a satisfaction survey model from the passenger point of view to determine the weighting factor for each model index system, through the use of quadrants propose the measures and

recommendations for the taxi industry to improve the satisfaction. Wang Xiaobo[5] in the background of the current rapid development of mobile Internet, dispatched and managed the resources for taxi flexibly and accurately, through the mobile Internet applications, it can make taxi drivers find passengers who need service faster, reduce empty consumption, make passengers quickly get services, and reduce urgency of waiting time.

II. THE ESTABLISHMENT OF PASSENGERS' SATISFACTION WITH THE QUALITY OF CAR MODEL

Analysis pre and post subsidy program introduced, "hard to take a taxi " issue whether the remission, from the passenger's point of view quantitative analysis of satisfaction pre and post the subsidy passenger ride. Fuzzy comprehensive evaluation[6] converts the qualitative appraisal to the quantitative evaluation, clear and systematic Solve the satisfaction of the problem is difficult to quantify.

According to considerations of passenger travel before taxi company subsidy program introduced, setting the waiting time, taxi risk, special time and special areas for the evaluation factors. Suppose evaluation factor set to $u_1 = (x_1, x_2, x_3, x_4)$. After the introduction of the subsidy scheme, passenger travel considerations Increased, evaluation factor changes, Setting the the waiting time, taxi risk, individual needs, additional income and software familiarity for the evaluation factors, scilicet $u_2 = (x_5, x_6, x_7, x_8, x_9)$.

In order to better illustrate the passengers on ride quality satisfaction, according to the data in taxi software market analysis report from 2013 to 2014, each evaluate factors of satisfaction degree will be divided into five levels, it is evaluate set. Passengers ride quality satisfaction rating classification in Table 1 below, the following study after the introduction of the subsidy program as an example:

TABLE 1 CLASSIFY THE EVALUATION SETS OF PASSENGERS TRAVELING SATISFIED WITH THE QUALITY

Num	Factors	A	B	C	D	E
1	waiting time	≤ 5	$5 < t < 10$	$10 \leq t < 20$	$20 \leq t < 30$	≥ 30
2	Taxi Risk	≤ 0.05	$0.05 < \lambda_1 \leq 0.1$	$0.1 < \lambda_1 \leq 0.2$	$0.2 < \lambda_1 \leq 0.3$	> 0.3

3	Individual needs	≤ 0.01	$0.01 < \lambda_2 \leq 0.1$	$0.1 < \lambda_2 \leq 0.2$	$0.2 < \lambda_2 \leq 0.3$	> 0.3
4	Additional income	≤ 0.1	$0.1 < \lambda_3 \leq 0.2$	$0.2 < \lambda_3 \leq 0.3$	$0.3 < \lambda_3 \leq 0.4$	> 0.4
5	Software familiarity	≤ 0.05	$0.05 < \lambda_4 \leq 0.1$	$0.1 < \lambda_4 \leq 0.2$	$0.2 < \lambda_4 \leq 0.3$	> 0.3

According to the five standard latency metrics, construct five levels of membership functions. Among them, evaluation factor in the waiting time evaluation index is based on a minimum of the optimal value, function as follows:

Establish the waiting time lower semi-trapezoid function[8]:

$$t(1) = \begin{cases} 1 & , 0 \leq t \leq 5 \\ \frac{30-x}{25} & , 5 \leq t \leq 30 \\ 0 & , t \geq 30 \end{cases}$$

$$t(2) = \begin{cases} \frac{x-5}{5} & 5 \leq t \leq 10 \\ \frac{30-x}{20} & 10 \leq t \leq 30 \\ 0 & t \leq 5, x \geq 30 \end{cases}$$

$$t(3) = \begin{cases} \frac{x-10}{5} & 10 \leq t \leq 20 \\ \frac{30-x}{20} & 20 \leq t \leq 30 \\ 0 & t \leq 10, t \geq 30 \end{cases}$$

$$t(4) = \begin{cases} \frac{x-20}{10} & 20 \leq t \leq 30 \\ 0 & t \geq 30 \\ 0 & t \leq 20 \end{cases}$$

Similarly, establish the taxi risk, individual needs, additional income and software familiarity lower semi-trapezoid function.

Through the evaluation factor membership functions do single factor evaluation, then fuzzy relation matrix R . According to the survey data obtains passenger waiting time membership subset, scilicet fuzzy evaluation matrix:

$$R_1 = [0.419 \ 0.880 \ 0.382 \ 0.206 \ 0.109]$$

Due to the different impact of waiting time, taxi risk, individual needs, additional income, software familiarity, therefore each index should be given different weights. According to the principles of large impact and weight Decide weights of passenger satisfaction factors.

Calculate the i-th items' proportion at the j-th index:

$$p_{ij} = \frac{r_{ij}}{\sum_{i=2}^m r_{ij}} \tag{1}$$

Calculate the j-th index' entropy e_j

$$e_j = -k \sum_{i=1}^m p_{ij} \cdot \ln p_{ij} \tag{2}$$

$$k = \frac{1}{\ln m}$$

Among them,

Calculate the j-th index' entropy weights w_j :

$$w_j = \frac{1 - e_j}{\sum_{j=1}^n 1 - e_j} \tag{3}$$

Determine the index of comprehensive weight: β_j

$$\beta_j = \frac{\alpha_j \omega_j}{\sum_{i=1}^m \alpha_i \omega_i} \tag{4}$$

Obtained the weight of C_1, C_2, C_3, C_4, C_5 is 0.362, 0.117, 0.223, 0.146, 0.152, which are Passengers in each evaluation factor weight after the heavy subsidies scheme set.

$$\omega_1 = [0.362 \ 0.117 \ 0.223 \ 0.146 \ 0.152]$$

Combining the weighting of evaluation factor with single factor matrix and getting fuzzy comprehensive results S, considering the waiting time of passengers after implement subsidy programs as an example:

$$S_1 = \omega_1 \times R_1 = [0.152, 0.103, 0.085, 0.030, 0.017]$$

Similarly, according to the above steps other evaluation factors of fuzzy comprehensive evaluation results can be got, fuzzy comprehensive evaluation matrix is:

$$\begin{bmatrix} S_2 \\ S_3 \\ S_4 \\ S_5 \end{bmatrix} = \begin{bmatrix} 0.337 & 0.337 & 0.211 & 0.079 & 0.045 \\ 0.349 & 0.367 & 0.149 & 0.107 & 0.049 \\ 0.132 & 0.162 & 0.401 & 0.249 & 0.057 \\ 0.324 & 0.318 & 0.158 & 0.142 & 0.058 \end{bmatrix}$$

Among them, S_2 is the taxi risks; S_3 is individual needs; S_4 is the additional revenue; S_5 is familiarity with the software.

Passengers ride quality
 $S = (S_1, S_2, S_3, S_4, S_5)$ can be obtained on the satisfaction of a fuzzy evaluation matrix, and then based on a fuzzy matrix composite calculation and normalization process to obtain passengers' satisfaction with vehicle quality fuzzy comprehensive evaluation vector: $Y_1 = \omega_1 * S = (0.39 \ 0.38 \ 0.28 \ 0.17 \ 0.06)$

Similarly, using fuzzy comprehensive evaluation method can obtain the fuzzy comprehensive evaluation matrix of each evaluation factor of the ride quality satisfaction:

$$\begin{bmatrix} S'_1 \\ S'_2 \\ S'_3 \\ S'_4 \end{bmatrix} = \begin{bmatrix} 0.168 & 0.102 & 0.070 & 0.034 & 0.012 \\ 0.328 & 0.305 & 0.217 & 0.092 & 0.040 \\ 0.116 & 0.230 & 0.325 & 0.116 & 0.095 \\ 0.087 & 0.113 & 0.136 & 0.097 & 0.331 \end{bmatrix}$$

Among them, S'_1 is the waiting time; S'_2 is the taxi risk; S'_3 is special period; S'_4 is a special area for the evaluation factor.

Compositing operation and normalizing fuzzy evaluation matrix, and then the fuzzy evaluation vector of ride quality satisfaction to passengers before the introduction of the subsidy scheme carried out can be obtained:

$$Y'_1 = (0.212 \ 0.236 \ 0.257 \ 0.116 \ 0.179)$$

Before and after the implementation of the subsidy program selected, passenger waiting time and passengers taxi risks, the two factors' fuzzy comprehensive evaluation result drawing is compared, shown in Fig. 1, and then analyze the passenger satisfaction.

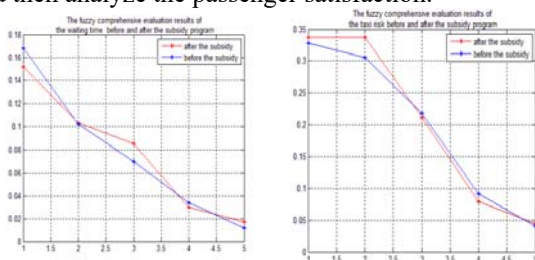


Fig.1 Fuzzy comprehensive evaluation of the subsidy program and the waiting time before and after the implementation of the results of the risk of a taxi

Combination of the above model, from the passenger's point of view, evaluate ride quality satisfaction before and after the implementation of subsidies :

Terms of waiting time: A considerable part of the fuzzy comprehensive evaluation matrix values before the subsidy scheme is implemented is greater than the value of fuzzy after the implementation of the subsidy program, but there is still less than the value after the implementation of the subsidy program, this shows that the taxi software company after the implementation of the subsidy program, passenger waiting time can be

reduced to some extent, but do not rule out the waiting time to be too long because of the driver pick passenger or rejection.

Terms of taxi risks: After the implementation of the subsidy program, a taxi was no significant change in the risk index, showing that the reliability of passenger to taxi software companies as well as the driver is high, and pay less attention to the driver defaults, black car and pay risk.

By the analysis of the fuzzy comprehensive evaluation matrix after established, it found that the implementation of the subsidy program can be greatly improved demand of individual passenger, while additional revenue of drivers is also increased in a small margin. Because you can use a taxi software to reduce travel costs, familiarity passengers software also gradually improved. Before the implementation of the subsidy program, passengers at special time, such as: rainy days, rush hour and mountains and other remote areas' need can't be satisfied. Visible use of certain subsidy programs in these areas, it is a good initiative to improve these problems.

III. CONCLUSION

It can be drawn from the above analysis that each company implemented subsidy programs in a certain extent, ease the difficulty in a taxi passenger waiting time is too long, lower income drivers, passengers in special time, a special place travel difficult problem, especially for young mobile users' travel it played improvement. But at the same time, the various subsidy programs make the drivers appear excessive profit, no-load, rejection, pick off, even in violation of provisions of the taxi act, it also caused the attacks to the elderly or the people who less frequently used Internet tools, resulted in a more adverse effects to their travel.

REFERENCE

- [1] Cai Jiming, Jiang Ning. With the mobile Internet to promote market-oriented reform of the taxi industry [J] Chinese Cadres Tribune, 2015,05: 60-62.
- [2] Chang Yingzheng. The economics for mobile taxi software price war [J] Price Theory and Practice, 2014,04: 116-118.
- [3] Bian Yang, Wang Wei, Lu Jian. City taxi operators network equilibrium model [J] Transport Engineering, 2007,01: 93-98.
- [4] Tong Zhichen, Li Qingheng. Taxi passenger satisfaction evaluation index system [J]. People's Forum, 2010, (Section 8).
- [5] Wang Xiaobo. City Taxi Resources Mobile App Design and Implementation of share [D]. Jilin University, 2014.
- [6] Liu Honghong, Wang Ni, Xie Jiancang, Zhu Jiwei. Based on fuzzy comprehensive evaluation method the Weihe River ecological vulnerability assessment [J] Shenyang Agricultural University, 2014,01: 73-77.
- [7] Zhao Xiaoguang, Cui Chao. Based on fuzzy comprehensive evaluation model, the Government of public investment and public satisfaction [J] accounting communications, 2011,08: 59-60.
- [8] Liu Junjuan, Wang Wei, Cheng Lin. Based on the number of intervals trapezoid membership function fuzzy evaluation [J]. Systems Engineering and Electronics, 2009,02: 390-392.

Study On Situation And Comprehensive Utilization Of Blast Furnace Slag

Shang Yanxia¹, Liu Weixing², Zhang Yajing¹, Li Jie²

1. College of science of north china university of science and technology, Tangshan 063009, China;
2. North china university of science and technology, The ministry of education key laboratory with modern metallurgical technology, Tangshan 063000, China

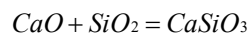
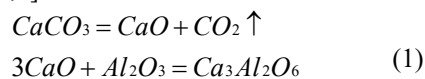
Abstract—The blast furnace mainly produced low value-added products such as slag cement and slag brick, only a small number of remolten modification slag used to produce slag cotton. The development condition, the existing problems and the future tendency of national blast furnace industry were analyzed in this paper. According to the comparison technology of liquid modification slag directly fibrosis and slag wool prepared by remolten slag. The directly fibrosis had advantage in terms of production technology, resources utilization, equipment investment and environmental protection which elaborated in detail.

Index Terms—blast furnace slag, development tendency, slag wool, comprehensive utilization

I. INTRODUCTION

During the 11th five-year, the crude steel production and iron production of China was first on earth in successive years which occupied about 50% of total world production. In 2010, the crude steel and iron production was 59021.8wt and 17700wt, respectively. The crude steel is about seven hundred million tons up to 2015, metallurgical slag production and processing slag can over 3 hundred million tons so that the significance assignment is realization of zero-emission metallurgical slag which can improve the recycling economy development, protect the ecological environment, realize the energy conservation, found the green steel and speed up the construction of “two- type society”. [1][14]

Iron ore contains a large number of silica and bauxite and has the reaction with flux such as CaCO_3 in smelting process generating soluble substances such as calcium aluminate and forming slag water. The main reactions show as follows [2,3].



The molten iron and slag water has different discharging way in blast furnace slag production, the iron let out at regular intervals time, but the slag water put out continuously. The slag water forms the solid slag after process known as the blast furnace slag.

The selected mineral composition and the kinds of pig iron can decide the blast furnace slag chemical composition, at the same time the production technology has little impact on it. The ordinary blast furnace slag mainly contains calcium oxide, silica and alumina, all of them mass fraction are over 90%, meanwhile, a small amount of magnesium oxide, ferrous oxide and sulfide also exists. In addition, it also has a small amount of chloride, manganese oxide, phosphorus pentoxide, Na_2O , K_2O and V_2O_5 which has little impact on the quality of slag.[2]

The mineral composition of blast furnace slag is mainly influenced by iron ore type and cooling way and it has closely relationship with the blast furnace slag type. Generally high acidic slag is mainly composed of melilite, wollastonite, plagioclase and pyroxene. The high alkaline slag is mainly composed of gehlenite and calcium magnesium melilite. Meanwhile, it also contains a small amount of dicalcium silicate, wollastonite, calcium feldspar magnesium, calcium and magnesium olivine, rose stone and magnesium scapolite. Therefore, the blast furnace slag with special elements contains a variety of other complex minerals.

The main part of metallurgical slag was blast furnace slag. At present, the blast furnace slag could discharge about 30 million tons every year in China. If it is not properly used, it would not only take up a lot of land but also pollute the environment formatting pollution, so it is important to use blast furnace slag properly. Presently the blast furnace slag mostly applies to construction, material, chemical industry, metallurgy, agriculture, and so on which show as follows.[4-13]

1) the blast furnace is used as producing cement, coarse aggregate for concrete, sand concrete water quenching slag slurry, slag making brick, concrete block or color tile making, production of various kinds of brick of pottery and porcelain and pavement brick, produce baking-free brick, road materials, production of gypsum, slag particle board, make artificial foundation and so on in terms of construction industry.

2) It can produce slag wool, high property stone wool, long-fiber glass and composite material etc.

3) It can produce the blast furnace slag powder, silicon fertilizer production, production of hydrated silica, and extraction of valuable components etc.

4) It can use as the tundish covering agent of basic material and sand material etc.

5) It can found the artificial algae field.

Generally, the blast furnace slag has low-added value in terms of construction, chemical industry, metallurgy and agriculture. However, it has high-adder value to material application.

Since the 21st century, the government release the circular economy promotion law, the resource utilization of blast furnace slag has made important progress.

The comprehensive utilization scale expands gradually by improvement of high technology slag processing equipment and increasing the capital investment and scientific research strength

Most of iron and steel enterprises can achieve the discharge and processing continuously by improvement of high technology processing equipment during the period of 11th five year plan. It has some achievement at the end of the 11th five-year plan.

It develop independent intellectual property rights of new technology equipment about water quench process

basically on the INBA abroad, it achieved less pollution, high-quality cinder flushing and high steam recovery effect. In addition, vertical roller mill with independent intellectual property right is widely applied in the country which study on the grinding equipment of granulated blast furnace slag powder. The yield of graining blast furnace slag powder increases almost 50 times in 2009 compared with 2000 by introducing advanced equipment and technology innovation. Furthermore, the specific surface area is up 400m²/kg which can replace the same weight of cement concrete increasing the concrete strength durability and performance. It has been listed as the environmental protection technology and the green construction products.[1,14][14-15]

It impose restrictions on introducing professional equipment, exploiting high value product and effective utilization resources that is crude slag process by the small size treatment plant of slag. It also can not meet the market development. Therefore, more and more professional processing enterprises is establishing rapidly, at the same time, they cooperate with scientific research institutes to carry out the research and development comprehensive utilization of high value-added slag promoting zero-emissions. It is conducive to increase use rate and make economic benefit for this operation model.[1,15]

There are 32 items to set out by metallurgical construction research institute of China at the end of 2010 including basic standards, product standards etc. it have laid a foundation of comprehensive utilization and promotion zero emissions of slag.[1,15][16]

II. THE PROBLEMS IN THE DEVELOPMENT PROCESS OF SLAG

The simple processing slag was landfill or relegated to the outskirts of city, rather than excavate its resource potential and application value. The comprehensive utilization consciousness was weaken which could not promote it to the construction of "two type society".[1,16]

The domestic units of professional study on the processing equipment is few which could not meet the domestic market so that almost all equipment rely on imported advanced equipment abroad. It is slowly to promote new technology, new processes and new equipment for the lower innovation ability. In addition, there is not theoretical and technical support on the production standard system. The comprehensive utilization of blast furnace slag is only 76.7% which is less than the national standard. Therefore, the potential value of blast furnace slag has not developed very well with low-added value product.[14-16]

The state does not make preferential tax and effective incentive mechanism to the utilization of metallurgical slag, so the product can not write into the renewable resources context. The state could not set out the prefect and effective scientific operation mechanism promoting industry development reasonable orderly and rapid which lead to the development utilization of metallurgical slag in central and eastern regions is better than the western. In addition, the funds give priority to found the main project rather than improvement of processing technology innovation and introducing advanced equipment. The enterprise also has the backward investment philosophy and mechanism.[1,17]

The government has not found a system and management system which can find the metallurgical slag data, information statistic and statistical standards. Furthermore, the present statistical data is incomplete and disunity which can not use as the basis.

III. COMPREHENSIVE UTILIZATION OF SLAG

The future development tendency of slag industry is indicated as follows combined with 12th five-year plan and adjust and revitalization plan of iron and steel industry.

For the resources and energy utilization, it saves the water consumption Developing the resource potential of blast furnace slag, taping the potential of high added value. Such as: making slag wool, rock wool, long fiber glass and preparing composite materials high and other value-added by blast furnace slag.

The optimization and innovation of high slag production process and technology.

Recovering high liquid slag sensible heat and increasing its effective utilization, directly utilizing its sensible heat production is the most direct and efficient way. It is the important way to achieve low-carbon of iron and steel enterprises, green growth, resource efficient utilization, production process intensification, energy saving, emission reduction.

Establishing and improving the basic theory, technical standards and regulations regulate of the use of the products that blast furnace slag produces, so as to promote the comprehensive development of blast furnace slag, recycling and promote the "zero emissions" of slag. Such as: the standard system that slag wool, rock wool and glass wool is produced by blast furnace slag has not been established.

Water quenched blast furnace slag separates slag wool and liquid blast furnace slag that is fibrosis directly after quenching to prepare slag wool.

For original technology, after the slag discharged water from the high road by Pakistani law (INBA) or bottom filter method (OCP) of water quenching process, to acquire granulated blast furnace slag, and then granulate blast furnace slag remolten. According to the differences of blast furnace slag composition and slag wool composition, modifier (iron tailing, basalt or fly ash, etc.) is added to quench. After the various indicators of blast furnace slag whose composition, temperature and etc meet the requirement, it is discharged, and then by high-speed compression gas injection, centralization or centrifugal blowing liquid slag is made slag wool[18-21].

For new technology, the slag water that is discharged from the blast furnace is directly into the furnace, modification agents which is iron tailing, basalt or fly ash add to quench according to the differences in composition of blast furnace slag and composition of slag wool, rock wool, glass wool. After the various indicators of blast furnace slag whose composition, temperature and etc meet the requirement, it is discharged. Then, by high-speed compression gas injection, centralization or centrifugal blowing liquid slag make slag wool.

New technology compared to the original process simplifies the liquid blast furnace slag water quenching process.

It is more simple and easy to product in process

For resources and energy utilization, it saves the water consumption from water quenching process and remolten

slag energy consumption. Meanwhile, the sensible heat of the liquid blast furnace slag is used to produce slag without other conversion, so that it can shorten the waste heat recycle and increase the utilization rate.

For the equipment construction and investment, the new process reduces the occupied area of the water treatment and remelting equipment and the factory construction which saves the investment cost.

For environmental protection, high temperature steam in the water quenching process and exhaust gas in the remelting process are not produced in the new process which is more environmentally.

The liquid blast furnace slag through quenching direct fibrosis and high slag resource utilization is very consistent.

IV. CONCLUSIONS

Although the directly fibrosis technology with liquid modification slag is correspondence with utilization development of slag. More and more research should do on the technology process. The main aspects show as follows.

- 1) The study is modification mechanism and method.
- 2) It is impact mechanism on physical and chemical performance, mineral composition and microstructure of blast furnace slag that is the kinds of modification agent, the amount of modification agent and composition of it.
- 3) The influence mechanism is the kinds of modification agent, the amount of it and composition of it to the fiber-forming rate, length of fiber and the diameter of fiber.
- 4) The study is what kinds of slag wool prepared by slag which contains mineral cotton rock wool, glass wool and aluminum silicate refractory fiber.
- 5) The innovation technology of preparation slag cotton is studied.
- 6) The heat flow and conversion rate in the preparation mineral wool with liquid slag is studied, high liquid slag in the process of preparation of mineral wool heat flow and the conversion of research.
- 7) The optimization and innovation of mineral cotton products molding process is studied.
- 8) The optimization research is on the development of new mineral wool products and their properties which are water absorption, thermal conductivity, bulk density and high temperature resistant performance.

In conclusion, it is not only conducive to saving energy and reducing emissions, but also achieves the comprehensive utilization and low carbon and green development that are the modification slag forming-fiber directly under the condition of indicating technology and theoretical research. The process is one of high effective comprehensive utilization, intensification of the production process and lower pollution emission which is corresponding with 12th five year policy and adjust and revitalization plan of iron and steel industry.

REFERENCE

- [1] China scrap iron and Steel Association. Development and utilization industry "Twelfth Five Year Plan"[J]. Waste iron and steel in China, 2010(6):12-20.
- [2] Lu Hongxia, Li Lijian, Guan Shaokang. Study on the property and application of Angang bf slag[J]. Henan Metallurgy, 2007-4(15).
- [3] Hao Hongshun, Xu Lihua, ZHANG Zuoshun, Yang Zengchao, Zhang Xiaomeng, Xie Zhipeng. Development of Green Inorganic Material from Blast Furnace Slag[N]. Materials review, 2010-11(24).
- [4] Hu Junge. Development of Comprehensive Utilization Technology of Blast Furnace Slag at Home and Abroad and Suggestion for Angang[J]. Angang Technology, 2003(3):8211.
- [5] Qin Yue-lin, Qiu Gui-bao, Bai Chen-guang, Lü Xue-wei, DENG Qing-yu. Development of Studies on Sensible Heat Recovery From Blast Furnace Slag by Chemical Methods[J]. China Metallurgy, 2011, 21(4): 2.
- [6] Zhou Wen-bo, Ke Chang-ming, Zhang Qin, Zhang Ke-ning, Du Shu-fang. Application of Pangang Blast-furnace Slag in Consstry[J]. Comprehensive utilization of mineral resources, 2007(3):35.
- [7] Liang Yushan, Lv Qinghua, Chen Zhaohui. Application of Linggang slag as road base materials[J]. Liaoning transportation science and technology, 2000,(2):12.
- [8] Cui Yuncheng, Sun Xueyu, Jin Yadong, Sui Changqing, Yan Yongsheng, Ma Yongchun. Comprehensive Utilization of Slag of Blast Furnace in Chemistry[J]. Songliao Journal(Natural Science Edition), 1997,(3):25.
- [9] Guo Wenhua. Construction and Detection of Foundation Stabilization with Dynamic Compaction[J]. Tech in Formation Development and Economy, 2001,11(5):121.
- [10] Lin Qinv, Li Zhifeng, Guan Shanji, Yang Guangyi. Study on Hydrated Silicon Produced by Blast Furnace Slag[J]. China Resources Comprehensive Utilization, 2010,28(6):33.
- [11] Sun Peng, Chen Yunman, Guan Shanji, Li Liancheng, Sun Bo. Present Situation and Forecast of Blast Furnace Slag Comprehensive Utilization[J]. Angang Technology, 2008(3):8.
- [12] Meng Bingchen, Zhang Chaohui, Ju Jiantao. New Approach and Present Situation of Recycling Utilization of Blast Furnace Slag[J]. Hydrometallurgy of China, 2011,30(1):8.
- [13] Zhang Zhaofu. Production of long fiber glass with blast furnace slag[J]. Material regeneration in China, 1995,(10):13.
- [14] Wei Ruili. Analysis on the Utilization Status of the Main Solid Wastes from Iron and Steel Industry[D]. Xi'an: Xi'an University Of Architecture And Technology, 2010.
- [15] Ji Min. Study on Reverse Logistics System for Steel Enterprise in Recycling Economy Mode[D]. Tianjin: Tianjin University, 2008.
- [16] Ma Zhongmin, Zhai Guoying, Liu Sanjun. Discussion of Iron Slag Circulation Utilization in Angang[J]. Henan Metallurgy, 2010,18(5):26.
- [17] Wei Xiang, Li Yuan, Cai Min. Comments Comprehensive Utilization of Iron and Steel Slag[J]. Shanxi Metallurgy, 2011,4:5.
- [18] Gong Yuanling, Zhai Huawei. Blast Furnace Slag Treatment Technologies[J]. Science and Technology of Baoyou Steel Group Corporation, 2009,35:81.
- [19] Wang Haifeng, Zhang Chunxia, Qi Yuanhong. Status and Development Trend of Treatment and Heat Recovery Technology for Blast Furnace Slag[J]. China Metallurgy, 2007,17(6):53.
- [20] Wang Haifeng, Zhang Chunxia, Qi Yuanhong, Dai Xiaotian, Yan Dingliu. Present Situation and Development Trend of Blast Furnace Slag Treatment[J]. Iron and Steel, 2007,42(6):85.
- [21] Yan Zhaomin, Zhou Yangmin, Yang Zhiyuan, Yi Chuijie. Present situation and development trend of blast furnace slag comprehensive utilization[J]. Research on Iron Steel, 2010,38(2):54.

A Way Of Disease Treatment Based On The People Density In Different Regions And The Speed Of The Virus Spread

Wen Xiaocan,Zhang Guanghe,Feng Jianyao, Yang Aimin*,Xu Yanghuan,Tangyu
North China University of Science and Technology, Tangshan, 063000, Hebei, China

Abstract—For the model of the spreading of the Ebola virus, we divided the whole district into different restrictions according to the people density. And so we can find the amount of medicine (vaccine) to stop the infection. Based on the speed of epidemics model, we guess the spreading of the virus might obey the population growth model, which is proved by the data of CDC. Through analyzing the epidemic speed growth and the spreading pattern of each country, the relation between the numbers of the cases and the epidemic speed could be figured. Then it is easy to make the transportation plan. It's important for people to change their bad habits efficiently, or they would still suffering the higher risk of being infected by other kinds of epidemics.

Index Terms—growth of the population; Model of Spreading; speed of epidemics spreads; Infectious Disease Model

I. INTRODUCTION

Infectious Disease Model has been researching for a long time [3].In 1927, Kermack and McKendrick built the famous SIR Model for spread of disease when they researching the spread regularity of London in 1655 to 1666 and an epidemic of Bombay in 1906.It played an important role of the research of infectious diseases. And then they came up with the “Threshold theory” to distinguish weather a kind of disease is epidemic or not, laying a solid foundation to the Epidemic Dynamics. Herbert and others have researched a infectious disease model with quarantine item. When entering constants, the model will provide SIQS and SIQR model with bilinear and standard occurrence rate, which discuss the stability of Balance Point.

Ebola is spreading fast in West Africa; the poor condition there make it open to the virus, also make us using the natural growth model(Logistic) to deal with it; based on this, we can find the amount of medicine(vaccine) to stop the infection.

(1) The spreading of the virus: according to the characters of Ebola, we divided the whole district into restrictions that people could not get out of; furthermore, we get each restriction into three round regions by the distance from the exploring area. At different regions we choose one or more ways of isolation, prevention and treatment to deal with.

(2) The speed of epidemics: from the condition of West Africa, we guess the spreading of the virus might obey the population growth model, which is proved by the data of CDC. With further considering, Guinea, Liberia and Sierra Leone are great- resistance-spreading, small-resistance-spreading and non-resistance-spreading, respectively.

(3) After the division, the epidemic speed growth and the spreading pattern of each country could be analyzed; added with the epidemic environment in each restriction

of every countries, the relation between the numbers of the cases and the epidemic speed could be figured; that's the key to the needs of drugs in each restriction, the whole should be the total need, then the transportation plan also be born.

At the end of 2013, Ebola virus reached West Africa. Then it broke out, and becomes the most serious epidemic of the history of Ebola virus disease^[1]. The Ebola virus epidemic of this time attracts the whole world's attention because of its high mortality rate, a wide range of Epidemic and it is difficult to control^[2]. Our job is building a mathematic model that considers the spread of the disease and other factors to optimize the eradication of Ebola, or at least its current strain.

II. THE MODEL OF SPREADING (WITHOUT MEDICINE OR VACCINE, BASED ON THE CONDITION OF THE WEST AFRICA)

The Spreading Model explains how Ebola epidemic spread and from it we can know how many drugs we should put to a certain area. But when a patient realize that he is a patient, he will receive medical treatment on his own initiative or passively. And he will also take measures such as do not go out or self-quarantine to limit the disease continuing to spread ,so as to reduce the risk of infection to others.

From the memo we could see that except the herb doctor and the teacher, the transmission speed is regular. So, our thought is based on the better case; that is, flow of people is strictly forbidden (without any people moving inside or outside a restriction). In the other hand, we assume the medicine could CURE the patient and the vaccine could only prevent the HEALTHY PEOPLE but COULD NOT cure the patient.

III. MODEL BACKGROUND

Then, after the epidemic explore we put every restriction into three kinds: the center region as the dangerous region, where the medicine should be send to; then a nearer area as the pseudo-safe region, where the medicine and the vaccine should be send to; a further area as the quasi-safe region, where only need to send the vaccine. The area of the regions, the amount of medicine and vaccine are depended by the measure of the speed of the epidemic.

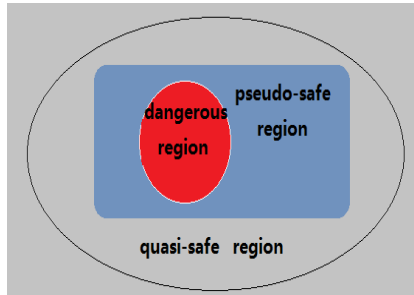


Figure 1 Schematic diagram of model 1

We assume $i(t)$ as the sickness number at time t ; the area of dangerous region is s when $t=0$; the density of the considered area is λ (average); the speed of epidemic is K_0 per sicko per unit time, Initial conditions: $i(0) = i_0, s(0) = s_0$.

The addition sickies in Δt is:

$$i(t + \Delta t) - i(t) = K_0 i(t) \Delta t \tag{1}$$

$$s(t + \Delta t) - s(t) = K_0 s(t) \Delta t \tag{2}$$

From the differential equations:

$$\begin{cases} \frac{di(t)}{dt} = K_0 i(t) \\ i(0) = i_0 \end{cases} \tag{3}$$

We get the solution:

$$i(t) = i_0 e^{k_0 t} \tag{4}$$

That means the transmission in the dangerous region is obey the exponential function. At the early times, the healthy people is much more than the influents, so the speed is high; with the transmission going on, the number of sickos would be equal to or more than that of the healthy people. So, we make a modification to describe the latter case.

We denote $y(t)$ and $n(t)$ as the number of influents and the healthy people respectively. Assume:

$K_0 = Ks(t)$; (The speed of infection is proportional to the number of non-influents).

One sicko will not cure or die while the Infectious period; (corpse still could spread the virus; the funeral of West Africa).

The population is N ; that is $y(t) + n(t) = N$.

Then we get the modified differential equations:

$$\begin{cases} \frac{dy(t)}{dt} = ky(t)n(t) \\ y(t) + n(t) = N \\ i(0) = i_0 \end{cases} \tag{5}$$

The solution:

$$y(t) = 1 + \begin{pmatrix} N & N \\ i_0 & -1 \end{pmatrix} e^{-KNt} \tag{6}$$

$$\frac{di}{dt} = \frac{kN^2 \left(\frac{N}{i_0} - 1\right) e^{-KNt}}{\left[1 + \left(\frac{N}{i_0} - 1\right) e^{-KNt}\right]^2} \tag{7}$$

When $\frac{d^2 i(t)}{dt^2} = 0$, we get the

maximum $t_1 = \frac{\ln\left(\frac{N}{i_0} - 1\right)}{kN}$; that means t_1 will be small as K or N becoming big. That is, if the virus is easier to spread or the number of population is bigger, then the summit of the spread would coming soon. This is coincide with the reality, it's likely that we can predict the peak of the influence.

From the analysis above, we can find that the virus-spreading likes the growth of the population. So, our result would be based on it with the different condition in Liberia, Guinea and Sierra Leone. The key point is the summit of the transmission, as we have found above.

TABLE I THE DEVELOPMENT OF THE EPIDEMIC

Country	The number of cases (as of February 1, 2015 published data)	Deaths (with the number of cases)
Guinea	2975	1944
Liberia	8745	8991
Sierra Leone	10740	3746

In a limitless environment: the growth obeys the exponential equation (J-type); that is,

In which N is the population, r is the increase ratio, t is the time.

In an environment with limit: the growth will be limited by the number of population and other restrictions. Now the Logistic model shows the type of growth (S-type):

$$\frac{dN}{dt} = rN \left(1 - \frac{N}{K}\right) \tag{8}$$

Where K is the capacity of the environment (based on technology, species, etc.)

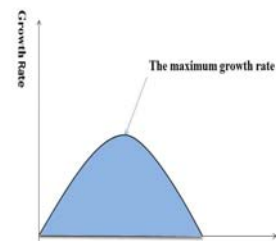


Figure 2 Population growth graph 1

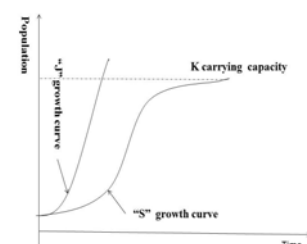


Figure 3 Population growth graph 2

Till now, the Ebola virus growth like the S-type (except the 2 events happened in Sala Leon). At the beginning, the health-care-less West Africa is the paradise of Ebola; after the fast spreading period, many factors appeared to slow down the speed (the high mortality rate, the interposition of government and the international aid).

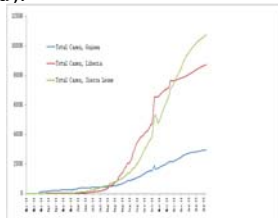


Figure 4 The growth of change of the three countries of West Africa

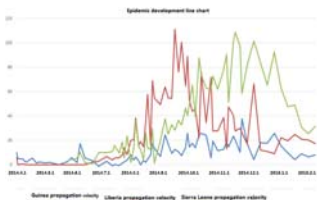


Figure 5 The growth rate of change of the three countries of West Africa

The spreading-speed in the three country:

Table2: The fitting formula of the rate of change

Country	Rate of change
Guinea	$y = 0.3367x - 14067$
Liberia	$y = 0.1378x - 5742.6$
Sierra Leone	$y = 0.3367x - 14067$

Then we could do a calculation to test our guess and get more concise results.

Assumption:

t: the time(days) since the epidemic begin;

p_i ($i=1, 2, 3... n$ (n is the number of patients of a region)): the amount of medicine needed in a restriction.

D: the total amount of medicine needed in the whole country or region considered.

$v(t)$: the speed of spreading at some time point t.

$N(t)$: the number of cases at some time point t.

Now our main point is: estimate the amount of medicine needed at time $t+1$. (For the character of the virus infection, we assume the medicine could 100% cure the patient.)

The amount of medicine needed in a restriction:

$$p_i = v(t) + N(t)$$

The amount of medicine needed of the country:

$$P = \sum_i^n p_i \tag{9}$$

Then we can get the delivery amount in any state, any country. For the production is far away from West Africa, so aero plane is the best chance. (But the cleaning is

important to prevent the spreading! Also the inner-country transport should be ware about that.)

Detailed information of the results showed below in the table:

Table3: The quantity of drugs sent to Guinea provinces

Province	The number of cases in the province	Min	Increased drug delivery day	Drug delivery per day	The overall amount of drug delivery
Conakry		501	14.89375	515.89375	10167.9023
Nzerekore	4	101	3.6226	104.6226	10266.9823
Kindia	4	101	3.6226	104.6226	10266.9823
And Kankan	3	21	3.6226	24.6226	10286.7983
Kindia	3	21	3.6226	24.6226	10286.7983
Keya	5	501	14.89375	515.89375	10167.9023
Dubr�eka	3	21	3.6226	24.6226	10286.7983
For�ecaria h	3	21	3.6226	24.6226	10286.7983
T�elim�el�e	3	21	3.6226	24.6226	10286.7983
Boke	1	1	3.6226	4.6226	10291.7523

IV. CONCLUSION

This solution is fully including the reality as the first thing as clear as the information could be found in order to recognize the difference between distinct regions. Our suggestions are reasonable and objective, fully considered the common situation and the living atmosphere in West Africa.

However, the only problem troubles most is the lack of data, and the credibility about data which we have got. Something accord that in some days there are less total amount of people dead in Ebola than the day before, which confused us much in some time point.

REFERENCES

- [1] Chen Huaxin, tang liu ying. The research progress of ebola haemorrhagic fever [J]. Journal of clinical medical. 2000 (04)
- [2] Yangyang Pan,Wen Zhang,Li Cui,Xiuguo Hua,Meng Wang,Qiaoying Zeng. Reston virus in domestic pigs in China[J]. Archives of Virology . 2014 (5)
- [3] Heinz Feldmann,Thomas W Geisbert. Ebola haemorrhagic fever[J]. The Lancet . 2011 (9768)
- [4] MA zhien, ZHOU yicang, WANG wendi, Mathematical modeling and study the dynamics of infectious diseases [M]. Peking: Science Press, 2004.
- [5] Van den Driessche P, Watmough J. Reproduction numbers and sub-threshold endemic equi-libria for compartmental models of disease transmission [J]. Mathematical Biosciences, 2002,180: 29-48.
- [6] ZHANG Su-xia, HU Gang. The analysis of an epidemic model with treatment [J].Applied Mathematics. 2014, 29(1): 1-10

The Location-Method Research Based on the Coordinate of Sun Shadow

Xu Yanghuan, Tang Yu, Wen Xiaocan, Yang Aimin*

North China University of Science And Technology, Mechanical Engineering Academy, Hebei Tangshan, 063000, China

Abstract—At present, location technology is widely applied in the fields of life, atmosphere, energy, aerospace and so on. This thesis expresses the regularity of shadow length through analyzing the discipline of sun movement and building the relationship model of time nodes and shadow length; it gets the target position through applying the relationship of longitude and zone time and the connection of solar elevation angle and latitude. Meanwhile, according to the camera model and shadow track calculation, the author turns video image into plane image and picks up the coordinate of shadows, which finishes the location research of video image.

Index Terms—solar elevation angle, latitude-angle model, camera model, shadow track calculation

I. THE ESTABLISHMENT OF THE TIME NODES AND SHADOW-LENGTH MODEL

In theory, the earth moves around the sun, while on the surface of the earth, it can be seen as the sun around the earth. In relative motion, all planets (including the sun) in the sphere around the earth do the rotation which regards the earth as the center and makes the imaginary sphere in any length. Equatorial coordinate system make the earth and latitude coordinate system extend to the celestial, earth and the equatorial plane parallel to the circles of latitude, on the celestial sphere called the declination; through the north and south poles of the earth longitude coil on the celestial sphere called circle, with the angle of declination and said that the sun's position, as shown in Figure 1. When the angle is the angle between the time of the sun and the time when the pole is through the South Pole, the time is the unit. From the north celestial pole, the position of the sun with a clockwise direction angle, the celestial sphere in the day time rotate 360 degrees per hour rotated 15 degrees. The ground coordinates are based on the horizon, and the position of the sun in the sky is determined by the angle of the sun at the same time, as shown in Figure 2. The angle between the solar rays and the ground plane is the angle of the sun. Angle of direct solar radiation on the ground plane projection line and the ground plane to south the folder is the solar azimuth angle, usually in the south pole is 0 degrees, West is positive and East is negative[1].

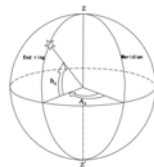
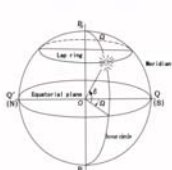


Figure1 azimuth angle and height angle Figure2 hour angle and declination of the sun

According to the geometrical relationship between the solar zenith angle and the shadow length

$$l = \frac{H}{\tan h_s} \tag{1}$$

L means the shadow length and H means the length of the test rod.

The summer solstice in the azimuth angle is corresponding to the maximum value of the year; the winter solstice value is corresponding to the minimum height of the sun. On this basis, we can know that the cover condition of solar rays in one year of, which is the function of the solar zenith angle [2]:

$$\sinh_s = \sin \varphi \sin \sigma + \cos \varphi \cos \sigma \cos \Omega \tag{2}$$

$$\sin \delta = 0.39795 \cos [N - 173] \tag{3}$$

$$\Omega = (TT - 12) \times 15^\circ \tag{4}$$

$$TT = C_T + L_C + E_Q \tag{5}$$

φ is the local latitude, so the author chooses a decimal; δ for the declination of the sun, it means the hour angle of the sun; Besides, C_T is the Beijing time and L_C is the longitude correction (4min/ degree). If the local meridian is located in the east of Beijing meridian, then L_C is negative and E_Q is jet lag.

The author selects the time nodes between 9:00-15:00 every 12 minutes in October 22, 2015 Beijing time, according to the above model to calculate the shadow of 3 meters high pole in Tiananmen square, we can see the node of solar zenith angle and the shadow length in the corresponding time from table 1.

Table1 solar zenith angle and the shadow length in the corresponding time

time	solar zenith angle	the shadow length	time	solar zenith angle	the shadow length
9:00	24.9	6.522	12:12	40.00	3.576
9:12	26.64	6.000	12:24	39.77	3.605
9:24	28.32	5.555	12:36	39.37	3.654
9:48	31.41	5.172	12:48	38.83	3.750
10:00	32.82	4.918	13:00	38.15	3.816
10:12	34.13	4.688	13:12	37.32	3.937
10:24	35.33	4.412	13:24	36.37	4.076
10:36	36.41	4.225	13:36	35.28	4.237
10:48	37.36	4.054	13:48	34.08	4.431
11:00	38.18	3.947	14:00	32.77	4.658
11:12	38.86	3.704	14:12	31.36	4.926
11:24	39.39	3.659	14:24	29.85	5.226
11:36	39.78	3.614	14:36	28.25	5.587
11:48	40.01	3.571	14:48	26.58	6.000
12:00	40.08	3.565	15:00	24.82	6.493

The author makes out the changing curve of the pole shadow length by applying mat lab.

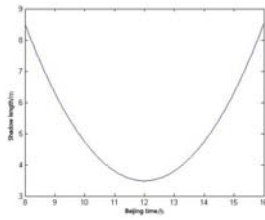


Figure3. The Changing Curve Of The Pole Shadow Length

II. THE ESTABLISHMENT OF LONGITUDE AND LATITUDE MODEL

The height of the sun is constantly changing within a day. The midday sun height is the max solar elevation, which has the largest solar altitude angle and the sun height of direct local's longitude. When the earth is at noon with the largest solar zenith angle, the length of the shadow appears the shortest value [4].

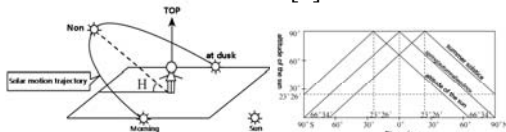


Figure4 the movement track of the sun within a day Figure5 the changing discipline of latitude at noon

Corresponding curve equation can be obtained according to the shadow length change, and then we can

know the lowest point x_0 . At this time, x_0 accords with the local noon time. Finally, through noon local time and Beijing East eight time zone of 12:00, we can get the location of longitude.

The author builds the Latitude angle model according to solar zenith angle and solar azimuth angle.

$$\begin{cases} \sinh_s = \sin \varphi \sin \delta + \cos \varphi \cos \delta \cos \Omega \\ \cos A_s = \frac{\sin \delta \cos \varphi - \cos \delta \cos \varphi \cos \Omega}{\sinh_s} \\ \Omega = (TT - 12) \times 15^\circ \\ TT = C_T + L_C + E_Q \end{cases} \quad (6)$$

The relationship between the sun azimuth α and the azimuth of the shadow A_s is $\alpha = A_s + 180^\circ$. The φ represents the local latitude and the expression is $\Omega = (TT - 12) \times 15^\circ$. At noon, when $TT = 0$, for the sun, δ is the sun and the earth's equatorial plane and the angle between the sun and the earth line, the expression is $\sin \delta = 0.39795 \cos[0.98563(d - 173)]$, the d means accumulated days. From the beginning of January 1st each year, December 31st notes as $d = 365$ (except leap year). The shadow position angle can be available from the vertex coordinate.

$$\tan \alpha = \frac{y_i}{x_i} \quad (7)$$

Because of the multi - value of trigonometric function, the sun azimuth in the formula has changed, and the continuity of the solar motion trajectory is not in conformity with the result:

$$A'_s = \begin{cases} A_s; T < 12, dA_s / dt \geq 0 \\ \pi - A_s; dA_s / dt < 0 \\ 2\pi + A_s; T \geq 12, dA_s / dt \geq 0 \end{cases} \quad (8)$$

So the longitude and latitude of the position are obtained.

III. THE DETERMINATION OF POSITION FOR THE SHADOW VIDEO

The author considers the point of space can see through into plane photo. If perspective center is placed in the origin of the European space, then the plane is called the projection plane or focal plane. In this camera model, the point of the 3D space is mapped to a point $(X, Y, Z)^T$ on the projection plane by a straight line connecting the point $(fX/Z, fY/Z, f)^T$ with the camera,

which means $(X, Y, Z)^T \rightarrow (fX/Z, fY/Z)^T$. Therefore,

this kind of mapping makes the 3D European space map to the coordinates of the two-dimensional space. The mapping center calls the camera center which is also named the center of optics. The vertical lines which cross the camera center and parallel the picture plane are the main axis of the camera. The main point is the intersection of the main axis and the picture plane. If we use homogeneous coordinates to describe the center pivot, the relationship between the world coordinate and the center of the image points can be expressed as a simple mapping between a homogeneous coordinate. This mapping can be expressed as a matrix:

The 3D world can be mapped to the 2D plane by camera. In this paper, the model of the camera is mainly used the center mapping and applied the model of the pinhole camera.

$$\begin{pmatrix} X \\ Y \\ Z \\ 1 \end{pmatrix} \text{ a } \begin{pmatrix} fX \\ fY \\ Z \end{pmatrix} = \begin{bmatrix} f & 0 \\ & f & 0 \\ & & 1 & 0 \end{bmatrix} \begin{pmatrix} X \\ Y \\ Z \\ 1 \end{pmatrix} \quad (9)$$

In world coordinates, the point X is expressed as the four-dimensional vector $(X, Y, Z, 1)^T$, and the projection points are three-dimensional homogeneous vector. This relationship can be understood as

$$x = PX \quad (10)$$

The camera matrix of the pinhole camera can be defined as $P = \text{diag}(f, f, 1)[I | 0]$.

In practical application, the origin point of the photo plane is not the main point of the camera, then the mapping relationship between the world coordinate space and the plane can be defined as:

$$(X, Y, Z)^T \text{ a } (fX/Z + p_x, fY/Z + p_y)^T,$$

And $(p_x, p_y)^T$ is the main point coordinates of the camera. In this case, the formula (4.18) is written as follows:

$$\begin{pmatrix} X \\ Y \\ Z \\ 1 \end{pmatrix} \text{ a } \begin{pmatrix} fX + Zp_x \\ fY + Zp_y \\ Z \end{pmatrix} = \begin{bmatrix} f & p_x & 0 \\ f & p_y & 0 \\ & & 1 \\ & & & 0 \end{bmatrix} \begin{pmatrix} X \\ Y \\ Z \\ 1 \end{pmatrix} \quad (11)$$

Where $K = \begin{bmatrix} f & p_x \\ f & p_y \\ & & 1 \end{bmatrix}$ is defined, then the formula

(3.3) can be expressed as $x = K [I | 0] X_{cam}$. The matrix K is the camera calibration matrix, and it

defines $(X, Y, Z, 1)^T$ as X_{cam} , which emphasize the camera position in the space of the Euclidean coordinate system, meanwhile the camera's axis is parallel to the normal direction of the Z axis.

An effective semi-automatic method is adopted to detect the shadow path of the input video [5]. First of all, the author sets a background picture to the inputting group photos $V = \{I_1, I_2, L, I_K\}$;

$$B(x, y) = \max_{i \in [1, K]} (I_i(x, y)) \quad (12)$$

In the B , each pixel (x, y) is the brightest pixel of V . The brightest pixels in B are based on the gray level. After using the background shear technology and setting the absolute difference, the shadow points can be displayed. After choosing a point in the shadow region, *floodfill* is used to calculate the shadow points. Finally the prominent shadow points were obtained by principal component analysis.

Background shear technology is the realization of a series of photographs taken by a fixed camera, which can detect all the foreground objects. The implementation of this technology is mainly through the comparison of the input images and the estimation of the model without the foreground object. In the picture plane, the biggest difference between the input image and the estimated model is the position of the foreground object. So by this technique, people can estimate the photo and set threshold to get the foreground objects from the input picture cut. In this topic, background shear technology archives the shadow region through cutting estimation model without a shadow from the shadow track photos. This action can do preparation for cynical point.

The calculation of *floodfill* [6] can be achieved by depth first search, breadth first search or breadth first scan. Its implementation is to find an unmarked node and then to expand the node. The nodes of the same label form a connected sub graph. In this paper, we use the most simple implementation mechanism, that is, the depth first search. For depth search, every step of the algorithm to consider the adjacent nodes, obviously these nodes are not identified, and then the nodes are identified and recursive traversal of them. The method steps are as follows: first in the broad shadow region manually enter a shadow and its logo, then uses the depth first search, based on a rectangular area division experience all the pixels set to the node identifier of the proximal nodes with less than certain que value of gray value, the

unlabeled nodes into the connected subgraph in. Such a loop traversal of all rectangular regions of the pixel [7] can be found in the shadow region. After using principal component analysis method, we can determine the shadow sharp point.

Principal component analysis method [8] is constructed a new set of latent variables, so as to reduce the dimensionality of the original data space, obtaining information from the new mapping spatial and statistical features, the structure of understanding of the original data. The basic idea is to find a new set of variables instead of the original [9], and the new variable and the original variables are linear combinations. The number of new variables is less than the number of the original variables, while the maximum degree of retention of the original variable is the useful information.

According to the above model, a series of coordinates can be extracted from the video. The model can be obtained by using the model in 1.

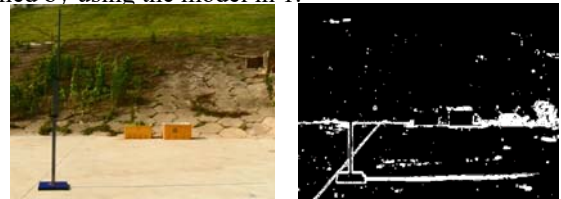


Figure 6 track coordinate effects

IV. CONCLUSION

It is challenging but very meaningful to estimate the geographic information by applying photos. The sun shadow location technology is a kind of accurate and feasible information analysis technology, so it is of great significance for the analysis and research of the technology.

REFERENCE

- [1] China Meteorological Bureau, Ground Meteorological Observation Standard [S]. Beijing: Meteorology Press, 2003:133.
- [2] Wu Mengda, Cheng Lizhi et al, Mathematical Modeling Course [M], Changsha: Higher Education Press, 2011.
- [3] Chen Xiaoyong, Zheng Keke, the formula of the hour angle and declination of the sun in the building sunshine calculation, Zhejiang building, 28 (9): 7-122011.
- [4] Xi'an University Of Architecture And Technology. Physics of Construction. Beijing: China Building Industry Press, 3.
- [5] Wu Lin, Cao Xiaochun, the study of the latitude and longitude estimation technology based on the sun shadow track, Tianjin University, 2010.
- [6] Duan Xiaojuan, Shi Haoshan. An Improvement Based on Obstacle Detection of Infrared Imaging, Electronic and Information Engineering Department, Northwestern Polytechnical University, 2009.
- [7] Cheng Guang, Gong Jian, Ding Wei. The Real-Time Anomaly Detection Model of High-Speed Network Based on Sampling Measurement. Journal of Software, Vol. 13, No. 4, 2002.
- [8] Q. Chen, H. Wu, T. Wada, Camera calibration with two arbitrary coplanar circles, in: Proceedings of the ECCV, 2004, 521~532.
- [9] Y. Chuang, D. Goldman, B. Curless, D. Salesin, R. Szeliski, Shadow matting and compositing, ACM Trans. Graph. 2003, 22 (3): 494~500.

Research of Urban Logistics Node Layout Solution

Peng Liu, Yan Yan *, Jianjian Zhang, Baosheng Jiang, Yajuan Qiao ,Baona Sun
North China University of Science and Technology, Tangshan, 063000, China

Abstract—In view of the city logistics nodes is not reasonable, the current situation of express transport efficiency is too low, Research on urban logistics node layout, Improve the efficiency of express transportation, This paper proposes a research plan: By considering the cheapest express business, the highest efficiency to establish the center location, the optimal delivery distribution path and built logistics node rapid transit Bi-level programming Site selection model. The model can achieve the optimal allocation of resources and improve the efficiency of the logistics system.

Index Terms—Center location, Distribution of path, Bi-level programming

I. INTRODUCTION

There is an inevitable connection between Logistics node layout and Regional economic development speed. The effective logistics node layout can improve the efficiency of express transportation, improve the regional status of the city and promote the development of urban economy [1].

The paper is based on optimization theory. In view of the urban logistics node layout and express the influence factors of transport efficiency, we study the construction and optimization of logistics system to achieve the optimal allocation of resources and improve the efficiency of thee logistics system[2].

II. ALLOCATING EXPRESS AXIAL RADIAL NETWORK MODEL

Express business include sorting, storing, transporting and transfer ingand so on many homework. This process will produce some costs. Because the store link and transportation service exist time error, so we mainly consider sorting costs, transportation costs and transit costs.[3]

Express between nodes $q_{ij}, i, j = 1, 2, 3, \dots, n$, n is the number of nodes in the network. Node k has n_k the sorting direction. Sorting fees [4] $s_k(n_k)$:

$$\sum_{i=1}^n \sum_{j=1}^n q_{ij} \left(\sum_{k \in I_{ij} - \{j\}} s_k \right) \quad (1)$$

Road (u, v) 's fixed fee is f_{uv} , The unit variable cost c_{uv} , Delivery quantity:

$$R_{uv} = \sum_{i=1}^n \sum_{(u,v) \in L_{ij}} q_{ij} \quad (2)$$

$$(u, v) \in N \times M \quad (3)$$

Road transport cost is:

$$f_{uv} + c_{uv} \sum_{(u,v) \in L_{ij}} q_{ij} \quad (4)$$

Transportation costs:

$$\begin{aligned} & \sum_{R_{uv}>0} \left(f_{uv} + c_{uv} \sum_{(u,v) \in L_{ij}} q_{ij} \right) \\ &= \sum_{R_{uv}>0} f_{uv} + \sum_{R_{uv}>0} \left(c_{uv} \sum_{(u,v) \in L_{ij}} q_{ij} \right) \\ &= \sum_{R_{uv}>0} f_{uv} + \sum_{i=1}^n \sum_{j=1}^n q_{ij} \sum_{(u,v) \in L_{ij}} c_{uv} \end{aligned} \quad (5)$$

Assume that nodes as k . The unit transfer fee as g_k , so The transit costs:

$$\sum_{i=1}^n \sum_{j=1}^n q_{ij} \left(\sum_{k \in L_{ij} - \{i, j\}} g_k \right) \quad (6)$$

Nod set as $N = \{1, 2, \dots, n\}$, Delivery quantity between the nodes $q_{ij}, i, j = 1, 2, \dots, n$

Determine[5]:

- ① Express network hub set as $H \subset N$, H : hub set
- ② Each distribution center $i \in M$'s Distribution hub for the collection $V_i = \{k \in H : (i, j) \in E\}$ V_i primary node E : between two points of express highway
- ③ The transport path between any two points $L_{ij}, i, j \in N$

The total cost:

$$\begin{aligned} Z_0 &= \sum_{i=1}^n \sum_{j=1}^n q_{ij} \left(\sum_{k \in L_{ij}} s_k(n_k) \right) + \left(\sum_{R_{uv}>0} f_{uv} + \sum_{i=1}^n \sum_{j=1}^n q_{ij} \sum_{(u,v) \in L_{ij}} c_{uv} \right) \\ &+ \sum_{i=1}^n \sum_{j=1}^n q_{ij} \left(\sum_{k \in L_{ij} - \{i, j\}} g_k \right) \\ &= \sum_{R_{uv}>0} f_{uv} + \sum_{i=1}^n \sum_{j=1}^n q_{ij} \left(\sum_{k \in L_{ij}} (s_k(n_k) + g_k) + \sum_{(u,v) \in L_{ij}} c_{uv} \right) \\ &- \sum_{i=1}^n \sum_{j=1}^n q_{ij} s_j(n_j) - \sum_{i=1}^n \sum_{j=1}^n q_{ij} (g_i + g_j) \end{aligned} \quad (7)$$

We know

$$\sum_{i=1}^n \sum_{j=1}^n q_{ij} s_j(n_j) + \sum_{i=1}^n \sum_{j=1}^n q_{ij} (g_i + g_j) \quad (8)$$

is constant and the objective function adds a constant does not affect its optimality[6].We get Assign Courier shaft radial network design optimization model as

$$z = \sum_{R_{uv}} f_{uv} + \sum_{i=1}^n \sum_{j=1}^n q_{ij} \left(\sum_{k \in L_{ij}} (S_k(N_k)) + \sum_{(u,v) \in L_{ij}} c_{uv} \right) \quad (9)$$

$$S.t. \quad R_{uv} = \sum_{i=1}^n \sum_{j=1}^n q_{ij} \quad (10)$$

$$(u, v) \in N \times M$$

First for any

$$(i, j) \in H \times H \cup M \times H \cup H \times M, i \neq j \quad (11)$$

Second for any

$$\text{if } t_{ik} + t_{kj} \leq T_{ij} \quad \text{and} \quad l_{ij} > r_{ij} + r_{kj}, \quad (12)$$

$$(i, j) \in M \times H \times H \cup M \times H \times M$$

Third for any

$$(i, j) \in M \times H \times H \times M \quad (13)$$

if $l_{ij} = +\infty$ then $t_{ij}^p = +\infty$ for any $k \in H$ carry out[7]:

$$\left\{ \begin{aligned} &t_{ij}^p > t_{ik} + t_{kj}, l_{ij} = r_{ik} + r_{kj}, p_{ij} = k, \\ &t_{ij}^p = t_{ik} + t_{kj}, t_{ij}^p < +\infty, t_{ij}^p = t_{ij} + t_{kj}, \\ &l_{ij} > r_{ik} + r_{kj}, l_{ij} = r_{ij} + r_{kj} \end{aligned} \right\} \quad (14)$$

Forth

$$\text{for any } (i, j, k) \in M \times H \times M$$

$$\text{among them } i \neq j \text{ if } l_{ij} = +\infty$$

and

$$l_{ij} > r_{ik} + r_{kj}$$

$$\text{then } l_{ij} = r_{ik} + l_{kj} \quad p_{ij} = k, t_{ij}^p = t_{ik} + t_{kj}^p$$

$$\text{Fifth for any } (i, j) \in M \times M$$

$$\text{among them } i \neq j, \text{ if } l_{ij} = +\infty$$

$$\text{then } t_{ij}^p = +\infty$$

$$\text{for any } k \in H$$

carry out :

$$\left\{ \begin{aligned} &t_{ij}^p > t_{ik} + t_{kj}, l_{ij} = r_{ij} + r_{kj}, p_{ij} = k, \\ &t_{ij}^p = t_{ij}, t_{ij}^p < +\infty, t_{ij}^p = t_{ik} + t_{kj}, \\ &l_{ij} > r_{ik} + r_{kj}, l_{ij} = r_{ik} + r_{kj} \end{aligned} \right\} \quad (15)$$

$$\text{Sixth for any } H \{V_i : i \in M, M = N - H\}$$

III. USE SIMULATED ANNEALING METHOD TO CALCULATE THE OBJECTIVE FUNCTION

Use Simulated annealing method to search[8]

$$H \{V_i : i \in M, M = N - H\} \quad (16)$$

We already known the express the amount between any two points and Sections of variable cost, the road transportation time and transportation cost of fixed cost and shipping time budget value.[9]We can get the sorting function:

$$s_k(n_k) = s_k \cdot \ln(n_k), k = 1, 2, \dots, 6 \quad (17)$$

After that we use the Simulated annealing method to solve: The initial temperature is 2000,The temperature drop rate is 0.95.If the temperature is below 10 degrees, we use Such as step down. Step length is 0.5,The same temperature number of iterations are 200,The temperature dropped to 0.5 or the objective function In the 15 iteration ends when algorithm cannot be changed[10].

IV. CONCLUSIONS

It is concluded that the express freight path matrix $[p_{ij}]_{n \times n}$ by finding the optimal objective function value to determine the specific type of node. The minimum corresponding node type the optimal network structure is the node functional allocation.

ACKNOWLEDGMENTS

Work is supported by College Students' Innovative Project in North China University of Science and Technology(X2015225).

REFERENCES

- [1] Li Fengyan,Hou Xianyun, "Shaft radial grain logistics network of lateral coordination", Economic geography, 2014/02.
- [2] He Minghe , Cheng Hongjing , "Air freight express enterprise network construction" , Strategy and management",2013/06.
- [3] Sun Zhizhong,Zhang Xiaoyan, "Gansu province logistics industry development countermeasure", The development of research,2014/01.
- [4] He Dengcai , Cha Yingxin , Li Jinying , Hong Tao, "China's rural logistics development report" , China's economic cooperation,2013/09.
- [5] Wang Dongqing,Shi Jing, "Based on the operation target of logistics customer service cost measurement and control research", Logistics technology,2013/03.
- [6] Min Jianing, "Based on the strategy of greedy one-to-many delivery vehicle routing optimization" , Logistics technology,2015/13.
- [7] Fang Chenyang, "Effective measures to reduce express transportation cost in logistics", Chinese trade,2014/28.
- [8] Jiang Min. "More than a loss risk value of bi-level programming model and its application conditions.Systems engineering theory and practice",2013/04.
- [9] Qi Jianxun,Su Zhixiong,Zhang Lihui, "Undirected network the most positive short circuit model and theoretical analysis.Systems engineering theory and practice",2012/10.
- [10] Mi Linglin,Shi Feng, "To allocate express shaft radial network hub location and distribution optimization method",Systems engineering theory and practice,2012/02.

Research On Fire Resistance Of Reinforced Concrete Columns

Yu Junpeng^{1,2}, Li Qiuming^{1,2}, Zhang Haojie³

1. North China University of Science and Technology, Construction and Engineering College, Tangshan 063009, Hebei, China

2. Hebei Earthquake Engineering Research Center, Tangshan 063009, Hebei, China

3. The Third Construction Engineering Company LTD. Of China Construction Second Engineering Bureau Fengtai, Beijing 100070, China

Abstract—With the development of human society, we are seeking more and more sturdy building. In this paper, we mainly study the high temperature fire resistance of reinforced concrete columns. First, we studied the high temperature mechanical properties of concrete and the mechanical properties of the steel bar. Then we combine the finite element method and ANSYS software to simulate the reinforced concrete columns subjected to fire and calculated its ultimate bearing capacity. Finally come to the conclusion: In the design of China's fire code, need to be added the request which for concrete protective layer thickness and so on.

Abstract—Reinforced concrete column; Fire resistance; Ultimate bearing capacity; Numerical simulation

I. INTRODUCTION

Fire prevention is always a long-term and arduous task for us humankind. Fire resistance of structures is an important and difficult problem in structural engineering. Reinforced concrete structures are one of the most familiar structures in structural engineering, and its fire resistance is better than other structures such as steel structures and wood structures, but it will become disabled under conflagration too. To begin with, fire resistance of reinforced concrete columns should be studied, because columns are one of the most important elements in structures. If the columns are disabled, the whole structure will collapse or overturn. In addition, the research on fire resistance of reinforced concrete columns provide the foundation for study on other rising combined columns such as concrete filled steel tubular

columns and steel reinforced concrete columns. So we research reinforced concrete structures in order to make my own contribution in Structure fire resistance.

II. HIGH TEMPERATURE MECHANICAL PROPERTIES OF CONCRETE

The compressive strength of concrete is one of the most important and basic parameters in the mechanical properties of the concrete, and it is often used as a basic parameter to determine the level and quality of concrete, and to determine other mechanical properties, such as tensile strength, elastic modulus and peak strain. At high temperature, this feature is still set up.

At high temperature, the strength and deformation of concrete are deteriorated, and the main reasons are summarized as three points: (1) Internal cracks and voids formed after evaporation;(2) The thermal performance of the coarse aggregate and cement paste is not the same, the deformation difference and the internal stress, and the cracks in the interface form;(3) Thermal expansion and rupture of coarse aggregate. These internal injuries continue to develop and accumulate with the increase of temperature, which is more serious.

At the same temperature, the concrete strength grade ($C20 \sim C50$) is high, and its relative high temperature strength is low, but the difference is not significant. As shown in table 1:

Table1 Effect of concrete strength grade on high temperature strength

Concrete	$f_{cu}(T) / N \cdot mm^{-2} \quad (f_{cu}(T) / f_{cu}(0))$					
	Room temperature	100°C	300°C	500°C	700°C	900°C
C20	30.5	28.2(0.925)	32.5(1.066)	24.7(0.810)	10.6(0.348)	3.6(0.118)
C40	55.0	50.3(0.915)	56.7(1.031)	43.7(0.795)	21.4(0.389)	5.0(0.009)

Short term high temperature creep of concrete $\varepsilon_{cr}(T, \sigma, t)$ is the strain that increases with time under the action of stress. According to the research data of Tsinghua University, the concrete short-term high temperature creep value greatly exceeds the normal temperature decades of creep values, but with the changes of room temperature creep similar: high temperature creep in the initial stage of loading development rapidly, and then the growth rate decreasing. Concrete of short-term high temperature creep is the

internal cracks of massive expansion and extension caused by, the main influencing factors [1]: temperature, stress level and duration of the aggregate species and with ratio, the existing test variables measured data quite discrete, a difference of several times [2]. In addition to the factors affecting the creep, the change range is big, the high temperature test method is not unified and the variable measurement technique is also important reason.

in view of the short - term high temperature creep of ordinary silica concrete, the Swedish Anderberg gives the following formula [3]:

$$\epsilon_{cr}(T, \sigma, t) = -\frac{\sigma}{f_c(T)} \sqrt{\frac{t}{3}} e^{\frac{3.04(T-20)}{1000}} \times 530 \times 10^{-6} \quad (1)$$

In formula (1), t is the time of the fire. (unit h), T is the Temperature of concrete (unit $^{\circ}C$).

By the comparison of two hours and 2 hours, the temperature of the high temperature creep of concrete after 2 hours can be obtained: As shown in Figure 1

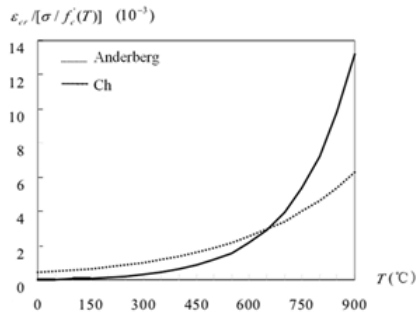


Figure 1.2 hours after the high temperature creep of concrete with temperature curve

It can be seen from Figure 1: The two models had little difference before 700, but the gap was gradually expanded at 700, and the difference was nearly two times when it reached 900, Therefore, the model should be selected reasonably in the analysis of the structure of the temperature exceeding 700.

III. HIGH TEMPERATURE MECHANICAL PROPERTIES OF STEEL BARS

At present, many scholars at home and abroad have done a high temperature tensile strength test, in the test can be observed in many similar high temperature characteristics of steel. The color of the bar surface gradually changes during the heating process: When the temperature is less than 300 DEG C, the surface is gray. After the temperature is more than 400, the color is deepened, When temperature reached 600, it was displayed as red. After the temperature reached 700, it display as black red.

Professor Lv Tongguang of China carry out high temperature tensile test of five kinds of steel bars, and derive the high temperature limit of the steel bar as shown in the formula:

$$\text{I, II, III, IV Steel} \quad \frac{f_u(T)}{f_u} = \frac{1}{1 + 36\left(\frac{T}{1000}\right)^{6.2}} \quad (2)$$

$$\text{V Steel} \quad \frac{f_u(T)}{f_u} = \frac{1}{1 + 56\left(\frac{T}{1000}\right)^{4.4}} \quad (3)$$

In formula (2) and formula (3), f_u represents the ultimate tensile strength of steel at room temperature.

The foreign experimental research has also shown that the V grade steel than other grades of steel of relatively high temperature, ultimate strength low, when the temperature difference between up to 25% ~ 35%. V grade steels used for concrete structure, at high temperatures the largest loss of strength, so the fire resistance of the component should pay more attention to.

IV. NUMERICAL CALCULATION OF ULTIMATE BEARING CAPACITY OF REINFORCED CONCRETE COLUMNS UNDER FIRE

With the continuous development of computer technology and finite element theory, the finite element method has become a common method to analyze complex problems in various disciplines. With the development of the constitutive relation of steel and concrete, the numerical simulation of reinforced concrete columns can be realized by combining the finite element method with the finite element method.

For numerical calculation of reinforced concrete column, the following basic assumption is generally taken:

1) The temperature field of the column section is unchanged along the axis of the column, and has nothing to do with the stress, strain, whether or not of the concrete: The temperature field of reinforced concrete column is only determined by the heat exchange of the surrounding environment, which has nothing to do with the stress and strain of the material. The temperature distribution near the surface of the cylinder will be affected, and the temperature distribution near the surface of the cylinder will be affected, and the distribution of the heat will be affected.

2) Flat cross section deformation: Section of the column is much smaller than the length of the column. In concrete cracking front, even by the high temperature of the role of a large, uneven temperature deformation, is still subject to external and internal constraints to maintain the role of flat cross section deformation.

3) There is no slip between steel bars and concrete: Good bond between steel and concrete is the basis of their common work. Before cracking of reinforced concrete column, the deformation of the two is equal and no relative slip. Due to the lack of research on the slip between steel bars and concrete at high temperatures, the lack of data. So we Hypothesis there is no relative slip between the two.

This paper mainly through the column limit axial force envelope of bending moment to determine the three pillars of the ultimate bearing capacity of surface , As shown in Figure 2:

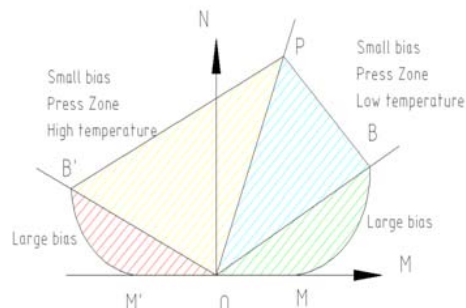


Figure 2 Ultimate axial force envelope diagram of the three high temperature column

The calculation method of ultimate bearing capacity of the reinforced concrete column is summarized as follows five steps:

1) Bending member, calculating the ultimate moment, and determining the envelope, M , M' two points;

2) Identify two directions of the large and small bias failure of the boundary points, B , B' two points, the calculation of the corresponding ultimate bearing capacity;

3) When the extreme eccentricity is greater than the limit, the ultimate load bearing capacity is solved by the large bias;

4) Calculation section of extremely strong bearing capacity, determine the P point

5) Established the envelope line of small bias, and the ultimate load bearing capacity is calculated by the insertion method.

Surrounded by the pillar of ultimate bearing capacity formula of the axis as shown below:

$$N_{ut} = (k_c \times A_c \times f'_c) / (1 + 1.0 \times k_\phi) + k_s \times A_s \times \sigma_{0.5}(T_m) \quad (5)$$

In formula (5): A_c represents the equivalent section area of concrete, m^2 ; A_s represents the area of reinforcement, m^2 ; k_c , k_ϕ , k_s represents the coefficient of the ratio of the length to the length of the reinforcement, the reinforcement and the strength of the concrete. Which needs to check the specification; T_m represents the average temperature of steel bars, °C; $\sigma_{0.5}(T_m)$ represents the stress corresponding to the 0.5% strain, MPa.

For the eccentric compression columns of four sides, the influence of the two order effects must be taken into consideration, and the moment amplification coefficient is used to enlarge the initial bending moment::

$$M_{Tot} = M_0 / C \quad (6)$$

Among them:

M_{Tot} represents the total bending moment acting on the cross section;

M_0 represents the initial bending moment of load;

C represents the moment amplification factor, need to check the specification to get.

After getting the section axial force and bending moment, the formula for calculating the ultimate bearing capacity of the section is as follows:

$$N = f'_c(T) \times 0.8 \times x \times b + \sum (f'_s(\epsilon'_s, T) \times A'_s) - \sum (f_s(\epsilon_s, T) \times A_s) \quad (7)$$

$$M_{Tot} = f'_c(T) \times 0.8 \times x \times b \times (h_0 - 0.4x) + \sum (f'_s(\epsilon'_s, T) \times (h_0 - a'_s)) \quad (8)$$

Among them, in addition to the high temperature strength of steel, concrete, and other symbols are

equivalent to the normal temperature of the calculation of the ultimate bearing capacity of the symbol.

V. CONCLUSION

In this paper, the fire resistance of reinforced concrete columns is analyzed theoretically and compared with that of the existing steel, concrete and high temperature mechanical properties, and the fire resistance analysis and design method of reinforced concrete columns are discussed. A new simplified calculation method is presented.

First, we summarize and compare the thermal performance of steel and concrete, the thermal performance and thermal model of concrete, and find out the similarities and differences of the models used in the analysis of other countries.

Then, through theoretical research on the structure of reinforced concrete columns, the influence of increasing the section size, ratio of longitudinal reinforcement, concrete strength grade and so on can effectively improve the fire resistance limit of reinforced concrete columns, and it is suggested that the design code of fire protection code for reinforced concrete columns should be added to the requirements of the thickness of concrete cover.

REFERENCE

- [1] Geymayer H G.. Effect of temperature on creep of concrete: A Literature Review[J]. ACI SP 34-31, Detroit, 1972. 565-589
- [2] Crispino E. Studies on the technology of concrete under thermal conditions[J]. ACI SP 34-25, Detroit, 1972. 443-479
- [3] Tan K H, Yao Y. Fire resistance of four-face heated reinforced concrete columns[J]. ASCE Journal of Structural Engineering, 2003, 129(9): 1220-1229.
- [4] Schneider U, Haksever A. Evaluation of the equivalent fire duration of reinforced concrete beams in natural fires. In: Final Research Report of Technical University of Braunschweig[J]. German, 1977, 53-63
- [5] Parra-Montesinos, Gustavo J, Bobet A, et al. Evaluation of soil-structure interaction and structural collapse in Daikai subway station during Kobe earthquake[J]. ACI Structural Journal, 2013, 103(1): 113-122.
- [6] An X H, Shawky A A, Maekawa K. The collapse mechanism of a subway station during the great Hanshin earthquake[J]. Cement and Concrete Composites, 2012, 19(3): 241-257.
- [7] Samata S, Ohuchi H, Matsuda T. A study of the damage of subway structures during the 1995 Hanshin-Awaji earthquake[J]. Cement and Concrete Composites, 2009, 19(3): 223-239.

The Comparison Of Regression Analysis And Grey Prediction And Joint Use

Qi Zhou, Shaoqian Huang, Haiyu Kan, Aimin Yang*

North China University of Science and Technology Tangshan of China, 063000, China

Abstract—This article in view of the prediction problem, first of all, forming standard for amount of random and nonrandom quantity is determined from the symbol in the regression analysis, and then through regression function and the mathematical expectation, regression equation will be established. Next, analyze the several kinds of information which failed passing the hypothesis test; Secondly, the grey data column and time parameters are to be samples. For grey prediction, from the regression analysis—regression function point of view, the grey forecasting time response will be established and longitudinal data will be dealt with the horizontal data, trying to realize unified modeling process of different kinds of data; According to the different features of regression analysis and grey forecasting, putting forward regression analysis and grey prediction is applied to the system problem of great prospects.

Index Terms—Regression analysis; Grey prediction; Longitudinal data; The horizontal data; The joint application

I. THE INTRODUCTION

About regression analysis to the current domestic works sort is various, for the perspective of the regression equation is also varied, and for the use of regression analysis of mathematical symbols is not standard, so this paper is to give the regression equation established from the perspective of mathematical expectation, the use of mathematical statistics on the overall about sample related symbols to establish the regression equation, and gives several reasons for regression equation failed the hypothesis test specific, the other grey prediction itself still has strong randomness, itself still have random mathematics related attributes, so after the specification of the regression analysis is given to express, this paper further longitudinal data combined with the regression method of the grey prediction in accordance with the horizontal data processing, to achieve a "predict" the form of unification, can better realize the unification process.

II. THE ESTABLISHMENT OF THE REGRESSION EQUATION

Regression analysis, as one of the prediction tool, obviously has the nature of good, besides regression analysis can be based on the mathematical statistics, implementation with mathematical statistics about the overall good fusion with samples, with the aid of mathematical statistics the related concepts of complete relevant operation, is conducive to implementing software operation, most of the traditional regression analysis has the disadvantage of symbol confusion, random concept with the concept of nonrandom mix as well as the analysis model fragmented, related concepts in this paper by means of mathematical statistics and for the regression analysis from the perspective of random

and nonrandom angle, giving the regression equation, a regression analysis of the exact system are presented.

Simple regression analysis as a special case of multiple regression analysis, obviously the vast majority of information can be reflected in the multiple linear regression, so only with multiple regression analysis as an example to establish regression analysis system

First of all to this rule symbol overall, sample, sample observation value:

Overall and indicators:

$$X = (X_1, X_2, \dots, X_p) \tag{1}$$

$$x = (x_1, x_2, \dots, x_p) \tag{2}$$

Regression analysis is first overall relationship, such as table 1:

Table 1 the relationship between the overall

	$X_{(1)}$	$X_{(2)}$	$X_{(3)}$	$X_{(n)}$
X	$x_{(1)}$	$x_{(2)}$	$x_{(3)}$	$x_{(n)}$
Y	y_1	y_2	y_3	y_n
	Y_1	Y_2	Y_3	Y_n

Regression analysis was presented for statistics and related relations. The two "a relationship" build exact function of the overall form—namely regression function. Observations are made to get a sample. So prediction is obtained.

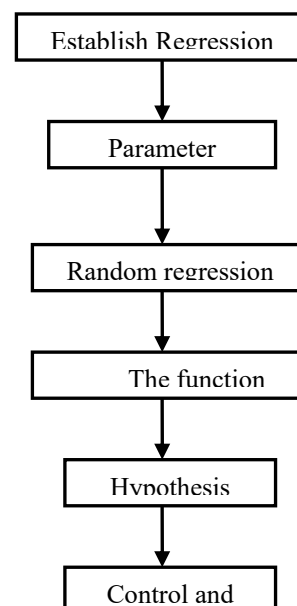


Figure 1 the process of establishing regression analysis

After a given observation, Mathematical expectation is used to predict, namely by the conditional expectation of prediction. But expected value and true value is obviously has the error and, in fact, after all, prediction is

not true. And there are some error between the true value and prediction. Because Y is a random variable, so the formation of random errors will be here: $Y = E(Y | \mathbf{X} = \mathbf{x}) + \varepsilon$

the form of $E(Y | X = x)$:

$$f(\mathbf{x}) = f(x_1, x_2, \dots, x_p) = E(Y | \mathbf{X} = \mathbf{x}) = \beta_0 + \beta_1 x_1 + \beta_2 x_2 + \dots + \beta_p x_p \quad (3)$$

$$f(\mathbf{x}_{(i)}) = f(x_{i1}, x_{i2}, \dots, x_{ip}) = E(Y | \mathbf{X} = \mathbf{x}_{(i)}) = \beta_0 + \beta_1 x_{i1} + \beta_2 x_{i2} + \dots + \beta_p x_{ip} \quad (4)$$

by the least squares principle, to determine the parameter values.

$$\hat{y} = \hat{\beta}_0 + \hat{\beta}_1 x_1 + \hat{\beta}_2 x_2 + \dots + \hat{\beta}_p x_p \quad (5)$$

F testing:

Reject H_0 :

All the independent variables of the whole has a significant linear relationship

Receive H_0

All of the independent variables has no significant linear relationship with Y . This can be explained from two aspects:

Compared to the traditional regression analysis, More according to the random variables in this paper, the regression analysis has been explained. Symbols and expression are standardized.

II THE ESTABLISHMENT OF THE GREY PREDICTION MODEL

Often grey prediction is always from the perspective of data column and time response type definition and push to, and grey forecasting is clearly still with a lot of randomness, so with the help of regression analysis of grey prediction model is set up, there is a reason, and in the framework of stochastic unified programming steps is given

For the form of regression function, determined by the solution of differential equation:

$$\frac{df(t)}{dt} + af(t) = b \quad (7)$$

Arrange to get:

$$X^{(1)} = \left[x^{(0)}(t_i) - \frac{b}{a} \right] e^a e^{-at} + \frac{b}{a} + \varepsilon = \left[x^{(0)}(t_i) - \frac{b}{a} \right] e^{-a(t-1)} + \frac{b}{a} + \varepsilon \quad (8)$$

The time discretization, get:

$$\hat{X}^{(1)} = \left[x^{(0)}(1) - \frac{\hat{b}}{\hat{a}} \right] e^{-\hat{a}(k-1)} + \frac{\hat{b}}{\hat{a}} \text{ or}$$

$$\hat{x}^{(1)} = \left[x^{(0)}(1) - \frac{\hat{b}}{\hat{a}} \right] e^{-\hat{a}(k-1)} + \frac{\hat{b}}{\hat{a}} \quad k = 1, 2, 3, \dots \quad (9)$$

In order to close to the regression analysis, and overall, as an ordinary regression analysis is the study of the cross section data, and the data source can be regarded as the same time different people were observed, and the grey prediction of the data attribute is the longitudinal data, by using regression function, also the longitudinal data to deal with the horizontal method of data processing, and horizontal longitudinal data unified process.

III. JOINT APPLICATION

Regression analysis depends on a large amount of data, and grey forecasting in only a small amount of data can be complete forecast process. In real life, often for a system, we should consider the component part of the system of related indicators, and the index of different have different sources of data, including some data source is adequate, some data source is limited, so by regression analysis and the combination of grey forecasting applications often can realize the complementary advantages, to achieve the purpose of solving the problem of system.

Now more and more problem is no longer a simple question, but a complex system problems, this requires some kind of method can juggle various problems in the system properties, so the joint using regression analysis and grey prediction is has a great prospect.

REFERENCES

- [1] Lianfu Liu. Several determining methods in unary linear regression equation of regression coefficient [J]. Journal of Shenyang Normal University (Natural science edition), 2008, 406:406-408.
- [2] Juanjuan Zhang. Robust linear regression in renewable power the effectiveness of the least squares method research [D]. Taiyuan University of Technology, 2013.
- [3] Huiwen Wang, Jie Meng. Modeling method of multivariate linear regression prediction [J]. Journal of Beihang University, 2007, 2007:500-504.
- [4] Yushan Zhang. Multiple linear regression analysis of case study [J]. Journal of Information technology, 2009,09:54-56.
- [5] Xiuying Chen, Hao Gu. Gray linear regression model in the application of port throughput prediction [J]. Port & waterway engineering, 2010, 12:89-92.
- [6] Yongfeng Ji. Grey multiple linear regression analysis and its application research [D]. Northeast Normal University, 2008.
- [7] Jun Zhang. The grey prediction model is improved and its application [D]. Xi'an University of Technology, 2008.
- [8] Yi Lu. Grey prediction model and its application [D]. Zhejiang Sci-tech University, 2014.

An Investigation On The Influence Of Network Games On College Students

NA Hao , LI Zhi-yang, LIN Xiao-tan, LI Jie, HAN Chuang-chuang, XIN Zi-cheng, LIU Zhen-chao
 North china university of science and technology, Hebei, The ministry of education key laboratory with modern metallurgical technology, Hebei, Tangshan 063000, China

Abstract—Aiming at the university students obsession to the network game, through the questionnaire survey, understanding to now college students internet basic situation, contact network game channels and network game type and frequency of games to play, and network game between men and women, so that present situation of relationship between college students with network game and existing problems and aiming at the present situation and the question proposed corresponding suggestions.

Index Terms—online games, physical and mental, health hazard

I. INTRODUCTION

Along with the popularization of computer and the improvement of College Students' living standards, college students have become more and more closely related to the Internet[1-3]. The time of the Internet has gradually increased. Most students have become a hobby.

II. COLLEGE STUDENTS' RELATIONSHIP WITH THE NETWORK GAME STATUS QUO AND EXISTING PROBLEMS

This paper to investigate college students in Tangshan area, adopting the questionnaire form, aiming at the condition of the college students to get to the Internet and the influence of online games on college students in the investigation.

(1) The basic situation of college students on the Internet

The investigation object, freshman and sophomore students proportion is higher, at 75.8% of net age up to 62.27% for five years, a total of 82.6% of more than 3 years. According to the survey, surf the Internet every day of time 1 to 2 hours (33.3%), 2-4 hours (32.7%), four hours or more 19.6% of the total, among them, 39.2% of respondents to get to the Internet to play games, 67.3% will see a movie, 65.4% is given priority to with learning, browse news, 66% will chat friends, sending and receiving E-mail.

(2) The network game

We through the survey found that 39.2% of respondents infatuated with online games, that is the main thing is to play games online, with 19.6% of the respondents almost every day to play, play a two or three days, 22.9% and 30.1% of the time playing games up to 1-3 hours, 17% longer than 3 hours. From the point of view of the perception of respondents, 62.1% of respondents said the time control of the online gaming in the hands of their own, roughly 25.5% of the said sometimes addicted, but most of the time will be enough is enough. In addition, the online game often lead to

problems in study and life, can also be interpreted as "online games sequela, such as 24.8% of the students thought that the end of the game will always be thinking about things related to the game, what is more, 11.8% of the students after playing the games, more less than once upon a time to participate in collective activities such as friends in real life, outing, etc.

(3) Contact network channels and network game type

The rapid development of network game has produced different kinds of network game type, all kinds of games are actually with the help of props, imitation of life, production and fighting, in the online world of virtual people in individual or social activities, realize the interaction between players, irresistible for college students. Nearly 70% of the respondents is by classmates, friends, access to the network game, 37.2% is through the network come into contact with the media and advertisement propaganda way. Of these, 53.6% often play chess game (such as The Three Kingdoms, lianliankan), 40.5% are usually casual online games, 35.3% often play role-playing, 33.3 usually play racing games, music (e.g., kartrider, QQ dazzle dance).

(4) The boys and girls affected by online games.

In general, the boys compared with 58.8% of the survey, women was 41.2%

Table 1 The purpose of college students' Internet boys and girls compared

gender	The main thing is to play games online
male	15.79%
female	7.96%

Among them, the boys love of network game level reached almost twice as many girls, so, many online game content is challenging and casino, this longing for impulsive, aggressive, stimulate the boy is very full of temptation, they hope to online games to release myself, reality is difficult to get from the online gaming experience, while girls mainly for entertainment, gain happiness. Now most of the online game for boys, so the number of boys playing online games than girls. However, 36.24% of women prefer small game, 36% of men tend to role-playing games, it has to do with the men and women have different hobbies.

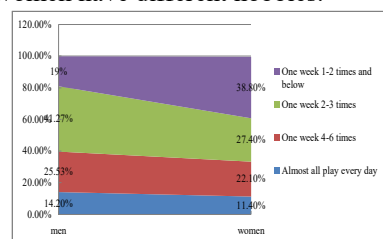


Fig.1 Play frequency histogram investigation

According to our investigation: playing games frequency on the problem, as shown in the above, most of the boys in 2 to 3 times a week, while girls in 1 to 2 times a week. In every day to play games of male students (14.2%), female students accounted for 11.4%. This is mainly because the girl have a shopping, leisure activities, such as do hair, take their time. Now the network game mainly war strategy, action fantasy is given priority to, casual games relative to less, so lead to average boys play games more than girls. Investigations, we also found that respondents monthly living expenses 800-1000 accounted for 38.6%, 36.66%, 1000-1200, 1200 yuan of above 20.3%, and on the network game's average monthly cost of 100 yuan of less than 12.4%, 7.2% of 100-300 yuan, of course, there are 78.4% of the said not spend any money on online games.(5) the college students contact network game

Table 2 College students' attitude towards online games

option	The proportion
A. online games can get in real life, let me can't get something, so it's like	5.2%
B. network game can let I can relax in the strain of real life	15%
C. network game expanded my horizons, made many new friends, that will be helpful to growth	4.6%
D. network game influenced my study and life, now I regret it	1.3%
E. leisure"	73.9%

III. THE INFLUENCE OF THE COLLEGE STUDENTS ADDICT NETWORK GAME

Addict network game to the harm done by the students a lot, we group discussion after it is concluded that the harm to the following several aspects[4]:

3.1 The dangers of online games on college students' body

Addicted to online games has a lot of harm to the body, can lead to excessive with the eye, affect vision, can appear sometimes dazzling, and eye symptoms, serious can cause keratitis and temporary blindness. Addicted to online game the brain in a highly excited state for a long time, it's easy to have a nervous breakdown, at the same time also can cause an imbalance in the body of hormone, immune suppression.

3.2 The dangers of online games on college students' academic

Should college students with academic, addicted to online games seriously affect their studies. They will study most of the time and energy in the network game, can lead to some college students fail to pass the exam, the phenomenon such as make-up examination, rebuild, and even affect their graduation.

IV. THE REASONS OF COLLEGE STUDENTS ADDICT NETWORK GAME

Analysis of the questionnaire that most college students spend time on online games is more, some even indulge, unable to extricate themselves, only 30% of the students think online learning has certain adverse effect on life. According to the questionnaire, the cause of the addict network game of university students can be roughly summary for the following several aspects:

The characteristics of online game is a beautiful picture, the design process is full of suspense, stimulate students' curiosity, to continually produce passion play[5]. In addition, in the network game virtual sex, equality, open to let students experience is different from the real world of pleasure and freedom.

On the characteristics of college students themselves, has the following two points:

(1) Time, regulation and money problems, college students compare past have more free time, by the regulation is relatively small, can independently arrange time, resulting in part of self control ability is poor students easily addicted to the game. In addition, college students have a certain economic foundation, to have more control over free money, from the survey we found more than 20% of the students spend money on the game.

(2) Mentality problem - a lot of college students have a herd mentality, easy to follow classmates, friends, online game addiction. Now a lot of college students is only children, physical and mental development is not yet mature, facing with the situation of academic and employment pressure, relying on the network game to vent their tension, depressed mood, once the game is deeply addicted addiction, difficult to extricate themselves[6].

Now most college students are in residence, less communication between parents and children. Now lack guidance for college students' physical and mental education in colleges and universities, the phenomenon of Internet addiction games with no clear rules and regulations.

In conclusion, we found that the cause of the college students addict network game is from various aspects, various factors influence each other, can't the everyone addicted to a same point. However, each student has one of the most important reason, in order to solve the problem only suit the remedy to the case[7-8]. The simplest part, derived from complex will find the most accurate.

V. THE SUGGESTIONS ON COLLEGE STUDENTS TO GET RID OF THE ADDICT NETWORK GAME

According to the above analysis, we believe that the prevention and control of compulsive playing for college students can be divided into the following three aspects[9]:

Parents should strengthen the awareness of college students' Internet behavior, improve education methods. Since most college students are in residence, parents can't always supervise children, this requires between parents and children have a good and frequent

communication, always keep your eyes open for children change and psychological tendency. Parents should encourage them to take an active part in activities, solve the puzzle of interpersonal communication, more dedicated to the network, with people rather than let their pent-up emotions through normal interpersonal poured forth, to experience the real success of interpersonal communication, to help them rebuild confidence[10].

Schools should strengthen education and take the way to improve campus network. Schools ought to guide and control network education students to use more at ordinary times, colleges and organizations can be more activities to enrich students' college life, at the same time also can cultivate the students' skills, be well prepared for the future into society. Schools should also strengthen the psychological health education and psychological consultation work actively, and keep the communication channels open and clear, is the escort of the students' mental health.

College student I should also enhance their ability of self-control, set up the correct values and good living habits. College students is the main task of the study is given priority to, with freedom of action and thought of stable should also form rational judgment ability and self-control, and establish a correct concept of value and behavior habits, with healthy personality to resist from the bad influence of the network, to form the correct cognition to the network, realize the network game nature, to abandon bad merit.

In view of the network game's influence on college students, this paper through the questionnaire survey, learned that most of the college students addicted to online games, through the analysis, the main cause of this situation are: network game has developed rapidly in a variety of forms, college students themselves have plenty of energy and time, parents and schools and education for its lack of control. In order to solve this problem, this paper puts forward the following Suggestions: first, parents should strengthen the awareness of college students' Internet behavior, improve education methods. Second, schools should strengthen education and take the way to improve campus network. Third, college students should also enhance their ability of self-control, set up the correct values and good living habits.

ACKNOWLEDGMENTS

This work is supported by the College students' innovative projects of North china university of science and technology (no. X2015104).

REFERENCES

- [1] Anand Vivek. A study of time management: the correlation between video game usage and academic performance markers[J]. *Cyberpsychology & behavior: the impact of the Internet, multimedia and virtual reality on behavior and society*, 2007, 10(4), 552-559.
- [2] Eppright T, Allwood M, Stern B et al. Internet addiction: a new type of addiction[J]. *Missouri medicine*, 1999, 96(4), 133-136.
- [3] Zaheer Hussain, Glenn A. Williams, Mark D. Griffiths. An exploratory study of the association between online gaming addiction and enjoyment motivations for playing massively multiplayer online role-playing games [J]. *Computers in Human Behavior*, 2015, 50(1), 221-230.
- [4] Galanter M, Keller D S, Dermatis H et al. Use of the Internet for addiction education, Combining network therapy with pharmacotherapy[J]. *The American journal on addictions / American Academy of Psychiatrists in Alcoholism and Addictions*, 1998, 7(1), 7-13.
- [5] M. Hamizul, Nik Mohd Rahimi. Design and Development of Arabic Online Games – A Conceptual Paper [J]. *Procedia - Social and Behavioral Sciences*, 2015, 174 (12), 1428-1433.
- [6] Eleni Andreou, Hionia Svoli. The Association Between Internet User Characteristics and Dimensions of Internet Addiction Among Greek Adolescents[J]. *International Journal of Mental Health and Addiction*, 2013, 11(2), 139.
- [7] ELŻBIETA KRAJEWSKA-KUŁAK, WOJCIECH KUŁAK, JERZY TADEUSZ MARCINKOWSKI et al. Internet Addiction Among Students of the Medical University of Białystok[J]. *CIN: Computers, Informatics, Nursing*, 2011, 20(11), 657-661.
- [8] Didier Acier, Laurence Kern. Problematic Internet use: Perceptions of addiction counsellors[J]. *Computers & Education*, 2010, 56(4), 983-989.
- [9] Coniglio Maria Anna, Muni Viviana, Giammanco Giuseppe et al. Excessive Internet use and Internet addiction: emerging public health issues[J]. *Igiene e Sanita Pubblica*, 2008, 63(2), 127-136.
- [10] MIA SEO, HEE SUN KANG, YOUNG-HEE YOM. Internet Addiction and Interpersonal Problems in Korean Adolescents[J]. *CIN: Computers, Informatics, Nursing*, 2009, 27(4), 226-233.

The Metallurgy Professional College Students' Employment Research And Prediction

LI Yong, MA Lian-zheng, WANG Qi, LIU Wei-xing, HAN Chuang-chuang, XIN Zi-cheng, LIU Zhen-chao
 North china university of science and technology, Hebei, The ministry of education key laboratory with modern metallurgical technology, Hebei, Tangshan 063000, China

Abstract—In view of China's steel industry downturn, the problem such as the number of college graduates increases year by year, by means of metallurgical related professional college students' employment in recent years, the employment rate, employment forms and graduation to analysis, puts forward some Suggestions on college students' future employment.

Index Terms—metallurgical, industry employment, employment guidance

I. INTRODUCTION

In recent years, China's number of college graduates increased year by year, college students face the grim problem of employment, the employment facing unprecedented challenges, students in the smooth employment after graduation, to become a hot issue of common concern to the whole society[1]. Metallurgical industry as the basic industry of national economy in our country, for the national economy sustained, stable and healthy development of our country has made great contributions to the metallurgical industry is China's largest base material industrial sector, but now the metallurgy related professional college students' employment situation is not optimistic, in this paper, the current college students employment situation is analyzed[2].

II. TANGSHAN REGION METALLURGY RELATED PROFESSIONAL COLLEGE STUDENTS' EMPLOYMENT SITUATION INVESTIGATION AND THE ANALYSIS OF THE RESULTS

Research method: a questionnaire survey was conducted on campus, field investigation, literature survey, ask teachers and interview survey

(1) Tang shan area of metallurgy related basic situation in recent years, graduates are shown in figure 1.

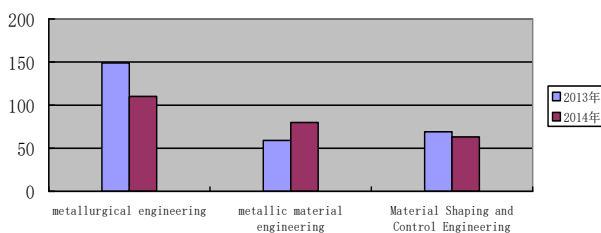


Fig.1 Tangshan metallurgy related professional graduates basic situation in recent years

Metallurgical engineering in tangshan some school graduates in 2013 is 149, metal material engineering is

59, material forming and control engineering is 69; Metallurgical engineering is 110, 2014 graduates in the metal material engineering is 80, material forming and control engineering is 63[3,4].

Decline in metallurgical engineering graduates in recent years; Metal material engineering graduates increased; Decline in material forming and control engineering graduates, but is not obvious.

(2) The professional employment trends

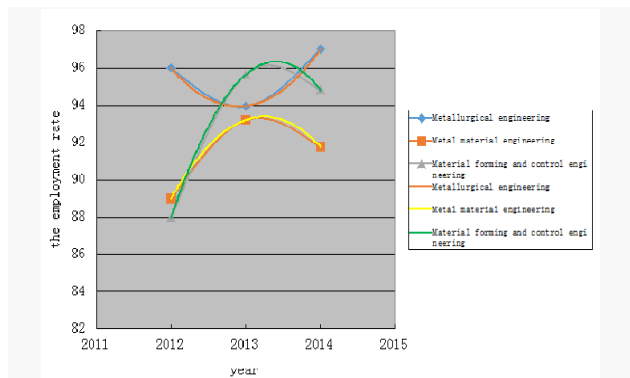


Fig.2 Each major employment trends

Metallurgical engineering employment is: 2012 96.00% 2013 93.96%, 2014 97.01%; Metal material engineering employment is: 2012 89.00% 2013 93.22%, 2014 91.78%; Material forming and control engineering employment: 2012 87.96%, 2013 95.65%, 2014 94.83%;

The above curve fitting equation is[5]:

Metallurgical engineering: $2.545 10245.665 x + y = 10311847.500$

Metal material engineering: $y = 2.830 + 11394.970 x 11394.970$

Material forming and control engineering: $y = 4.255 + 17134.065 x 17134.065$

The above chart and equation shows: in recent years the employment trend of present form of quadratic function, the metallurgical engineering present a tendency of increasing employment; Metal material engineering employment rate showed a trend of decline; The employment of material forming and control engineering also showed a trend of decline.

(3) the employment of graduates

In recent years, graduate employment forms include entrance, the unit contract, personnel agency, flexible employment and employment as shown in figure 3[6].

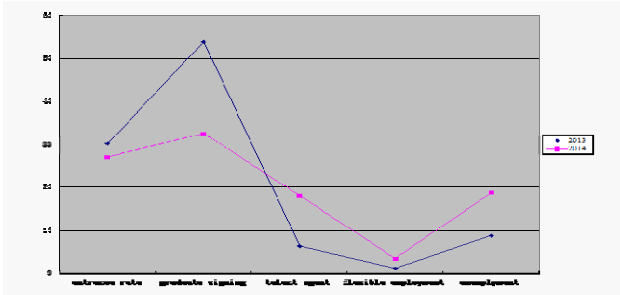


Fig.3 Graduates employment form

Seen from Fig.3 employment form, 2013 graduates signing at a rate of 54.08%, one's deceased father grind rate was 30.21%, to 6.48% talent agent, flexible employment proportion is 1.2%; Graduates signing at a rate of 32.64% in 2014, one's deceased father grind rate was 27.08%, the talent agent ratio of 18.06%, to 3.47% of flexible obtain employment.

The line chart shows that entrance rate dropped in recent years, the unit contract scale to drop, talent agency rise, increase in the number of flexible obtain employment, employment is also on the rise.

(4)raduates graduated in 2014 to as shown in Fig. 4.

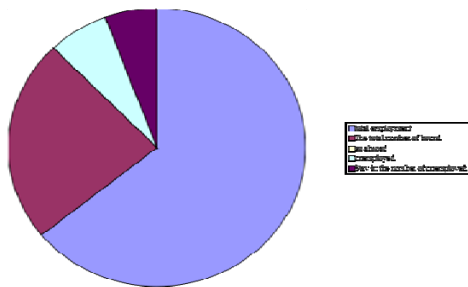


Fig.4 Graduates to graduation

Total employment of 212 people, accounting for 68% of the total, the entrance to the total number of 78, accounting for 25% of the total, the total number of going abroad to 0, accounting for 0% of the total, back to the city of 22, the total number of underemployed accounted for 7% of the total, stay to 19, the total number of underemployed accounted for 6% of the total.

Choice of 2014 graduates, direct employment is still dominant, occupying 68% of the total; Entrance second, occupying 25% of the total; Did not work and stay, a total of 13%.

(1) Proportion reducescontinue studies, most of the graduates due to the social pressure, working pressure and the influence of personal factors, lead to declining proportion ascending[7].

(2) Although the professional obtain employment situation is not stable, but the overall employment trend is good, have gradually rising trend.

(3) Talent agent, flexible employment proportion increase, some students begin to choose talent agent to enhance their own competitiveness, flexible obtain employment is to offer the students a broader direction of employment.

(4) Graduates are not to go abroad in recent years, more choice in the domestic employment, choose a dream job.

(5) Did not have obvious upward trend in the employment of graduates, most of the unemployed graduates after failing to find an ideal job and choose to give up, obtain employment is small due to failed to learn at school, after graduation can not work related[8].

III. THE PROFESSIONAL OBTAIN EMPLOYMENT SITUATION PREDICTION ANDSUGGESTION

According to the survey data fitting of metallurgical engineering employment change formula to predict employment growth in 2015 and 2016. According to the survey data fitting out the metal material engineering employment change formula can be predicted in 2015 and 2016, the employment rate has continued to decline, according to the survey data fitting out the metal material engineering employment change formula can be predicted in 2015 and 2016, the employment rate has continued to decline, in conclusion, metallurgical engineering employment has certain advantages over the next two years, metal material engineering and material forming and control engineering employment is relatively serious, but the overall trend is not optimistic[9].

(1) Improve the ability of planning study, planning the ability that college students should learn according to their career development trend, and combined with the needs of the development of the personal choice learning content, learning method or way of ability. It is a long-term activity, college students have to know what and when to learn, where learning, etc. Timely adjust their learning methods, flexible to adapt to the complex environment, finally achieve their goals.

(2) To make their own career planning, improve employment ability. First, to establish the normal professional ideal. Second, the right to self analysis and professional analysis. Third, build a reasonable knowledge structure. Fourth, cultivate professional need to practice ability. In addition to build a reasonable knowledge structure, but also need to be engaged in the industry's basic ability and professional ability. College students will only reasonable knowledge structure and applicable to unify all kinds of social ability, can be in an impregnable position.

(3) Improve the social adaptation ability of self, some enterprises in the selection and hiring university graduates, the same condition, tend to give priority to those who once participated in social practice, has certain organization management ability of graduates and don't choose the undergraduate of lack of justice experience and life experience. This requires college students to employment of cultivating the ability to adapt to society, to integrate itself.

(4) With the aid of social practice platform, improve college students' ability of organization and management, psychology to bear ability, interpersonal skills and strain capacity, etc. In addition, you can make them understand the employment environment, policy and situation, and help them find their own knowledge level, personality traits and ability quality matching occupations.

(5) To develop excellent psychological quality, college students during the period of school, only pay attention to professional knowledge, ignore the psychological quality of some people in the face of adversity and confused, always at a loss, affect their job choices. Therefore, college students should pay attention to improve the psychological quality in the process of studying, especially pay attention to exercise their tenacious character in our daily life[10].

IV. CONCLUSION

China's steel industry downturn, the number of university graduates increase, lead to metallurgy professional college students' employment outlook is not optimistic. In a university in tangshan metallurgy in recent years was analyzed through investigation of relevant professional graduates employment situation, it is concluded that the next few years metallurgy related severe employment situation, employment prospects are unknown, the overall trend is not optimistic, to enhance their competitiveness and puts forward some Suggestions on the contemporary college students, contemporary college students need to improve the ability of planning learning, seriously do a good job in their own career planning, enhance the social adaptation ability of self, with the aid of social practice platform, improve students' ability of organization and management, psychology to bear ability, interpersonal skills and strain capacity, for our future construction contributes an own strength.

ACKNOWLEDGMENTS

This work is supported by the College students' innovative projects of North china university of science and technology (no. X2015103).

REFERENCES

- [1] Rong Yu. The research of how to effective implementation the political education in employment guidance for university students[J]. IERI Procedia,2012,1:238-242.
- [2] Judith Scott-Clayton, Veronica Minaya. Should student employment be subsidized? Conditional counterfactuals and the outcomes of work-study participation[J]. Economics of Education Review,2015:1-18.
- [3] Geying Zhang. Metallurgical work in the new mode of graduates[J]. Abroad and Employment (Employment Edition), 2010,23:73-75.
- [4] Xiaoliang Cui , Jin Zhang , Yong Chen , Yi Tian , Xiaohuan Dong. Chongqing university of science and metallurgy industry related employment status of students[J]. Chongqing University of Science and Technology(Social Sciences), 2014,02:142-145.
- [5] Xiaotian Feng. Current situation and problems of college students' employment in China-Take 30 key empirical studies as an example[J]. Journal of Nanjing University(Philosophy, Humanities, Social Sciences) ,2014,01:60-69+158.
- [6] Taotao Ni , Wenlong Nie , Jia Guo. Research on the influence mechanism of college students' comprehensive quality on employment performance[J]. Contemporary education theory and Practice,2015,04:168-170.
- [7] Senay Sezgin Nartgün , Rasit Özen. Investigating pedagogical formation students' opinions about ideal teacher, teaching profession, curriculum, responsibility, public personnel selection examination (ppse) and employment: A metaphor study[J]. Procedia-Social and Behavioral Sciences,2015,174:2674-2683.
- [8] Noordeen Shoqirat , Ma'en Zaid Abu-Qamar. From placement to employment: Career preferences of jordanian nursing students[J]. Nurse Education in Practice,2015,15(5):366-372.
- [9] Zorica Marković , Biljana Blaževska Stoilkovska. Final year university students' beliefs about future employment relationships[J]. Procedia - Social and Behavioral Sciences,2015,171:76-82.
- [10] Hui Liu. Discussion on how to obtain the successful employment of the metallurgical engineering graduates[J]. China Education Innovation Herald, 2009,11:182.

Three-Way Decisions Model Based on Set Pair-Information Entropy and Applications

BAI Bin, LI Li-hong, Li Yan and Wang Li-ya

College of Science, North China University Science and Technology, Tangshan 063009, Hebei, China

Abstract—Three-way decision is a kind of decision model very according with human cognitive, three-way decision model based on set pair-information entropy explains decision domain. First, the approximation set of set pair was structured based on rough operator, set pair-information entropy was defined and basic properties were discussed in the sense of information system. It was proved that the Set pair-information entropy degraded into the information entropy when collections of set pair expended the whole region. Secondly, decision rules of three-way decision were structured based on set pair-information entropy, the risk evaluation of three-way decision reliability was discussed. Finally, it is given that three-way decision changed into two-way decision when the value of different entropy was zero.

Index Terms—Rough set, Set pair-information entropy, Three-way decisions.

I. INTRODUCTION

Three-way decisions is a new decision analysis theory and method processing inaccurate and incomplete information given by Yao Yi Yu based on rough set[1-2] and DTRS[3-5] and develop two-way decisions[6-7]. Disclaimer is used as a third selection state when the knowledge we got is not able to decide to accept or reject in three-way decisions that considers fully the uncertainty factors. In recent years, three-way decisions transforms gradually into decision-making theory system containing theory, model and applied research form decision-making ideas. Meanwhile, these new concepts of three-way decision model based on set pair analysis[8] and three-way said about formal concept are given when three-way decision overlaps and fusions with Other subjects. At present, three-way decision has been widely used in data mining, machine learning, cluster analysis, and pattern recognition fields, etc[9].

The information entropy is the measurement defined by American mathematician Shannon which quantized the size of a discrete random variable. In recent years, the information entropy has been widely introduced into the rough set, explaining the roughness of knowledge from the perspective of information. These new concepts of knowledge entropy, rough entropy and conditional entropy[10], etc are given that define mainly The importance of attributes and measure the uncertainty of information system, having achieved successful application of attribute reduction[11], feature selection[12], decision analysis[13] and other important research content in rough set. Meanwhile, these new models of approximate decision entropy[14-15] and granularity entropy[16] are given, which solve different problems based different models.

Based on this, three-way decision model based on set pair-information entropy is given when set pair-information entropy explains accept domain, refused to domain and no commitment of three-way decision from the perspective of information. The new idea expanding the method of three-way decision-making and improving the theory of decision-making is given, in this paper.

II PRELIMINARY KNOWLEDGE

These related definitions and basic properties of Set pair-information entropy are briefly introduced.

Definition 1 $K = (U, A)$ is the information system in which U and A are non-empty and finite collections representing universe of discourse and attribute set, in form. $\forall a \in A, a: U \rightarrow V_a$ is a mapping and V_a is a Value set of a .

Order $P \subseteq A$, the indistinguishable relationship $IND(P)$ decide by P is

$$IND(P) = \{(x, y) \in U \times U \mid \forall a \in P, f(x, a) = f(y, a)\} \quad (1)$$

If $(x, y) \in IND(P)$, x and y is indistinguishable. It is easy to prove that $IND(P)$ is the equivalence relation.

The equivalence partitioning is written by $U/P = \{X_1, X_2, \dots, X_n\}, 1 \leq n \leq |U|$.

Definition 2 The upper and lower approximation set about $X \subseteq U$ are $\bar{P}(X) = \cup\{X_i \in U/P : X_i \cap X \neq \emptyset\}$, $\underline{P}(X) = \cup\{X_i \in U/P : X_i \subseteq X\}$.

U is divided into positive region $POS(X)$, negative region $NEG(X)$ and boundary region $BND(X)$ based on $(\bar{P}(X), \underline{P}(X))$, $POS(X) = \underline{P}(X)$, $BND(X) = \bar{P}(X) - \underline{P}(X)$, $NEG(X) = U - \bar{P}(X)$.

Definition 3 $K = (U, A)$ and $P \subseteq A$ are given. $p(X_i) = |X_i|/|U|, 1 \leq i \leq n$ is established based on U/P .

$$H(P) = -\sum_{i=1}^n p(X_i) \log p(X_i) = -\sum_{i=1}^n \frac{|X_i|}{|U|} \log \frac{|X_i|}{|U|}$$

is called Knowledge entropy or Information entropy of P .

$$\text{If } P = A, H(A) = -\sum_{i=1}^n \frac{|X_i|}{|U|} \log \frac{|X_i|}{|U|}$$

is called Information entropy of K .

Definition 4 The upper and lower approximation set pair about $H(X, Y)$ composed by $X, Y \subseteq U$ are

$$\bar{P}(X, Y) = \bar{P}(X \cap Y) = \bar{P}(X) \cap \bar{P}(Y)$$

$$\underline{P}(X, Y) = \underline{P}(X \cap Y) = \underline{P}(X) \cap \underline{P}(Y)$$

U is divided into positive region $POS(X, Y)$, negative region $NEG(X, Y)$, boundary region $BND(X, Y)$ and $U - \bar{P}(X \cup Y)$ based on $(\bar{P}(X, Y), \underline{P}(X, Y))$,

$$POS(X, Y) = \underline{P}(X, Y), NEG(X, Y) = \bar{P}(X \cup Y) - \underline{P}(X, Y)$$

$$BND(X, Y) = \bar{P}(X, Y) - \underline{P}(X, Y), \bar{P}(X \cup Y) = \bar{P}(X) \cup \bar{P}(Y)$$

Definition 5 $K = (U, A)$ and $P \subseteq A$ are given.

$p_i^p = |X_i^p|/|\bar{P}(X \cup Y)|$, $p_i^N = |X_i^N|/|\bar{P}(X \cup Y)|$ and $p_i^B = |X_i^B|/|\bar{P}(X \cup Y)|$ are established conversely in $POS(X, Y)$, $NEG(X, Y)$ and $BND(X, Y)$ based on U/P , in which there is $\sum_{i=1}^m p_i^p + \sum_{i=1}^j p_i^N + \sum_{i=1}^l p_i^B = 1$.

$$H_p^p(X, Y) = -\sum_{i=1}^m p_i^p \log p_i^p$$

$$H_p^N(X, Y) = -\sum_{i=1}^j p_i^N \log p_i^N$$

$$H_p^B(X, Y) = -\sum_{i=1}^l p_i^B \log p_i^B$$

$$SH_p(X, Y) = H_p^p(X, Y) + iH_p^N(X, Y) + jH_p^B(X, Y)$$

are called Positive entropy, Negative entropy, Different entropy and Set pair-information entropy. There are senses about value and mark symbol of i, j .

III. THREE-WAY DECISION MODEL BASED ON SET PAIR-INFORMATION ENTROPY

The three-way decision theory is given based on Granular computing and Rough set theory. The reasonable Semantic interpretation is provided by three-way decision for positive region, negative region and boundary region in rough set. That is to say, positive region, negative region and boundary region are described conversely as accept domain (R), refused to domain (L) and no commitment (M).

$K = (U, A)$ and $P \subseteq A$ are given. Three-way decision represented by $POS(X)$, $NEG(X)$ and $BND(X)$ of $X \subseteq U$ is as follow:

$$R(X) = \{x \in U / f_A(x) = T\} = \{x \in U / [x] \subseteq X\} = POS(X)$$

$$L(X) = \{x \in U / f_A^c(x) = T\} = \{x \in U / [x] \subseteq X^c\} = NEG(X)$$

$$M(X) = \{x \in U / \neg([x] \subseteq X) \wedge \neg([x] \subseteq X^c)\} = BND(X)$$

Clearly, the acceptance rule is taken because $[x] \subseteq X$ is true and the refusal rule is taken because $[x] \subseteq X^c$ is true. There is no mistake that we make the decision of accept or reject, at this point. There is a no commitment rule when objects cannot be determined in positive or negative region.

Positive region $POS(X, Y)$, negative region $NEG(X, Y)$ and boundary region $BND(X, Y)$ are measured with Positive entropy $H_p^p(X, Y)$, Negative entropy $H_p^N(X, Y)$ and Different entropy $H_p^B(X, Y)$ in $SH_p(X, Y)$ from the perspective of information. Three-way decision rule is established based on $H_p^p(X, Y)$, $H_p^N(X, Y)$ and $H_p^B(X, Y)$. The acceptance rule is structured from $H_p^p(X, Y)$ and the refusal rule is structured from $H_p^N(X, Y)$. The option of no commitment is elected based on $H_p^B(X, Y)$.

$K = (U, A)$ and $P \subseteq A$ are given. There are decision problem W , factor set $X \subseteq U$ to evaluate and standard set $Y \subseteq U$ of evaluation. Three-way decision based on $SH_p(X, Y)$ is as follow:

$$R(X) = \{x \in X / \max\{H_p^p(X, Y), H_p^N(X, Y), H_p^B(X, Y)\} = H_p^p(X, Y)\}$$

$$L(X) = \{x \in X / \max\{H_p^p(X, Y), H_p^N(X, Y), H_p^B(X, Y)\} = H_p^N(X, Y)\}$$

$$M(X) = \{x \in X / \max\{H_p^p(X, Y), H_p^N(X, Y), H_p^B(X, Y)\} = H_p^B(X, Y)\}$$

Clearly,

if there is $\max\{H_p^p(X, Y), H_p^N(X, Y), H_p^B(X, Y)\} = H_p^p(X, Y)$, the acceptance rule is structured, accepting X .

If there is $\max\{H_p^p(X, Y), H_p^N(X, Y), H_p^B(X, Y)\} = H_p^N(X, Y)$, the refusal rule is structured, rejecting X .

If there is $\max\{H_p^p(X, Y), H_p^N(X, Y), H_p^B(X, Y)\} = H_p^B(X, Y)$, the no commitment rule is structured. It is necessary to further decide to accept X or reject X .

$K = (U, A)$ and $P \subseteq A$ are given. Assuming, X is a non-empty collection called decision region to make decision and Y is a non-empty collection of decision conditions called condition region.

$SH_p(X, Y)$ is used as the evaluation function of three-way decision. The minimum risk principle of decision is used.

The accept domain of decision is correspond to $H_p^p(X, Y)$, so the risk of acceptance rule based on Y must be less than refusal and no commitment rule's. The refusal domain of decision is correspond to $H_p^N(X, Y)$, so the risk of refusal rule based on Y must be less than acceptance and no commitment rule's. The no commitment is correspond to $H_p^B(X, Y)$, so the risk of no commitment rule based on Y must be less than acceptance and refusal rule's. It is the situation of minimum risk of decision rule structured by three-way decision.

The acceptance rule is stronger than refusal and no commitment rule, when there is $\max\{H_p^p(X, Y), H_p^N(X, Y), H_p^B(X, Y)\} = H_p^p(X, Y)$. The reliability of correct decision is depend on two factors:

(1) The closer to 1 of the ratio of $H_p^p(X, Y) / H_p^N(X, Y)$, the lower of the reliability of making correctly acceptance decision.

(2) Comparing $H_p^B(X, Y) + H_p^N(X, Y)$ with $H_p^p(X, Y)$
 ① The reliability of correct decision is large, when there is $H_p^B(X, Y) + H_p^N(X, Y) < H_p^p(X, Y)$. That is to say, $H_p^p(X, Y)$ plays a major role in $SH_p(X, Y)$.

② The reliability of correct decision is small, when there is $H_p^B(X, Y) + H_p^N(X, Y) > H_p^p(X, Y)$. That is to say, $H_p^N(X, Y)$ plays a secondary role in $SH_p(X, Y)$.

The refusal rule is stronger than acceptance and no commitment rule, when there is $\max\{H_p^p(X, Y), H_p^N(X, Y), H_p^B(X, Y)\} = H_p^N(X, Y)$. The reliability of correct decision is depend on two factors:

(1) The closer to 1 of the ratio of $H_p^p(X, Y) / H_p^N(X, Y)$, the lower of the reliability of making correctly refusal decision.

(2) Comparing $H_p^B(X, Y) + H_p^p(X, Y)$ with $H_p^N(X, Y)$
 ① The reliability of correct decision is large, when there is $H_p^B(X, Y) + H_p^p(X, Y) < H_p^N(X, Y)$. That is to say, $H_p^N(X, Y)$ plays a major role in $SH_p(X, Y)$.

② The reliability of correct decision is small, when there is

$H_P^B(X, Y) + H_P^P(X, Y) < H_P^N(X, Y)$. That is to say, $H_P^N(X, Y)$ plays a secondary role in $SH_P(X, Y)$. The no commitment rule is stronger than acceptance and refusal rule, when there is $\max\{H_P^P(X, Y), H_P^N(X, Y), H_P^B(X, Y)\} = H_P^B(X, Y)$. The reliability of making correctly decision. is depend the value of $H_P^B(X, Y)$. The higher of reliability of making correctly decision, the larger of the value of $H_P^B(X, Y)$.

IV. THREE-WAY DECISION CHANGE INTO TWO-WAY DECISION

In fact, on the premise of making sure collection X to make decision, collection Y of decision condition and cognitive P , the three-way decision model based on set pair-information entropy is given. The no commitment rule in three-way decision in is no real purpose in some decision problem. It is necessary to further analyze the no commitment. The change is not will of subjective but reasonable and scientific cognitive decision. For example, the set X of patient is divided into these patients need immediately to receive treatment, don't treat and don't promise to treat based on standard set Y of evaluation in decision problem W about medical. In order to make decision of receive treatment or not, doctors need to collect new information from test. It is the process that three-way decision change into two-way decision based on actual needs.

With the in-depth study of the problem, the $[x]_P$ is reduced and $H_P^B(X, Y)$ is decomposed gradually. The process turning three-way decision to two-way decision is the decomposition course of $H_P^B(X, Y)$.

The decomposition course of $H_P^B(X, Y)$ is shown in figure1

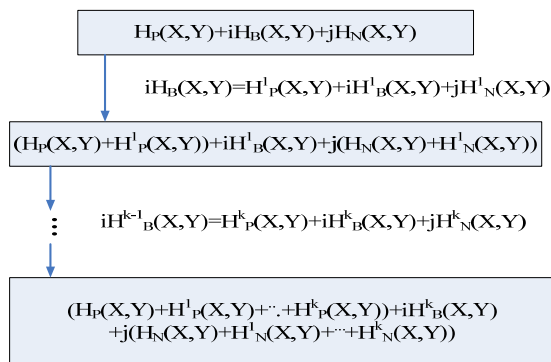


Fig.1 The three to two decisions

The three-way decision change into two-way decision

when there is $\forall x_i \in U, [x_i]_P = \{x_i\}$.
 That is to say, there are $U/P = \{\{x_1\}, \{x_2\}, \dots, \{x_{|U|}\}\}, H_P^B(X, Y) = 0$.

V. CONCLUSION

The three-way decision model based on set pair-information entropy explains the reliability of making decision from the perspective of information based on the point of three-way decision and information theory and decision theory is improved. Meanwhile, the new problem to predict advanced the risk of making no commitment decision is given.

ACKNOWLEDGMENTS

This paper is supported by NCFC grant No. 61370168.

REFERENCE

- [1] Pawlak Z. Rough sets. International Journal of Computer and Information Sciences, 1982, 11:341-356.
- [2] Wang G Y, Yao Y Y, Yu H.A Survey on Rough Set Theory and Tts Application [J]. Chinese Journal of Computers, 2009, 32(7):1229-1246.
- [3] Yao Y Y, Wong S K, Lingras P.A decision-theoretic rough set model//The 5th International Symposium on Methodologies for Intelligent Systems, 1990.
- [4] Liu D, Yao Y Y, Li T R. Three-way Decision-theoretic Rough Sets[J]. Computer Science, 2011, 38:246-250.
- [5] Zhang X Y, Miao D Q. A new type of classification region and relevant comparison analyses of the decision-theoretic rough set[J]. Systems Engineering-Theory & Practice, 2014, 12(12):3204-3211.
- [6] Yao Y Y. An outline of a theory of three-way decisions//Proceedings of the 8th International RSCTC Conference, 2012, 7413:1-17.
- [7] Yao Y Y. several issues researched by Three-way Decision// Liu D, Li T R, Miao D Q. Three-way Decision & Granular computing[M]. Beijing, Science press, 2013:1-13.
- [8] Lihong Li, Yan Li*, Jie Sun and Baoxiang Liu. Application of set pair analysis in three-way decisions. Journal of Chemical and Pharmaceutical Research, 2015, 7(3):1170-1175
- [9] Yu H, Wang G Y, Li T R. Three-way Decision: Methods and Practices for Complex Problem Solving [M]. Beijing, Science press, 2015, 7.
- [10] Liang J Y, Qian Y H. Information granule and Entropy theory in Information System [J]. Science In China, 2008, (12):2048-2065.
- [11] Wu S Z, Gou P Z. Attribute Reduction Algorithm on Rough Set and Information Entropy and Its Application [J]. Computer Engineering, 2011, 37(7):56-58.
- [12] Meng Y, Zhao F. Feature selection algorithm based on dynamic programming and comentropy [J]. Computer Engineering and Design, 2010, 31(17):3879-3881.
- [13] Yang C L. Application for Multi-Attribute Decision Making Based on Attribute Reduction of Information Entropy[J]. Mathematics in Practice and Theory, 2013, 43(3):97-102.
- [14] Jiang F, Wang S S, Du J W. Attribute reduction based on approximation decision entropy [J]. Control and Decision. , 2015, 30(1):65-70.
- [15] Zhao H B, Jiang F, Wang C P. An approximation decision entropy based decision tree algorithm and its application in intrusion detection. Proc of the 6th Int Conf on Rough Set and Knowledge Technology. Chengdu: Springer-Verlag, 2012:101-106.
- [16] Zhang X. Application of Knowledge Reduction Algorithm Based on Granularity Entropy [J]. Development and application of the computer, 2015,

The Spread and Control Research of Disease Based on the SIR Model and Individual Radiation Motion Model

Zhang Di, Wu Wenrui, Li Tan, Yang Aimin*, Han Yang, Luo Xingjun
North China University of Science and Technology, Tangshan, 063000, China

Abstract—This article focuses on the individual motion model and radiation model, and combined with the two models to put forward individual radiation motion model. Firstly using SIR model, combined with the number of infected population in A region, susceptible population, easily sicken population, and concluded that the needed speed of producing A vaccine or drug in the region. Secondly combining the individual movement model and the radiation model, and put forward individual movement radiation model, analysis the number of flows condition in various region around, and concluded that the effective control radius of A region, so provides effective basis for suppress the spread of disease.

Index Terms—SIR model; Individual radiation motion model; Radius of prevention

I. INTRODUCTION

With the improvement of social economic level, people's quality of life also has improved generally, the people's attention to health is also higher, and also have more and more attention on the measures of how to effectively control the spread of the virus. And with the improvement of health level and the progress of human society, such as infectious diseases of SARS, a (H1N1) influenza that wreak havoc the world has no longer scary, however some virus continues to change, playing a waiting game to invade the body, (such as Ebola virus recently began to free all over the world, led to tens of millions of people lost their lives), so in addition to study the corresponding treatment, studying how to control the spread of the epidemic is also very important.

The burgeoning of the complex network theory provides a new perspective for the population flow research among the regions. Strogatz and Watts [1] proposed the small world network model which fused general network advantages in 1998. It has both rules of the network's high aggregation, and small average path distance, such as random network. So it can better reflect the real network system. Barabási and Albert in 1999 [2] found that the world wide web's point and degree distribution fit in the characteristics of power law, and this is called a scale-free network, which together with the small world network commonly showed the preferred select characteristics of the new node connect. To explore complex network's structure and its evolution rule, many scholars had different degrees of improvement for the basic models, and which is widely used in nerve tissue, knowledge network, interpersonal relationship, traffic network, etc. Hou Heping [3], in 2013, firstly trying to take complex network theory as the instruction, with the radiation model based on spatial accessibility to measure population flow intensity between the villages and towns, thorough discussed that under the different geographical distribution, population

flows connection among regions and its spatial structure characteristics.

Pastor-Satorras studied the spread of behavior based on Barabási-Albert (BA) scale-free networks [4], found that when the network scale increases indefinitely, the critical threshold of the epidemic spread tends to zero, which is the lack of critical spread threshold, changed many conclusions in traditional study of the infectious diseases dynamics, inspired a lot of studies of epidemic spreading behavior under the complex topology structure. Miramontes O, Luque B [5] rules based on two-dimensional lattice, puts forward a simple individual motion model, allowing individuals had local motion within eight neighbors, also allows the individual to had random motion in the crystal lattice with a particular probability, combining SIS model to analysis individual movement's influence on the spreading behavior.

Y. Enatsu, Y. Nakata, Y. Muroya in the Global stability for a class of discrete SIR epidemic models, *math.h Biosci* [6] through using backward Euler method to the continuous delay SIR epidemic model to get a new discrete SIR epidemic model; Says Pastor-Satorras [7] based on complex network transmission dynamics research, using the mean field theory to study the disease spread of homogeneous and heterogeneous networks; In 2009, Xia Chengyi and others in the "The modeling and simulation of the disease spread based on the SIS model in dynamic network" based on two-dimensional rule lattice [8], put forward a improved SIS transmission model which considering individual movement to study spreading behavior of the disease in the dynamic network structure.

This paper successfully applied radiation model to the field of the virus spread, and combined the improved SIR model, put forward individual radiation model, concluded the effective radius size of the virus control.

II. SPEED MODEL OF PRODUCTION OF VACCINES OR DRUGS

Production speed refers to the production of the organism at any one time. The amount of the biological production process used as an indicator, previously known as productivity or productive power, is mainly used to represent human beings in general engaged in various production activities to create value in the process rate, but also represents various types of bio-energy production per unit of time.

In order to meet the needs of the patients, in the case of the best possible control of the transport time, but also pay attention to the speed of the production of drugs. In practice, the speed of the production of drugs and the level of economic development, the supply of raw materials, the production of technical level and some other external factors are related. Specific relationship shown in Fig.1:

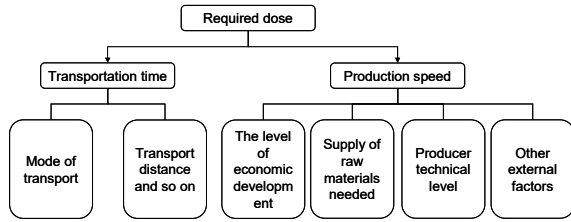


Fig.1 Production graph

In order to reduce the number of new patients as soon as possible, so that people susceptible to restore as quickly as possible, it must be possible to increase productivity, speed up the production rate of the drug. Assuming a vaccine or pharmaceutical production speed is v_m , the number of new patients per unit time is v_p , the transport speed of v_0 . Establishing a mathematical model of infectious diseases only by propagation mechanism, not from a medical point of view, then calculate the speed of a vaccine or drug production.

Assuming that each patient can make $\delta NS(t)$ healthy person into a patient per day, the total number of patients is $NI(t)$, so there are $\delta NS(t)I(t)$ healthy people are infected every day, the patient's rate of increase as follows:

$$\frac{\partial S(t)}{\partial t} = -\delta S(t)I(t) \tag{1}$$

Patients convert mainly refers to the increase in the number of patients infected with $S(t)NI(t)$ minus cure and death (i.e. $(\phi + \xi)I(t)$). Thus, the patient's conversion rate can be expressed as:

$$\frac{\partial I(t)}{\partial t} = \delta S(t)I(t) - (\phi + \xi)I(t) \tag{2}$$

The conversion between the onset of the population and the cure rate, and the change in the unit time to cure the population is equal to the amount of the population. That is:

$$\frac{\partial R(t)}{\partial t} = \phi I(t) \tag{3}$$

To sum up, SIR model is the total population of roughly divided into three categories, namely: vulnerable population S , sick people I and cure disease number R , satisfy the relationship between the three models are as follows:

$$\begin{cases} S(t) + I(t) + R(t) = 1 \\ \frac{\partial S(t)}{\partial t} = -\delta S(t)I(t) \\ \frac{\partial I(t)}{\partial t} = \delta S(t)I(t) - (\phi + \xi)I(t) \\ \frac{\partial R(t)}{\partial t} = \phi I(t) \end{cases} \tag{4}$$

In the numerical solution of differential equations, the four order Runge-Kutta method is used to solve the model (4) $I(t)$, $S(t)$, $R(t)$, i.e.:

$$y_{n+1} = y_n + \frac{h}{6}(K_1 + 2K_2 + 2K_3 + K_4) \tag{5}$$

Among them:

$$K_1 = f(t_n, y_n) \quad K_2 = f(t_n + \frac{h}{2}, y_n + \frac{hK_1}{2})$$

$$K_3 = f(t_n + \frac{h}{2}, y_n + \frac{hK_2}{2})$$

$$K_4 = f(t_n + h, y_n + hK_3) \quad y_0 = \chi$$

Making:

$$f(t, i) = \delta S(t)I(t) - (\phi + \xi)I(t)$$

$$f(t, s) = -\delta S(t)I(t), \quad f(t, r) = \phi I(t)$$

As can be found in the corresponding data, using MATLAB to calculate the value of $(\phi + \xi)$, δ , you can get the following conclusions:

Drug Production speed:
 $v_m \geq v_0 / t_1 \geq v_p (t_1 + t_2) / t_1$, that is when the supply rate of the drug faster than the speed of new patients, in order to achieve the demand for drugs, and then to really achieve the purpose of controlling and even cure the virus. In order to achieve this production rate, we can start with the main factors that affect the production rate, improve these factors, and then achieve the supply of energy should be.

III. INDIVIDUAL RADIATION MOTION MODEL TO SOLVE THE PREVENTION RADIUS

In view of the above models take into account only the delivery of drugs to reduce the number of infections, inhibit the spread of the disease, but did not play an effective role in the prevention of infection of personnel flows, which virtually increases the chances of a healthy number of contagious people, very The number of patients may lead to new multi-day variations. In order to better control the disease, the use of self-motion model [7] combined with radiation approximation model to simulate the spread of the epidemic prevention movement of individual radiation model, and then come to a radius of effective prevention, preventing further spread of the disease.

Let the individual motion model shown in Fig.2, the black circles represent individuals already be infected, the white circles represent temporary uninfected individuals. At the beginning, the individual is randomly assigned to a periodic boundary condition $L \times L$, in which the individual density in the plane space

is $\rho = \frac{N}{L^2}$, V_i and $\theta_i (-\pi \leq \theta \leq \pi)$ set for the i ($i = 1, 2, 3 \dots N$) velocity and direction of the individual, $V_i \approx (v \cos \theta_i, v \sin \theta_i)$ That individual is on a two-dimensional plane V can be random movement speed radius. In addition, individuals can make a certain probability p_j ($0 \leq p_j \leq 1$) long distance movement.

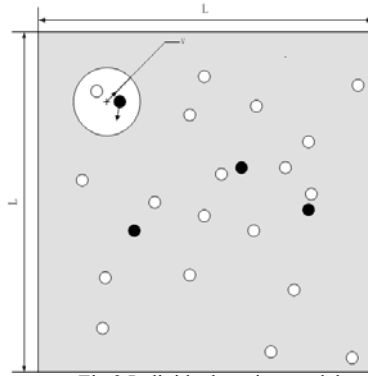


Fig.2 Individual motion model

There will be some differences to stating different individual movement, the main reasons are:

1) Because the prevalence of infection are contagious and isolated, they can only do some local motions and do not be a long way away movement, namely $p_j = 0$; the prevalence that without infection either do local motions can do long-range movement.

2) In general, uninfected persons has a self-adaptive for infected person, If there is no infection, Direction angle θ of the infected person is no longer 360 degrees, but in the range of less than 360 degrees of random movement, the general motion range of 180 degrees, as shown in Fig.3.

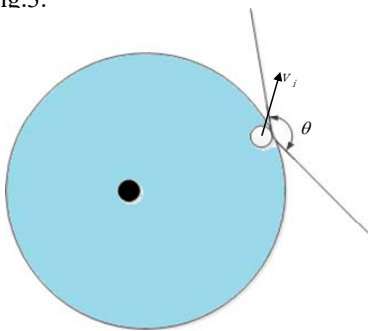


Fig.3 Movement schematic of uninfected individuals

Consider the individual's response to this reaction, and the person who is not infected will be far away from the infection, for example, in Figure 3 gives a hint of the direction of the movement of the individual. When infected in a certain radius of a non infected person, the person will not be infected with the most distant from the infection of the direction of movement.

In the model of radiation, movement of population is considered as a random process governed by the joint probability, which is influenced by the distribution of the population, the destination and the influence range. The equation of the radiation model is derived from theory, and the equation of the radiation model (formula 6, 7),

$$T_{ij} = T_i \frac{m_i n_j}{(m_i + s_{ij})(m_i + n_j + s_{ij})}$$

$$T_i = m_i V \tag{7}$$

About formula : T_{ij} as predicted i, j migration intensity between the two places, m_i, m_j respectively departure i and destination j of the total

population, S_{ij} for i to j population movements between the scope of the total population, T_i for i as the flow of population, V for i the proportion of the floating population.

Based on the spatial geographical differences, the isotime circle is used to determine the extent of heterogeneity of population flow from the perspective of space accessibility. According to the definition of the influence range of the radiation model, suppose the time cost of i to j is t_{ij} , the isotime circle of i is the scope of population flow between i and j , also known as heterogeneous sphere of influence. The total population S'_{ij} in that range is the total population isochronous circle around, without the population of i and j , the time cost of i to any place within the scope of the heterogeneity is less than that of i to j .

$$S'_{ij} = \sum_{k \neq i, j} O_k (t_{ik} \leq t_{ij}) \tag{8}$$

Above formula, S'_{ij} is the total population of the heterogeneous influence range from i to j , O_k is the population of k in the heterogeneous influence rang, t_{ik} is the time cost from i to k , t_{ij} is the time cost from i to j .

According to the description of the above two models, the model of individual radiation is obtained, calculating

the size r_2 of the prevention radius, in other words, using the radiation model, calculate the flow intensity of the infected area to other areas, combined with the characteristics of individual motion model, the radius of the radiation r_3 is estimated by a proper value of the intensity of the population flow, come to the size $r_2 = r_1 + r_3$ of the prevention radius.

In the model of individual radiation motion, assuming that the individual is in 5 states, which divides a population into 5 kinds of people including the susceptible individuals (S), the latent individual (E), the infected people (I), the rehabilitation group (R) and the inoculated population (V). In the course of disease transmission, there are 2 networks of infection network and control network, the control network is a subset of the network. We use to infection radius (r_1) and prevention radius (r_2) to characterize the infection radius network and control network quantitatively. From the microscopic view, we analyze the influence of the degree of local spread of the disease and the extent of disease control on the overall spread of disease, as shown in Fig.4.

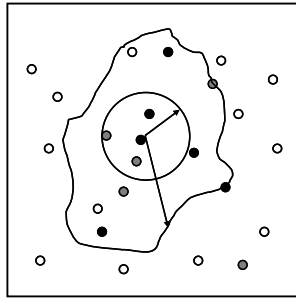


Fig.4 Radius of infection and prevention of radius

Among them, the black circle represents the infected individual I , the grey circle represents the vaccinated individuals V , the white circle represents the individual in other states. The susceptible individuals S can not infect other people, but it could be infected; the individual is already infected with the latent infectious E and other individual ability but not having

symptoms of people, the infected people I are showed symptoms of illness and infectious, probability β to the disease transmitted to the r_1 radius of the circular range of the susceptible population S , with probability γ was cured to enter the rehabilitation state R . In addition, the infected individual I to trigger the corresponding control action, all individuals in a circular range of r_2 around the radius of a circular range are inoculated with probability μ .

IV. CONCLUSION

Find a regional change in patient data on the WHO web site, can get in Table 1 below:

Table 1 patient changes Total 140 groups

death toll	time	The number of infections	Susceptible persons	Cure Listings	The total number of people (10000)	Susceptibility rate	Prevalence	mortality rate
4922	10.2	10141	11727909	2028	1174.5	0.998545	0.000863	0.00042
4922	10.3	13703	11723634	2743	1174.5	0.998181	0.001167	0.00042
4951	10.3	13567	11723770	2713	1174.5	0.998192	0.001155	0.00042
.....
11279	7.2	27688	11700500	5533	1174.5	0.996211	0.002357	0.00096
11283	7.2	27734	11700440	5543	1174.5	0.996206	0.002361	0.00096
11284	7.2	27742	11700427	5547	1174.5	0.996205	0.002362	0.00096

According to the description of model I can be obtain:

The values of $(\phi + \xi)$ and δ are 0.026,0.041. Supposing manufacture of a medicament for the time and transportation time are t_1 and t_2 , The speed of the production of the drug is $v_m \geq v_p(t_1 + t_2)/t_1$. Drug production plant according to the conditions of transport and their own different conditions, needing to improve some of the main factors affecting the production rate, Such as increasing the supply of raw materials needed, additional laboratories, increased pharmacy professionals, etc., to improve some of the relatively large weight of their influence factors for energy should seek to achieve the real purpose of inhibiting the development of the epidemic.

Model II individual radiation motion model combines the characteristics of individual sports model and the radiation model, that is, within a certain range, the smaller the radius prevention, disease suppression as possible, in line with population flow intensity calculation method mentioned radiation model. Finally get that when people flow strength is 0.8 can obtain the optimum radiation radius. The most appropriate

prevention radius is $r_2 = r_1 + r_3$. Individual radiation combines individual sports model and radiation characteristics of the model sports model, Within a certain range, can effectively find the most appropriate prevention radius, which can inhibit the development of the epidemic and better use of migration intensity

calculation method mentioned in radiation model, If we know the time cost of the total population of each region and between the two places, you can find the radius of the region's population, combined with the radius of the outbreak of infection, and thus prevent the outbreak can be determined radius, reaching epidemic prevention effect.

REFERENCES

- [1] Watts D J, Storgatz S H. Collective dynamics of 'small world' networks[J]. Nature,1998, (393):440-442.
- [2] Barabasi A L, Albert R.Emergence of sealing in random networks[J],Sience,1999, (393):400-422.
- [3] Hou Heping. Study on Population Mobility Network among Towns Based on Improved Radiation Model [J]. China population, resources and environment,No.8,2013.
- [4] Fu XC, Small M,Walker DM, et al. Epidemic dynamics on scale-free networks with piecewise linear infectivity and immunization . Physical Review E,2008,77: 036113.
- [5] Miramontes O,Luque B. Dynamical small world behavior in an epidemiological model of mobile individuals. Physica D, 2002, 168-169:379-385.
- [6] Y. Enatsu, Y. Nakata. Global stability for a class of discrete SIR epidemic models [J], Math. Biosci.Engin, 7(2010) 347-361.
- [7] Pastor-Satorras R,Vespignani A. Epidemic spreading in scale-free networks[J]. Physical Review Letters, 2001, 86(14) : 3200-3203.
- [8] Xia Chengyi. Modeling and Simulation of Disease Propagation Based on SIS model in Dynamical Networks [J]. Journal of System Simulation, Vol.21,No.15, 2009.8.

Supply Matching Degree Evaluation Model Based on Gene Analysis

Luo Xingjun, Zhang Di, Wu Wenrui, Yang Aimin*, Han Yang, Zhou Qi
North China University of Science and Technology, Tangshan, 063000, China

Abstract—This paper combines the control variable method, use Factor Analysis Method, and set up supply matching degree evaluation model based on factor analysis, and the same time, mileage utilization in different spaces, vehicle load factor and ten thousand people three indexes were analyzed, and the same time, robbed single time under different space, a taxi degree of difficulty, the car hit demand / taxi distribution the four indicators were analyzed, obtained at the different time, the taxi supply matching degree in Chinese major cities provides a realistic basis for our country's taxi in promotion and development of the era of Internet.

Index Terms—Factor analysis; Control variable method; matching of supply and demand

I. INTRODUCTION

With the advent of the era of "Internet +" and the establishment of several taxi service platform, realizing the communication between the passengers and the driver, how to design a more reasonable subsidy scheme promotion platform to ease a taxi difficult problem has become the focus of each enterprise focus, studying under the different time and space, the degree of taxi resources "the matching of supply and demand" also becomes very important.

Wang Liming in his article "taxi resource configuration and scheduling model" by the analyzing the allocation difficult problem in the public "taxi difficulty" and taxi resource allocation scheduling in time and space, set up in different space and time period of two indicators for the distribution of the taxi and subsidies, the taxi resources supply and demand matching" degree of multi-index comprehensive evaluation model [1].

Li Xuejuan, Chen Xizhen in their article "structural equation model of factor analysis" used the result of exploratory factor analysis under SPSS Analysis and the confirmatory factor analysis result of structure equation model to compare, and obtained that under the structural equation model of confirmatory factor analysis of factor loading is higher than exploratory factor analysis of factor loading, and at the same time made the opinion that when the data is analyzed by factor analysis, the two method should be combined when using [2].

Ma Qinghua, Li Yonghua, Liang Lisong, Li Qin, etc in their article "Factor analysis and comprehensive evaluation of winter jujube superior individual fruit quality" used Subordinate function to transform the indicators data, used SPSS 13.0 software to make factor analysis, and used the fourth largest rotation method to obtain factor gain loading matrix, saw common factor contribution rate as weights, and calculate sample's six common factor score and the plus of the corresponding weights of accumulation to get the complex score, and combined with the common factor of two figure of superior individual selection, and explored the main impact factor winter-jujube fruit quality evaluation [3].

Lin Haiming in his article "the interpretation of some common problems in the application of factor analysis" used the factor analysis model L recent improvement, solved these problems one by one, proposes a factor analysis with decision-making relevance, and analyzed of the application process more in-depth, then exemplified its effectiveness [4].

Wang Binhui, Li Xiongying in their article "the construction and comparative study of robust factor analysis method" improved the traditional method of factor analysis, built a robust algorithm Factor Analysis in order to overcome the impact of outliers, and made this method be simulated and empirical analysis [5].

This paper is based on the factor analysis in the above a few papers of dimension reduction, begins with the study of internal dependence of primitive variable correlation matrix, puts some variables with complex relations to attribute to the integrated factor. With minimal loss of information, the numerous original variables condensed into a few factors, and make factor variables have strong interpretability advantages to solve the problem of the influence of taxi resources "supply and demand mismatch" degree in different times.

II. MODEL PREPARATION

Factor analysis [6,7] basic idea is to classify the observed variables, the correlation is higher, that is closely linked to the same class, and the correlation between different variables is lower, then each kind of variable actually represents a basic structure, that is, the public factor. For the problem of the study, The linear function of the common factor and the special factor are used to describe each component of the original observation.

Notes:

① When determining the number of factors, select the first characteristic value of the cumulative contribution rate of more than or equal to 85 percent of the corresponding ranking position, combined with the rotated factor loading matrix variables, does not appear to be lost to determine the number of factor M.

② Factor score function Z . Expression :
 $Z_i = b'_i X$, Which b_i is the factor score coefficient matrix of the i column vector.

③ Comprehensive factor score (evaluation) formula:
 $Z_{syn} = \sum_{i=1}^m (v_i / p) Z_i$, Contribution rate of i to the number of v_i / p in feature values.

III. ESTABLISHMENT OF MODEL

In order to be more objective and systematic analysis of the impact of various factors on taxi resource "supply and demand matching", we need to discuss the two

aspects of the space dimension, the time dimension of the same space.

(1) Time must, space is not fixed

Several main indexes of the "supply and demand matching" degree of taxi resources : several main indexes of the "supply and demand matching" degree of taxi resources: x_1 , Vehicle load: x_2 , Million people: x_3 , they are known as the "three indicators."

$$x_1 = \frac{l}{L} \times 100\%$$

Among them, l represents passenger traffic mileage, L represents the total mileage of a taxi.

Taxi mileage utilization rate reflects the efficiency of the vehicle, the proportion is too high, the proportion of passenger travel is too high, the proportion of empty driving is low, less taxis can be used for passengers, and waiting time for passengers will increase, there will be tension between supply and demand.

$$x_2 = \frac{P}{P} \times 100\%$$

Among them, P represents the number of passengers load, P represents the total number by car.

In the actual operation, the proper balance between the capacity and the traffic volume is achieved by controlling the full load rate of the taxi.

$$x_3 = \frac{m}{M}$$

Among them, m represents the total number of taxis, M represents the population size.

From the statistical yearbook of traffic to find out the 15 cities of the mileage, vehicle load rate, million people with data, as shown in table 1:

Table 1 Statistical table of the three indicators of each city

cities	Mileage utilization ratio	Taxi million people	Vehicle load ratio
Dalian	0.6551	36	0.695

Table 3 Total variance

ingredients	The initial eigenvalue					
	Summary	of the variance%	Total%	summary	Loading extract square and variance%	total%
1	1.447	48.248	48.248	1.447	48.248	48.248
2	1.024	34.128	82.377	1.024	34.128	82.377
3	0.529	17.623	100.000			

Then, the final index of the total variance is obtained by using table 3.

$$F = 0.586F_1 + 0.414F_2 \tag{4.3}$$

Take the formula (4.1) and (4.2) into (4.3) to obtain the total index:

$$F = -0.384x_1 + 0.452x_2 + 0.231x_3 \tag{4.4}$$

By the formula (4.4) it can be seen that the final comprehensive index is negatively correlated with the mileage utilization ratio, and it is positively related to the vehicle load rate and the million people.

Shenyang	0.574	34	0.741
Beijing	0.68	34	0.865
Guangzhou	0.7379	32	0.652
Harbin	0.841	29	0.532
Xian	0.7	25	0.852
Wuhan	0.6902	24	0.736
Nanjing	0.654	23.77	0.765
Chengdu	0.6788	23.5	0.569
Xiamen	0.72	22.78	0.768
Qingdao	0.6451	22	0.713
Ningbo	0.68	20	0.682
Hangzhou	0.6925	19.6	0.741
Jinan	0.717	15.5	0.632
Shenzhen	0.691	10.86	0.82

We Use factor analysis to extract common factors from variable group. Factor analysis based on the correlation coefficient matrix, using principal component analysis to extract the total contribution of 85% of the ingredients. After the principal component analysis, it is decided to retain a principal component. Then, the square sum of a feature vector is obtained, which is used as a common property, and is used to replace the diagonal matrix of the correlation matrix. On the basis of the matrix of the correlation coefficient matrix, the coefficient of the factor and the factor of the factor is determined by the method of repeatedly seeking eigenvalues and eigenvectors. As shown in table 2.

Table 2 Component score coefficient matrix

The three major indicators	ingredients	
	1	2
The mileage utilization	-0.593	-0.088
Vehicle load factors	0.099	0.951
Ten thousand people ownership	0.574	-0.255

Set mileage utilization rate as x_1 , the vehicle load rate as x_2 , and ten thousand people ownership as x_3 . The formula for dealing with the data available on the table 1 is:

$$F_1 = -0.593x_1 + 0.099x_2 + 0.574x_3 \tag{1}$$

Formula for component 2:

$$F_2 = -0.088x_1 + 0.951x_2 - 0.255x_3 \tag{2}$$

The total score difference as shown in table 3

The above different cities of the data in the form of non dimensional (4.4), can be obtained as the following fig.2:

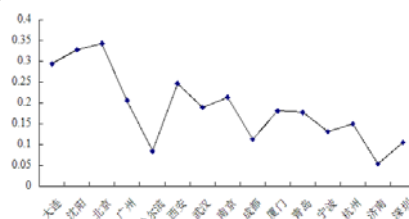


Fig.2 Different cities of the same period of time integrated indicators

From Fig.2 it can be seen that the 15 cities, Beijing has the best matching degree, Jinan and Harbin, have the worst matching degree.

(2) Certain space, uncertain time

Taking Beijing as an example, by collecting a day in Beijing, the time of the order was robbed, demand taxi, taxi distribution data, coupled with the difficulty of the qualitative taxi, Data obtained are shown in Table 4

Table 4 The situation of taking a taxi in Beijing one day

Time slot	Ease of taxi	Taxi Demand / Taxi Distribution	the time of the order was robbed /s
0:00-2:00	1.6	0.15	40
2:00-4:00	1.4	0.184615	38
4:00-6:00	1.5	0.218182	39
6:00-8:00	1.6	0.233333	40
8:00-10:00	2.2	0.18	41
10:00-12:00	2.4	0.144444	42
12:00-14:00	2.4	0.152941	42
14:00-16:00	2.4	0.1625	41
16:00-18:00	2.4	0.157576	40
18:00-20:00	2.2	0.17284	40
20:00-22:00	2.0	0.16875	38
22:00-24:00	1.6	0.151899	40

Factor analysis was carried out on the data in table 4, get the component score coefficient matrix as shown in table 5.

Table 5 Component score coefficient matrix.

Three indicators	ingredients
	1
Ease of taxi	0.894
Taxi Demand / Taxi Distribution	0.842
the time of the order was robbed	-0.752

Set y_1 as the ease of taxi, y_2 as the demand for taxi demand / taxi distribution, y_3 as the time of the order was robbed. The above table shows that the composition of formula 1 is:

$$N_1 = 0.894y_1 + 0.842y_2 - 0.752y_3$$

(4.5)

From equation (4.5) can be seen: the final comprehensive index and the time of the order was robbed into negatively correlated with taxi difficult easy degree, taxi demand / taxi distribution, into positive correlation. And when the absolute value of the index N, the matching degree of supply and demand is better, and the actual situation is more in line with the actual situation.

Put the Beijing city a day of data into the formula (4.5), the calculation of the data obtained, can be obtained as shown in fig.3:

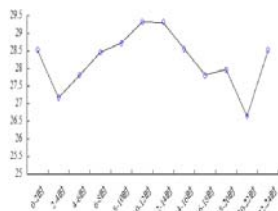


Fig.3 The integrated indicator of the change of the time in Beijing within a day

From Figure 3, we can see that the 12 time periods that selected in Beijing, the 2:00-4:00 and 20:00-22:00 time interval is the best matching degree, 10:00-12:00 and 12:00-14:00 time interval is the matching degree worst.

III. CONCLUSION

This paper mainly use factor analysis, establishing the degree of matching supply evaluation model based on factor analysis, from the spatial dimensions, same spatial dimension of time under the same time, evaluating the various factors on the taxi Resources "matching supply and demand," the extent of the impact, obtained at different time, Chinese major cities in taxi supply matches the level, providing a realistic basis for the promotion and development of the Internet era of + for our taxi.

Under the same time, different space, the degree of matching the best in Beijing of the fifteen cities, Jinan and Harbin matching degree are the worst. The main reason lies in the level of economic development and the impact of the total urban population of the three indicators, software promotion on the Internet, while a taxi should adopt different marketing strategies for different levels of Taxi matching city.

Other in the same space and different time, in Beijing, for example, 12 periods in Beijing, 2-4 and 20-22 period, matching level are the best, 10-12 and 12-14 period, matching degree are the worst. The reason is that the degree of information symmetry between the taxi and passenger and urban economy and population are unevenly distributed have impact on the three major factors. In the taxi software promotion process, we should consider how to promote the degree of matching supply and demand in order to make the city more "uniform".

REFERENCES

- [1] Wang Liming. Model research of taxi resource allocation and scheduling [J]. Suppliers, 2015, 36: 255.
- [2] Li Xuejuan, Chen Xizhen. Factor structural equation modeling analysis under [J]. Science Technology and Engineering, 2010,23: 5708-5711.
- [3] Ma Qinghua, Li Yonghong, Liang Lisong, Liqin. Jujube fruit quality fine individual factor analysis and comprehensive evaluation [J]. Chinese Agricultural Science, 2010, 12: 2491-2499.
- [4] Lin Haiming. Factor analysis to resolve some common problems with the application [J]. Statistics and Decision, 2012, 15: 65-69.
- [5] Wang Binhui, Li Xiongying. Build robust factor analysis and comparative study [J]. Statistical Research, 2015, 05: 84-90.
- [6] Wu Mengda, Cheng Lizhi. Mathematical modeling tutorial [M] Changsha: Higher Education Press, 2011.
- [7] Ren Shenggang, Peng Jianhua. Based on the evaluation and comparison of Chinese regional innovation capacity factor analysis [J]. Systems Engineering, 2007,(02):87-92.

AOSLO Video Image Stabilization Algorithm Based on Harris-sift

Guang-qiu CHEN, Bin-bin HUO, Fei TONG, Bao-kun ZHU

School of Electronic and Information Engineering, Changchun University of Science and Technology, Changchun 130022, China

Abstract—Confocal scanning laser ophthalmoscope based on adaptive optics can correct the aberrations, which can achieve high resolution imaging in vivo retinal. But because of the micro tremor of the patient and the jitter of the device, the video image of the adaptive optics scanning laser ophthalmoscopy (AOSLO) output is blurred. To solve this problem, an AOSLO image stabilization algorithm based on Harris-SIFT is proposed. Firstly, Harris-SIFT algorithm is used to match feature vector, then the RANSAC algorithm is used to verify the match accuracy, the motion vector value estimated is obtained. Finally, the fixed frame compensation method is used to realize the motion compensation. Experimental results show that the proposed algorithm can effectively remove jitter and enhance the contrast of video image.

Index-terms —AOSLO, RANSAC, SIFT

I. INTRODUCTION

AOSLO is that adaptive optics is used to correct the aberrations of the eye and high resolution retinal cell video image is realized by combined with confocal scanning laser ophthalmoscope (CSLO) technology. During the doctor checking patient's condition by AOSLO, the micro tremor of the patient and the jitter of the device make the observed video image blur. So it is necessary to stabilize video image by stabilization algorithm, so that better video image can be obtained to assist the doctor to make an accurate judgment. In this paper, AOSLO video image stabilization algorithm based on Harris-SIFT is proposed. For improving the matching speed, the Harris-SIFT algorithm is used to match the feature vector of the video image. For improving the matching accuracy and stability, the RANSAC algorithm is used to verify the matching accuracy to obtain the motion vector estimation. The motion compensation is realized by the fixed frame compensation method to output stable video image.

II. SCALE-INVARIANT FEATURE TRANSFORM(SIFT)

Scale-invariant feature transform (SIFT) algorithm is a new image local feature description algorithm based on scale space, image scaling, rotation and affine transform on the basis of the summary on the existing feature detection method by the invariant technology, which can be divided into 4 steps[1][2]

The scale space theory first appeared in the field of computer vision, and whose purpose is to simulate the multi-scale characteristics of image data. In reference [3], It is proved that the Gauss convolution kernel is the only

transform kernel in realizing scale transform, and the only linear kernel. Given a 2D image, the scale space representation at different scales can be obtained from the image and Gauss kernel convolution

$$L(x, y, \sigma) = G(x, y, \sigma) * I(x, y) \quad (1)$$

Where (x, y) represents spatial coordinate, σ represents scale coordinate, $G(x, y, \sigma)$ represents Gaussian function with scale variable

$$G(x, y, \sigma) = \frac{1}{2\pi\sigma^2} e^{-\frac{(x^2+y^2)}{2\sigma^2}} \quad (2)$$

For effectively detect the stable feature points in the scale space, the difference of Gaussian (DOG) scale space is proposed, which is the approximation of the LOG operator with scale normalization. DOG operator is simple, which can be generated by Gauss difference kernel in different scales and image convolution.

$$\begin{aligned} D(x, y, \sigma) &= (G(x, y, k\sigma) - G(x, y, \sigma)) * I(x, y) \\ &= L(x, y, k\sigma) - L(x, y, \sigma) \end{aligned} \quad (3)$$

For finding the extreme points in the scale space, each sampling point should be compared with its adjacent points to see whether it is larger or smaller than the adjacent points in the image domain and the scale domain.

The position and scale of the feature points can be accurately located and the characteristic points with the low contrast and the unstable edge response points (the DOG operator can generate strong edge response) can be removed by fitting 3D quadratic function, which can enhance the matching stability and improve the ability of anti noise. The accurate location of the feature points position and scale coordinates (sub-pixel accuracy) can be obtained by two order Taylor expansion interpolation

of DOG function $D(X)$.

$$D(X) = D + \frac{\partial D^T}{\partial X} X + \frac{1}{2} X^T \frac{\partial^2 D}{\partial X^2} X \quad (4)$$

Where $X = (x, y, \sigma)$ represents the position and scale offset between the sampling point and the feature point. The first derivative of the formula (4) is set to 0, the offset vector for the accurate position of the feature points can be obtained

$$\hat{X} = -\frac{\partial^2 D^{-1}}{\partial X^2} \frac{\partial D}{\partial X} \quad (5)$$

\hat{X} is added to the original rough feature points coordinate X and the accurate sub pixel interpolation estimates of the feature points can be obtained. The substitution of equation (5) in equation (4) can be obtained:

$$D(\hat{X}) = D + \frac{1}{2} \frac{\partial D}{\partial X} \hat{X} \quad (6)$$

When $|D(X)|$ is less than a certain threshold, the feature points can be rounded, usually this feature is sensitive to noise, therefore unstable. Furthermore, the edge response points with unstable should be eliminated. The tangential principal curvature at the edge is larger and that at vertical direction vertical is smaller in this kind of extreme point in DOG function. For detecting whether the principal curvature is less than a certain threshold, it is only necessary to detect whether the following inequality is satisfied

$$\frac{Tr(H)^2}{Det(H)} < \frac{(r+1)^2}{r} \quad (7)$$

Where H represents Hessian matrix of DOG function,

$$H = \begin{pmatrix} D_{xx} & D_{xy} \\ D_{xy} & D_{yy} \end{pmatrix}, \text{ In the course of the experiment, } r = 10$$

By the gradient direction distribution characteristic of the neighborhood pixels of the feature points, the parameters of each feature point are specified, which makes the operator rotation invariance. Firstly, Gradient mode and orientation of feature points are computed in Gauss space by the following equation

$$\begin{cases} m(x, y) = \\ \sqrt{(L(x+1, y) - L(x-1, y))^2 + (L(x, y+1) - L(x, y-1))^2} \\ \theta(x, y) = \\ \tan^{-1}(L(x, y+1) - L(x, y-1)) / (L(x+1, y) - L(x-1, y)) \end{cases} \quad (8)$$

Then a gradient direction histogram is created by the sampling in the neighborhood of the feature points in Gauss space. Histogram of each 10 degree as a column, a total of 36 columns, and then each sampling point in the neighborhood is placed into the appropriate column according to the gradient direction θ , gradient modulus m is used as contribution weight. Finally, the main peak value is regarded as the main direction of the feature point, the local peak of more than 80% main peak value is selected as auxiliary direction. So a feature point may be specified with multiple directions, which can enhance matching robust.

The coordinate axis is rotated into the direction of the feature points to ensure rotation invariance. The feature points are taken as the center to select a window, the size is 8×8 , then the gradient direction histogram in 8 directions is calculated on each 4×4 block. The cumulative value in each gradient direction can be

computed to form a seed. The neighborhood directional information association algorithm can enhance the ability of anti noise, and also provide a better fault tolerance for the feature matching with localization error. In the actual calculation process, for enhancing the matching robustness, each feature point is described by 4×4 , a total of 16 seeds. So a feature point can produce 128 data, which can generate 128 dimensional SIFT feature vector. Now the SIFT feature vector has removed the influence of scale change, rotation and other geometric distortion factors, furthermore, the length of the feature vector is normalized, the influence of the illumination change can be removed.

III. HARRIS-SIFT

When SIFT feature extraction and matching algorithms are applied in the AOSLO video image stabilization system with high real-time requirement, it exits three main problems[4][5]

- (1) The complexity of Feature extraction is too high and the computation time is too long.
- (2) The feature points generated are too much, which can affect the matching and searching speed.
- (3) The overall significance of the feature set is poor.

For solving the real-time problem of SIFT algorithm, the other more effective feature point detection operator should be considered to replace the extreme point extraction algorithm in SIFT. Harris operator is an effective point feature extraction operator, as following

$$R = det(C) - ktr^2(C) \quad (9)$$

Where det represents the determinant of a matrix, tr represents matrix trace, C represents correlation matrix

$$C(x) = \begin{bmatrix} I_u^2(x) & I_{uv}(x) \\ I_{uv}(x) & I_v^2(x) \end{bmatrix} \quad (10)$$

Where $I_u(x)$, $I_v(x)$ and $I_{uv}(x)$ represent partial derivative and two order mixed partial derivative, k is a empirical value, usually take 0.04-0.06.

When the Harris operator R of a certain point is larger than the threshold value T , the point is the corner point. The merit s of the Harris operator are that: (1) simple calculation (2) The feature points are uniform and reasonable, which can reflect the structure of the image (3) Feature corner points can be extracted quantitatively (4) Even in the presence of image rotation, gray level changes, noise effects and viewpoint transformation, it is also the most stable point feature extraction algorithm. So the extreme points in SIFT algorithm is replaced by the Harris feature points, then defines the main direction of each feature point and produces feature vector description for each feature points, which is called Harris-SIFT algorithm. When the feature vectors of the two image feature points are generated, the Euclidean distance of the feature points is used as the similarity measurement of the feature points.

IV. RANSAC MATCHING VERIFICATION AND MOTION COMPENSATION

In AOSLO video image, the target is are similar, which is easy to enhance the similarity of the feature point, which can result in false matching. These false matching points make the processing speed of the algorithm is affected, and the accuracy of the results is reduced. For reducing the error and improve the stability, the Random Sample Consensus (RANSAC) algorithm is used to verify the matching accuracy. RANSAC algorithm steps are as follows

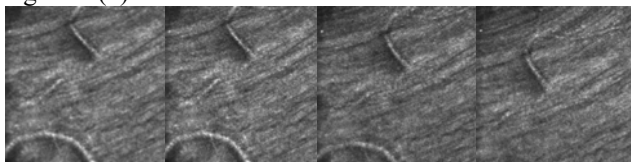
- (1) The samples were randomly selected from a sample of RANSAC, namely 4 matching points.
- (2) According to these 4 matching points to calculate the transformation matrix M
- (3) According to the sample set, the transform matrix M , and the error metric function, the consensus of the current transform matrix is calculated and returns the number of the consensus elements
- (4) According to the elements number of the current consensus to determine whether the optimal consensus, if it is true, the current consensus is updated.
- (5) Update the current error probability p , if p is greater than the allowable minimum error probability , repeat (1) to (4) , continue, until the current error probability p is less than the minimum error probability.

The above steps is repeated, image stabilization is outputted.

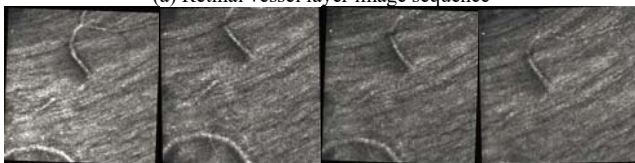
As can be seen from the imaging characteristics of AOSLO, objects mainly move in the form of translational motion, very little rotation and scaling, so the motion angle can be negligible. So the fixed frame compensation method is used to compensate the motion of the video image.

V. SIMULATION AND RESULTS ANALYSIS

For demonstrating the effectiveness and stability of the proposed method, the proposed algorithm is used to stabilize the retinal vessel layer and the retinal cell layer image sequence obtained by AOSLO. The original image sequence is shown in figure 1(a) and figure 2(a), the stabilization image sequence is shown in figure 1 (b) and figure 2 (b).

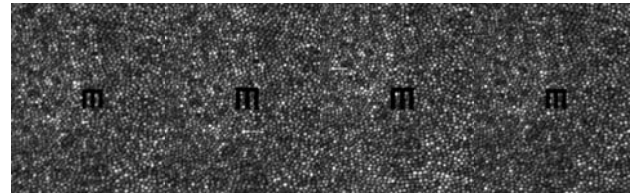


(a) Retinal vessel layer image sequence

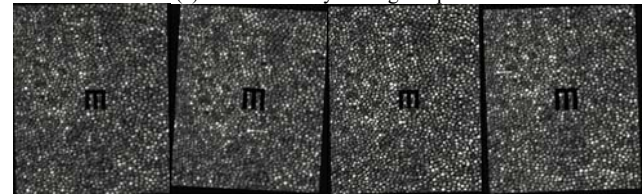


(b) Stabilized retinal vessel layer image sequence

Figure1 Image sequence stabilization of retinal vessel layer



(a) Retinal cell layer image sequence



(b) Stabilized retinal cell layer image sequence

Figure 2 Image sequence stabilization of retinal cell layer

As can be seen in figure 1(b) and figure 2 (b) , the effect of video stabilization is more and more obvious, which shows that the proposed algorithm has better stabilization effect for retinal vascular layer image and retinal cell layer image.

VI.CONCLUSION

Aiming at the defects of existing AOSLO equipment output video image, an AOSLO video image stabilization algorithm based on Harris-SIFT is proposed. Many invariant feature points can be extracted by the SIFT algorithm with good scale, rotation, perspective and illumination invariance, but when it is applied to AOSLO video image with high real-time requirement , the complexity is high and real-time is poor, and the scale invariant feature is difficult to be reflected. The operator proposed Harris-SIFT is a successful improvement for SIFT, which can reduce the complexity of feature extraction and feature matching, greatly improve the real-time.

RANSAC matching verification and motion compensation improve the stability and accuracy of the algorithm. The experimental results show that the proposed image stabilization algorithm has achieved good results in improving the AOSLO video image.

REFERENCE

- [1] LOWE D G, "Distinctive image features from scale-invariant key points," *International Journal of Computer Vision*,2004, Vol.60,NO.2,pp: 91-110.
- [2] LOWE D G, " Object recognition from local scale-invariant features," *Proceedings of the International Conference on Computer Vision*, 1999,pp: 1150-1157.
- [3] LINDBERG T, " Feature detection with automatic scale selection ,". *International Journal of Computer Vision*,1998, Vol.30,NO.2: 79-116.
- [4] MIKOLAJCZYK K, SCHMID C , "A performance evaluation of local descriptors ," *IEEE Transactions on Pattern Analysis and Machine Intelligence*, 2005, Vol.27,NO.10,pp: 1615-1630.
- [5] MIKOLAJCZYK K, TUYTELAARS T, SCHMID C, et al. , "A comparison of affine region detectors and descriptors ," *International Journal of Computer Vision*, 2005, Vol.65,No.1,pp:43-72.

Infrared Dim Small Target Detection Algorithm Based on Adaptive Pipeline Filtering

Guang-qiu CHEN, Fang XING, Yang-mei SUN, Bao-kun ZHU

School of Electronic and Information Engineering, Changchun University of Science and Technology, Changchun 130022, China

Abstract—Aiming at the pipeline size fixing in the traditional pipeline filtering algorithm, when the size of the target is larger than the pipe diameter, the pipeline filtering algorithm based on the adaptive pipe diameter is proposed. The adaptive learning theory is introduced in this algorithm, which can modify the displacement of the pipeline center and the pipe diameter in real time according to the target location. The experimental results show that compared with the traditional method, this method can effectively suppress the influence of noise and effectively detect the trajectory of the small target.

Index-terms — pipeline filtering, dim small target, adaptive pipe diameter

I. INTRODUCTION

Pipeline filtering is one of the commonly used methods in infrared dim small target detection, which is taking the motion characteristics of small targets (motion trajectory space, motion velocity or acceleration) as a separable feature to detect the target. The basic principle of the algorithm is that: a spatial pipeline is established with the target as its center at the spatial location in n frame infrared video images (n is called pipeline length), the diameter of the pipeline (pipe is circular) represents the neighborhood size around the target, the length of the pipeline represents the required number of the image frames. According to the temporal and spatial continuity of moving target, if the target is detected in the pipeline with a specified length (such as m frames), is based on the theory of target track continuity and random noise correlation, it is considered that there is a target in the pipeline, whose theoretical basis is that the target trajectory is continuous and random noise is not correlated. The diameter in the traditional pipeline filtering algorithm is fixed, the relative motion between the target and the observer and the noise of the infrared detection system make the size of the small motion target changing, but the pipeline filtering algorithm can only detect the target with the diameter smaller than the diameter, and the diameter can not change with the target size. When the size of the target is larger than the diameter of the pipe, it will cause the target to overflow from the pipe. In this paper, a novel pipeline filtering algorithm is proposed, which can be adapted to the change the diameter of the pipe with the target size. The adaptive learning theory is introduced in this algorithm, which can modify the displacement of the pipeline center and the pipe diameter in real time according to the target location, which can effectively suppress the noise interference on the detection on target sequence[1].

II. PIPELINE FILTERING ALGORITHM WITH ADAPTIVE PIPE DIAMETER

Two important parameters are required in pipeline filtering algorithm with adaptive pipe diameter [2], which are the center coordinates of the pipeline and the target size respectively. Target diameter estimation and pipe diameter can be computed as following

$$\begin{cases} d = 2\sqrt{2}\sigma \\ D = 2d \end{cases} \quad (1)$$

Where σ represents space scale, d represents target diameter, D represents pipe diameter. E.g. if σ is equal to 1.4, the target diameter is 4×4 , pipe diameter is 8×8 .

The estimation coordinate of the pipeline center is that

$$\begin{cases} \hat{x}_i = x_{i-1} + m(x_i - x_{i-1}) \\ \hat{y}_i = y_{i-1} + n(y_i - y_{i-1}) \end{cases} \quad (2)$$

Where (x_i, y_i) and (x_{i-1}, y_{i-1}) represent target center coordinate in i th and $i-1$ th frame, (\hat{x}_i, \hat{y}_i) represents pipeline center coordinate in i th frame[3]. The weighted values m and n are as follows:

$$m = \begin{cases} 0 & \frac{x_i - x_{i-1}}{R} < 0 \\ 1 & 0 \leq \frac{x_i - x_{i-1}}{R} < \mu \\ \frac{C_x}{(x_i - x_{i-1})} & \frac{x_i - x_{i-1}}{R} > \mu \end{cases} \quad (3)$$

$$n = \begin{cases} 0 & \frac{y_i - y_{i-1}}{R} < 0 \\ 1 & 0 \leq \frac{y_i - y_{i-1}}{R} < \mu \\ \frac{C_y}{(y_i - y_{i-1})} & \frac{y_i - y_{i-1}}{R} > \mu \end{cases} \quad (4)$$

Where C_x and C_y are constant, μ is controllable factor. The controllable factor μ can get in the n th frame and those in the $(n-1)$ th frame is moving speed, so speed constraint is that

$$m = \begin{cases} 0 & \frac{x_i - x_{i-1}}{R} < 0 \\ 1 & 0 \leq \frac{x_i - x_{i-1}}{R} < \mu \\ \frac{C_x}{(x_i - x_{i-1})} & \frac{x_i - x_{i-1}}{R} > \mu \end{cases} \quad (5)$$

Target speed variation constraint is that

$$n = \begin{cases} 0 & \frac{y_i - y_{i-1}}{R} < 0 \\ 1 & 0 \leq \frac{y_i - y_{i-1}}{R} < \mu \\ \frac{C_y}{(y_i - y_{i-1})} & \frac{y_i - y_{i-1}}{R} > \mu \end{cases} \quad (6)$$

Where u_i and v_i are moving speed in x and y direction respectively, α_u , α_v and α_w are the maximum moving amount of the target center between two adjacent frames. Candidate targets are considered to be correct only if the above three inequalities are satisfied. On the contrary, it is considered to be noise interference. If the target speed exceeds the constraint condition in the current frame detection, the center

coordinate of the pipeline will not be updated, and still maintain the center coordinate of the pipeline in the last frame[4].

The specific steps of the pipeline filtering algorithm with adaptive pipe diameter is following

(1) Pipeline parameter initialization. Set the diameter and length, length N is determined by the requirements of the detection task

(2) Input sequence image. The first frame image is the starting image, and continuous input N frame images in the stack mode.

(3) Establish a pipeline for each candidate target, when the pipeline is filled with N frame images, start detecting the pipeline image in turn, then new image is entered by first-in first-out and the old image is removed.

(4) Speed constraint condition discriminates, counter updates. All the candidate targets in the current frame are observed that whether there are suspicious targets in their pipeline area in the next frame, If there is a suspected target, target appears counter plus 1, otherwise plus 0. To determine whether the target location is changed, then update the target position change counter.

(5) Update pipeline parameters. If the small target in the pipeline meets the constraints, the diameter of the pipe and the center coordinates of the pipeline are updated according to the formula (1) and (2).

(6) Distinguish between true and false target. After N frame image processed, the output value of each counter is observed. If the value of the counter is greater than or equal to K and the value of the target position change counter is less than or equal to R, the candidate target is determined to be a true target, otherwise it will be regarded as a false target.

(7) Updating the pipeline image until all the image sequences are processed.

(8) Output target trajectory.

III. SIMULATION AND RESULT ANALYSIS

For demonstrating the effectiveness and stability of the proposed algorithm, the proposed algorithm is used to detect dim small targets airplane in a set of infrared video image sequences, as can be shown in figure1. The airplane in the video image sequence gradually becomes larger in the field of view, the length is 50 frames, the size of the image is 320×240 . The original video image is shown in figure 1 (a)-(f), the residual images are shown in figure 1 (a)-(f), the target trajectory images of the classical pipeline filtering algorithm and the proposed algorithm are shown in figure 3(a)(b).

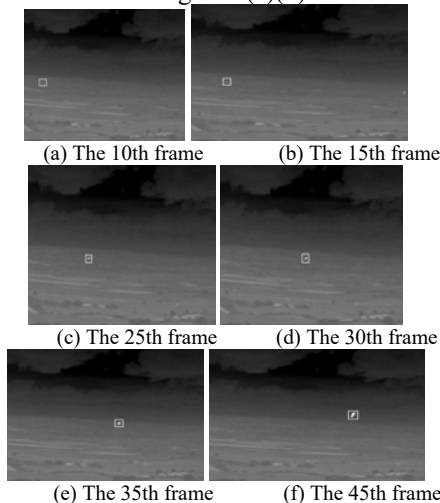


Figure 1 The different frames captured from the original video image

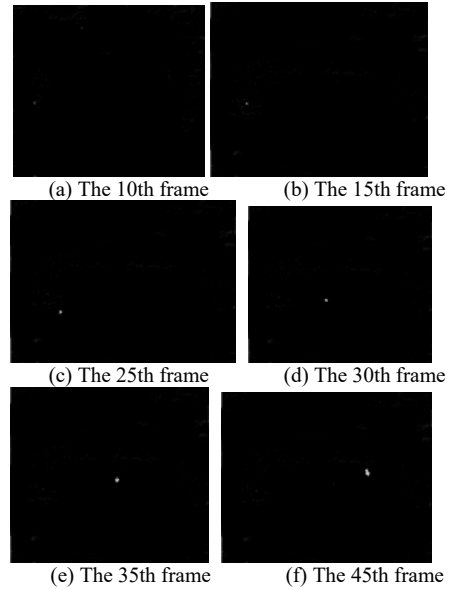


Figure 2 Residual image obtained by background suppression

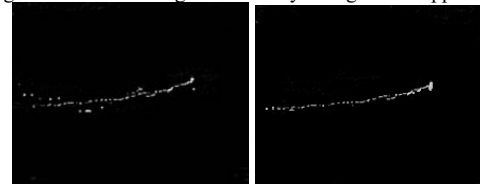


Figure3 Target motion trajectories by the different filtering algorithm

As can be seen in the above experimental results, the fixed position noise is still retained in the result obtained by the traditional pipeline filtering algorithm. The leakage alarm rate increases with the size of the dim small target gradually becoming larger. The proposed algorithm can suppress the edge noise and the fixed noise in the pipeline, the target can be captured when the size gradually become larger with the small target from far and near

IV. CONCLUSION

In this paper, aiming at the defects of the traditional pipeline filtering algorithm in infrared dim target detection, an adaptive pipe diameter filtering algorithm is proposed, which can effectively restrain the edge noise and the fixed noise. When the size of the dim small target in the field of view gradually becomes larger, the target can be effectively captured. Experimental results show that the proposed algorithm is superior to the traditional pipeline filtering algorithm in small target detection.

REFERENCE

- [1] Li Dawei, "SMALL DIM TARGETS DETECTION IN INFRARED VIDEO WITH COMPLEX BACKGROUND," *Master Thesis of Harbin Institute of Technology*,2013,pp:32-35.
- [2] SUN Ji-Gang, "Research on algorithm of infrared small target detection and tracking in image sequence," *Changchun Institute of Optics, Fine Mechanics and Physics Chinese Academy of Sciences*,2014,pp:77-79.
- [3] DONG Wei-ke,ZHANG Jian-qi, LIU De-lian, et al, "Pipeline Filter Algorithm Based on Movement Direction Estimation,"*ACTA PHOTONICA SINICA*, 2013,Vol.42,NO.4,pp:471-474.
- [4] ZHAO Xiao-ming, Yuan Sheng-chun, Ma Xiao-li, et al, "Research on Infrared Small Target Detection Technique Based on Moving Pipeline Filtering,"*Infrared Technology*,2009,Vol.31 , NO.5,pp:295-297.

The Structural Analysis and the Grey Situation Decision-making Research of Sustainable Forest Management Engineering Systems

Nansheng Wu¹, Zaohong Zhou², Liming Zen³

1.College of Forestry, Jiangxi Agricultural University, Nanchang, P.R.China

2.Department of Engineering management, Jiangxi university of economic and finance, Nanchang, P.R.China

3.Jiangxi Jinggangshan National Nature Reserve Administration, Jinggangshan, P.R.China

Abstract—Sustainable forest management is an important measure to achieve sustainable economic and social development, in order to achieve this goal, a number of construction projects have been implemented in various parts of China, but the structural problems and scientific decision-making issues of this construction project have not caused any concern. This paper takes Sustainable forest management project in the National Nature Reserve of Jiangxi Jinggangshan as an example, regard this project as a system, applying ISM model to analyze the structure of the system, on this basis, applying the gray situation decision-making theory, regard sustainable forest management project as situation countermeasure, and conduct the process of quantification and effectiveness value whitening, establish the model of gray situation decision, obtain the optimized decision-making scheme of the sustainable forest management projects, which will undoubtedly be a beneficial theoretical exploration to the current sustainable forest management project.

Index Terms— system structural, ISM model; gray situation decision model, engineering; sustainable forest management, National Nature Reserve of Jinggangshan in Jiangxi province

I. INTRODUCTION

In February 2011, on the Ninth General Assembly of the United Nations Forum on Forests, when discussed the issues of forests benefit people and alleviate poverty, the delegates pointed out that forests play an important role in the development of the green economy and forestry should be placed in priority areas[1,2]. In recent years, some major countries put forward several ways of green economic development. The United States take the Green New Deal as the basic concept in order to promote their development of green economy. EU advises that develop green economy to revitalize the regional economy[3]. Japan plans to be the world's first low-carbon green country. China advocates the view of scientific development, building resource-saving and environment-friendly society, emphasizing people-oriented, improving people's livelihood. The director of State Forestry Bureau Zhao Shucong stressed that". To implement the forestry ecological construction-oriented development strategy, we must hold high the two flags of ecology and people's livelihood, accelerating the pace of afforestation and industry development, not only providing ecological protection for scientific development, but also providing strong support for the improvement of people's livelihood[4], to take more advantages of the functions of the forests, producing better comprehensive efficiency, producing better comprehensive efficiency, it is necessary to carry out a high level scientific forest sustainable management[4]. To strengthening the forest management is an inevitable road of forestry promoting green growth[5]. Our forest resources inventory results show that the forestry "double increase" target which China have promised to international community is progressing well[6]. But forest quality of China is not very high, the

task of China's forest sustainable management is still very arduous. To meet the demand of China's ecological construction, strengthening forest management is a very important measure to enhance the ecological carrying capacity and achieve sustainable economic and social development [7].

The National Nature Reserve of Jinggangshan in Jiangxi Province belongs to the territory of the revolutionary sites of Jinggangshan, which located in the middle of Luoxiaoshan Ridge in the central part of Wanyangshan Mountain at the junction of Hunan and Jiangxi provinces in the southwest of Jiangxi, belongs to the nature reserve of forest ecological type, covers an area of 21,499 hectares. It is a World Biosphere Reserve areas, national education base of ecological civilization. It is the national demonstration nature reserves. It is the national epidemic sources and disease monitoring stations of terrestrial and wild animal. It is the national science education base and forestry science base. And it is also the youth science and technology Education Base and ecological education base in Jiangxi Province. The main protected object is the ecosystems of the humid subtropical evergreen broad-leaf forest and its biodiversity. Sustainable forest management a very important role in the development of the National Nature Reserve of Jinggangshan Mountain. In order to explore the model of sustainable forest management, in accordance with the relevant requirements of the demonstration construction of Chinese sustainable forest management, the National Nature Reserve of Jinggangshan authorized and implemented "the implement plan of the sustainable forest management of the Jinggangshan National Nature Reserve", establishing the ecological construction-oriented way of sustainable forestry development, adhere to ruling forests in accordance with the law, revitalizing the forest with science and technology, deepen the reform of forestry property rights system. Through a unified planning and rational arrangement, implemented step by step, building the forest cultivation system, management system, monitoring and evaluation system, resource protection systems and safeguards system which conform to the requirements of sustainable management. And fostering, protecting and take advantage of forest resources vigorously to achieve the goal of sustainable forest management, promoting the harmonious development between man and nature, make great efforts to achieve the comprehensive, coordinated and sustainable development of our social and economic.

II. THE KEY PROJECT AND CONSTRUCTION CONTENT OF SUSTAINABLE FOREST MANAGEMENT IN THE NATIONAL NATURE RESERVE OF JINGANGSHAN

The main construction contents of the "sustainable forest management implement plan" in the National Nature Reserve of Jinggangshan Mountain contain the following list below. First, strengthen the construction of

forest resources cultivation system:① Adjusting measures to local conditions, fortify as the harm extent, focusing on the main point, making rational distribution, regard these as the principles of sustainable development. Considering forming a forest ecological network system to protect the security of region ecological zone as the goal, focusing on the nature reserve forest, water conservation forest, soil and water conservation forest, scenic forests, environmental protection forests and road protection forests, building public welfare ecological forest;② Organic combining the afforestation and economic development to form a new rural economic growth point, prospering regional economy, and develop commercial forests construction actively, which includes the fast growing high yield timber base construction, industrial raw material forest base construction, Bamboo base construction, economic forest construction and seedlings forests base construction; ③ Through the measures of adjustment of forest species, trees species and the structure of trees-age, improve and optimize the structure of forest resources. Second, strengthen the construction of the monitoring and evaluation system of forest resources. According to the relevant regulations and technical standards of China National Forest Inventory, carry out analysis of survey results of forest resources based on "3S" technology, provide basic data and information for authorizing detailed implementary planning, detailed planning and design of key construction projects, forest management plan, forest resource assets assessment and evaluation of the monitoring of construction effectiveness. The third is to strengthen the utilization system of forest resource, considering the variety demand for forest ecosystem services and forest products in the economic and social development in experimental demonstration area, formulating the content, layout, strength and way of forest utilization, and ensure sustainable forest products and optimization production, take full advantage of the multiple benefits and utilization value. The fourth is to strengthen forest management system, through the research explore of the aspects of concept, criteria, indicators and research practices ways of sustainable forest management, adhere to the theory and ideology of sustainable development, study the sustainable management methods techniques and model of Southern China Collective forest resources. Fifth, strengthen the construction of forest ecology and conservation. Biodiversity conservation and sustainable use of sustainable is an important goal in forest sustainable management, we must consider the impact of our forest management activities on biodiversity. Forest pests and forest fires are major factors which affecting the sustainable management of forests, in the whole process of forest management we must stick to the policy of "prevention first, scientific prevention and control, governance according to the law, health promotion", strengthen the management of forestry pest and forest fire. Woodland is the material basis of forest development, the woodland protection and utilization project of Nation Nature Reserves Jingangshan in Jiangxi province should be well done in the process of sustainable forest management, including strengthen the use management of woodland, maintenance ecological safety, prevent degradation of forest ecosystems and forest soil fertility, establishing monitoring system of the plantations ecosystem and forest soil fertility changes.

In order to achieve the construction content of the implementation plan for sustainable forest management in Jingangshan National Nature Reserve in Jiangxi province, Jiangxi Jingangshan National Nature Reserve established the "construction of leading group of sustainable forest management". According to the requirement of the national demonstration construction of sustainable forest management, organize the implement the supplementary investigation of division of forestry

classified management, and organize experts to evaluate the status quo of forest resources and sustainable forest management, conform the main construction task of sustainable forest management, and putting forward 18 construction project of sustainable forest management in the National Nature Reserve of Jingangshan in Jiangxi province, including ecological construction project, commercial forest construction project, evaluation standard of sustainable forest management, forest ecology and resource monitoring system construction, geographic information system of forest resources management, bamboo comprehensive utilization project, forest ecotourism project, development of non-wood forest products, timber comprehensive utilization project, the project of revitalizing forest through science and technology series, the new type of forestry system and demonstration forest construction, media-term and long-term planning of forest management, forest classification management, comprehensive treatment engineering of forest important fire danger division, forest ecology and wildlife protection engineering, natural reserve construction project, forest land use planning and forestry harmful biological control engineering. These engineering provide important guarantee for the construction of sustainable forest management, and is conducive to the sustainable development of Jiangxi Jingangshan National Nature Reserve. From the view of system, these projects constitute a system together, and the system has an internal structure, aiming at achieve sustainable forest management better. However, in practice work, structural problems and scientific decision of these engineering have cause no concern. Therefore, it is necessary to analyze the systematic structure problems of these engineering, and provide theoretical basis for scientific decision of projects.

III. THE SYSTEM STRUCTURE ANALYSIS OF FOREST SUSTAINABLE MANAGEMENT PROJECT BASED ON THE ISM MODEL

Structural analysis model is a set of method which analysis related problems of complex system, it split multiple complex system into subsystems, combining with our practice knowledge and experience, through complex calculation of computer, eventually obtain a multi-stage structural model, thus helping researchers analyze key issues more clearly. Now we applied ISM model in the sustainable forest management of Jingangshan National Nature Reserve to do system structure analysis to determine its hierarchy relation.

A. Establish correlation matrix among various engineering

Regarding the sustainable forest management engineering of Jingangshan National Nature Reserve as a system, combining with the actual situation and the relevant theoretical knowledge in the sustainable forest management projects of Jingangshan National Nature Reserve, analyzing the relationship of mutual influence between 18 project .

In the system, there is a certain internal logic contact between mutal project, he contact information form the structure of the system[6]. In the process of the project of constructing Jingangshan National Nature Reserve sustainable forest management system, set up "ecological forest construction project" for the system elements "S1", set up "commercial forest construction" for "S2", ..., "forestry harmful Biological Control project "for the system elements" S18",we take the interests relationship between the projects as logical structure, such as" ecological forest construction S1 "is good for" forest ecology and resource monitoring system S4 ", "commercial forest construction project "is good for

"bamboo utilization project S6" and so on, by this logic link analysis, exploring the structure of the system.

According to this analysis method, making decision according to the following rules. If the line S_i has a "direct or indirect benefit" effect to the column S_j ($i, j = 1, 2, \dots, 10$), assign it as "1". If the line S_i has no "direct or indirect beneficial" effect to the column S_j , assign it as "0", establish a binary relation adjacency matrix A [7]. We can obtain binary adjacency matrix A of sustainable forest management project in Jingangshan National Nature Reserve, which shown in Figure 1.

	S_1	S_2	S_3	S_4	S_5	S_6	S_7	S_8	S_9	S_{10}	S_{11}	S_{12}	S_{13}	S_{14}	S_{15}	S_{16}	S_{17}	S_{18}
S_1	0	0	0	1	1	0	1	0	0	1	1	0	1	0	1	1	1	0
S_2	0	0	0	0	0	1	0	1	1	1	1	0	1	1	0	0	0	1
S_3	1	1	0	0	0	1	1	1	1	1	1	1	1	1	1	1	1	1
S_4	1	0	0	0	1	1	1	1	1	1	1	1	1	1	1	1	1	1
S_5	1	1	0	0	0	1	1	1	1	1	1	1	1	1	1	1	1	1
S_6	0	1	0	0	0	0	0	1	0	1	1	1	1	1	1	1	1	1
S_7	1	0	0	0	1	0	0	0	0	1	1	1	1	1	0	1	1	0
S_8	0	1	0	0	0	0	0	0	0	1	1	1	1	1	1	1	1	1
S_9	0	1	0	0	0	1	0	1	0	1	1	1	1	1	1	1	1	1
S_{10}	1	1	1	1	1	1	1	1	1	0	1	1	1	1	1	1	1	1
S_{11}	1	1	1	0	0	1	1	1	1	0	1	1	1	1	1	1	1	1
S_{12}	1	1	1	1	1	1	1	1	1	1	0	1	1	1	1	1	1	1
S_{13}	1	1	1	0	0	1	1	1	1	1	1	0	1	1	1	1	1	0
S_{14}	0	1	0	1	1	1	0	1	1	1	1	1	1	1	0	1	1	1
S_{15}	1	0	0	1	1	0	1	0	0	1	0	1	0	1	0	1	1	1
S_{16}	1	0	1	1	1	0	1	0	1	1	1	1	1	1	1	0	1	1
S_{17}	1	1	1	1	1	1	1	1	1	1	1	1	1	1	1	1	0	1
S_{18}	0	1	0	0	0	1	0	1	1	1	1	1	1	1	1	1	1	0

Figure1. Binary adjacency matrix A of sustainable forest management project in Jingangshan National Nature Reserve

B. Building up a reachable matrix

Reachable matrix is to use a matrix to reflects the extent of the length which can be reached through a certain length way between the nodes in the system directed connection diagram. The principle is: Use the operation rules of the Boolean algebra (ie, $0 + 0 = 0, 0 + 1 = 1, 1 + 0 = 1, 1 + 1 = 1, 0 \times 0 = 0, 0 \times 1 = 0, 1 \times 0 = 0, 1 \times 1 = 1$) and the following equation (1), we can obtain the reachable matrix M [8]:

$$(A + I)^{K-1} \neq (A + I)^K = (A + I)^{K+1}, K \geq 1 \tag{1}$$

In this equation, I is the same order unit matrix of adjacency matrix.

By calculation, we can obtain reachabe matrix R :

$$R = (A + I)^K \tag{2}$$

We can get the reachabe matrix R among the sustainable forest management projects in Jingangshan National Nature Reserve, which is shown in Figure 2.

	S_1	S_2	S_3	S_4	S_5	S_6	S_7	S_8	S_9	S_{10}	S_{11}	S_{12}	S_{13}	S_{14}	S_{15}	S_{16}	S_{17}	S_{18}
S_1	1	0	0	0	1	0	1	0	0	1	1	1	1	1	1	1	1	1
S_2	0	1	0	0	0	1	0	1	1	1	1	1	1	1	1	1	1	1
S_3	1	1	1	0	1	1	1	1	1	1	1	1	1	1	1	1	1	1
S_4	1	0	0	1	1	1	1	1	1	1	1	1	1	1	1	1	1	1
S_5	1	0	0	0	1	0	1	0	0	1	1	1	1	1	1	1	1	1
S_6	0	0	0	0	0	1	0	1	0	1	1	1	1	1	1	1	1	1
S_7	1	0	0	0	1	0	1	0	0	1	1	1	1	1	1	1	1	1
S_8	0	0	0	0	0	0	1	0	1	1	1	1	1	1	1	1	1	1
S_9	0	0	0	0	0	1	0	1	1	1	1	1	1	1	1	1	1	1
S_{10}	0	0	0	0	0	0	0	0	0	1	1	1	1	1	1	1	1	1
S_{11}	0	0	0	0	0	0	0	0	0	1	1	1	1	1	1	1	1	1
S_{12}	0	0	0	0	0	0	0	0	0	1	1	1	1	1	1	1	1	1
S_{13}	0	0	0	0	0	0	0	0	0	1	1	1	1	1	1	1	1	1
S_{14}	0	0	0	0	0	0	0	0	0	1	1	1	1	1	1	1	1	1
S_{15}	0	0	0	0	0	0	0	0	0	0	0	0	0	0	1	1	1	1
S_{16}	0	0	0	0	0	0	0	0	0	0	0	0	0	0	1	1	1	1
S_{17}	0	0	0	0	0	0	0	0	0	0	0	0	0	0	1	1	1	1
S_{18}	0	0	0	0	0	0	0	0	0	0	0	0	0	0	1	1	1	1

Figure2. The reachable matrix M of the sustainable forest management project of Jingangshan National Nature Reserve

C. Generating hierarchical ladder structure model

After we get the reachable matrix, the relationship between class of engineering system and class is not clear yet, therefore we need to arrange it sequentially, get the reduced matrix R' [9]. The approach is: In the reachable

matrix R , if there are identical row and the corresponding column (S_1, S_5 and S_7 are identical, S_{10} - S_{14} are identical, S_{15} - S_{18} are identical), we can conduct reduce process and remove the same row and column, then we can get treated reduced matrix R' . The reachable reduced matrix R' among the sustainable forest management projects of Jingangshan National Nature Reserve to is shown in Figure 3.

	$S_{1,5,7}$	S_2	S_3	S_4	S_6	S_8	S_9	S_{10-14}	S_{15-18}
$S_{1,5,7}$	1	0	0	0	0	0	0	1	1
S_2	0	1	0	0	1	1	1	1	1
S_3	1	1	1	0	1	1	1	1	1
S_4	1	0	0	1	1	1	1	1	1
S_6	0	0	0	0	1	1	0	1	1
S_8	0	0	0	0	0	1	0	1	1
S_9	0	0	0	0	1	1	1	1	1
S_{10-14}	0	0	0	0	0	0	0	1	1
S_{15-18}	0	0	0	0	0	0	0	0	1

Figure3. The reachable reduced matrix R' among the sustainable forest management projects of Jingangshan National Nature Reserve

After we get the reachable reduced matrix R' , rearranging all the elements sequentially according to the number of "1", forming an matrix where the number in right corner are all "0", this matrix is the backbone matrix R^* [10], then we can get the backbone matrix R^* among the sustainable forest management projects of Jingangshan National Nature Reserve, which is shown in Figure 4.

	$S_{1,5,7}$	S_2	S_3	S_4	S_6	S_8	S_9	S_{10-14}	S_{15-18}
$S_{1,5,7}$	1	0	0	0	0	0	0	1	1
S_2	0	1	0	0	1	1	1	1	1
S_3	1	1	1	0	1	1	1	1	1
S_4	1	0	0	1	1	1	1	1	1
S_6	0	0	0	0	1	1	0	1	1
S_8	0	0	0	0	0	1	0	1	1
S_9	0	0	0	0	1	1	1	1	1
S_{10-14}	0	0	0	0	0	0	0	1	1
S_{15-18}	0	0	0	0	0	0	0	0	1

Figure4. The backbone matrix R^* among the sustainable forest management projects

After the division above, we can constitute a systematic structure model, which is the model of the sustainable forest management projects in Jingangshan National Nature Reserve (As is shown in Figure 5).

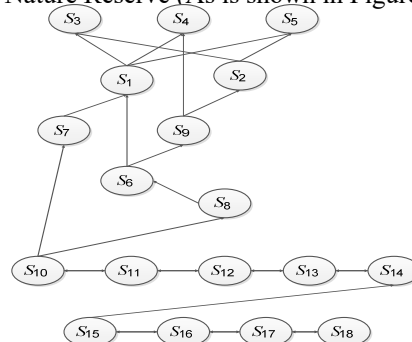


Figure5. The systematic structure model of the sustainable forest management projects in Jingangshan National Nature Reserve

As it can be seen in the structural model of the system in the sustainable forest management projects of Jingangshan National Nature Reserve, the key projects of sustainable forest management in Jingangshan National Nature Reserve can be divided into seven levels:

First layer: The evaluate of sustainable forest management criteria S3, the construction of forest ecology and resource monitoring system S4, the geographic information system of forest resource management S5.

Second layer: Ecological forest construction project S1, commercial forest construction project S2.

Third layer: Forest eco-tourism project S7, wood intergated utilization project S9.

Fourth layer: Bamboo intergated utilization project S6.

Fifth floor: NTFP development project S8.

Sixth Layer: The project of revitalizing forest through science and technology, new silvicultural systems and demonstration forest construction S11, the medium-term and long-term planning of forest management S12, forestry classified management S13,integrated treatment project in forest major fire district S14.

Seventh layer: Forest ecology and wildlife protection projects S15, construction of Nature Reserve S16, forest protection and utilization planning S17, forestry pest control project S18.

Taking into account that the division should not be too thin, some levels can be combined, such as the fifth layer and the fourth layer can be combined into the third layer. After merged like that, the system structure of the sustainable forest management project in Jing Gang Mountain National Nature Reserve can be simply divided into five levels:

First layer: The evaluate of sustainable forest management criteria S3, the construction of forest ecology and resource monitoring system S4, the geographic information system of forest resource management S5, this layer can be call as "Forest resources monitoring and evaluation layer."

Second layer: Ecological forest construction project S1, commercial forest construction project S2, this layer can be call as" forest resources cultivation layer."

Third layer: Forest eco-tourism project S7, wood intergated utilization project S9,bamboo intergated utilization project S6,NTFP development project S8,this layer is called "forest resource utilization layers".

Fourth layer: The project of revitalizing forest through science and technology, new silvicultural systems and demonstration forest construction S11, the medium-term and long-term planning of forest management S12, forestry classified management S13,integrated treatment project in forest major fire district S14, this layer can be call as "Forest operations and management layer."

The fifth layer: Forest ecology and wildlife protection projects S15, construction of Nature Reserve S16, forest protection and utilization planning S17, forestry pest control project S18, this layer can be call as: "Forest ecology and resource protection layer."

D. Analysis of the structural model

From the ISM model of sustainable forest management engineering system in Jingangshan National Nature Reserve, we can clearly see the direct relationship between each project and the importance degree layer where each project is located, then we can learn the internal mechanism of the engineering system from it.

The projects in the first layer of the sustainable forest management system in Jing Gang Mountain National Nature Reserve are three engineerings in forest resources monitoring and evaluation layer: The evaluate of sustainable forest management criteria S3, the construction of forest ecology and resource monitoring system S4, the geographic information system of forest resource management S5, the projects of this layer is the fundamental factor which have a direct impact on Jingangshan National Nature Reserve sustainable forest management, and have a significant effects for the sustainable forest management system construction of the National Nature Reserve in Jing Gang Mountain in

Jiangxi province. In practice, to guarantee the objective of the sustainable forest management in Jing Gang Mountain National Nature Reserve, the most fundamental measure is to construct these three systems engineerings well: The evaluation of sustainable forest management criteria S3,forest ecology and resource monitoring system construction S4 and the geographic information of forest resource management S5.

The project of the second layer is the two projects in the layers of forest resource cultivation: the ecological forest construction S1 and commercial forest construction S2,the project of this layer is the underlying factors which impact sustainable forest management system of Jing Gang Mountain National Nature Reserve, these projects are the premise to achieve the objectives of the sustainable forest management system in Jing Gang Mountain National Nature Reserve.

The project of third layer are the four engineerings in forest resource utilization layers: bamboo integrated utilization project S6, forest eco-tourism project S7,development of non-wood forest products project S8 and timber utilization project S9, the project of this layer is the main project which influence sustainable forest management system of the National Nature Reserve of Jing Gang Mountain in Jiangxi province, these projects form the core of the National Nature Reserve of Jing Gang Mountain in Jiangxi province, play an important role in achieving the goal of sustainable forest management system in the National Nature Reserve of Jing Gang Mountain in Jiangxi province.

The project of the fourth layer is the five projects in forest operation and management layer: The project of revitalizing forest through science and technology, new silvicultural systems and demonstration forest construction S11, the medium-term and long-term planning of forest management S12, forestry classified management S13,integrated treatment project in forest major fire district S14, the project of this layer is to the acting path which influence the sustainable forest management system in National Nature Reserve of Jing Gang Mountain in Jiangxi province, and the primary path to achieve the sustainable forest management system in the National Nature Reserve of Jing Gang Mountain in Jiangxi province, at the same time, the project of this layer Engineering is strongly connected modules and a strong association projects, play a connecting role and play a very important supporting role in the system.

The fifth layer is the surface factor influence the sustainable forest management in National Nature Reserve of Jingangshan, including the four projects in "forest ecology and resource protection layer": Forest ecology and wildlife protection projects S15, construction of Nature Reserve S16, forest protection and utilization planning S17, forestry pest control project S18, staying at the bottom of ISM model, means that these projects have an impact on rest projects, they are the underlying engineerings of the model, called the input feature of engineering systems, which is the foundation projects of the sustainable forest management in National Nature Reserve of Jing Gang Mountain in Jiangxi province .

Through ISM model, the logical relationship among the sustainable forest management in National Nature Reserve of Jingangshan in Jiangxi province is reflected, which is in favour of grasping the formation and development mechanism of the sustainable forest management in National Nature Reserve of Jingangshan in Jiangxi province.

IV. GRAY SITUATION DECISION OF THE SUSTAINABLE FOREST MANAGEMENT IN NATIONAL NATURE RESERVE OF JINGANGSHAN IN JIANGXI PROVINCE

Optimization Decision of the engineering is a key step to implement the project, because of engineering

decisions, we need to consider the social, economic, technical, environmental and other factors, taking into account that some elements are lack of information, based on this condition, this study conducted Grey Situation Decision analysis. Grey Situation Decision Method is an important decision-making method of the gray system theory, it is a decision analysis method which considers the 4 decisions considering elements of event, strategies, results, goals and so on. The most important feature of this method is that the data it deals with contain grey elements, which is the decision problem of incomplete information[11]. Using grey situation decision to construct every situation of sustainable forest management in National Nature Reserve of Jingangshan in Jiangxi province, and conduct advantage analysis and comprehensive evaluation, through the result of grey situation decision, confirm the optimal solution of sustainable forest management in National Nature Reserve of Jingangshan in Jiangxi province, which is the useful exploration in project decision-making process.

A. Grey situation decision method and procedure

Grey Situation Decision optimization principle is to turn the indicators of various programs into the effect measure of dimensionless within a certain range, and then the combine effect measure value of each index to become a general effect measure, deciding and evaluating the merits of the project by the size of the general effect measure value. Grey Situation Decision contains four basic elements, namely the event(Issues to be addressed), measures(measures to deal with an issue), effects(the practical effect of using a countermeasure to deal with an event)and the target (the guidelines of the evaluating effect). Noting the events as a_i , countermeasures as b_j , binary combinations of countermeasures and events (a_i, b_j)note as for the situation S_{ij} , effect that countermeasures to deal with the events note as γ_{ij} , the ratio of the results and the corresponding situation r_{ij}/s_{ij} noted as decision-making elements, for the multi-objective decision-making, the decision element under the k th goals, and thus form the effect measure matrix

$M^{(k)}$ composed of row $i \times$ columns j , the integrated decision-making element synthesize the k targets is $r_{ij}(\sum)/S_{ij}$, thereby set up an integrated measurement matrix composed of row $i \times$ columns j , transforming the elements of the matrix $M^{(\Sigma)}$ into a better order by row and column, in order to get excellent sequence decision matrix M^* , the final decision is based on the effect measure size.

Grey situation decision calculation steps are as followings: (1) given event a_i and countermeasures b_j . (2) constructing situation S_{ij} ; (3) given target k_p ; (4) given practical effect of different target γ_{ij} ; (5) calculating the effect measure matrix of different target. (6) calculating integrated effect measure matrix $M(\sum)$. (7) $M(\sum)$ will be in an optimal transformation, obtain optimal sequence decision matrix M^* , according to the maximum effect measure, choose the best situation for decision-making; (8) Decision result analysis.

B. Gray situation decision of the sustainable forest management in National Nature Reserve of Jingangshan in Jiangxi province

- Event set (a_i) and countermeasures set (b_j)

Put the forest resources monitoring and evaluation layer, forest resources cultivation layer, forest resource utilization layers, forest operations and management layer, forest ecology and resource protection layer into event set(a_i), suppose the forest resources monitoring and evaluation layer as a_1 , forest resources cultivation layer as a_2 , forest resource utilization layers as a_3 , forest

operations and management layer as a_4 , forest ecology and resource protection layer as a_5 , then we have:

$$a_i=(a_1, a_2, \dots, a_5) \tag{3}$$

Different events have different countermeasure, their set constitute countermeasures set, suppose engineering as countermeasures set (b_j), specific measures are: ecological forest construction (b_1), commercial forest construction (b_2), evaluation of sustainable forest management standards (b_3), the construction of forest ecology and resource monitoring system (b_4), geographic information system construction of forest resource management (b_5), the project of bamboo comprehensive utilization of (b_6), forest eco-tourism project (b_7), the development of non-wood forest products (b_8), project of wood integrated utilization (b_9), the series projects of revitalizing forest through science and technology (b_{10}), silvicultural systems and demonstration of new forest construction (b_{11}), medium-term and long-term planning of forest management (b_{12}), forest classification management (b_{13}), the comprehensive treatment project of forest focus fire areas (b_{14}), forest ecology and wildlife protection projects (b_{15}), Nature Reserve construction (b_{16}), forest protection and utilization planning (b_{17}) and forestry pest control engineering (b_{18}), then we get:

$$(b_j)=(b_1, b_2, \dots, b_{18}) \tag{4}$$

- Construct situation S_{ii}

The situation (S_{ii}) is the binary combinations of event a_i ($i = 1, 2, \dots, 5$) and countermeasures b_j ($j = 1, 2, \dots, 18$). namely $S_{ii} = (a_i, b_j)$. In the present case, the five kinds of events and responses 18 above constitute the situation matrix of rows $5 \times$ columns 18.

- Target collection (K_p)

There are three project objectives, namely, investment size, technical difficulty and implementation effect, set a target set $k_p = (k_1, k_2, k_3) =$ (investment size, technical difficulty, implementation effect).

- Decision Matrix mode

Since there are three decision-making objectives of this study, we need to carry out the multi-objective decision-making, which including the three single-objective decision-making matrix ($k=1,2,3$) and an integrated decision-making matrix $M(\sum)$. These four matrices should all be the multi-dimensional matrix of rows $5 \times$ columns 18. These decision matrix model $M^{(k)}$ is:

$$M^{(k)} = (M_1^{(k)}, M_2^{(k)}, \dots, M_5^{(k)}) = \begin{matrix} \begin{matrix} \gamma_{11}^{(k)} & \gamma_{12}^{(k)} & \dots & \gamma_{118}^{(k)} \\ S_{11} & S_{12} & \dots & S_{118} \\ \gamma_{21}^{(k)} & \gamma_{22}^{(k)} & \dots & \gamma_{218}^{(k)} \\ S_{21} & S_{22} & \dots & S_{218} \\ \vdots & \vdots & & \vdots \\ \gamma_{51}^{(k)} & \gamma_{52}^{(k)} & \dots & \gamma_{518}^{(k)} \\ S_{51} & S_{52} & \dots & S_{518} \end{matrix} \end{matrix} \tag{5}$$

In the formula(5): $\gamma_{ij}^{(k)}$ ($i=1,2,\dots,5$ $j=1,2,\dots,18$) is the effect measure under the k th ($k=1,2,3$) target, $S_{ij}=(a_i, b_j)$ is the situation.

- The calculation of effect Measure $\gamma_{ij}^{(k)}$

The determine of effect measure is an important link of gray situation decision. Effect measure is the measure of comparing the actual effect that various situations arised, usually including up limit effect measure, lower limit measure, and moderation limit measure. Different goals have different effect measure calculation methods.

Up limit effect measure:

$$\gamma_{ij}^{(k)} = \frac{U_{ij}^{(k)}}{\max_i \max_j U_{ij}^{(k)}} \tag{6}$$

Lower limit effect measure:

$$\gamma_{ij}^{(k)} = \frac{\min_i \min_j U_{ij}^{(k)}}{U_{ij}^{(k)}} \tag{7}$$

moderation limit measure:

$$\gamma_{ij}^{(k)} = \frac{U_0}{|U_{ij}^{(k)} - U_0| + U_0} \tag{8}$$

In these formulas, $\gamma_{ij}^{(k)}$ is the effect measure of the situation S_{ij} under k -th goal. $U_{ij}^{(k)}$ is for the actual effect measure of the situation S_{ij} under k -th goal. $\max_j U_{ij}^{(k)}$ and $\min_i U_{ij}^{(k)}$ are the maximum and minimum of the actual effect in all situations under the k -th goal. U_0 is the moderate specified value.

Listing the $\gamma_{ij}^{(k)}$ calculated by matrix, which is the effect measure matrix $M_{ij}^{(k)}$. Obviously, the values of $\gamma_{ij}^{(k)}$ are all less than 1 [12].

There are three goals in this study: investment size k_1 , technical difficulty k_2 and the implementation effect k_3 . In the study process, weighting these three goals first, this study adopt subjective weighting method, inviting 16 engineering and technical staff of the "Sustainable Forest Management Project" in the National Nature Reserve of Jing Gang Mountain to constitute the expert members

$M^{(1)}$	0.19	0.21	0.88	0.86	0.91	0.41	0.28	0.14	0.23	0.31	0.24	0.32	0.19	0.31	0.29	0.31	0.29	0.27
	0.91	0.80	0.18	0.21	0.29	0.17	0.32	0.25	0.19	0.23	0.22	0.34	0.23	0.27	0.18	0.38	0.21	0.29
	0.21	0.12	0.31	0.22	0.17	0.89	0.80	0.89	0.90	0.19	0.21	0.28	0.31	0.24	0.23	0.22	0.31	0.29
	0.28	0.23	0.30	0.29	0.26	0.36	0.28	0.20	0.23	0.70	0.83	0.88	0.80	0.81	0.21	0.20	0.31	0.31
	0.23	0.21	0.19	0.22	0.31	0.28	0.19	0.37	0.27	0.31	0.25	0.36	0.19	0.26	0.77	0.82	0.88	0.76
$M^{(2)}$	0.39	0.24	0.83	0.83	0.90	0.29	0.26	0.18	0.43	0.28	0.36	0.32	0.23	0.23	0.25	0.37	0.42	0.31
	0.93	0.79	0.28	0.35	0.38	0.04	0.01	0.29	0.37	0.42	0.32	0.28	0.21	0.36	0.46	0.31	0.41	0.39
	0.38	0.29	0.32	0.21	0.41	0.82	0.81	0.85	0.83	0.27	0.22	0.39	0.24	0.35	0.31	0.22	0.32	0.18
	0.14	0.21	0.24	0.35	0.36	0.21	0.29	0.36	0.28	0.76	0.80	0.85	0.90	0.77	0.19	0.21	0.32	0.27
	0.19	0.19	0.26	0.35	0.21	0.38	0.28	0.37	0.38	0.17	0.41	0.21	0.34	0.21	0.76	0.94	0.95	0.80
	0.33	0.08	0.89	0.94	0.98	0.29	0.04	0.36	0.31	0.42	0.43	0.39	0.21	0.26	0.23	0.36	0.34	0.24
	0.85	0.88	0.40	0.43	0.21	0.41	0.39	0.23	0.38	0.27	0.42	0.22	0.40	0.18	0.32	0.45	0.39	0.43
$M^{(3)}$	0.24	0.27	0.48	0.29	0.33	0.78	0.77	0.89	0.84	0.19	0.39	0.21	0.35	0.27	0.32	0.22	0.34	0.31
	0.31	0.26	0.29	0.38	0.29	0.31	0.26	0.31	0.23	0.82	0.86	0.94	0.84	0.77	0.23	0.31	0.28	0.27
	0.33	0.25	0.22	0.19	0.23	0.37	0.21	0.26	0.29	0.35	0.21	0.34	0.29	0.24	0.72	0.78	0.86	0.82

Taking into account the requirements of the project, the measure of "investment size" goal should not simply be considered as smaller as possible, moderate measure were appropriate to conduct effect measure calculate in this objective measure, getting 80% of the mean value more appropriate as moderate values [13], which is 0.35,

$M_{ij}^{(1)}$	0.69	0.71	0.40	0.41	0.38	0.85	0.83	0.63	0.74	0.90	0.76	0.92	0.69	0.90	0.85	0.90	0.85	0.81
	0.38	0.40	0.67	0.71	0.85	0.66	0.92	0.78	0.69	0.74	0.73	0.97	0.74	0.81	0.67	0.92	0.71	0.85
	0.71	0.60	0.90	0.73	0.66	0.39	0.44	0.39	0.39	0.69	0.71	0.83	0.90	0.76	0.74	0.73	0.90	0.85
	0.83	0.74	0.88	0.85	0.80	0.97	0.83	0.70	0.74	0.50	0.42	0.40	0.44	0.43	0.71	0.70	0.90	0.90
	0.74	0.71	0.69	0.73	0.90	0.83	0.69	0.95	0.82	0.90	0.78	0.97	0.69	0.80	0.45	0.43	0.40	0.46
$M_{ij}^{(2)}$	0.41	0.25	0.87	0.87	0.95	0.31	0.27	0.19	0.45	0.29	0.38	0.34	0.24	0.24	0.26	0.39	0.44	0.33
	0.98	0.83	0.29	0.37	0.40	0.04	0.01	0.31	0.39	0.44	0.34	0.29	0.22	0.38	0.48	0.33	0.43	0.41
	0.40	0.31	0.34	0.22	0.43	0.86	0.85	0.89	0.87	0.28	0.23	0.41	0.25	0.37	0.33	0.23	0.34	0.19
	0.15	0.22	0.25	0.37	0.38	0.22	0.31	0.38	0.29	0.80	0.84	0.89	0.95	0.81	0.20	0.22	0.34	0.28
	0.20	0.20	0.27	0.37	0.22	0.40	0.29	0.39	0.40	0.18	0.43	0.22	0.36	0.22	0.80	0.99	1	0.84
	0.34	0.08	0.91	0.96	1	0.30	0.04	0.37	0.32	0.43	0.44	0.40	0.21	0.27	0.23	0.37	0.35	0.24
$M_{ij}^{(3)}$	0.87	0.90	0.41	0.44	0.21	0.42	0.40	0.23	0.39	0.28	0.43	0.22	0.41	0.18	0.33	0.46	0.40	0.44
	0.24	0.28	0.49	0.30	0.34	0.80	0.79	0.91	0.86	0.19	0.40	0.21	0.36	0.28	0.33	0.22	0.35	0.32
	0.32	0.27	0.30	0.39	0.30	0.32	0.27	0.32	0.23	0.84	0.88	0.96	0.86	0.79	0.23	0.32	0.29	0.28
	0.34	0.26	0.22	0.19	0.23	0.38	0.21	0.27	0.30	0.36	0.21	0.35	0.30	0.24	0.73	0.80	0.88	0.84

- The calculation of comprehensive effect measure $M^{(k)}$

By calculating the effect measure of each single objective, actually carried out dimensionless normalize

group, first weighting three goals, taking the mean values of all the experts as weighted value of each goals, get:

$$k_1: k_2: k_3 = 0.35: 0.25: 0.40$$

Secondly, experts construct the decision matrix $M(k)$ of the three goals, every goal divided into five level, and quantify as the order of difficult \rightarrow easily or the large \rightarrow small or good \rightarrow poor in 5 levels. Considering the differences between the data, and to compare with each other more convenient, normalizing the data quantized by the experts as following:

$$y_{ij} = \frac{x_{ij} - x_{j\min}}{x_{j\max} - x_{j\min}} \tag{9}$$

In this formula, $X_j \max$ is the maximum value of the j -th index, $X_j \min$ is the minimum value of the j -th index.

Seen from the formula, the index value is between 0-1 after treated.

Take the normalized mean value respectively to construct three single-objective decision-making structure matrix $M_{ij}^{(k)}$ ($k = 1,2,3$), which are the target decision matrix of the investment size, technical difficulties and implement results in "Sustainable Forest Management Project". After data processing, getting the decision matrix ($k = 1,2,3$) of the three objectives as follows:

"technical difficulty" is metered as the order of "hard \rightarrow easy", so it is the upper limit measure, "implementation effect" is also metered as upper limit measure. Based on measure calculation method, we can get three goals effect measure matrix $M_{ij}^{(k)}$ ($k = 1,2,3$) as follows:

dispose of effect whitening value under different targets, it is convenient to calculate the comprehensive effect measure.

Based on the judgment result of experts, the weight of targets M1, M2 and M3 are 0.35, 0.25, 0.40, through $M_j^{(1)}, M_j^{(2)}, M_j^{(3)}$ we can get the comprehensive effect measure of the situation $M_j^{(\Sigma)}$:

$$M_j^{(\Sigma)} = 0.35 \times M_j^{(1)} + 0.25 \times M_j^{(2)} + 0.40 \times M_j^{(3)} \quad (10)$$

And get comprehensive effect measure matrix:

$$M^{(\Sigma)} = \begin{bmatrix} 0.48 & 0.35 & 0.72 & 0.74 & 0.77 & 0.49 & 0.38 & 0.41 & 0.50 & 0.56 & 0.54 & 0.57 & 0.39 & 0.48 & 0.46 & 0.56 & 0.55 & 0.46 \\ 0.73 & 0.72 & 0.47 & 0.52 & 0.48 & 0.41 & 0.48 & 0.44 & 0.49 & 0.48 & 0.51 & 0.50 & 0.48 & 0.45 & 0.49 & 0.59 & 0.52 & 0.58 \\ 0.45 & 0.40 & 0.59 & 0.43 & 0.47 & 0.67 & 0.68 & 0.72 & 0.70 & 0.39 & 0.47 & 0.48 & 0.52 & 0.47 & 0.47 & 0.40 & 0.54 & 0.47 \\ 0.46 & 0.42 & 0.49 & 0.55 & 0.49 & 0.52 & 0.47 & 0.47 & 0.43 & 0.71 & 0.71 & 0.75 & 0.73 & 0.67 & 0.39 & 0.43 & 0.51 & 0.50 \\ 0.45 & 0.40 & 0.40 & 0.42 & 0.46 & 0.54 & 0.40 & 0.53 & 0.50 & 0.50 & 0.47 & 0.53 & 0.45 & 0.43 & 0.65 & 0.72 & 0.74 & 0.71 \end{bmatrix}$$

We can get comprehensive strategy of the five events, the optimal situation of first event is the 5th countermeasure, the value is 0.77. The optimal situation of second event is 1st countermeasure, the value is 0.73. The optimal situation of 3th event is the 8th countermeasures, the value is 0.72. The optimal situation of 4th event is 12th countermeasures, the value is 0.75. The optimal situation of the 5th event is the 17th countermeasures, the value is 0.74. Seen from integrated effect measure, countermeasures optimize sequence of different events can refer to the countermeasures optimized sequence as Table 1 shown:

TABLE V. THE OPTIMIZATION DECISION RESULTS OF THE SUSTAINABLE FOREST MANAGEMENT PROJECT OF THE NATIONAL NATURE RESERVE OF JINGANGSHAN IN JIANGXI PROVINCE

Incidents ai	Sort Optimization of Countermeasure bj
Forest Resources Monitoring and Evaluation Layer a1	b5>b4>b3
Forest Resources Cultivating Layer a2	b1>b2
Forest Resources Utilizing Layer a3	b8>b9>b7>b6
Forest Managing Layer a4	b11>b12>b10> b 13
Forest Ecology and Resources Protecting Layer a5	b17>b16>b18>b15>b 14

The study applied gray situation decision method to analyze optimizing decisions in the sustainable forest management projects of the National Nature Reserve of Jingangshan in Jiangxi province. Through this research, we can confirm the optimize strategies in different measures, and also conform the sequence of various measures. The research results is conform to the economic, technical and effect situation of the sustainable forest management projects of the National Nature Reserve of Jingangshan in Jiangxi province, the application of gray situation decision method in decision and implement of the sustainable forest management projects of the National Nature Reserve of Jingangshan in Jiangxi province is a good technological dependence.

IV. CONCLUSIONS

From the term of systematic science, the article analyze the system structure of sustainable forest management project of Jingangshan National Nature Reserve, exploring the constitutive property of the level in the system, representing clearly the system structure of the National Nature Reserve Jingangshan, on this basis, applying the gray situation decision theory, regard the sustainable forest management project as situation countermeasure, set up multiple targets to do comprehensive measure, establish the gray situation decision model, get the optimized decision making case of the sustainable forest management program, and obviously it is more accurate and reliable than the result of single factor analysis. It is no doubt that the research methods will be a theoretical exploration of construction and management of the current sustainable forest management.

REFERENCES

[1] Keenan, R.J., Reams, G. A., Achard, F. "Dynamics of global forest area: Results from the FAO Global Forest

Resources Assessment 2015". *Forestry Economy and Management*, vol.352, pp.9-20, September 2015.
 [2] Xu Bin, Zhang Decheng, Huyan Jie, et al. "World Forestry Development Issues and Trends". *Forestry Economy*, vol. 35, pp.99-106, January 2013.
 [3] Howson, P., Kindon, S. "Analysing access to the local REDD plus benefits of Sungai Lamandau, Central Kalimantan, Indonesia". *Asia Pacific Viewpoint*, vol.56, pp.96-110, April 2015.
 [4] Agnoletti M., Santoro A. "Cultural values and sustainable forest management: the case of Europe". *Journal of Forestry Research*, vol. 20, pp. 438-444, October 2015.
 [5] Keenan J. "Climate change impacts and adaptation in forest management: a review". *Annals of Forestry Science*, vol. 72, pp.145-167, March 2015.
 [6] Chomba S., Treue T., Sinclair F. "The political economy of forest entitlements: can community based forest management reduce vulnerability at the forest margin?". *Forestry Policy and Economics*, vol.58, pp.37-46, September 2015.
 [7] Wei Xia Qing, Qin Guowei. "Forestry economic development is a vivid practice of eco-forestry and livelihood forestry - Take Anhui Province as an example". *Forestry Economy*, vol. 35, pp. 31-34, March 2013.
 [8] Shen Guofang. "Natural Forest Protection Project and the Sustainable Forest Management". *Forestry Economy*, vol. 31, pp. 15-16, November 2009.
 [9] Wang Zhu Xiong, Gao Junkai, Jiang Sannai. "Strengthen forest management and promote green growth". *Forestry Economy*, vol. 34, pp. 20-23, June 2012.
 [10] Zhou Shaozhou. "Thoughts on promoting the forest resources growth of China". *Chinese national conditions and strength*, vol.11, pp. 35-36, April 2014.
 [11] Zhou Dequn, Zhang ling. "Research of Classification of complex system-level of integration DEMATEL / ISM's". *Management Science Journal*, vol.45, pp. 20-26, February 2008.
 [12] Zhuangzhao Rong, Guo Dongqiang. "Evaluation model of Knowledge transfer factors of transforming enterprise based on ISM and ANP". *Information Science*, vol. 37, pp. 109-114, November 2013.
 [13] Yuan Lin, Jiang Yu jie, Yu Xiaozhong. "Analysis of the factors of the cooperation strategy of petroleum enterprises base on ISM and DEMATEL". *Petroleum Technology Forum*, vol. 35, pp.29-32 + 35 + 69, January 2012.
 [14] Yu Songqing, Linsheng. "The sustainable development research of electricity demand in Shandong Province based on improved ISM Method". *Henan Science*, vol. 41, pp. 1724, October 2013.
 [15] Lao Shishuai, Zhang Shu. "Two kinds of improved algorithm ISM's". *Applied Science and Technology*, vol. 39, pp. 26-29, November 2010.
 [16] Deng Julong. *Grey prediction and decision-making*. Wuhan: Huazhong University of Science Press, 1986, 168-171.
 [17] Liu Sifeng, Dang Yaogu, Fang Zhigeng, et al. *Grey system theory and its applications*. 6th ed., Beijing: Science Press, 2010, 143-148.
 [18] Wang Hui, Su Lining. "The achievement, problems and improvement of the performance evaluation in county government". *Chinese administration*, vol. 41, pp. 19-21, December 2006.

Financial Risk Modeling and Simulation based on Vector Auto Regressive Model

WU Yan*

School of Economics and Resource Management, Beijing Normal University, Beijing 100875, China.

*Corresponding Author Email:bnuwuyan@163.com

Abstract—This paper introduce threshold value rule into wavelet threshold estimating value, and apply wavelet transform modulus to check out the possible change points (thus eliminate the noise’s influence on valuation of income rate density function), then divide the wavelet coefficient into several subblock according to these change points to get the calculation formula of threshold value of density function: VaR multi-scale estimation mode proposed basing on this quantile definition to transfer VaR’s calculation accuracy into convergence analysis of estimation error of wavelet threshold estimating value so as to infer indirectly that the convergence rate of VaR multi-scale estimation mode’s estimation error correlate with income rate density function’s smoothness and sample capacity. Finally this paper supports this robust result with simulation examples and empirical analysis.

Index Terms—financial risk, simulation, vector auto regressive model

I. INTRODUCTION

As VaR plays an essential role in financial risk management, it is crucial to improve VaR’s calculation accuracy. VaR estimation methods includes parametric method, semi-parametric method and nonparametric method, etc [1].As for improving VaR’s calculation accuracy, This paper assumes that how to improve VaR’s calculation accuracy lies on finding out or constructing a probability model which can quantify the assents income distribution precisely as well as how to deduce the model’s parameter by statistical method [2]. As sample’s nonstationarity endows the related probability density function with local characteristics like being aiguille and fat-tail, some relatively smooth distribution function may be unable to satisfy the requirement of VaR’s calculation accuracy [3]. It is very likely to underestimate or overestimate the market’s risk like that, which will go against high-quality management on market risk and investment decision [4]. Thus This paper explores the influences of assets income rate distribution density function’s partial characteristics and its related influencing factors on VaR’s calculation accuracy from probability density function’s space perspective [5].

II. METHODS

This paper introduce threshold value rule into wavelet

threshold estimating value, and apply wavelet transform modulus to check out the possible change points (thus eliminate the noise’s influence on valuation of income rate density function), then divide the wavelet coefficient into several subblock according to these change points to get the calculation formula of threshold value of density

function: VaR multi-scale estimation mode proposed basing on this quantile definition to transfer VaR’s calculation accuracy into convergence analysis of estimation error of wavelet threshold estimating value so as to infer indirectly that the convergence rate of VaR multi-scale estimation mode’s estimation error correlate with income rate density function’s smoothness and sample capacity[6]. Finally This paper support this analysis result with simulation examples and empirical analysis[7].

Multi-scale algorithms in wavelet analysis provide visual, embedded hierarchic thought for space decomposition of density function [8-11]. If the scale function and wavelet function of $L^2(\mathbb{R})$ orthogonal multi-scale decomposition is respective, any wavelet of density function $p(x)$ for proper original scale J_0 can be displayed in this way:

$$p(x) = \sum_{k \in I_j} a_{J_0,k}(x) + \sum_{j \geq J_0} \sum_{k \in I_j} d_{j,k}(x), \quad (1)$$

Where

$$\begin{aligned} (a_{J_0,k} = \int_{-\infty}^{\infty} \phi_{J_0,k}(x) p(x) dx, d_{j,k} = \int_{-\infty}^{\infty} \psi_{j,k}(x) p(x) dx, \phi_{j,k}(x) = 2^{j/2} \phi(2^j x - k), \\ \psi_{j,k}(x) = 2^{j/2} \psi(2^j x - k), I_j = \{1, 2, \dots, 2^{j-1}\}, j \geq J_0. \end{aligned}$$

Assume that $\{x_n\}_{n=1}^T$ is extracted from $p(x)$, then the factor’s sample estimation is

$$\hat{a}_{J,k} = \frac{1}{T} \sum_{n=1}^T \phi_{J_0,k}(x_n), \hat{d}_{j,k} = \frac{1}{T} \sum_{n=1}^T \psi_{j,k}(x_n). \quad (2)$$

Theorem 1: Sample estimation which is obtained by this should be:

$$\hat{p}(x) = \sum_{k \in I_{J_0}} \hat{a}_{J_0,k}(x) + \sum_{j \geq J_0} \sum_{k \in I_j} \hat{d}_{j,k} \psi_{j,k}(x) \quad (3)$$

For limited samples, in formula <3> $J_0 \leq j \leq J_{\max}$ ($J_0 = 0, J_{\max} = 2\sqrt{\log(T)}$), J_{\max} is the maximum resolving scale. If conduct wavelet linear estimation by scale truncation method, two problems will arise when calculating factor according to formula <2>:

(1) How to select truncation scale j to make $\hat{p}(x)$ can reflect $p(x)$ overall trend characteristics and partial detailed characteristics; (2) How to select threshold value to process $\hat{d}_{j,k}$ to weaken sample’s abnormal new information’s innovation influence on wavelet factor. Donoho and other researchers [12] held that linear threshold value rule and nonlinear threshold value rule are applicable to modification of factor $\hat{a}_{J_0,k}$ and factor

$\hat{d}_{j,k}$. L rule $\tilde{a}_{j_0,k} = \hat{a}_{j_0,k}$ and $\tilde{d}_{j,k} = 0$ retains density function's trend but ignore the details, therefore rigid threshold value (H) and soft threshold value (S) in N rule are applied to modify wavelet factor.

$$\tilde{d}_{j,k}^{(GS)} = \left(\left| \hat{d}_{j,k} \right| - \sigma_T \right) \text{sgn} \left(\hat{d}_{j,k} \right), \tilde{d}_{j,k}^{(GH)} = \hat{d}_{j,k} I \left(\left| \hat{d}_{j,k} \right| \geq \sigma_T \right). \quad (4)$$

Here nonlinear threshold factor σ_T processes the wavelet factor at the same scale with the same criterion. For unstable sample, this may distort the original sample's complex characteristic. Here, we adopt method of wavelet model maximum value [13] combining with changing-point distinguishing technology to any possible changing points at any scale and then take advantage of partial block self-adaptive threshold value rule to obtain the four kinds of calculation formulas for the estimated threshold value of probability density [14-16]. In concrete speaking, it is divided into three steps:

The changing points in formula <4> divide wavelet with scale of "j" into L pieces of blocks; correspondently, the wavelet's variance is

$$\sigma_{j,l}^2 = \frac{1}{l} \sum_{k=L_{l-1}+1}^{L_l} \left(d_{j,k} \right)^2, \left\{ d_{j,k} \right\}_{k=0}^{2^j-1} = \bigcup_{l=1}^L B_{j,l}.$$

(2) The parameter of block threshold value is $\sigma_{j,l}^2$ the wavelet threshold value should be adjusted to:

$$\tilde{d}_{j,k}^{(BH)} = \hat{d}_{j,k} I \left(\sum_{k \in B_{j,k}} \hat{d}_{j,k}^2 > \sigma_{j,l}^2 \right), \tilde{d}_{j,k}^{(BS)} = \left(\left| \hat{d}_{j,k} \right| - \sigma_{j,l} \right) \text{sgn} \left(\hat{d}_{j,k} \right). \quad (5)$$

The wavelet's estimated threshold value of density function p(x) should be

$$\tilde{p}(x) = \sum_{k \in J_0} \tilde{a}_{j_0,k} \phi_{j_0,k}(x) + \sum_{j=J_0}^{J_{\max}} \sum_{k \in I} \mu_{j,k}^{(N)} \psi_{j,k}(x). \quad (6)$$

Here $\mu_{j,k}^{(N)} = \tilde{d}_{j,k}^{(N)}$ ($N \in \{GS, GH, BS, BH\}$) denote respectively the wavelet factor of overall soft threshold rule, overall rigid threshold rule, partial soft threshold rule and partial rigid threshold rule.

So, in high-frequency financial data analysis, N rule can characterize the partial features of income rate density. Thus, this article will focus on three questions while using <6> formula to estimate assets market risk: 1) proposing VaR multi-scale estimation mode; 2) analyzing the four threshold rules' respective influence on VaR estimation error and convergence 3) prove the analysis conclusion above with simulation tests.

III. SIMULATION EXAMPLE

This section analyses $\tilde{VaR}(\mathcal{G})$ convergence rate of estimation accuracy in different sample size, then verify the result of theorem 1.

A. The Generation of Simulation Samples

Normal distribution $p_{\mu,\sigma}(x) = \frac{1}{\sqrt{2\pi}\sigma} \exp \left\{ -\frac{(x-\mu)^2}{2\sigma^2} \right\}$,

frequently used in financial econometrics, shows a proper regularity and smoothness. Let mean $\mu=0$, variance $\sigma=1$, then get a standard normal density p(x). As p(x) is often used to describe residual distribution of the SV model [17], we make simulation analysis for p(x).

Fourier transform of p(x) is $p(\omega) = \exp \left\{ -\omega^2 / 2 \right\}$. The parameters in theorem 1 are $y=0, \alpha=0, v=1$ and $\rho=1$. We use random number generator of statistics toolbox inside the software MATLAB2010a, then get three samples that means are equal to 0 and variances are 1. Here, the separate capacities are $T=500, 1000, 2000$. This section uses Meyer function [18] to make the simulation analysis, that shows sample histogram and Meyer function.

B. Estimation Algorithm of VaR

Following the previous analysis idea, this section takes the corresponding quantiles of density p(x) of normal fitting as exact values of VaR. Then apply samples with various capacities and four threshold rules to threshold wavelet estimation of density p(x) and multiscale estimation of VaR. Please see detailed six steps below:

Step 1: Follow formula <2> to calculate wavelet coefficient and scale coefficient. Here $J_{\max} = 2 \log_2 T$;

Step 2: Get the sample estimator $p(x_n)$ of accurate density from formula <3>;

Step 3: Separately follow formula <4> and <5> to make revision for the coefficient calculated from step one;

Step 4: Follow formula <6> to calculate wavelet threshold estimator $\tilde{p}(x)$;

Step 5: Follow formula <6> to calculate sample estimator of mean square error

$$MSE(\tilde{p}) = \frac{1}{T} \sum_{n=1}^T \left(\tilde{p}(x_n) - p(x_n) \right)^2;$$

Step 6: Calculate $\tilde{VaR}(\mathcal{G})$ and its relative deviation.

$$eVaR(\mathcal{G}) = 100 \times (\tilde{VaR}(\mathcal{G}) - VaR(\mathcal{G})) / VaR(\mathcal{G}), \mathcal{G} = 0.9, 0.95, 0.99$$

C. Estimator Result Analysis

This section programmed by WavLab8.5 toolbox, implement estimator algorithm step 1-5 to calculate threshold wavelet estimator of sample density: implement algorithm step 5-6 to calculate estimator accuracy and multiscale estimator of VaR and its relative deviation with various confidence level. See that and formula <2> for results separately.

1. Density estimator $\tilde{p}(x)$ is closer to actual density p(x) with the increasing sample capacity, which indicates a better estimation effect of these four nonlinear threshold methods.

2. The preferential order of $\tilde{p}(x)$ is $BS \gg GH \gg BH \gg$

GS , the left tail estimation order of $\tilde{p}(x)$ is $BS \gg GH \gg BH \gg GS$, the right tail estimation order of $\tilde{p}(x)$ is $BS \gg GH \gg BH \gg GS$, so there is some certain differences of these four threshold rules for quantification of density's local features. In formula <1>, variation trend of $MSE(\tilde{p})$ proves that the optimal estimator of density is $\tilde{p}(x)$ which is based on the BS rule.

On the whole: (1) We can see from the simulation analysis above that density estimator $\tilde{p}(x)$ which is based on BS rules would be better for the improvement of $VaR(\mathcal{G})$'s calculating accuracy. Under various

confidence level, $VaR(\vartheta)$ increases with sample capacity T, the estimation error of $VaR(\vartheta)$ is smaller and its convergence rate accelerates, which proves the accuracy of model <7> in the theorem. (2) For financial institutions, accurate estimation of VaR would help make more reasonable use of funds. Underestimated VaR will bring huge risk for financial institutions, while overestimated one will be unable to make full use of funds. Therefore, none of financial institutions are willing to accept an overestimated or underestimated VaR value, and because of that, multiscale estimator model of VaR has an application potential in risk management.

IV. PARAMETER ESTIMATION AND CORRECTION

To remove the effect which innovation makes to affect asymmetry feature of return-dispersion shock of four great stock indexes to distribution density's local feature in the greater China region, according to the test result of formula <3> and positivistic experience of available literatures, we start the GJR-GARCH(1,1)-N model for return series at first. Then estimate a wavelet estimator of information sequence density, and next adjust parameter of normal density through minimizing MSE. Lastly, calculate VaR values separately. See steps as follows:

Step 1: Fitting GJR-GARCH(1,1)-N Parameters

$$\begin{cases} r_t = c_0 + \varepsilon_t, \\ \varepsilon_t = \sigma_t z_t, z_t \sim ii.N(0,1), \\ \sigma_t^2 = \omega + \alpha_1 \sigma_{t-1}^2 + \beta_1 \varepsilon_{t-1}^2 + \gamma_1 s_{t-1} \varepsilon_{t-1}^2; \end{cases}$$

Step 2: Follow formula(6) to calculate the wavelet threshold estimator $\tilde{p}(z)$ for the density function of Z1.

Step 3: Benchmarked against $\tilde{p}(z)$, make parameter correction of $p(z)=N(0,1)$ standard normal density set ahead of time through optimal method, which is $(\hat{\mu}, \hat{\sigma}) = \arg_{(\mu, \sigma) \in R^2} \min MSE(p, \mu, \sigma)$.

Here,
$$MSE(p, \mu, \sigma) = \frac{1}{T} \sum_{t=1}^T (p(z_t) - \tilde{p}(z_t))^2,$$

$$p(z_t) = \frac{1}{\sqrt{2\pi}\sigma} \exp\left\{-\frac{(z_t - \mu)^2}{2\sigma^2}\right\}$$
 are normal density;

Step 4 Calculate $\tilde{VaR}(\vartheta), \vartheta = 0.9, 0.95, 0.99$ through multiscale model.

Programming through WavLab8.5 toolbox again, we can see the calculation results above from formula <4> and <3>. It's found out that positivistic results of density estimator $\tilde{g}(z)$ are the best based on BS rules.

V. CONCLUSION

This paper through research indicates that block threshold rule fully shows the local number about distribution density function of single scale return rate from multiscale perspective. Therefore, this paper improves the estimation method about distribution density of return rate and multiscale model based on that is an improvement for VaR estimation method. Investors can start multiscale estimation analysis for the risk from

asset market, choose minimum-risk assets according to risk preference, and then implement high-quality investment decision as well as risk management.

REFERENCES

- [1] Cuske C, Dickopp T, Seedorf S. J Onto Risk: An Ontology-based Platform for Knowledge-based Simulation Modeling in Financial Risk Management[J]. Social Science Electronic Publishing, 2005.
- [2] Zhou H, Zhang F. Calculation of Short-term Financial Risk in Electricity Market by VAR Historical Simulation Method [J]. Automation of Electric Power Systems, 2004, 28(3):14-18.
- [3] Squicciarini A, Rajasekaran S D, Mont M C. Using Modeling and Simulation to Evaluate Enterprises' Risk Exposure to Social Networks[M] IEEE, 2011:1-1.
- [4] Barsade J, Conlon J A, Gutierrez T, et al. Financial risk cover analysis, modeling control and monitoring system: US, US8224734[P]. 2012.
- [5] Duffey E A D M. Optimal Capital Structure and Financial Risk of Project Finance Investments: A Simulation Optimization Model With Chance Constraints[J]. Engineering Economist, 2013, 58(1):19-34.
- [6] Janabi M.A. Incorporating Asset Liquidity Effects in Risk-Capital Modeling[J]. Review of Middle East Economics & Finance, 2010, 6(1):3-3.
- [7] Danielsson J, Morimoto Y. Forecasting Extreme Financial Risk: A Critical Analysis of Practical Methods for the Japanese Market[J]. Monetary & Economic Studies, 2000, 18(2):25-48
- [8] Qin Z, Cheng L, Du J, et al. The Correlation Study Based on VAR Model between Major Financial Risk Indicators and Economic Growth[M] Advances in Information Technology and Education. Springer Berlin Heidelberg, 2011:45-54.
- [9] O'Brien J M, Szerszen P. An Evaluation of Bank VaR Measures for Market Risk During and Before the Financial Crisis[J]. Social Science Electronic Publishing, 2014.
- [10] Jasemi M, Kimiagari A M, Memariani A. Development of A More Applied Version of Coherency Called' Sensible Coherency' for Assessment of Financial Risk Measures:[J]. South African Journal of Industrial Engineering, 2010, 21(1).
- [11] Yang Q, Xue Y N, Ke J. Quantitative Models Remediating VaR to Measure Extreme Financial Risk[J]. Journal of Fudan University, 2009, 48(6):783-774.
- [12] Shu T, Murata H, Tanaka S, et al. Monte Carlo Grid for Financial Risk Management[J]. Future Generation Computer Systems, 2005, 21(5):811 - 821.
- [13] Koutmos G. Financial Risk Management: Dynamic Versus Static Hedging[J]. Global Business & Economics Review, 1999, 1(1):60-75.
- [14] Liu H W, Sun W T, Science S O, et al. Application and Model of the VaR Method in Financial Risk Management of China[J]. Journal of Lanzhou University of Arts & Science, 2014.
- [15] Zhou S, Shi B, Wen Z. Analysis of mean-VaR model for financial risk control[J]. Systems Engineering Procedia, 2012, 4:40 - 45.
- [16] Tian H X, Zhang X D, Liu Q, et al. Review of VaR Way Used in Management of Financial Risk[J]. Journal of Social Science of Jiamusi University, 2008.
- [17] Bhattacharyya M. Contemporary Financial Risk Management: The Role of Value at Risk (VaR) Models[J]. IIMB Management Review (Indian Institute of Management Bangalore), 2008.
- [18] Xue H G, Xu C X, Li S P, et al. VaR Method and Its Empirical Research in Financial Risk Management.[J]. Gongcheng Shuxue Xuebao, 2004, (6):941-946,924.

Modeling and Simulation of earnings management of listing Corporation based on Chinese data

Yiru Yang¹, Hong Liu²

¹School of Accounting, Economics and Finance, University of Wollongong, Wollongong, 2500, Australia

²Computer and Information Engineering College, Hohai University, Nanjing ,210098, China;

Abstract—During the practical earnings management, due to the information asymmetry, institutional investors often fail to obtain the correct information. In this way, the earnings obtained are expressed as the interval information. The interval probability is introduced to earnings management in this paper. The earnings function and the payoff matrix of the dynamic game between the two earnings management sides under the uncertain information are built. PSO is adopted to solve the Nash equilibrium solution of the dynamic game under the uncertain information. The optimal strategy that both sides might choose is adopted so as to maximize the managers in the listed company and the institutional managers.

Index Terms—Chinese Data, Listing Corporation, Earnings Management, Simulation

I. INTRODUCTION

Emerging as a frontier research topic in the accounting field since the 1980s, earnings management has still been a critical field of modern accounting theoretic research, and an important index to measure operation performance of enterprises [1]. Investors, managers, creditors and government departments have paid great attention to it. Enterprises' earnings represent the earnings of investors, and are basis of various securities in the capital market, which could influence the compensation level of managers [2]. Government's taxation is also connected with enterprises' earnings [3]. Due to the important role of accounting earnings, enterprises try every means to manipulate their earnings, thus leading to the popularity of earnings management among listed enterprises. In January 2013, Research Institute of the Commerce Ministry issued Financial Safety Analysis Report of Non-Financial Chinese Listed Enterprises in 2012, which showed that 823 out of 1698 listed enterprise samples or 48.79% of the total whitewashed their financial statements to different degrees up to the third quarter of 2012 [4]. Research suggested that, due to the pressure of stock price, supervision and delisting, the greater financial risks enterprises are faced with, the stronger their motive and willing to whitewash the financial statements and the higher the probability of whitewashing the financial statements [5]. All in all, the financial safety status of non-financial listed enterprises declined sharply.

①

Earnings management is different from financial frauds. However, excessive earnings management might result in financial frauds [6]. However, the boundary between the two is hard to define both theoretically and practically. Most financial scandals exploding worldwide in the early 21st century were a result of excessive earnings management. Levitt (2001), former president of

SEC (the U.S. Securities and Exchange Commission), pointed out in his speech entitled Digital Game that accounting rules are abused [7]; managers adopt various "creative accounting methods" to glorify the financial statements; enterprises' earnings reflect wishes of the administrative level instead of the practical operation performance of enterprises; earnings management is wandering in the grey zone between legality and illegality, thus seriously jeopardizing the quality of financial statements, dealing a heavy blow to the confidence of investors and seriously influencing the efficiency of resource allocation. Considering the serious economic results of earnings management, earnings management of listed companies has been an issue of great concern to the academic circles, practitioners and supervision departments.

To study earnings management under an uncertain environment is an emerging research topic. First, earnings functions of the dynamic game and the payoff matrix between two earnings management sides against the backdrop of uncertain information are built respectively. The extended dynamic game is transferred into the dynamic strategy-based game. The probability formula of interval numbers is employed to compare the payment value of managers and in listed enterprises and institutional investors in the form of interval numbers so as to obtain the complementary probability matrix. Second, PSO (Particle Swarm Optimization) is adopted to work out the Nash equilibrium solution of the dynamic game under the situation of uncertain information. At last, the optimal decision-making strategy for earnings management under the asymmetric information environment is worked out.

II. DYNAMIC GAME MODEL OF EARNINGS MANAGEMENT BASED ON THE UNCERTAIN INFORMATION

Dynamic game strategy set of earnings management. During the earnings management process, institutional investors and managers of listed enterprises are regarded as two players. The dynamic game counteraction during the interval of k is adopted. (See Fig. 1)

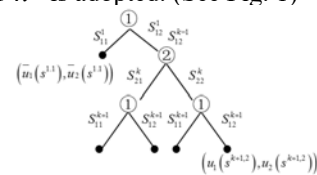


Fig. 1 Extended dynamic game of two earnings management sides during the interval of k

The extended dynamic game model under the

situation of uncertain information can be expressed as $\bar{G} = \{N, S, \bar{U}\}$, where $N = \{1, 2\}$ and N stands for two participants in the game with 1 representing the institutional investor and 2 as the manager of listed enterprises. First, the institutional investor might make the choice of whether to supervise or not and then the manager of listed enterprises is in a position to decide whether to conduct earnings management.^{23]}

$S = \{s_{1i}^k, s_{2j}^k\}$ stands for the action strategy set of two sides in the game; s_{1i}^k stands for the i action strategy of the institutional investor during the interval of k ; s_{2j}^k stands for the j action strategy of the manager of listed enterprises; $\bar{U} = \{\bar{u}_1(s^{k,j}), \bar{u}_2(s^{k,j})\}$ stands for the earnings interval corresponding to every action group which might be chosen by the institutional investor and the manager of listed enterprises.

In Fig. 1, the action circumstances during the k interval of the game can be expressed by an information set. Therefore, the action strategies of the institutional investor and the manager of listed enterprises are in fact the action rules of two sides in every general collection. H_i can express the information set, I_j , of the institutional investor, namely $H_i = \{I_j\}$. $A_i(I_j)$ can express the action set in the information set, I_j , of the institutional investor. Therefore, the pure strategy set of the institutional investor can be expressed by the

Cartesian product, $S_i \prod_{I_j \in H_i} A_i(I_j)$, on the action set of every general information set. Similarly, the manager of listed companies can also be expressed in this way.

III. SIMULATION EXPERIMENT

In this paper, a listed company is taken as an example. The due compensation of managers of the company in 2012 was $e \in [2, 5]$ million; the remaining earnings of institutional investors were $v = 20$ million; the excess earnings of managers were $s \in [6, 80]$ million; the probability of earnings management actions to be revealed was $p = 0.4$; the fines for managers after their management behaviors were revealed were $F \in [10, 60]$ million; the supervision cost was $c = 0.1$ million; the shareholding percentage of institutional investors was $\beta = 20\%$. Then, the earnings management counteraction strategy set between institutional investors and managers in listed companies during the three stages were shown in Table 1.

From Table 1, it can be seen that the zero-sum payoff matrix showing the counteraction between institutional investors and managers of the listed company is a 2*2 dimensional one. The attack-defense confrontation during three stages forms a 8*8 dimensional matrix. According to the operation rules of the interval numbers, the payoff matrix of the earnings management confrontation 8*8 dimensional strategy game between two sides during three stages can be worked out:

	$(S_{21} S_{21} S_{21})$	$(S_{21} S_{22} S_{21})$	$(S_{21} S_{21} S_{22})$	$(S_{21} S_{22} S_{22})$	$(S_{22} S_{21} S_{21})$	$(S_{22} S_{21} S_{22})$	$(S_{22} S_{22} S_{21})$	$(S_{22} S_{22} S_{22})$
$\bar{A} =$	$(S_{11} S_{11} S_{11})$	$(S_{11} S_{11} S_{12})$	$(S_{11} S_{12} S_{11})$	$(S_{11} S_{12} S_{12})$	$(S_{12} S_{11} S_{11})$	$(S_{12} S_{11} S_{12})$	$(S_{12} S_{12} S_{11})$	$(S_{12} S_{12} S_{12})$
	$[-459.3, 113.7]$	$[-463.2, 89.8]$	$[-463.2, 89.9]$	$[-347.231.9]$	$[-463.5, 89.5]$	$[-346.231.7]$	$[-346.231.8]$	$[-471.42]$
	$[-383.2, 95.5]$	$[-387.2, 71.8]$	$[-387.5, 71.6]$	$[-271.213.2]$	$[-387.7, 71.6]$	$[-275.213.5]$	$[-271.6, 13.7]$	$[-397.25]$
	$[-383.3, 95.7]$	$[-387.3, 71.9]$	$[-387.6, 71.6]$	$[-272.213.8]$	$[-387.5, 71.5]$	$[-277.213.4]$	$[-271.5, 213.8]$	$[-396.22]$
	$[-307.2, 77.6]$	$[-311.3, 53.7]$	$[-311.6, 53.9]$	$[-196.195.8]$	$[-311.53.5]$	$[-195.195.9]$	$[-199.195.4]$	$[-314.6.2]$
	$[-383.4, 95.6]$	$[-387.2, 71.8]$	$[-387.4, 71.7]$	$[-271.213.9]$	$[-387.5, 71.4]$	$[-271.6, 13.5]$	$[-271.8, 213.2]$	$[-395.24]$
	$[-307.4, 77.4]$	$[-311.4, 53.6]$	$[-311.1, 53.5]$	$[-195.195.9]$	$[-311.5, 53.3]$	$[-194.195.4]$	$[-192.195.6]$	$[-315.6.8]$
	$[-307.3, 77.7]$	$[-311.2, 53.8]$	$[-311.8, 53.2]$	$[-197.195.6]$	$[-311.7, 53.1]$	$[-198.195.7]$	$[-197.195.9]$	$[-319.6]$
	$[-171.3, -0.3]$	$[-235.2, 35.8]$	$[-235.3, 35.6]$	$[-119, 177.9]$	$[-235.35.7]$	$[-117, 177.6]$	$[-120, 177.2]$	$[-243, -12]$

Table 1 Earnings counteraction strategy set of two sides during three stages

Stage	Strategies of managers in listed companies	Strategies of institutional investors
1	Managers of the listed company conduct earnings management	With the supervision of institutional investors
	Managers of the listed company conduct no earnings management.	Without the supervision of institutional investors
2	The game strategies of both sides in Stage 2 is similar to those in Stage 1	
3	The game strategies of both sides in Stage 3 is similar to those in Stage 1	

The element in every row of the game payoff matrix is used to express the strategies of managers in the listed companies. Among them, $(S|S|S)$ can express the strategies adopted by managers of the listed company for earnings management in Stage 1. In Stage 2 and Stage 3, the same earnings management strategies are adopted. The element of every row stands for the strategy of

institutional investors. Among them, $(S|S|S)$ stands for the supervision strategy that institutional managers adopt during Stage 1. During Stage 2, no supervision strategies are adopted; while, supervision strategies are adopted during Stage 3.

The fitness value of the earnings management game between the two sides under the situation of uncertain information can be obtained through PSO:

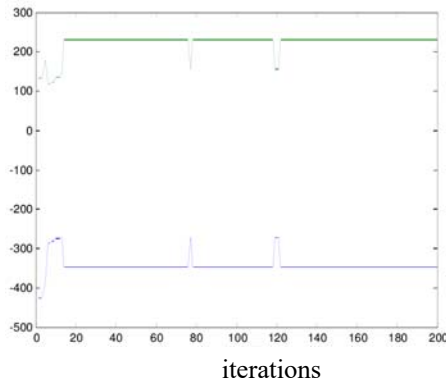


Fig. 2 Fitness variation curve for institutional investors

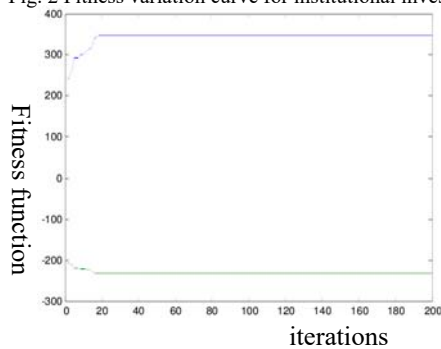


Fig. 3 Fitness variation curve for managers in the listed company

Based on the simulation experiment, the Nash equilibrium solution of institutional investors during the three stages can be obtained, $x^* = (0, 0, 0, 0, 0.68, 0, 0.29, 0.029, 0)$; the payoff value is $v = -346.626$. In other words, the probability for institutional investors to adopt the fifth, seventh and eighth strategy is 0.68, 0.29 and 0.029, respectively. In terms of the fifth strategy, institutional investors adopt non-supervision strategies in Stage 1, but adopt supervision strategies in Stage 2 and Stage 3. In terms of the seventh strategy, institutional investors adopt non-supervision strategies in Stage 1 and Stage 2, but adopt supervision strategies in Stage 3. In terms of the eighth strategy, institutional investors adopt non-supervision strategies during three stages.

The Nash equilibrium solution of managers in the listed company during three stages is $y^* = (1, 0, 0, 0, 0, 0, 0, 0, 0)$; the payoff value is $v = 347$. In other words the probability for the listed company to choose the first strategy is 1, which means that the listed company adopts the earnings management strategy during three stages. It shows the absoluteness of earnings management behaviors of managers in the listed company. Under the circumstance, institutional investors should enhance the restriction of their behaviors so as to prevent their benefits from being infringed.

The Nash equilibrium solution of the two sides

during three stages is defined as that institutional investor and managers of the listed company choose strategies at the probability of x^* and y^* . The equilibrium between the two is an optimal choice for the two. If any party destroys the balanced state, earnings of the side might be reduced.

IV.CHAPTER SUMMARY

This paper studies the issue of dynamic game of earnings management under the uncertain environment. During the practical earnings management, due to the information asymmetry, institutional investors often fail to obtain the correct information. In this way, the earnings obtained are expressed as the interval information. The interval probability is introduced to earnings management in this paper. The earnings function and the payoff matrix of the dynamic game between the two earnings management sides under the uncertain information are built. PSO is adopted to solve the Nash equilibrium solution of the dynamic game under the uncertain information. The optimal strategy that both sides might choose is adopted so as to maximize the managers in the listed company and the institutional managers.

REFERENCES

- [1] Stubben S R. Discretionary Revenues as a Measure of Earnings Management[J]. Accounting Review, 2009, 85(2):695-717.
- [2] Chia-Ling Chao, Richard L. Kelsey, Shwu-Min Horng, et al. EVIDENCE OF EARNINGS MANAGEMENT FROM THE MEASUREMENT OF THE DEFERRED TAX ALLOWANCE ACCOUNT[J]. Engineering Economist A Journal Devoted to the Problems of Capital Investment, 2010, volume 49(1):63-93.
- [3] Wu H, Wang X, Chen X, et al. On Earnings Management Strategy Based on Fuzzy Game[J]. Reformation & Strategy, 2014.
- [4] Tsai B. Earnings Management before Rights Issues and the Subsequent Cash Transfer in Chinese Firms[C]// COMPUTATIONAL METHODS IN SCIENCE AND ENGINEERING: Advances in Computational Science: Lectures presented at the International Conference on Computational Methods in Sciences and Engineering 2008 (ICCMSE 2008)AIP Publishing, 2009:489-492.
- [5] Shivakumar L. Estimating Abnormal Accruals for Detection of Earnings Management[J]. Social Science Electronic Publishing, 1996.
- [6] Mashoka T Z. Earnings management and loss reversal[J]. Brunel University, 2010.
- [7] Yim A, Yim A. Earnings Distribution Discontinuity from a Continuous Model of Earnings Management[J]. Ssrn Electronic Journal, 2012.

Research on Vocational Skill Training of Newly Established Local Universities

Jiafan TAN, Zhou YUE and Li TAN
Hunan University of Humanities, Science and Technology, Loudi, China

Xiao YUAN ^{Corresponding author}
Wuhan Military Representation Bureau of GAD, Yueyang, China

Abstract—Confronting the situation of national economy transformation and industrial structure adjustment, newly established local undergraduate colleges ought to adapt the needing of applied talents, and try out effective exploring on talent training mode. This paper studies the professional skill training of newly established local undergraduate colleges, and proposes an idea of emphasizing professional skills while paying attention to basic college education, some topics including the necessity of professional skill training, the research status, and the methods of training are thoroughly discussed.

Index Terms—Local Undergraduate Colleges, Vocational Skills, Professional skills, Training, Teaching

I. INTRODUCTION

Under a background of economic globalization and popularization of higher education, confronting the situation of national economy transformation and industrial structure adjustment, newly established local undergraduate colleges ought to meet the needs of market, and try out new ways on cultivating applied talents positively. In our practicing of teaching, an idea of *emphasizing professional skills while paying attention to basic college education* was proposed, the students' capability of engineering practicing and professional skills are enhanced with our effective research.

II. NECESSITY OF PROFESSIONAL SKILL TRAINING

A. The guiding of national higher education developing macro policy

In 1994, the requirement of *emphasizing both diploma and vocational qualification certificate* was firstly carried out according to Doc No. GF[1994]39 (Implementation advices on *Outlines of China Education Reforming and Developing* by The State Council). In 2010, vocational and technical education was stressed in another pamphlet *Outlines of Mid-term/Long-term National Education Reform and Development Plan*. In 2014, Doc No. GF[2014]19 *Decisions on Speeding up the Development of Modern Vocational Education* (Decisions for short) was released for fully deployment of speeding up modern vocational education development. According to the *Decisions*, the importance of vocational education should be fixed in the national talent cultivating system, with serving the purpose of national developing and prompting obtaining employments, our education should adapt the

improvement of technique and reformation of production mode, meet the needs of social public services, training billions of high quality workers and technical skilled talents. We should speed up the construction of modern vocational education system, co-ordinate the development of vocational education at all levels, guide a group of undergraduate colleges changing into the application style, strengthen the communication between vocational education and general education, develop further education positively, set up the rising channel from vocational school to graduate school, build *Interchange Bridges* for students to choose from variety options. We should improve the quality of students training; deepen the integration of production and education, the cooperation between school and enterprise, the combination of working and learning. The major setting should accord the industry needing, the curriculum content should accord the professional standards, and the teaching process should accord the production process. The professional qualification certificate should play the same role as graduation certificate; the vocational education should be supported by lifelong learning. The quality of personnel training should be improved and the function of vocational education in technical skills accumulation should be strengthened.[1] Therefore, there comes the ground truth that local colleges have taken the responsibility of high-tech training, thus the corresponding role should they play eventually.

B. The objective needs of undergraduate colleges to refine characteristics and create brands

By the end of 2013, there were 650 local newly established undergraduate colleges and universities (including private), accounting for 55.6% of the country's ordinary undergraduate colleges and Universities.[2] Its training objective is to serve the local economy or the regional economic development of high level professional talents. Compared with the old university, local newly established undergraduate colleges and universities have the poorer quality of students. At the present stage of higher education popularization, their selectivity of the students is less, the conditions and history of the school itself does not have the advantage in the undergraduate education. If follow the method of traditional undergraduate education to develop a new colleges, in a long time, it will be difficult to form characteristics of the school, the social influence of the

school could not be changed as well. But local undergraduate colleges have advantages of cultivating professional talents, if take use of it, actively explore new ways to develop connotation of vocational undergraduate education and strengthen the cultivation of professional skills at the same time, in this way to optimize the knowledge structure of students, cultivate practical talents mastering high technology. It will improve the students' social adaptability and market competitiveness, reinforce the features of running, and build the brand of school.

C. Social needs forced New Local Colleges to implement Vocational skills training

In 2000 the number of college and university graduates was 1.07 million, which increased to 7.27 million in 2014, and will be 7.49 million in 2015. The increasing number of graduates is one reason for employment difficulty of university students. Structural contradiction is the other reason. Knowledge Structure of university graduates is incompatible with market demand, the level of knowledge and ability could not competent the market provided, especially in the era of knowledge economy, emerged a large number of new jobs, which require job applicants to have both theory knowledge and strong ability. Such a phenomenon occurs on the job market: on the one hand, "somebody is unemployed", employment pressure of university graduates is increasing, on the other hand, "some job no competent", particularly some gray-collar type of new jobs, in which the grey collar refers as talented person with higher level of knowledge and stronger ability to innovate and master skilled mental skill. China has become the world's manufacturing center, gray collar talent become a scarce resource in the continuous development of the manufacturing sector and the whole economy, this situation directly affects the absorption of the technical aspects of China's industrial modernization, the business of high-tech value-added products and even normal production. Gray collar talent becoming popular signifies that gray collar will become the mainstream of the employment of university graduates for a long time.[3] The contradiction proposed new requirements to New Local University about their talents location, demanding for high-tech skilled personnel need New Local University to think more. After calmly and objectively analyze the condition of students and self-Running, in order to achieve the best combination of undergraduate knowledge structure, solve skilled talent shortage, ease the employment pressure, new Local Colleges should focus on undergraduate education connotation and strengthen vocational skill training for students at the same time, strive to cultivate gray-collar talent.

III. ANALYSIS ON RESEARCH STATUS IN AND ABROAD

The system of vocational qualification certificate in China began at the 50th last century, while the system of workers' grade evaluation prevailed in the enterprises. With the uninterrupted developing in the past 10 years, we achieved the common idea that diploma and

vocational qualification certificate should be equally treated, and the operation-based education should be equally recognized as research-based education. In recent years, vocational skill training and authenticating evolves smoothly in many universities, the roll number increases day by day.[4] At the time when the first students enrolled by expansion polices graduated from school, most of them chose to enter a vocational school for the difficulties they've faced while finding a job. The profound significant of this phenomenon caught attention of society and colleges. Some school aggrandized the status of vocational education by augmenting relative courses into curriculum plan and making the certification a necessary condition of graduation, some even established special center for vocational skill training. Nevertheless, this topic remains controversial. There exists no common view on how to develop undergraduate education with vocational training elements, the effect of combining two kinds of education needs further discussing.

Out of China, the vocational education system matured for a long time, and possessed a firm status accordingly. Many UK colleges remain the traditional characteristic known as Sandwich, even after they upgraded as universities. In the theoretic domain of high-skill talent training in applied universities, a lot of new ideas and achievement well up. John Dugger from College of Technology Eastern Michigan University distilled the experience of Work-based learning; TAFE college of Australia developed a pattern of cooperation with the enterprises; Chris Chinien from UNESCO proposed the integration of human resource development and continuing Education; University of Bremen suggested Modernizing Apprenticeship etc.

IV. APPROACHES OF VOCATIONAL SKILL TRAINING

A. Reflecting the Vocational Requirement in Talent Cultivation Program

According to the cultivation plan, many newly established local colleges implement an elite oriented mode copied from so-called 985 and 211 universities. However, this mode doesn't suit well, for the students are often at a lower capability level, the duplicate education mode could not generate desired effect. When the students graduate from school, they'll be at a weaker position compared to those elites. After thorough investigation, we proposed a training mode of *emphasizing professional skills while paying attention to basic college education*. The training plan based on this mode reflexes actually vocational requirement, in order to improve the knowledge structure of students, and provide more choices when they graduate. Litter part of them could succeed in entering a graduate school to accept further education or acquire the RD jobs, most of them will devote themselves to applied position such as maintenance and marketing.

B. Increasing Skill Training as Supplement to Classroom Experiments

A certain amount of experiments are compulsory to satisfy under graduate requirement. At the same time, we devise more practicing content to strength the students' manipulation ability. As examples, in the *Circuit* course of auto major, students are told to design and install civil lighting circuit, learn to use measurement apparatus, and try to design a power distribution cabinet etc. In the *Motor and Drag* course, a training of three phase motor disassembly and fixing is required. In the *Electrical Control and PLC* course, lessons of control circuit installation and testing are added. In those teaching practicing, corresponding skill training are fulfilled, which lays the foundation for engineering application.

C. Applying Skill Enhancement Together and Organizing Certification Examination

After the practice training with the courses, the students need a procedure of concentrated practicing for strengthening, which integrate the knowledge they've accepted before. The courses often last for 4 to 6 weeks, in which period a higher level training will be provided, which means it will require more devotion from students. The students will try to pass certain examination hold by national facilities and get certification accordingly. The exams are official proof of the students' skill; at the same time can be a motivation for them to improved their applied abilities.

D. Encouraging Participating in Contests to Improve Operation Skills

Contests of each subject are excises of mental ability beyond textbooks, which can be considered as important carriers of cultivating the students' comprehensive competence and innovation spirit, and work well on encouraging the trends of studying, and motivating the cooperation and practicing abilities of students. Within the contests, students are told to fulfill certain productions, which include the process of manufacturing, testing, and instruction making. The systematic engineering of integration challenges students rigorously. For example, to participate in the NUEDC contest, one should handle electronic components, IC, executive components etc. crafty, which urges hard practicing potentially. Therefore, encouraging participating in contests is a good way to improve skills.

E. Reinforcing the Devotion of Lab/Training Center Construction

In the past, local under graduate schools were often lack of sites for practical skill training, or faced severe deficiencies in equipment and facilities. To achieve a reverse of this situation, the ideas out of date should be abandoned; the school should raise enough funds in a short time, and pay more attentions to skill training, construct lab or training center rapidly, eventually provide proper conditions for application talents training in time.

F. Bringing Up Teachers of Dual Type

The *Dual Type* of teacher became the key point and special trait of local undergraduate school. Nowadays, there exists an emergent need of high level dual type teachers. A practical resolution is training recruited teachers into dual type according to well framed schedule. Assigning them to factories or enterprises, organizing them together to implement training, sending them to classes for vocational skill, all these approaches can be effective. On the other hand, the colleges can introduce engineers as part-time teacher, to strengthen the cooperation between school and enterprises.

ACKNOWLEDGMENT

This work was supported in part by The Education Department Of Hunan Province, with a grant from XJT[2011]315-407#.

REFERENCES

- [1] Liu Guangming. "Reviews on China Education Events 2014". <http://blog.sciencenet.cn/blog-359436-856296.html>.
- [2] Li Jianping. "How Long Will the Pain of Newly Established Local Universities Reformation Last?" *China Youth Daily*. 2014, 3rd, July, pp. 3.
- [3] Tan Jiafan, Tian Hanping, Cao Feng, Zhang Yinhe. "Discussing and Analysis on the Specialized Skill Training of the Local Normal College Engineering Students". *Journal of Hunan Institute of Humanities, Science and Technology*, 2006, No.6, pp.
- [4] Zhang Jintong, Bi Xin, Cao Yuan. "University Student Vocational Skill Training Present Situation and Improvement Measure". *Value Engineering*. No.6, 2010, pp. 208.

Distal Tibiofibular Dislocation Fixation: A Meta-analysis on Syndesmotic Screw Versus Suture-button

Shadab Fasih Khan, Yu Deng, Shaobo Zhu*

Department of orthopaedic surgery, Zhongnan Hospital of Wuhan University, Wuhan, China, 430071

*Corresponding Author

Abstract—Syndesmosis is an important part of maintaining the structural stability of the ankle joint, in all ankle injuries syndesmosis injury accounts for 1-11%. Diagnostic errors and inappropriate treatment of their injuries will affect treatment outcome, lead to changes in the anatomical position of the ankle joint, may develop secondary to chronic ankle instability, which leads to long-term ankle pain and traumatic arthritis, and anterior ankle impingement syndrome and other complications. Finite element method is a very effective numerical tool that can be used to study irregular geometry and internal morphology having mechanical analysis of complex material structure, stress and strain. Finite element model can also be arbitrarily modified to simulate a variety of pathological conditions. Foot and ankle research carried out using the finite element method is a current research focus discipline sector, compared with traditional methods, which not only can more adequately reflect the shape of the various parts inside the ankle, stress, strain and displacement, etc., which is able to a variety of internal fixation devices and fixation methods were evaluated.

Index Terms—Syndesmosis, Suture-buttons system, Screws, Separated

I. INTRODUCTION

Syndesmosis, also known as the inferior tibiofibular joint, may vary with the movement of the ankle when the physiological state of a corresponding movement, is a micro-elastic joints. Clinically ankle fractures and other injuries and more with syndesmosis injury, due syndesmosis ankle injury can cause loss of stability if not treated or not treated properly, often under the influence of tibiofibular joint function, as well as will left ankle dysfunction, late can lead to serious complications. When the treatment of lower tibiofibular joint fractures especially associated with inferior tibiofibular joint separation, should be fully taken into account only to the repair of articular fractures around the ankle to heal it so that the joint is stable, and should maximize the recovery of ankle function, and concurrent disease is reduced to a minimum.

According to the length of time after inferior tibiofibular joint damage can be divided into: acute syndesmosis injury, injury time in 3 weeks; subacute syndesmosis injury, injury time is more than three weeks, but less than three months; obsolete That chronic injury syndesmosis injury, injury time over three months [18]. In acute syndesmosis injury, according to X-ray examination revealed the situation, it can be divided into three types, including: type I is simply no inferior tibiofibular ligament inferior tibiofibular joint separation: Type II is potentially inferior tibiofibular joint separation, conventional X-ray no abnormalities, but under stress of the X-ray is displayed tibiofibular joint separation; III type is obviously inferior tibiofibular joint separation, which can be found under the tibia in a conventional X-ray film Philippians joint separation [1].

Compared with the traditional mechanical methods, finite element method is a very effective numerical tool

that can be used to study the geometry of irregular shape and having an internal structure of complex objects, mechanical analysis of stress and strain. We can also change the loading, material properties and other methods of individual mechanics research, experiments can't provide normal physiological information to obtain the results of the experiment is difficult to obtain an objective entity, the more fully reflect the internal structure of the various parts of the form, stress, strain and displacement, etc., and to the various internal fixation devices and fixation methods evaluated.

II. MATERIALS AND METHODS

A. Meta-analysis Development

In recent years, with the rapid development of computer technology, medical imaging technology and virtual technology, finite element analysis, as a relatively new biomechanical research method, gradually applied to the foot and ankle biomechanics research. This study was based on CT scan data DICOM formats, the use of Mimics, Geo-magic Studio. UG software, ankle and surrounding bone structure three-dimensional reconstruction, the establishment of a virtual digital simulation model geometry structure looks clear, vivid, visual effect is good, you can Any combination of display for each part or in whole, stereoscopic. We can also observe the internal structural relationships through different aspects, and it is possible at any angle of rotation and scaling observation, and dynamic display. The model can be directly output to the appropriate file format conversion software finite element, finite element model for further biomechanical research [2].

When analyzed using the finite element method, the result gives a visual impression; the use of virtual reality technology can also transform any angle, you can select any target observation point; and can make use of interactive performance finite element method, a variety of real-time changes data to facilitate a variety of programs and the results were compared. Specific operation is determined by the level of organization Click to select the seed zone, and then click on the region growing command, the computer automatically selected seeds and other organizations distinguish. Because the bone marrow cavity and uneven cancellous bone often displayed as bones of the inner contour line in CT image data, so that the model generated three-dimensional reconstruction Mimic internal pores, is not conducive to the establishment of three-dimensional surface model. We need to use manual editing methods, at each level of CT scan images of the holes within the outline of each bone filling regional separation tibia, ribs, talus,

calcaneus, and navicular bone from soft tissue and noise points, Fig.1 show the 3-D model [3].



Fig. 1.The 3-D model

B. Finite Element Calculation

Import solid model above calculation module, application software boo-lean functions to remove part of the bone screw holes occupy, and then to various parts mesh, mesh is to make early preparations for all types of finite element analysis, meshing quality directly affects the result of the subsequent calculation. Theory of the grid division finer, higher accuracy analysis of the results, but consumes longer time. Principle is not to reduce the accuracy of the results is provided at a reasonable cost without the dual demands considerable resources meshing parameters. Grid size parameter can be set according to the needs of users in a certain range, but still can be freely changed after the establishment of complete solid model. In this study, cut syndesmotic, simulation syndesmosis ligament injury, meshing settings before processing the material properties of the solid model, boundary conditions and load, and finally guide the mesh model [4]. Fig.2 and Fig.3 show the surgery simulation and finite element model.

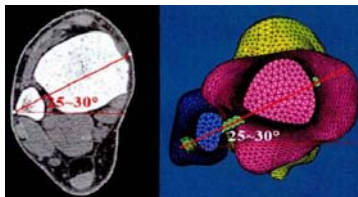


Fig. 2.The surgery simulation



Fig. 3.The finite element model

At the same time, boundary conditions of the calcaneus and navicular bone fixation, tibia, fibula center to the upper end of a cross-sectional front view of the reference plane X, Y fixed in both directions so that the model is stable, other bone can be active, and then loaded on the tibia and fibula sectional size of 600N, the direction of gravity pressure to simulate human standstill single foot stomp joint to withstand the force of the body weight when standing neutral position, contact is established between the joint surfaces. In an ideal use, close bond between the screw and the bone should be no slip between them, on both sides of the cell contact interface node translational and rotational freedom should be coupled with each other, using the sticky constraints [5].

Analysis of button suture system for ankle fracture tibiofibular syndesmosis separation merge the treatment and screw fixation of the results, and on the basis, we

have the clinical comparative analysis of the tibiofibular syndesmosis injury in the merger of ankle fracture treatment selected. Button suture system is the ideal surgical approach. For treating the separation of tibiofibular syndesmosis, its effect is comparable to the screw fixation.

C. The Application Analysis

Established within 12 kinds, including bone, ligament syndesmosis screws isolated single dimensional finite element model between models 7525378108 nodes number 2246123182 7 unit has between. Its various parts geometry from a different angle, the biomedical model and the CT reconstruction are satisfactory similarity; its shape reproduction is good, the effect is more ideal reconstruction obtained satisfactory detailed three-dimensional information. Under the same boundary and loading conditions, inferior tibiofibular joint separation after a single cortical screw fixation in different ways, displacement finite element model of the tibia and fibula screw stress distribution and value as shown [6]. Fig.4 shows the a. b. c stand for the screw is 2/3/4cm above the articular surface of ankle joint.

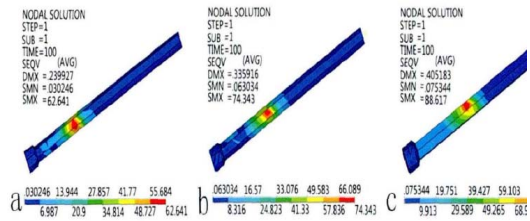


Fig. 4.The von Mises stress distribution of the 3.5mm screw which is fixed through four layers of cortical bone.

It can be seen through the rear lower tibiofibular joint separation 4 with a single layer of cortical bone fixation cortical screws, screw Von Mises peak appeared at the tibia and fibula gap, in which the maximum in diameter from 3.5mm screw fixed ankle flat 4cm 88.62 MPa, the maximum displacement of the tibia fibula maximum displacement of 1.95mm is 1.39mm; minimum in diameter screw 4. 5mm from ankle 2cm fixed plane when 36.36MPa, the maximum displacement of the fibula is 0.41 mm, the maximum displacement of the fibula 0.30mm [7].

In summary, different internal screw fixation of tibia and fibula stress distribution and displacement different, all models focused on the tibial screw stress gaps ribs, this situation consistent treatment of tibial fat screw joint after surgery on broken nails and clinical. In the same load boundary conditions, using 4.4mm diameter screws from the ankle 2cm plane through four layers of cortical bone fixation screws von Mises stress minimum, maximum displacement of the tibia and fibula minimum value; at the same screw diameter and position, through four layers of cortical bone ratio when crossing the three layers of cortical bone screw von Mises stress is small; at the same position and the same cortical bone through layers opposite 3.5mm 4.5mm screw von Mises stress reduced the carrying capacity of stronger relative displacement of tibia and fibula reduce better stability [8].

The Actual efficacy Analysis

In recent years, a method of fixing syndesmosis more, currently the most common clinical method is the cortical bone screws or lag screws transverse fixation, its therapeutic effect has been affirmed large number of scholars, but the distance between the screw position and the number of screw ankle, crossing

several cortical screw diameter of the screw implant position so controversial. New surgical methods are absorbable screw fixation, ligament reconstruction, buttons suture fixation, all kinds of new ways in minimally invasive surgery, reducing surgical trauma, recovery inferior tibiofibular joint function and other aspects have some breakthroughs, each with its own unique advantages. Under the new joint separation surgery tibia fat, as opposed to ordinary screw simple, stable fixation, better able to restore normal anatomy between tibiofibular is an ideal method for treating syndesmosis separation [9].

Syndesmosis fixation method most commonly used currently in clinical cortical bone screws or lag screws laterally fixed. As Syndesmotic separation using cortical screws or tension screw fixed for the time being there is no uniform standard. Many scholars believe that the application will result in lag screws tight affect syndesmosis ankle function that such step will lag screw hole with a smaller load so that the patient walking more concentrated stress on the screw fixing screw breakage under tibia In vitro studies have found that fixed pressing Philippians maximum ankle dorsiflexion activities before and after surgery the difference was not significant [10].

Suture-button system fully reflects the flexible fixed point for Stationary syndesmosis separation, the joint do tunnel through syndesmotic by introducing an elastic fixing material, both ends of the tibia, the bone surface fat hanging with buttons In the tunnel mouth. Efficacy screw fixation syndesmosis separation affirmed its fixed and treatment satisfaction, but often the risk of breakage exists. Button suture system as a new surgical treatment of tibial joint separation of fat, having allowed tibiofibular inching presence and early weight bearing, more physiological characteristics, there is no fatigue fracture of the implant, the results will not reset lost, no complications, no routine removal and many other advantages. Button suture system and screw two surgical ways treatment syndesmosis separation of fixed and treatment rather, it has achieved a good therapeutic effect [11].

III. CONCLUSION

Compared with the traditional mechanical methods, finite element method is a very effective numerical tool that can be individualized by changing the loading mechanics, material properties and other methods, experiments can't provide normal physiological information to obtain the objective entity experiment The results are difficult to get, more fully reflect the structure of the various parts of the internal morphology, stress, strain and displacement, etc., and to the various internal fixation devices and fixation

methods were evaluated. When the three-dimensional model-based ankle and surrounding bony structures established on the establishment of a different way of finite element model of fixed syndesmosis separation using a single cortical screw, model in a stationary state of human standing with one foot in neutral position stamp joint bear body weight load, the stress distribution of all models of consistency, screw stress gaps mainly in the tibia and fibula, which appears consistent with the position of the screw broken nails and clinically. Lower tibia joint horizontal row of screws can effectively control the syndesmosis injury caused by abnormal activity over the lower end of the tibia and fibula, results of this study show syndesmosis screws from stamp isolated cortical bone joint plane fixed, you can get a better biological mechanical stability.

REFERENCES

- [1] Gardner M J, Demetrakopoulos D, Briggs S M, et al. "Malreduction of the tibiofibular syndesmosis in ankle fractures" [J]. *Foot Ankle Int.* 2006, 27(10): 788 — 792. tibiofibular syndesmosis in ankle fractures [J]. *Foot Ankle Int.* 2006, 27(10):788-792.
- [2] Zalavras C, Thordarson D. "Ankle syndesmotic injury" [J]. *J Am Acad Orthop Surg.* 2007, 15 (6): 330-339.
- [3] Dattani R, Patnaik S, Kantak A, et al. "Injuries to the tibiofibular syndesmosis" [J]. *J Bone Joint Surg Br.* 2008, 90(4): 405-410.
- [4] Hansen M, Le L, Wertheimer S, et al. "Syndesmosis fixation: analysis of shear stress via axial load on 3.5-mm and 4.5-mm quadricortical syndesmotic screws" [J]. *J Foot Ankle Surg.* 2006, 45(2): 65-69.
- [5] Nousiainen M T, McConnell A J, Zdero R, et al. "The influence of the number of cortices of screw purchase and ankle position in Weber C ankle fracture fixation" [J]. *J Orthop Trauma.* 2008, 22(7): 473-478.
- [6] Hamid N, Loeffler B J, Braddy W, et al. "Outcome after fixation of ankle fractures with an injury to the syndesmosis: the effect of the syndesmosis screw" [J]. *T Bone Joint Surg Br.* 2009, 91(8): 1069-1073.
- [7] Miller A N, Paul O, Boraiah S, et al. "Functional outcomes after syndesmotic screw fixation and removal" [J]. *J Orthop Trauma.* 2010, 24(1):12-16.
- [8] Manjoo A, Sanders D W, Tieszer C, et al. "Functional and radiographic results of patients with syndesmotic screw fixation: implications for screw removal" [J]. *J Orthop Trauma.* 2010, 24(1):2-6.
- [9] Porter D A. "Evaluation and treatment of ankle syndesmosis injuries" [J]. *Instruction Course Lect.* 2009, 58:575-581.
- [10] Van den Bekerom M P, de Leeuw P A, van Dijk C N. "Delayed operative treatment of syndesmotic instability. Current concepts review" [J]. *Injury.* 2009, 40(11):1137-1142.
- [11] Yasui Y, Takao M, Miyamoto W, et al. "Anatomical reconstruction of the anterior inferior tibiofibular ligament for chronic disruption of the distal tibiofibular syndesmosis" [J]. *Knee Surg Sports Traumatol Arthrosc.* 2011, 19(4): 691-695.